

# Mind the gut

Citation for published version (APA):

Kakni, P. (2023). *Mind the gut: advancing intestinal organoid technologies*. [Doctoral Thesis, Maastricht University]. Maastricht University. <https://doi.org/10.26481/dis.20230203pk>

## Document status and date:

Published: 03/02/2023

## DOI:

[10.26481/dis.20230203pk](https://doi.org/10.26481/dis.20230203pk)

## Document Version:

Publisher's PDF, also known as Version of record

## Please check the document version of this publication:

- A submitted manuscript is the version of the article upon submission and before peer-review. There can be important differences between the submitted version and the official published version of record. People interested in the research are advised to contact the author for the final version of the publication, or visit the DOI to the publisher's website.
- The final author version and the galley proof are versions of the publication after peer review.
- The final published version features the final layout of the paper including the volume, issue and page numbers.

[Link to publication](#)

## General rights

Copyright and moral rights for the publications made accessible in the public portal are retained by the authors and/or other copyright owners and it is a condition of accessing publications that users recognise and abide by the legal requirements associated with these rights.

- Users may download and print one copy of any publication from the public portal for the purpose of private study or research.
- You may not further distribute the material or use it for any profit-making activity or commercial gain
- You may freely distribute the URL identifying the publication in the public portal.

If the publication is distributed under the terms of Article 25fa of the Dutch Copyright Act, indicated by the "Taverne" license above, please follow below link for the End User Agreement:

[www.umlib.nl/taverne-license](http://www.umlib.nl/taverne-license)

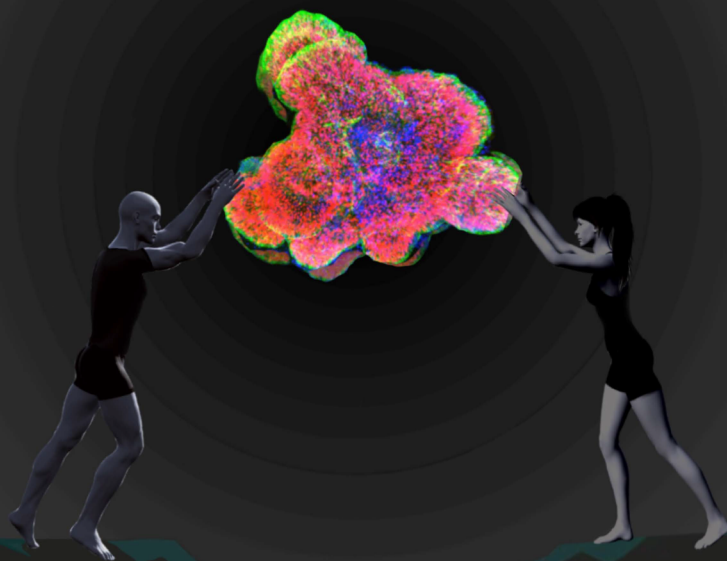
## Take down policy

If you believe that this document breaches copyright please contact us at:

[repository@maastrichtuniversity.nl](mailto:repository@maastrichtuniversity.nl)

providing details and we will investigate your claim.

# Mind the gut: Advancing intestinal organoid technology



*Panagiota Kakni*



**Mind the gut:  
Advancing intestinal  
organoid technologies**

Panagiota Kakni



Copyright © 2023 Panagiota Kakni

All rights reserved. No parts of this publication may be reproduced, stored in a retrieval system, or transmitted in any form or by any means, electronic, mechanical, photocopying, recording, or otherwise, without prior permission in writing from the author.

The work described in this thesis was carried out at the Department of Instructive Biomaterials Engineering of the MERLN Institute for Technology-Inspired Regenerative Medicine, Maastricht University, the Netherlands.

This study received funding from the Dutch Province of Limburg (program “Limburg INvesteert in haar Kenniseconomie/LINK”; SAS-2014-00837 and SAS-2018-02477).

ISBN:	9789464691832
Printed by:	ProefschriftMaken // <a href="http://www.proefschriftmaken.nl">www.proefschriftmaken.nl</a>
Layout by:	Panagiota Kakni
Cover design by:	Marianna Athanasouli

# **Mind the gut: Advancing intestinal organoid technologies**

Dissertation

To obtain the degree of Doctor at the Maastricht University,  
on the authority of the Rector Magnificus,  
Prof.dr. Pamela Habibovic  
in accordance with the decision of the Board of Deans,  
to be defended in public  
on Friday 3<sup>rd</sup> February 2023, at 10:00 hours

by

**Panagiota Kakni**

Born on 30<sup>th</sup> April 1994 in Thessaloniki, Greece

**Promotor:**

Prof.dr. Pamela Habibovic

**Co-promotors:**

Dr. Stefan Giselbrecht

Prof.dr. Roman Truckenmüller

**Assessment committee:**

Prof.dr. Lorenzo Moroni (chair)

Dr. Hans Bouwmeester, Wageningen U&R

Prof.dr. Daisy Jonkers

Prof.dr. Daniel Keszthelyi

Dr. Adrian Ranga, KU Leuven

# TABLE OF CONTENTS

<b><u>Chapter I</u></b>	
General introduction	6
<b><u>Chapter II</u></b>	
Challenges to, and prospects for, reverse engineering the gastrointestinal tract using organoids	14
<b><u>Chapter III</u></b>	
Intestinal organoid culture in polymer film-based microwell arrays	40
<b><u>Chapter IV</u></b>	
A microwell-based intestinal organoid-macrophage co-culture system to study intestinal inflammation	70
<b><u>Chapter V</u></b>	
Reversing epithelial polarity in pluripotent stem cell-derived intestinal organoids	100
<b><u>Chapter VI</u></b>	
Intestinal organoids with apical-out orientation as a tool to study nutrient uptake, drug absorption and metabolism	128
<b><u>Chapter VII</u></b>	
Hypoxia-tolerant apical-out intestinal organoids to model host-microbiome interactions	156
<b><u>Chapter VIII</u></b>	
General discussion	190
<b><u>Chapter IX</u></b>	
Impact paragraph	208
<b><u>Epilogue</u></b>	
Summary	216
Samenvatting	220
Acknowledgements	222
List of Publications	224
Curriculum vitae	225





# CHAPTER I

## **GENERAL INTRODUCTION**



The small intestine is the primary digestive organ of the body and it is located between the stomach and the large intestine. It constitutes the longest part of the gastrointestinal tract and it is comprised of three parts, which are, from proximal to distal: the duodenum, the jejunum and the ileum<sup>1</sup> (Figure 1A). Functionally, the small intestine is responsible for completing digestion and nutrient absorption. It forms a physical barrier against external factors and also plays a critical role in host immunity<sup>2</sup>. The primary organs of the alimentary canal consist of multiple layers. The innermost layer is the mucosa, which involves the glandular epithelium, the lamina propria and the muscularis mucosae<sup>3</sup>. Next, the submucosa offers a supportive layer of fibrous connective tissue is followed by the muscularis propria, which consists of an outer longitudinal and an inner circular smooth muscle layer and accounts for peristaltic movements. The outermost part is the adventitia or serosa. A unique feature of the small intestinal mucosa is the presence of circular folds, villi and microvilli (Figure 1B). The villi and microvilli extend tremendously the surface area of the epithelium (more than 30 m<sup>2</sup>) and together with the folds facilitate nutrient absorption. The villi protrude into the lumen of the small intestine and among them, deep crevices form, extending through the lamina propria to the muscularis mucosae, known as intestinal glands or crypts of Lieberkuhn<sup>3,4</sup>. The crypts, which have a secretory role, constitute the proliferative units of the mucosa<sup>3,5</sup>. Stem cells residing at the bottom of the crypts proliferate continuously to replenish themselves and give rise to transit amplifying cells that will then differentiate into mature epithelial cell types while migrating towards the villus. There are five types of differentiated cells in the villi: the secreting goblet and tuft cells, the absorptive enterocytes and M cells and the hormone-secreting enteroendocrine cells. Paneth cells are the only differentiated cell type that is accommodated solely in the crypts and does not migrate towards the villi<sup>3-6</sup>. Once the cells reach the villi tips, they undergo apoptosis and shed into the lumen. The intestinal epithelium has a rapid cell turnover rate and fully regenerates every five to seven days. These dynamic processes are orchestrated by epithelial-mesenchymal interactions. Furthermore, the intestinal epithelial cells are polarized and organize into an apical domain that faces the lumen, and a basolateral domain that faces the basement membrane and neighboring cells (Figure 1D). Establishment and maintenance of epithelial polarity is crucial for the proper function of the intestine<sup>7</sup>. Collectively, these features make the small intestine one of the most complex organs of the body, both structurally and functionally. So far, animal models and two-dimensional (2D) cell culture models do not accurately reflect the complexity and physiological responses of the human intestine, thus there is a great need for representative and robust human *in vitro* models<sup>8</sup>.

The establishment of small intestinal organoid models in the early 2000s revolutionized the *in vitro* research of intestinal physiology and disease. Organoids are 3D, self-organizing mini tissues that mimic multiple aspects of tissue structure and function. Specifically, intestinal organoids can recapitulate the crypt-villus architecture, as well as the polar apical-basolateral organization and the multicellular composition of the *in vivo* tissue<sup>9</sup>. Additionally, they perform intestinal functions, such as formation of a tight barrier, uptake and metabolism of nutrients and drugs, and modeling of host-microbiome interactions<sup>10</sup>. Therefore, organoid technology can be employed for several applications, including studies related to fundamental biology, regenerative medicine and drug discovery. However, one cannot neglect the challenges in the organoid field that remain untackled<sup>11</sup>. A major limitation is the use of poorly defined matrices as extracellular matrix substitutes, which are usually derived from animals and can cause high batch-to-batch variation within the culture system. Additionally, organoids lack the full complexity of the *in vivo* tissue and the surrounding tissues, which hinder their maturation and application in studies that require multiple key components of human physiology (e.g., immune responses). All these shortcomings limit the applicability and reliability of organoids for certain applications, such as drug screenings and other high-throughput assays, as well as translational research. Combining biological and engineering tools can promote the development of more advanced organoid models with higher efficiency, consistency and level of organization.

The main focus of the research outlined in this thesis was the development of 3D *in vitro* models that overcome some of the current limitations, aiming to expand the range of applications of intestinal organoids. Initially, in the review **chapter II** we provided an overview of the current challenges in gastrointestinal organoid models and discussed the approaches taken to overcome them<sup>12</sup>. Moreover, the future of organoids is envisioned as integrated models that recapitulate multiple regions of the digestive system in a single *in vitro* model. A combination of biology and engineering inspired methods seems to be the ultimate resolution for more advanced and physiologically representative *in vitro* models at the moment. Hence, through the following five experimental chapters, we describe intestinal organoid models developed with innovative bioengineering strategies.



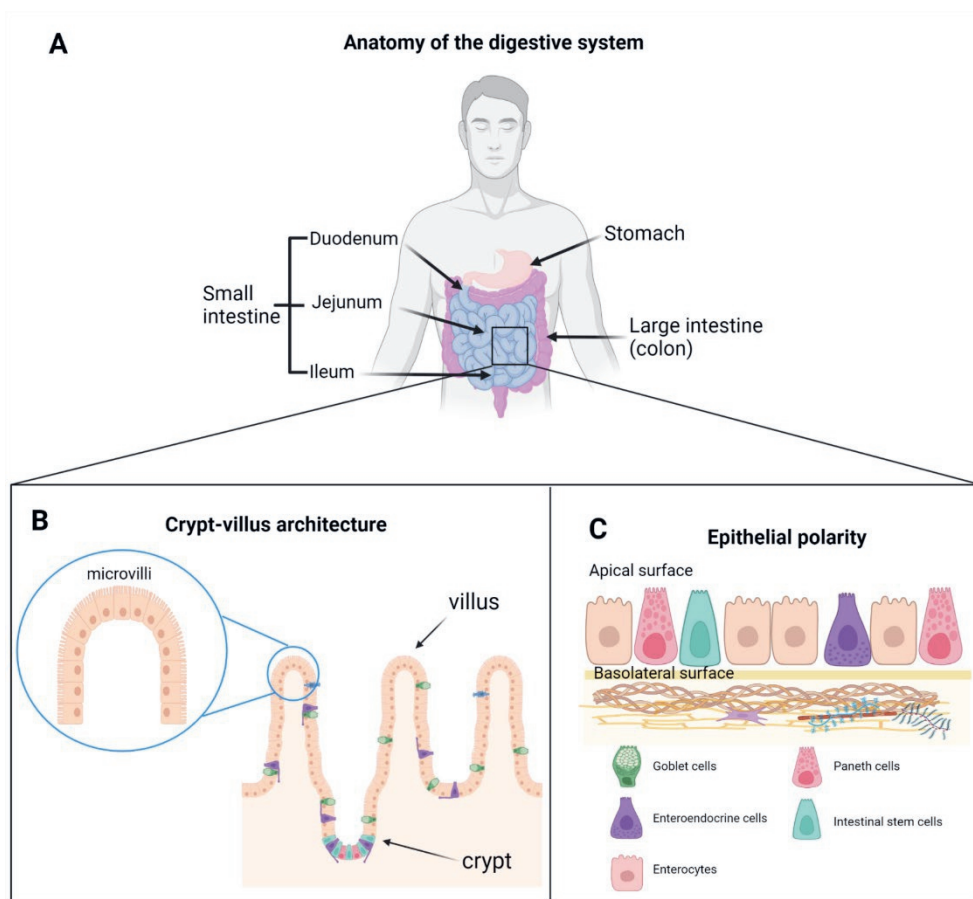


**Figure 1:** Structural characteristics of the small intestine. (A) The small intestine connects the stomach and the colon and it is subdivided into the duodenum, jejunum, and ileum. (B) The intestinal epithelium consists of characteristic, repetitive compartmentalized crypt-villus units. (C) Apical-basolateral polar organization of epithelial cells. Created with BioRender.com

In **chapter III**, the establishment of a microwell-based mouse intestinal organoid model was described<sup>13</sup>. Using microthermoforming, we fabricated ultrathin polymer film-based microwell arrays, which can accommodate almost 300 organoids in a single well of a 24-well plate and allow for *in situ* monitoring throughout the culture period and downstream experiments. In this platform, organoids showed multicellular composition, crypt-villus architecture and proper apical-basolateral polarity. Minimizing the use of extracellular matrix substitutes, the homogeneity in the system increased and the organoid viability was extended. This system provided exciting perspectives for the use of organoids in high-throughput applications and drug discovery.

In **chapter IV**, we demonstrated another valuable application of the microwell arrayed mouse intestinal organoid model. We established a versatile co-culture system that contained intestinal organoids and macrophages to study intestinal inflammation. We identified prominent differences when placing macrophages in close proximity to the organoids, by comparison of a direct (juxtacrine and paracrine signalling) with an indirect (only paracrine signalling) co-culture configuration. Quantification of a subpanel of cytokines related to intestine-macrophage interactions, suggested that co-culture systems provide a more holistic approach for the study of inflammatory responses when compared to exogenous treatments with pro-inflammatory cytokines (e.g., TNF- $\alpha$ ) and hinted an innate immunomodulatory function for the organoids. This microwell-based co-culture system could benefit studies related to the mechanisms underlying intestinal inflammation and facilitate the discovery of intestinal inflammatory disease related drugs.

In the following three experimental chapters, we focused on the generation and application of intestinal organoid models with reversed epithelial polarity. The use of intestinal organoid models to study nutrient/drug uptake and epithelial interactions with luminal contents (such as microorganisms) is currently hampered by the restricted access to the apical surface, which is located in an enclosed position, facing the lumen<sup>14</sup>. In the past few years, apical-out intestinal organoids were described using human<sup>14</sup>, chicken<sup>15</sup> and porcine<sup>16</sup> adult stem cells. In **chapter V**, we described the first apical-out intestinal organoid model derived from human pluripotent stem cells<sup>10</sup>. Unlike previous models, we initiated the differentiation process in a microwell platform that allowed for robust and scalable generation of organoids. By following a stepwise differentiation method that resembles the embryonic intestinal development and placing organoids in a suspension system, we generated mature intestinal organoids with apical-out orientation. The organoids contained all major intestinal cell types and maintained distinct apical and basolateral domains. The directly accessible apical surface can facilitate studies related to nutrient/drug uptake, metabolism and host-microbiome/pathogen interactions. Thus, in **chapter VI** we investigated the applications of apical-out intestinal organoids and showed that they successfully performed intestine-specific functions. More specifically, we demonstrated that apical-out organoids form a highly selective barrier through the presence of special junctional complexes, such as tight junctions, adherent junctions and desmosomes. Apical-out organoids showed an efficient uptake of nutrients from the culture medium, due to the apical transporters being directly accessible in the outer surface of the organoids. Additionally, we showed that apical-out organoids recapitulated intestinal metabolic functions and expressed

functional drug metabolizing enzymes and transporters, which could respond to drug treatments. Taking into account the system scalability, apical-out organoids may constitute a powerful new tool for nutrient studies and drug discovery.

As previously mentioned, host-microbiome/pathogen interaction studies can be facilitated with reversed epithelial polarity organoid models. However, the intestinal lumen *in vivo* is hypoxic and therefore, many of the residing microorganisms are obligate anaerobes. Thus, co-culture systems with apical-out organoids are not optimal with the current models, since the apical surface is exposed to high oxygen levels. To address this, in **chapter VII** we developed a novel hypoxia-tolerant apical-out intestinal organoid model. After assessing the differentiation capacity and functionality of these organoids, we demonstrated their ability to efficiently host anaerobic bacteria. We showed that the probiotic strains *Lactobacillus casei* and *Bifidobacterium longum* could colonize the apical surface of the organoids and we were able to identify probiotic effects on the organoids. This system offers a platform to explore unknown mechanisms related to host-microbiome interactions, which are essential for the proper function of the intestine. This system could also serve as a tool for developing microbiome-related therapeutics, the demand of which has immensely increased in the past decades.

Finally, in the discussion **chapter VIII**, we provided a general overview and discussed the future prospects of intestinal 3D *in vitro* models related to the experimental research described here and we discuss how they fit within the general panorama of intestinal models. Finally, we conclude with the impact paragraph **chapter IX**, where we highlighted the potential future scientific and social impact of our findings.

## **References**

1. Denbow, D. M. *Sturkie's Avian Physiology (Sixth Edition)*. (Elsevier Inc., 2015).
2. Chin, A. M., Hill, D. R., Aurora, M. & Spence, J. R. Seminars in Cell & Developmental Biology Morphogenesis and maturation of the embryonic and postnatal intestine. *Semin. Cell Dev. Biol.* **66**, 81–93 (2017).
3. Bass, L. M. & Wershil, B. K. *Anatomy, Histology, Embryology, and Developmental Anomalies of the Small and Large Intestine. Sleisenger and Fordtran's Gastrointestinal and Liver Disease* (Elsevier Inc., 2015).
4. Gehart, H. & Clevers, H. Tales from the crypt: new insights into intestinal stem cells. *Nature Reviews Gastroenterology and Hepatology* **16**, 19–34 (2019).

5. Bertram, T. A., Ludlow, J. W., Basu, J. & Muthupalani, S. *Digestive Tract. Haschek and Rousseaux's Handbook of Toxicologic Pathology* (Elsevier, 2013).
6. van der Flier, L. G. & Clevers, H. Stem Cells, Self-Renewal, and Differentiation in the Intestinal Epithelium. *Annu. Rev. Physiol.* **71**, 241–260 (2009).
7. Schneeberger, K., Roth, S., Nieuwenhuis, E. E. S. & Middendorp, S. Intestinal epithelial cell polarity defects in disease: lessons from microvillus inclusion disease. *Dis. Model. Mech.* **11**, dmm031088 (2018).
8. Chen, Y. *et al.* Robust bioengineered 3D functional human intestinal epithelium. *Sci. Reports 2015 51* **5**, 1–11 (2015).
9. Günther, C., Brevini, T., Sampaziotis, F. & Neurath, M. F. What gastroenterologists and hepatologists should know about organoids in 2019. *Digestive and Liver Disease* **51**, 753–760 (2019).
10. Kakni, P., López-Iglesias, C., Truckenmüller, R., Habibović, P. & Giselbrecht, S. Reversing Epithelial Polarity in Pluripotent Stem Cell-Derived Intestinal Organoids. *Front. Bioeng. Biotechnol.* **0**, 669 (2022).
11. Kim, J., Koo, B. K. & Knoblich, J. A. Human organoids: model systems for human biology and medicine. *Nat. Rev. Mol. Cell Biol.* *2020 2110* **21**, 571–584 (2020).
12. Kakni, P., Truckenmüller, R., Habibović, P. & Giselbrecht, S. Challenges to, and prospects for, reverse engineering the gastrointestinal tract using organoids. *Trends Biotechnol.* 932–944 (2022).
13. Kakni, P. *et al.* Intestinal Organoid Culture in Polymer Film-Based Microwell Arrays. *Adv. Biosyst.* 2000126 (2020).
14. Co, J. Y. *et al.* Controlling Epithelial Polarity: A Human Enteroid Model for Host-Pathogen Interactions. *Cell Rep.* **26**, 2509-2520.e4 (2019).
15. Nash, T. J., Morris, K. M., Mabbott, N. A. & Vervelde, L. Inside-out chicken enteroids with leukocyte component as a model to study host–pathogen interactions. *Commun. Biol.* *2021 41* **4**, 1–15 (2021).
16. Li, Y. *et al.* Next-Generation Porcine Intestinal Organoids: an Apical-Out Organoid Model for Swine Enteric Virus Infection and Immune Response Investigations. *J. Virol.* **94**, (2020).





## CHAPTER II

# **CHALLENGES TO, AND PROSPECTS FOR REVERSE ENGINEERING THE GASTROINTESTINAL TRACT USING ORGANOIDS**

Panagiota Kakni, Roman Truckenmüller,  
Pamela Habibović and Stefan Giselbrecht

*Trends in Biotechnology*  
40(8): 932-944 (2022)



## **Abstract**

For over a decade, organoids mimicking the development, physiology and disease of the digestive system have been a topic of broad interest and intense study. Establishing organoid models that recapitulate all distinct regions of the gastrointestinal tract (GI) has proven challenging since each tissue surrogate required tailor-made modifications of the original protocol to generate intestinal organoids. In this review, we discuss the challenges and current advances of the GI tract organoid models. Moreover, we envision the next-generation GI organoids as integrated organoid models, able to recapitulate structural and functional characteristics of multiple regions of the digestive tube in a single *in vitro* model. We discuss these new trends and provide an outlook for the future of GI *in vitro* models.

## **Current status of organoid models of the digestive system**

The emergence and rapid progress of organoid models has contributed significantly to the field of stem cell research. Organoids can be derived from two main stem cell types: **pluripotent** stem cells (PSCs; See Glossary) or organ-specific **adult stem cells** (ASCs). For PSC-derived models, both **embryonic** (ESCs) and **induced pluripotent** (iPSCs) stem cells can be utilized. The resulting organoids either contain both epithelial and mesenchymal cell types or only epithelial cells[1–4]. ASC-derived models are mostly employed for disease modeling, personalized medicine and to study tissue regeneration and homeostasis, whereas PSC-derived models are primarily used for studying development and developmental disorders. These self-organizing, three-dimensional (3D) models are promising tools to bridge the gap between *in vitro* monolayer cultures and *in vivo* studies, as they recapitulate tissue function and structure more accurately than conventional 2D cell cultures. Although they are characterized by an increased structural and functional complexity, they are amenable to the majority of the standard experimental techniques[5–8]. In this review, we focus on organoid models of the gastrointestinal (GI) tract and discuss the potential future directions to further approximate these models to the intricate complexity of a multiregional digestive tract by using recently developed technologies and bioengineering approaches (Figure 1, Key figure).

Insights into the development and homeostasis of the alimentary canal laid the foundation for the generation and culture of organoids (Box1). Intestinal organoids constitute the first organoid model described for a specific region of the

GI tract. In 2009, two pioneering models for growing intestinal organoids from adult mouse tissues were described. The first one was developed by Clever's team, who utilized previously identified  $Lgr5^+$  stem cells[9] to generate 3D epithelial organoids that resembled the crypt-villus architecture and expressed all the differentiated cell types present in the intestine *in vivo*[10]. The second model was described by Kuo's team, who embedded murine small and/or large intestinal fragments, including stromal cells, in collagen type I gels and placed them in a **3D air-liquid interface system** (ALI-3D)[11]. A couple of years later, the first PSC-derived intestinal organoid model was described. In this case, a stepwise differentiation method that mimics the embryonic intestinal development was required. Specifically, PSCs were initially differentiated towards the definitive endoderm, then hindgut and finally towards intestinal tissue[12]. Apart from the simple columnar epithelium, hPSC-derived intestinal organoids comprise a mesenchymal layer that develops along with the epithelium, thus indicating the importance of epithelial-mesenchymal interaction during intestine specification. Despite the common developmental origin, each part of the digestive system demonstrates a characteristic stem cell niche[13,14] and epithelial turnover[3]. This is reflected by the differences in the protocols to generate organoids mimicking other GI tissues[13,15–18]. Continuous efforts to tailor the culture conditions and niche factors according to the respective tissues lead to the development of the first protocols for gastric[19–22], colon[23–26] and esophageal[27–30] organoids. After a decade of intense research, today, numerous methods for generating and culturing organoids that mimic single distinct regions of the GI tract are available.

Despite the tremendous progress in this field, organoids are still far from being a perfect system and come with certain limitations and challenges, such as the use of undefined animal tumor-derived **extracellular matrix** (ECM), lack of complexity and surrounding tissues, low levels of maturation, uncontrolled growth and many others. In an attempt to improve this system, several approaches have been described focusing either solely on biological or on a combination of biological and engineering inspired methods. Specifically, to increase complexity and achieve further maturation, various co-culture systems, bioreactors and organoid-on-a-chip methods have been employed. Fully-defined, tunable, synthetic matrices and bioprinting techniques have also been established to replace poorly-defined matrices and better control organoid architecture. In this review, we provide an overview of methods that have been applied to tackle some of these issues. Mapping the landscape of the GI organoid field is an important step towards the next generation



of 3D *in vitro* models, which are capable of modelling multiregional architectures and functions by integrating multiple distinct regions of tissues or organs in one system. We discuss the role of advanced technologies in this endeavor, including roadmaps based on the compartmentalization strategy of organ-on-chip systems and the recently established organoid fusion techniques.

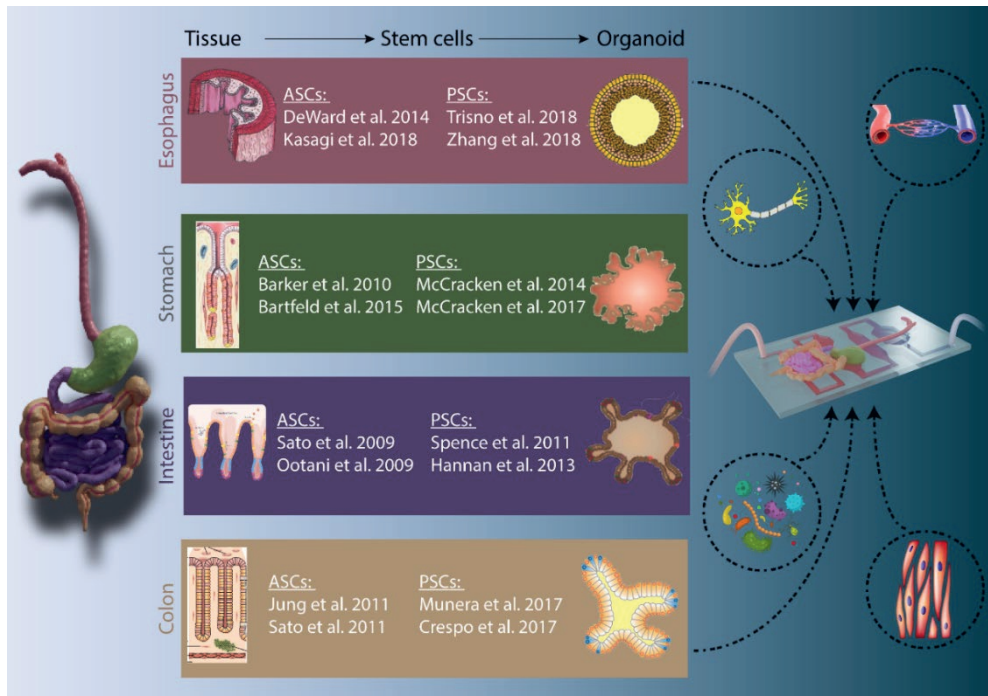


**Figure 1, Key Figure:** Schematic of organoid models of the GI tract and future on-chip applications. The current organoid models have been optimized to mimic structural and functional characteristics of specific single regions of the gastrointestinal tract. The next step in organoid research would be the generation of integrated organoid models that are capable of modelling multiple tissues and region-specific architectures and functions in one system using a combination of biology and engineering tools.

## **Hydrogels as ECM substitutes**

### Synthetic matrices

Gastrointestinal organoids have been widely used as an *in vitro* model to study development, physiology and disease. However, one limiting factor in extending their applicability in translational and clinical research is the use of poorly defined matrices (e.g. Matrigel, Cultrex or Geltrex). These ECM substitutes are derived from

mouse sarcoma cells. They also show batch-to-batch variability, their physical and chemical properties are difficult to control and they potentially transfer pathogens[31]. Hence, numerous groups have tried to replace those with other synthetic matrices. Initially, a hydrogel containing a fibronectin-derived, cell-adhesive, extended RGD (Arg-Gly-Asp) amino acid sequence and an elastin-like structural backbone was able to support the growth of mouse intestinal organoids under ALI-3D conditions[32]. Later on, enriched polyethylene glycol (PEG) hydrogels have been found to support the growth and differentiation of mouse intestinal stem cells into organoids[33]. The same hydrogel was used to culture human ASC-derived organoids but the efficiency was lower, suggesting that further optimization of the protocol was required[33]. For the culture of hPSCs-derived intestinal organoids, mid/hindgut spheroids were embedded in a PEG-4MAL (maleimide groups at each terminus) hydrogel functionalized with RGD peptides and expanded to mature intestinal organoids with similar efficiency to Matrigel[34]. Interestingly, these hydrogels were able to guide organoids towards intestinal mucosal wounds upon injection in mice, thus supporting localized engraftment of the organoids and more efficient wound closure[34,35]. Unmodified alginate, an algae-derived polysaccharide, has been proven capable of supporting the growth of PSC-derived intestinal organoids both *in vitro* and *in vivo* with similar efficiency to Matrigel. On the contrary, primary cell-derived organoids lacking mesenchyme failed to grow in this matrix[31]. A plant-based nanocellulose hydrogel functionalized with RGD peptides and glycine supported the culture of mouse intestinal organoids, which were initially formed in Matrigel, but failed to support the formation of organoids from freshly isolated mouse intestinal crypts [36]. All these studies demonstrate the versatility of synthetic matrices with regard to physical properties (stiffness, degradability, viscoelasticity etc.) and bioactivity of the organoid environment. Engineered ECM substitutes offer the possibility to tailor the biochemical and mechanical properties according to the organoid type and application. This will be of increasing importance once multiple organoid types need to be cultured and maintained in one single cell culture system. However, these synthetic and highly defined hydrogels are still in their infancy. They can only be used for certain applications and still cannot fully replace the widely used commercially available natural matrices.

#### Suspension and adherent organoid systems

Another downside of using these ill-defined, solid hydrogel matrices is that they usually hinder the use of organoids in high-throughput and pharmacological studies.

Embedding organoids in viscous hydrogels complicates their handling and downstream processing because they are usually randomly distributed in the matrix and their direct accessibility is impaired. Hydrogels seem to cause also a higher variation of size and shape of the organoids[37]. To overcome these issues, platforms that support the growth of organoids without a solid matrix have been described. It has been shown that murine intestinal stem cells cultured in flat-bottom plates require 10% Matrigel to generate organoids, whereas in V-shaped wells of 96-well plates, only 1% was sufficient. This set-up also allowed for an easier single-organoid tracking during the experiment and was used to study stem cell competition following irradiation[38]. Mouse intestinal organoids, derived from ASCs, have successfully been cultured in thermoformed polymer film-based microwell arrays using 5% of Matrigel as a media supplement[37]. Within this platform, organoids grew in a more controlled environment which improved the homogeneity of the organoids and allowed for an extended culture period. Furthermore, hydrogel microwell arrays have been shown to facilitate the culture of both mouse and human intestinal organoids with 2% Matrigel, achieving rapid and homogeneous organoid growth and facilitating automated high-throughput analysis. A proof of concept drug screening was also performed to demonstrate the potential of the system[39].

In a similar manner, Matsunaga's group placed midgut cells in EZSPHERE microwell plates to generate spheroids and then transferred them into ultralow-attachment plates and supplemented the media with 3% Matrigel for further culture[40]. These organoids expressed not only intestinal markers but also pharmacokinetic-related genes, and demonstrated transport and metabolic activity[40]. Uchida and coworkers obtained intestinal organoids suitable for pharmacological studies using a xenogeneic-free system. iPSCs were seeded on micropatterned glass surfaces and treated with the appropriate differentiation medium to generate mature and functional intestinal organoids[41]. A colonoid array, in which the organoids were grown on top of a thick Matrigel layer, was developed with the aim to increase the throughput of downstream applications. Automated microscopy and image analysis were performed to examine the position and size of organoids during culture and their response to different compounds[42]. Finally, a study was performed aiming to eliminate Matrigel while exploiting a cost-efficient suspension culture set-up for iPSC-derived organoids. However, the resulting organoids displayed differences in the expression of intestinal markers and a lower growth rate[43]. In these studies, researchers succeeded to reduce drastically the amount of Matrigel required to culture functional organoids by placing them in

suspension, culturing them on top of solid Matrigel and/or in microwell arrays. In this way, downstream analysis is facilitated since organoids are directly accessible, e.g. for exposing organoids to compounds which would diffuse only slowly in highly viscous matrices or to harvest organoids for further molecular analysis.

### **Co-culture systems**

Although organoids recapitulate multiple aspects of the *in vivo* tissue, they still fail to mimic the full complexity of the corresponding tissue. To improve this further, numerous co-culture systems and on-chip applications have been described. However, in most on-chip applications, organoids need to be dissociated into single cells and only serve as cell sources. The cells are integrated into the technical systems as 2D cell monolayers and the tissue-specific architecture is lost. However, the 3D multicellular context is of growing importance for future models, especially for models that aim to mimic multiple regions of the alimentary canal, e.g. with regard to the formation of stable tissue boundaries. In this article, we will therefore solely focus on complex organoid systems in which the 3D architecture of the organoids is maintained.

#### Co-culture with supportive cells

The enteric nervous system (ENS), known also as the “second brain”, plays a key role in multiple functions of the GI tract, including peristalsis/motility, hormone secretion and coordination of blood flow. Thus, numerous groups have tried to implement it in their organoid systems. **Neural crest cells (NCCs)** were combined with hindgut spheroids and formed intestinal organoids with a functional ENS[44]. To achieve further maturation of the ENS, Schlieve and colleagues, co-transplanted intestinal organoids and NCCs on scaffolds into immunodeficient mice[45]. Gastric organoids co-cultured with neural cells isolated from the myenteric plexus showed significantly improved growth[46]. A more complex gastric organoid system, incorporating both ENS and smooth muscle layers was achieved by the co-culture of posterior foregut spheroids with NCCs and splanchnic mesenchyme[47].

The crosstalk between the gastrointestinal epithelium and immune system is crucial to maintain barrier homeostasis since the epithelium is constantly in contact with foreign materials, viruses and microorganisms. In a study by Hahn and coworkers, mouse intestinal organoids were co-cultured with RAW 264.7 macrophages to model epithelial-to-mesenchymal transition[48]. Peripheral blood monocytes, when co-cultured with human intestinal organoids, were found to

migrate towards the mucosal organoids, interact with them and adopt a monocyte fate in a steady state[49]. In another study, low numbers of T effector memory cells were found to promote organoid growth, whereas higher numbers obstructed intestinal epithelial cell proliferation, thus indicating a dose-dependent effect on the organoid development[50,51]. In a more elaborate system, dissociated intestinal organoid cells were placed inside a microdevice that mimics the geometry of the native mouse intestinal crypts. The cells formed tubular organoids with crypt- and villus-like domains similar to the *in vivo* intestine and an accessible, perfusable lumen. When macrophages or endothelial cells were added to the system, these cells were found to communicate with the intestinal epithelium. Specifically, macrophages acquired a different morphology and performed phagocytosis and endothelial cells created blood vessel-like networks[52].

### Co-culture with microbiota/pathogens

The microbiota is a complex, dynamic population of microorganisms that constitute an indispensable part of the inner lumen of the gastrointestinal tract. Trillions of bacteria, fungi and other microbes reside there and contribute to nutrient degradation and absorption, defence against pathogens and the overall gut health. Alterations in the composition of the microbiota have been associated with inflammatory diseases. Thus, incorporation of microbiota and/or pathogens into organoids could greatly benefit the understanding of the digestive system's physiology and disease and could lead to more efficient therapeutic approaches. These kind of studies are usually technically challenging because of the hindered accessibility of the organoids' central lumen and the apical surface of the epithelium facing the inner lumen. To tackle this, two different strategies have been pursued; microinjection into the lumen and reversing **epithelial cell polarity** of the organoid.

Microinjections have been performed to study pathogen and commensal microbiomes both in PSC- and ASC-derived organoids. An advantage of this system is that the organoid lumen is a hypoxic environment, thus allowing the growth of oxygen-sensitive species. Intestinal and/or colonic organoids have been utilized to study the colonization of *Escherichia coli*[53–57], *Cryptosporidium*[58], *Salmonella Typhimurium*[59–61], *Clostridium difficile*[62–64] and *Bacteroides thetaiotaomicron*[65]. Infections by *Helicobacter pylori* have been extensively studied in gastric organoids[19,22,66,67]. Recently a comprehensive protocol to perform microinjections of microbes in organoids has been described[68]. Microinjections are beyond any doubt technically challenging, thus Williamson and

colleagues developed a semi-automated, high-throughput platform to expedite this intricate process. Apart from bacteria (both aerobic and anaerobic), healthy stool samples were injected in organoids within this platform, demonstrating that the environment of the organoid lumen is capable of supporting the growth of multiple microbial communities[69].

Reversal of the epithelial polarity is a very recently developed and non-invasive strategy aiming to provide access to the apical side of the epithelium. So far, this has only been shown with ASC-derived organoids of different organisms. In an apical-out human intestinal organoid system, *Salmonella Typhimurium* was found to invade more efficiently the apical surface, whereas *Listeria monocytogenes* showed a preference for the basal surface[70,71]. In a similar chicken organoid model, *Salmonella Typhimurium*, influenza A virus and *Eimeria tenella* successfully invaded the intestinal epithelium[72]. Immune responses following an infection by transmissible gastroenteritis virus were explored in a porcine apical-out intestinal organoid model[73]. Finally, a reversed polarity human gastric organoid model was utilized to study how SARS-CoV-2 infects gastric cells at different stages of development[74]. In all these studies, the apical side of the epithelium was located at the outer surface of the organoid, thus the microorganisms could simply be added to the medium to infect the organoids. This process seems to better mimic the natural infection process and overcomes the need for laborious microinjections. Tubular mini-guts formed in a hydrogel-containing microdevice were used to model the infection caused by *Cryptosporidium parvum*. In this system, access to the apical surface is granted by the inlet and outlet medium reservoirs that mediate perfusion of the lumen, thus there is no need for injection. Within the lumen of these organoids, *C. parvum* could successfully complete its life cycle and grow for long periods without affecting the epithelium[52]. All these co-culture systems show great potential to further increase the complexity of organoids and better model *in vivo* physiology and diseases. However, this field is still in its infancy and many questions remain unanswered. For example, can organoids which are co-cultured with immune cells respond in similar ways as the intestine during enteric infections and can we mimic the complexity of inflammatory processes *in vitro*? Would it be possible to co-culture multiple immune (or neuronal) cell types in the same system?

## **Future Perspectives**

An unmet challenge and a logical next step in organoid research is the development of systems featuring tissue-specific functions and architectures of multiple regions of the GI tract to mimic the complex interplay and communication between the different specialized tissues of this long tubular organ. In current cell culture systems, the organoid growth has limitations, but using bottom-up tissue engineering strategies, organoids can be used as complex building blocks to create multicellular superstructures. Lately, a lot of attention in the field has been directed towards a successful assembling of multiple organoids that resemble different regions of the same organ or even the body, in an effort to generate fully functional tissues in a dish. Since models capable of mimicking systemic and more physiological responses are urgently needed to better understand tissue-tissue interactions, such complex models could further close the gap between *in vitro* systems and animal experiments. An ideal scenario would be to grow multi-tissue organoid systems *in vitro* by making use of guided self-organization and directed differentiation. There are some first successful experiments by Silva and colleagues that point towards this direction. In this case, a multilineage organoid model integrating features of both the heart and the gut emerged from one single aggregate of mesendoderm progenitors by tightly controlling the temporal medium composition, thus laying the foundation for new methods to study multi-tissue interactions[75]. However, as long as we cannot grow and fully control such multilineage GI organoids *in vitro* by making use of guided self-organization and directed differentiation, we need to rely on more engineered approaches. So far, there have been two main bioengineering approaches to achieve this; first, the fusion method, where organoids resembling different tissues are co-cultured and eventually fuse to create a single functional organoid that displays characteristics from both regions of origin, and, second, based on the body-on-a-chip idea, where different types of organoids are grown in separate but still communicating compartments of a microfluidic chip.

### Organoid fusion

The fusion method has primarily been applied in the field of brain organoids. Already in 2017, the first three models of fused forebrain organoids were established and showed the potential of studying cortical interneuron migration during development[76–78]. In all three cases, the two region-specific organoids assembled into a multiregion neural 3D microphysiological system that maintained a spatial architecture and function similar to *in vivo* (Figure 2A). Likewise, thalamic organoids were fused with cortical organoids establishing reciprocal thalamocortical

axon projections just like their *in vivo* counterparts[79](Figure 2B). These studies laid the foundation for the generation of more advanced organoid systems, which are able to model complex interactions occurring in the brain during development, but also to model certain disorders. In the first integrated model related to the digestive system a foregut and a midgut spheroid were fused (Figure 2C). The resulting spheroid was embedded and matured in a Matrigel dome, a hepato-biliary-pancreatic organoid branched from the boundaries between the two spheroids[80]. These self-patterned multi-organ structures recapitulate the *in vivo* interactions taking place within the boundaries of foregut and midgut that precede the hepato-biliary-pancreatic organogenesis. However, one would expect gastric/esophageal and intestinal characteristics to be present in this system, since these tissues derive from the foregut and midgut respectively. This indicates lack of spatiotemporal control and guiding mechanisms in the system which should be more tightly regulated in future applications. Nevertheless, similar approaches could also be translated to other parts of the GI tract. For instance, at the hindgut stage, a fusion of proximal and distal spheroids, which can be derived using the same growth factors but different duration of exposure, could produce fused organoid constructs featuring characteristics of the duodenum, ileum and possibly even the jejunum, thus resulting in a more complete and multiregional intestinal organoid model. The integration of antral and fundic organoids could potentially result into a gastric organoid recapitulating closer the *in vivo* stomach. This assembly could be performed at the posterior foregut spheroid stage followed by ECM encapsulation. A spatial pattern of synthetic matrices, which offer the possibility to tailor the local microenvironment and support the growth of different organoid types, could benefit the control of the spheroid fusion and promote the development of specific tissues. Considering the different growth factors needed for the maturation and maintenance of each tissue surrogate, micro- and milli-fluidic platforms would be necessary in order to control the media supply and provide spatially distinct culture conditions. A spatially controlled, triple fusion of foregut, midgut and hindgut spheroids could yield innovative organoid models, considering that all the regions of the digestive system derive from primitive gut subdomains. However, to accomplish a spatiotemporally controlled, organized fusion, more sophisticated techniques using e.g. hydrodynamic flow focusing, microfluidic trapping and releasing, bioprinting and robotic pick and place techniques would need to be further adapted to the task of a controlled fusion of organoids on-chips. In a recent study, researchers used 3D bioprinting to generate macro-scale intestinal constructs featuring structural and functional *in vivo*-like characteristics[81]. The sequential printing of stomach and colon epithelial stem



cells lead to the formation of large tubes, which mimicked not only organ-specific properties but also the junction between stomach and intestine (Figure 2D).

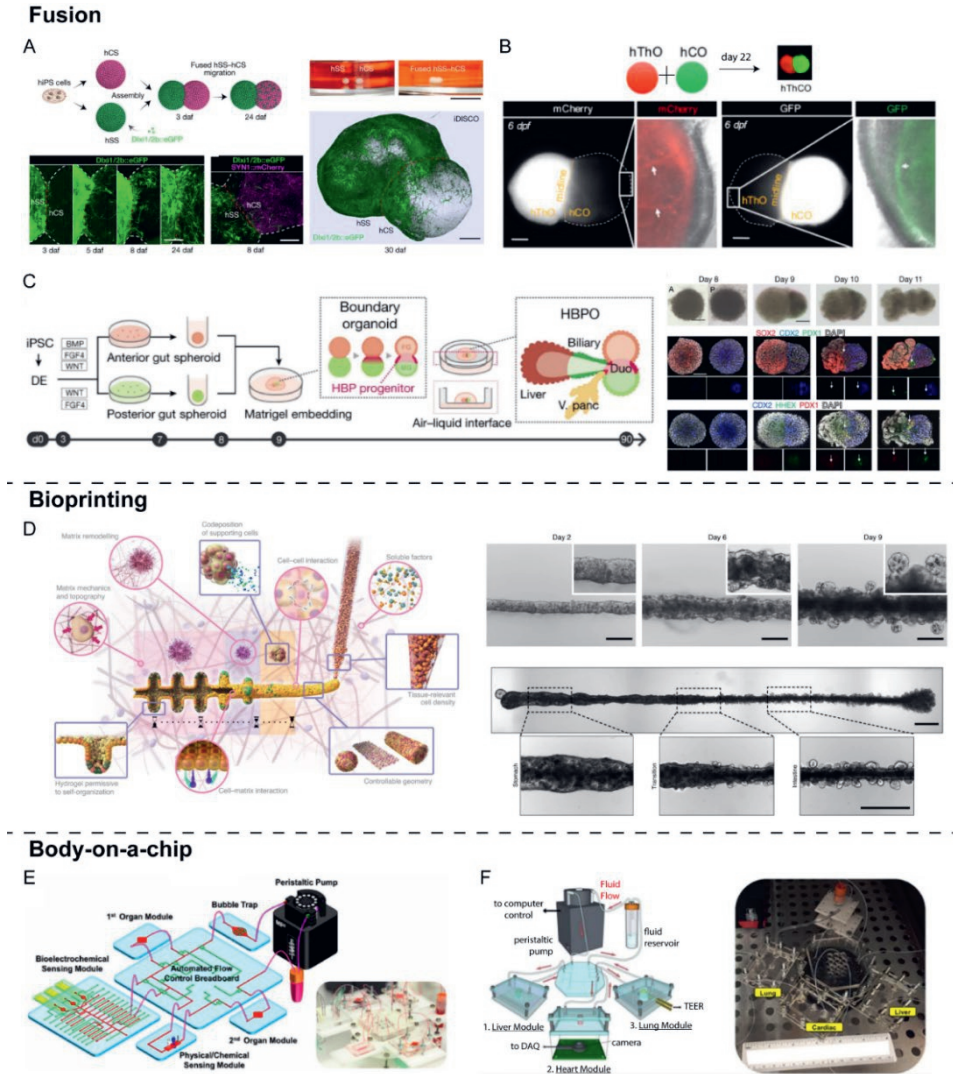


**Figure 2:** Currently available advanced organoid models. (A) A fusion model of dorsal and ventral forebrain organoids recapitulates the saltatory interneuron migration towards the cerebral cortex and their functional integration into microcircuits. hCS, human cortical spheroids; hSS, human subpallial spheroids[76]. (B) The assembly of thalamic and cortical organoids demonstrates reciprocal thalamocortical axon projections. hThO, human thalamic organoids; hCO, human cortical organoids[79]. (C) Following fusion of foregut and midgut spheroids, hepato-biliary-pancreatic organ domains emerge at the boundaries between the two spheroids. DE, definitive endoderm; HBPO, hepato-

biliary-pancreatic organoid[80]. (D) Illustration and bright-field images demonstrating bioprinted intestinal and gastrointestinal tissue constructs[81]. (E) An integrated multi-organoid on-a-chip platform comprising two microbioreactors for the organoids, physical and electrochemical sensors, bubble trap, medium reservoir and a breadboard[82]. (F) A three-tissue organ-on-a-chip platform integrating liver, heart and lung organoids accommodated in microreactors which are interconnected via a central fluid flow breadboard and continuously monitored with electrical sensors[83]. All the images are reproduced with permission from ref. [76, 80, 81, 83], Springer Nature, ref. [79] Elsevier and ref. [82]PNAS.

Although these methods to create more complex organoid models based on organoid fusion have demonstrated very promising results, the mechanisms underlying the formation of such assembled superstructures require further investigation (see Outstanding questions). An important point of consideration is the maintenance of distinct tissue borders in such integrated systems in order to avoid epithelial or mesenchymal cell migration across these borders that would “contaminate” the adjacent regions, thus making the model less physiologically relevant and applicable. A technical contingency plan for this could include the use of microfluidic devices where the organoids representing different regions are kept separated in compartments, similar to body-on-a-chip concepts (Figure 3A).

### Body-on-a-chip

Even though the body-on-a-chip approach has gained significant attention lately, it surprisingly remains less popular in the organoid field. One possible explanation is the heterogeneous and complex nature of the organoids that imposes challenges on the engineering of such devices. For example, some organoids grow at an ALI-3D whereas others grow embedded in viscous hydrogels. Additionally, there are differences in size and architecture; therefore, different chamber designs are required according to each organoid type. Apart from this, different organoids have different media requirements, thus having interconnected organoid chambers urges the need of a compatible medium that can facilitate the maintenance of multiple types of organoids. Another restraining factor associated with the interconnected media flow is to separately address the apical and basal sides of epithelial organoids enclosing a central lumen without disrupting their organotypic architecture. To overcome especially the limited access to the inner apical side of single or fused luminal organoids and to establish models, which enable controlled access to both the stromal and luminal compartment, more intelligent chip designs will be required. A controlled lumen-to-lumen medium flow, similar to the unidirectional flow of food and liquids in the digestive tract, would be a major step forward in organoid-on-chip

technology and would pave the way for a broad range of new applications. Further, it is important to determine at which stage of the culture protocols the organoids are transferred to the chip, considering the maturity level required for each downstream experiment and the fact that a compatible medium will most likely not support further growth or maturation. So far, only two such organoid systems have been established, which are not related to the GI tract; the first contains liver and cardiac organoids[82] (Figure 3E), while the second contains liver, cardiac and lung organoids[83](Figure 3F). In both systems, each organoid is cultured in a separate compartment of a microfluidic device and all the compartments are interconnected with tubes to enable a continuous fluid flow. Further, these chips are equipped with physical and biochemical sensors that enable continuous *in situ* monitoring of the organoids. Such systems have been used to study the response of the combined organoids to pharmaceutical compounds. On a larger scale, platforms such as the dynamic SIMulator of the GastroIntestinal tract (simgi®) and (TWIN-) SHIME® (Simulator of Human Intestinal Microbial Ecosystem) platform comprise several interconnected compartments, each representing a different part of the digestive system. These platforms are already applied in food and drug research. Likewise, a multi-chamber chip could be designed to accommodate organoids resembling the different regions of the alimentary canal and provide the opportunity to have a complete GI tract on a chip. According to the published protocols, there are several similarities between the culture conditions and timelines of the GI tract organoids. For instance, the duration of culture is similar and the same basal medium is used; hence, it should be possible to maintain these different organoids in the same medium for some time once they reach a certain maturity level. Even though the architecture is different, the dimensions of the different types of organoids are comparable, thus facilitating the chip fabrication process and simplifying seeding procedures. Considering all these, a GI-tract-on-a-chip platform appears plausible (Figure 3B). Thus, we envision that an organoid-based GI-tract-on-a-chip, potentially even with integrated advanced analytical tools, could become the new gold standard in studies of digestive system's development, function and disease.

Platforms integrating multiple types of organoids would greatly benefit both basic and translational research. Although organoids recapitulate many aspects of the *in vivo* physiology, one cannot neglect that neighboring and even remote tissues interact with each other in the human body. Hence, replicating the full spectrum of biochemical and biophysical interactions, including mechanical forces, paracrine and juxtacrine cell-cell interactions, are critical in every step of development. This

is particularly important when it comes to modeling the digestive tube, which consists of a series of interconnected organs, and to exploring complex mechanisms in developmental studies, which govern the patterning and regionalization of the GI tract.

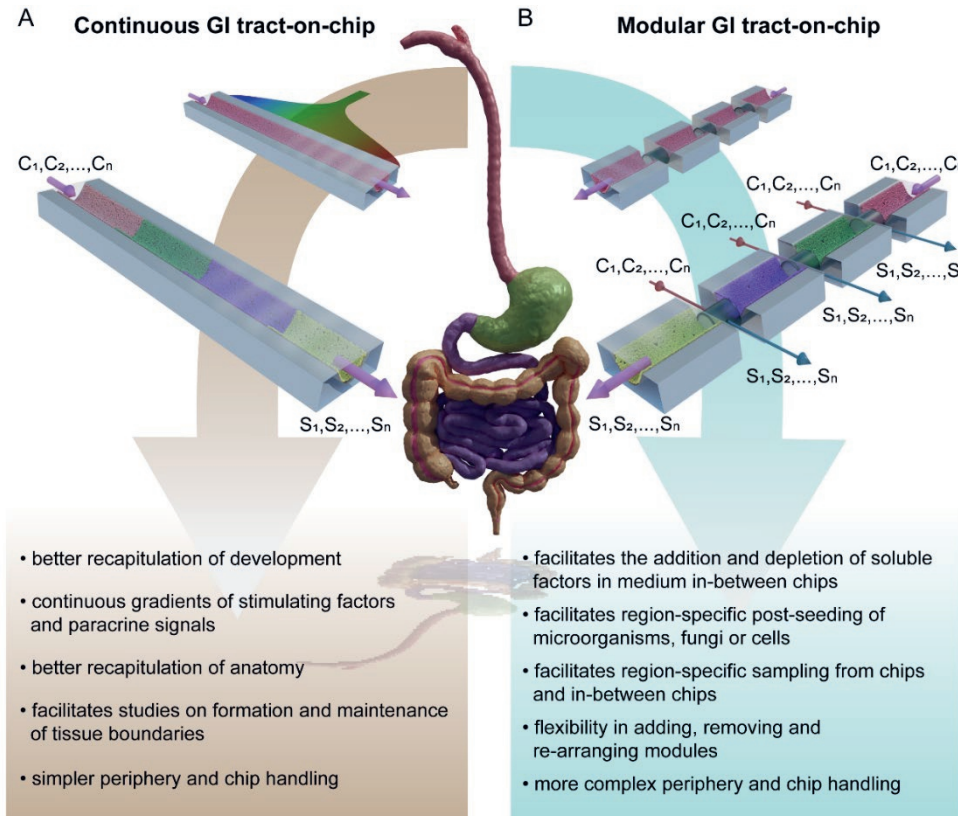


**Figure 3:** Brief assessment of the continuous (A) and modular (B) GI-tract-on-chip future concepts. On the one hand, a fused organoid model could be accommodated in a continuous system in order to achieve a better controlled growth and at the same time maintain the distinct boundaries between adjacent tissues. On the other hand, a modular chip could accommodate different organoids in each compartment allowing for more flexibility in the culture conditions, placement and interconnection of the organoids. C: medium component, S: sample.

## **Conclusion**

Organoids are one of the most exciting and rapidly advancing 3D in vitro models that have emerged in the last decade. The growing interest in more complex models

placed organoids in a unique position as a tool for a wide range of applications. It has been shown that all the important regions of the GI tract can separately be recapitulated by organoids representing both fetal and adult stages. Using organoids as building blocks to create more advanced integrated multiregion models seems to be the logical next step. Methods like organoid fusion, body-on-a-chip and bioprinting have already shown great potential to establish such organoid-based superstructures. Adding to that, considering the common developmental origins of these tissues, along with the similarities between the different organoid protocols, we foresee a high opportunity to reverse engineer a complete GI tract *in vitro* using organoids. Such a system would greatly benefit both fundamental and applied research and would serve a wide variety of applications.

## **References**

- 1 Broutier, L. *et al.* (2016) Culture and establishment of self-renewing human and mouse adult liver and pancreas 3D organoids and their genetic manipulation. *Nat. Protoc.* 11, 1724–1743
- 2 Rossi, G. *et al.* (2018) Progress and potential in organoid research. *Nat. Rev. Genet.* 19, 671–687
- 3 Günther, C. *et al.* (2019) What gastroenterologists and hepatologists should know about organoids in 2019. *Digestive and Liver Disease* 51, 753–760
- 4 Singh, A. *et al.* (2020) Gastrointestinal organoids: a next-generation tool for modeling human development. *Am. J. Physiol. Liver Physiol.* 319, G375–G381
- 5 Fatehullah, A. *et al.* (2016) Organoids as an *in vitro* model of human development and disease. *Nat. Cell Biol.* 18, 246–254
- 6 Min, S. *et al.* (2020) Gastrointestinal tract modeling using organoids engineered with cellular and microbiota niches. *Experimental and Molecular Medicine* 52, 227–237
- 7 Dedhia, P.H. *et al.* (2016) Organoid Models of Human Gastrointestinal Development and Disease. *Gastroenterology* 150, 1098–1112
- 8 Merker, S.R. *et al.* (2016) Gastrointestinal organoids: How they gut it out. *Developmental Biology* 420, 239–250
- 9 Barker, N. *et al.* (2007) Identification of stem cells in small intestine and colon by marker gene *Lgr5*. *Nature* 449, 1003–1007
- 10 Sato, T. *et al.* (2009) Single *Lgr5* stem cells build crypt-villus structures *in vitro* without a mesenchymal niche. *Nature* 459, 262–265
- 11 Ootani, A. *et al.* (2009) Sustained *in vitro* intestinal epithelial culture within a Wnt-dependent stem cell niche. *Nat. Med.* 15, 701–706

- 12 Spence, J.R. *et al.* (2011) Directed differentiation of human pluripotent stem cells into intestinal tissue in vitro. *Nature* 470, 105–109
- 13 Fujii, M. *et al.* (2019) Modeling Human Digestive Diseases With CRISPR-Cas9-Modified Organoids. *Gastroenterology* 156, 562–576
- 14 Date, S. and Sato, T. (2015) Mini-Gut Organoids: Reconstitution of the Stem Cell Niche. *Annu. Rev. Cell Dev. Biol.* 31, 269–289
- 15 In, J.G. *et al.* (2016) Human mini-guts: New insights into intestinal physiology and host-pathogen interactions. *Nature Reviews Gastroenterology and Hepatology* 13, 633–642
- 16 Merenda, A. *et al.* (2020) Wnt Signaling in 3D: Recent Advances in the Applications of Intestinal Organoids. *Trends in Cell Biology* 30, 60–73
- 17 Kechele, D.O. and Wells, J.M. (2019) Recent advances in deriving human endodermal tissues from pluripotent stem cells. *Current Opinion in Cell Biology* 61, 92–100
- 18 Daoud, A. and Múnera, J.O. (2019) Insights Into Human Development and Disease From Human Pluripotent Stem Cell Derived Intestinal Organoids. *Front. Med.* 6, <https://doi.org/10.3389/fmed.2019.00297>
- 19 Bartfeld, S. *et al.* (2015) In vitro expansion of human gastric epithelial stem cells and their responses to bacterial infection. *Gastroenterology* 148, 126-136.e6
- 20 Barker, N. *et al.* (2010) Lgr5+ve Stem Cells Drive Self-Renewal in the Stomach and Build Long-Lived Gastric Units In Vitro. *Cell Stem Cell* 6, 25–36
- 21 McCracken, K.W. *et al.* (2017) Wnt/ $\beta$ -catenin promotes gastric fundus specification in mice and humans. *Nature* 541, 182–187
- 22 McCracken, K.W. *et al.* (2014) Modelling human development and disease in pluripotent stem-cell-derived gastric organoids. *Nature* 516, 400–404
- 23 Jung, P. *et al.* (2011) Isolation and in vitro expansion of human colonic stem cells. *Nat. Med.* 17, 1225–1227
- 24 Sato, T. *et al.* (2011) Long-term Expansion of Epithelial Organoids From Human Colon, Adenoma, Adenocarcinoma, and Barrett’s Epithelium. *Gastroenterology* 141, 1762–1772
- 25 Múnera, J.O. *et al.* (2017) Differentiation of Human Pluripotent Stem Cells into Colonic Organoids via Transient Activation of BMP Signaling. *Cell Stem Cell* 21, 51-64.e6
- 26 Crespo, M. *et al.* (2017) Colonic organoids derived from human induced pluripotent stem cells for modeling colorectal cancer and drug testing. *Nat. Med.* 23, 878–884

- 27 DeWard, A.D. *et al.* (2014) Cellular heterogeneity in the mouse esophagus implicates the presence of a nonquiescent epithelial stem cell population. *Cell Rep.* 9, 701–711
- 28 Kasagi, Y. *et al.* (2018) The Esophageal Organoid System Reveals Functional Interplay Between Notch and Cytokines in Reactive Epithelial Changes. *CMGH* 5, 333–352
- 29 Trisno, S.L. *et al.* (2018) Esophageal Organoids from Human Pluripotent Stem Cells Delineate Sox2 Functions during Esophageal Specification. *Cell Stem Cell* 23, 501-515.e7
- 30 Zhang, Y. *et al.* (2018) 3D Modeling of Esophageal Development using Human PSC-Derived Basal Progenitors Reveals a Critical Role for Notch Signaling. *Cell Stem Cell* 23, 516-529.e5
- 31 Capeling, M.M. *et al.* (2019) Nonadhesive Alginate Hydrogels Support Growth of Pluripotent Stem Cell-Derived Intestinal Organoids. *Stem Cell Reports* 12, 381–394
- 32 DiMarco, R.L. *et al.* (2015) Protein-engineered scaffolds for in vitro 3D culture of primary adult intestinal organoids. *Biomater. Sci.* 3, 1376–1385
- 33 Gjorevski, N. *et al.* (2016) Designer matrices for intestinal stem cell and organoid culture. *Nature* 539, 560–564
- 34 Cruz-Acuña, R. *et al.* (2018) PEG-4MAL hydrogels for human organoid generation, culture, and in vivo delivery. *Nat. Protoc.* 13, 2102–2119
- 35 Spence, J. *et al.* (2017) PEG-4MAL Hydrogels for In Vitro Culture of Human Organoids and In Vivo Delivery to Sites of Injury. *Protoc. Exch.* DOI: 10.1038/protex.2017.098
- 36 Curvello, R. *et al.* (2021) Engineered Plant-Based Nanocellulose Hydrogel for Small Intestinal Organoid Growth. *Adv. Sci.* 8, 2002135
- 37 Kakni, P. *et al.* (2020) Intestinal Organoid Culture in Polymer Film-Based Microwell Arrays. *Adv. Biosyst.* DOI: 10.1002/adbi.202000126
- 38 Fujimichi, Y. *et al.* (2019) An Efficient Intestinal Organoid System of Direct Sorting to Evaluate Stem Cell Competition in Vitro. *Sci. Rep.* 9, 1–9
- 39 Brandenburg, N. *et al.* (2020) High-throughput automated organoid culture via stem-cell aggregation in microcavity arrays. *Nat. Biomed. Eng.* DOI: 10.1038/s41551-020-0565-2
- 40 Onozato, D. *et al.* (2018) Generation of intestinal organoids suitable for pharmacokinetic studies from human induced pluripotent stem cells. *Drug Metab. Dispos.* 46, 1572–1580

- 41 Uchida, H. *et al.* (2017) A xenogeneic-free system generating functional human gut organoids from pluripotent stem cells. *JCI Insight* 2,
- 42 Gunasekara, D.B. *et al.* (2018) Development of Arrayed Colonic Organoids for Screening of Secretagogues Associated with Enterotoxins. *Anal. Chem.* 90, 1941–1950
- 43 Takahashi, Y. *et al.* (2018) A Refined Culture System for Human Induced Pluripotent Stem Cell-Derived Intestinal Epithelial Organoids. *Stem Cell Reports* 10, 314–328
- 44 Workman, M.J. *et al.* (2017) Engineered human pluripotent-stem-cell-derived intestinal tissues with a functional enteric nervous system. *Nat. Med.* 23, 49–59
- 45 Schlieve, C.R. *et al.* (2017) Neural Crest Cell Implantation Restores Enteric Nervous System Function and Alters the Gastrointestinal Transcriptome in Human Tissue-Engineered Small Intestine. *Stem Cell Reports* 9, 883–896
- 46 Pastuła, A. *et al.* (2016) Three-Dimensional Gastrointestinal Organoid Culture in Combination with Nerves or Fibroblasts: A Method to Characterize the Gastrointestinal Stem Cell Niche. *Stem Cells Int.*, <https://doi.org/10.1155/2016/3710836>
- 47 Eicher, A.K. *et al.* (2021) Functional human gastrointestinal organoids can be engineered from three primary germ layers derived separately from pluripotent stem cells. *Cell Stem Cell*, <https://doi.org/10.1016/j.stem.2021.10.010>
- 48 Hahn, S. *et al.* (2017) Organoid-based epithelial to mesenchymal transition (OEMT) model: From an intestinal fibrosis perspective. *Scientific Reports* 7, 1–11
- 49 Jose, S.S. *et al.* (2020) Comparison of two human organoid models of lung and intestinal inflammation reveals Toll-like receptor signalling activation and monocyte recruitment. *Clin. Transl. Immunol.* 9, e1131
- 50 Schreurs, R.R.C.E. *et al.* (2019) Human Fetal TNF- $\alpha$ -Cytokine-Producing CD4+ Effector Memory T Cells Promote Intestinal Development and Mediate Inflammation Early in Life. *Immunity* 50, 462-476.e8
- 51 Schreurs, R.R.C.E. *et al.* (2021) In vitro co-culture of human intestinal organoids and lamina propria-derived CD4+ T cells. *STAR Protoc.* 2, 100519
- 52 Nikolaev, M. *et al.* (2020) Homeostatic mini-intestines through scaffold-guided organoid morphogenesis. *Nature* DOI: 10.1038/s41586-020-2724-8
- 53 Karve, S.S. *et al.* (2017) Intestinal organoids model human responses to infection by commensal and Shiga toxin producing Escherichia coli. *PLoS One* 12, e0178966
- 54 In, J. *et al.* (2016) Enterohemorrhagic Escherichia coli Reduces Mucus and Intermicrovillar Bridges in Human Stem Cell-Derived Colonoids. *Cell. Mol. Gastroenterol. Hepatol.* 2, 48-62.e3



- 55 VanDussen, K.L. *et al.* (2015) Development of an enhanced human gastrointestinal epithelial culture system to facilitate patient-based assays. *Gut* 64, 911–920
- 56 Pleguezuelos-Manzano, C. *et al.* (2020) Mutational signature in colorectal cancer caused by genotoxic pks+ *E. coli*. *Nat.* 580, 269–273
- 57 Hill, D.R. *et al.* (2017) Bacterial colonization stimulates a complex physiological response in the immature human intestinal epithelium. *Elife* 6, e29132
- 58 Heo, I. *et al.* (2018) Modelling *Cryptosporidium* infection in human small intestinal and lung organoids. *Nat. Microbiol.* 2018 37 3, 814–823
- 59 Wilson, S.S. *et al.* (2014) A small intestinal organoid model of non-invasive enteric pathogen–epithelial cell interactions. *Mucosal Immunol.* 2015 82 8, 352–361
- 60 Forbester, J.L. *et al.* (2015) Interaction of *Salmonella enterica* Serovar Typhimurium with Intestinal Organoids Derived from Human Induced Pluripotent Stem Cells. *Infect. Immun.* 83, 2926–34
- 61 Forbester, J.L. *et al.* (2015) Interaction of *salmonella enterica* serovar Typhimurium with intestinal organoids derived from human induced pluripotent stem cells. *Infect. Immun.* 83, 2926–2934
- 62 Engevik, M.A. *et al.* (2014) Human *Clostridium difficile* infection: Inhibition of NHE3 and microbiota profile. *Am. J. Physiol. - Gastrointest. Liver Physiol.* 308, G497–G509
- 63 Leslie, J.L. *et al.* (2015) Persistence and toxin production by *Clostridium difficile* within human intestinal organoids result in disruption of epithelial paracellular barrier function. *Infect. Immun.* 83, 138–145
- 64 Engevik, M.A. *et al.* (2014) Human *Clostridium difficile* infection: Altered mucus production and composition. *Am. J. Physiol. - Gastrointest. Liver Physiol.* 308, G510–G524
- 65 Engevik, M.A. *et al.* (2013) Loss of NHE3 alters gut microbiota composition and influences *Bacteroides thetaiotaomicron* growth. *Am. J. Physiol. Gastrointest. Liver Physiol.* 305, 697–711
- 66 Pompaiah, M. and Bartfeld, S. (2017) Gastric organoids: An emerging model system to study *Helicobacter pylori* pathogenesis. *Current Topics in Microbiology and Immunology* 400, 149–168
- 67 Bertaux-Skeirik, N. *et al.* (2015) CD44 Plays a Functional Role in *Helicobacter pylori*-induced Epithelial Cell Proliferation. *PLOS Pathog.* 11, e1004663
- 68 Puschhof, J. *et al.* (2021) Intestinal organoid cocultures with microbes. *Nat. Protoc.* 2021 1610 16, 4633–4649

- 69 Williamson, I.A. *et al.* (2018) A High-Throughput Organoid Microinjection Platform to Study Gastrointestinal Microbiota and Luminal Physiology. *Cmgh* 6, 301–319
- 70 Co, J.Y. *et al.* (2019) Controlling Epithelial Polarity: A Human Enteroid Model for Host-Pathogen Interactions. *Cell Rep.* 26, 2509-2520.e4
- 71 Co, J.Y. *et al.* (2021) Controlling the polarity of human gastrointestinal organoids to investigate epithelial biology and infectious diseases. *Nat. Protoc.* 16, 5171–5192
- 72 Nash, T.J. *et al.* (2021) Inside-out chicken enteroids with leukocyte component as a model to study host–pathogen interactions. *Commun. Biol.* 4, 1–15
- 73 Li, Y. *et al.* (2020) Next-Generation Porcine Intestinal Organoids: an Apical-Out Organoid Model for Swine Enteric Virus Infection and Immune Response Investigations. *J. Virol.* 94, <https://doi.org/10.1128/JVI.01006-20>
- 74 Giobbe, G.G. *et al.* (2021) SARS-CoV-2 infection and replication in human gastric organoids. *Nat. Commun.* 12, 1–14
- 75 Silva, A.C. *et al.* (2021) Co-emergence of cardiac and gut tissues promotes cardiomyocyte maturation within human iPSC-derived organoids. *Cell Stem Cell* 28, 2137-2152.e6
- 76 Birey, F. *et al.* (2017) Assembly of functionally integrated human forebrain spheroids. *Nature* 545, 54–59
- 77 Bagley, J.A. *et al.* (2017) Fused cerebral organoids model interactions between brain regions. *Nat. Methods* 14, 743–751
- 78 Xiang, Y. *et al.* (2017) Fusion of Regionally Specified hPSC-Derived Organoids Models Human Brain Development and Interneuron Migration. *Cell Stem Cell* 21, 383-398.e7
- 79 Xiang, Y. *et al.* (2019) hESC-Derived Thalamic Organoids Form Reciprocal Projections When Fused with Cortical Organoids. *Cell Stem Cell* 24, 487-497.e7
- 80 Koike, H. *et al.* (2019) Modelling human hepato-biliary-pancreatic organogenesis from the foregut–midgut boundary. *Nature* 574, 112–116
- 81 Brassard, J.A. *et al.* (2020) Recapitulating macro-scale tissue self-organization through organoid bioprinting. *Nat. Mater.* DOI: 10.1038/s41563-020-00803-5
- 82 Zhang, Y.S. *et al.* (2017) Multisensor-integrated organs-on-chips platform for automated and continual in situ monitoring of organoid behaviors. *Proc. Natl. Acad. Sci. U. S. A.* 114, E2293–E2302
- 83 Skardal, A. *et al.* (2017) Multi-tissue interactions in an integrated three-tissue organ-on-a-chip platform. *Sci. Rep.* 7, 1–16
- 84 Zorn, A.M. and Wells, J.M. (2009) Vertebrate Endoderm Development and Organ Formation. *Annu. Rev. Cell Dev. Biol.* 25, 221–251

- 85 Montgomery, R.K. *et al.* (1999) Development of the Human Gastrointestinal Tract: Twenty Years of Progress, *Gastroenterology* 3, P702-731
- 86 Wells, J.M. and Melton, D.A. (1999) Vertebrate Endoderm Development. *Annu. Rev. Cell Dev. Biol.* 15, 393–410
- 87 Gao, S. *et al.* (2018) Tracing the temporal-spatial transcriptome landscapes of the human fetal digestive tract using single-cell RNA-sequencing. *Nat. Cell Biol.* 20, 721–734
- 88 Kiefer, J.C. (2003) Molecular mechanisms of early gut organogenesis: A primer on development of the digestive tract. *Dev. Dyn.* 228, 287–291
- 89 Dunn, N.R. and Hogan, B.L.M. (2018) The endoderm from a diverse perspective. *Development* 145, <https://doi.org/10.1242/dev.163550>
- 90 Nowotschin, S. *et al.* (2019) The endoderm: A divergent cell lineage with many commonalities. *Development* 146, <https://doi.org/10.1242/dev.150920>
- 91 Zorn, A.M. and Wells, J.M. (2007) Molecular Basis of Vertebrate Endoderm Development. *International Review of Cytology* 259, 49–111
- 92 Sheaffer, K.L. and Kaestner, K.H. (2012) Transcriptional Networks in Liver and Intestinal Development 4, DOI: 10.1101/cshperspect.a008284
- 93 Grapin-Botton, A. and Melton, D.A. (2000) Endoderm development: From patterning to organogenesis. *Trends in Genetics* 16, 124–130

## **Glossary**

**Air-Liquid Interface (ALI):** cell culture method in which the basal surface of the cells is in direct contact with the culture medium and the apical one is exposed to air.

**Air-Liquid Interface 3D (ALI-3D):** organoid culture method in which the hydrogel (ECM substitute) that surrounds the embedded organoids is exposed to air.

**Adult Stem Cells (ASCs):** undifferentiated cells that are found between differentiated cells in a tissue. They have the capacity to self-renew and differentiate to specialized cell types. Unlike pluripotent stem cells, ASCs have a limited differentiation potential and can differentiate only into the cell types of the tissue of origin, thus they are multipotent or unipotent stem cells.

**Extracellular Matrix (ECM):** complex network of proteins and other macromolecules that provides biochemical and biomechanical support to cells and tissues. In addition, it plays a direct role in cellular interactions and in the repair of tissue damage.

**Epithelial cell polarity:** cells with intrinsic asymmetry in structural orientation. Epithelial cells establish distinct apical and basolateral compartments which are characterized by different protein composition and function.

**Enteric Nervous System (ENS):** the intrinsic nervous system of the digestive system, which is composed of a complex network of sensory neurons, motor neurons and interneurons.

**Embryonic Stem Cells (ESCs):** pluripotent stem cells derived from the inner cell mass of the blastocyst. They have an unlimited capacity for self-renewal and they can give rise to every cell type in the body.

**Induced Pluripotent Stem Cells (iPSCs):** pluripotent stem cell that have been produced by reprogramming adult somatic cells. They show a similar potential as embryonic stem cells.

**Neural crest cells (NCCs):** multipotent, migratory cell population that contributes to the formation of a wide range of tissues.

**Pluripotent Stem cells (PSCs):** stem cells that have the capacity to self-renew and produce any cell of the body.

## **Text Boxes**

### *Box 1: Development of the GI tract*

The human GI tract comprises a series of hollow organs joint in a long muscular tube running from the oral cavity to the anus. These organs are the esophagus, stomach, small intestine and large intestine. The embryonic development of the GI tract is a complex process initiated during gastrulation[84–89]. Gastrulation is a critical early step in developing multicellular organisms as it gives rise to the three primary germ layers: the endoderm, mesoderm and ectoderm[84–86,90]. Following gastrulation, the naïve endoderm transforms into a primitive gut tube, surrounded by splanchnic mesoderm, through a series of morphogenetic events[84,86,88,91]. During this time, three distinct regions, the foregut, the midgut and the hindgut, become prominent as the gut tube is patterned along the anterior-posterior (A-P) axis. Epithelial-mesenchymal interactions drive each one of these regions to undergo further patterning, in order to form specific primary organs. The foregut gives rise to the esophagus, trachea, stomach, lungs, thyroid, liver, biliary system and the pancreas; the midgut gives rise to the small intestine and the hindgut to the large intestine. As development proceeds, organ buds in conjunction with their surrounding mesenchyme continue to proliferate and differentiate into functional organs that eventually branch from the main tube[84,92]. During gut development, maintenance of regional identity relies on three mechanisms. First, the interplay between numerous signaling pathways, including the FGF, Wnt, Shh, BMP, RA and Notch, tightly coordinates local gene expression throughout development and function. Each region requires different combinations of transcription factors. The

## Chapter II

extracellular signaling factors also hold crucial stage-specific roles. Finally, morphogenetic processes and correct cell positioning are required for proper signaling between neighboring tissues[84,92,93].

Challenges to, and prospects for, reverse engineering  
the GI tract using organoids





## CHAPTER III

# **INTESTINAL ORGANOID CULTURE IN POLYMER FILM-BASED MICROWELL ARRAYS**

Panagiota Kakni, Rui Hueber, Kèvin Knoops,  
Carmen López-Iglesias, Roman Truckenmüller,  
Pamela Habibović and Stefan Giselbrecht

*Advanced Biosystems*  
4(10): 2000126 (2020)





## **Abstract**

As organoids offer a promising tool to study cell biology and model diseases, organoid technology has rapidly evolved over the last few years. Even though intestinal organoids are one of the most well-established organoid systems, they currently rely on the embedding into an excess amount of poorly defined, tumour-derived extracellular matrix. Here, we suggest a novel suspension method to grow mouse intestinal organoids inside thermoformed microwell arrays. This platform promotes the controlled growth of organoids under matrix-reduced conditions, with Matrigel only used as medium supplement. Hence, this system provides numerous advantages over the previously established methods. Based on our findings, viable and functional mouse intestinal organoids can be preserved for longer periods than in traditional Matrigel domes. Additionally, this microwell-based technique renders a novel organoid culture system in which the heterogeneity of the organoids is significantly reduced. Our method paves the way towards more controlled organoid culture systems that can also be beneficial for further downstream applications, such as automated imaging techniques and micromanipulations, which constitute valuable tools for high-throughput applications and translational studies.

## **Introduction**

The mammalian intestinal epithelium is a highly organized, self-renewing tissue composed of a single layer of columnar epithelial cells in a crypt-villus architecture. The crypt is a proliferative compartment occupied by continuously dividing cells at the bottom, which after differentiation migrate upwards towards the villus. In the villus, six different mature cell types are found, including secretory cells, such as goblet, Paneth, enteroendocrine and tuft cells, and also absorptive cells, such as enterocytes and microfold cells.<sup>[1-3]</sup> The intestinal epithelium serves two main functions, nutrient uptake and protection against harmful substances and pathogens. The presence of strong apical-basolateral compartmentalization is of critical importance for proper intestinal function.<sup>[3-7]</sup> Despite various advances in cell and tissue culture technologies<sup>[8-11]</sup> and organ-on-chip models<sup>[12]</sup> that have been used to study intestinal physiology over the past years, numerous morphological and functional aspects remain unknown.

Miniaturized three-dimensional, multicellular, stem cell-derived constructs that mimic *in vivo* tissue, called organoids, along with organ-on-chip systems represent culture systems able to recapitulate the complexity of an organ closer than any previously utilized technique.<sup>[13,14]</sup> Organoids have high self-organization

capacity and hold great potential as a research tool to explore unknown aspects of organ development, tissue regeneration, disease pathology, cell biology, and as drug-screening platforms. In the past few years, numerous protocols have been described to grow organoids that resemble various organs, such as liver, brain, intestine and lung.<sup>[15–21]</sup> Intestinal organoid culture is a relatively simple system, that typically involves the embedding of small multicellular fragments (containing LGR5<sup>+</sup> cells) in Matrigel, which serves as an extracellular matrix (ECM) mimic, supplemented with the right cocktail of growth factors.<sup>[16]</sup> This results in growing and self-sustaining intestinal organoids, which contain all the above mentioned cell types found *in vivo* and are organized in a crypt-villus structure that surrounds a central lumen, with strong apical-basolateral polarity.<sup>[13,22]</sup> Hence, these organoids have contributed significantly to the understanding of normal intestinal function and dysfunction in the last years.

Even though organoids are a powerful tool, their use still faces numerous limitations. Bioengineering approaches hold great potential in overcoming some constraints.<sup>[23–27]</sup> More specifically, mass transport in organoids is usually restricted by their size, a limitation which researchers hope to overcome with either the use of bioreactors, microfluidic chips or integration of vascular networks. Another limitation lays in the uncontrollable growth of organoids in terms of architecture. To overcome this, the use of synthetic materials with programmable properties that mimic the extracellular environment could be a valuable tool. In addition, embedding organoids in highly viscous gels entangles their handling and downstream processing and often accounts for variation between them. Co-culture with other cell types, such as stromal cells, could also lead to the formation and spatial organization of diverse tissues within a single organoid.<sup>[16,28,29]</sup> A multidisciplinary approach is considered crucial in order to overcome the challenges that come with the use of organoids.

Here we describe the fabrication of a thermoformed microwell array,<sup>[30]</sup> which is used as a platform for culturing intestinal organoids from adult mouse stem cells. By adapting previously described protocols,<sup>[13,22]</sup> we were able to grow organoids for up to 13 days without embedding them in Matrigel domes. Instead, we supplemented our medium with 5% Matrigel. We validated our platform by comparing the viability, morphology, size, apical-basolateral polarity, and expression of the main intestinal markers of organoids cultured in microwells to those grown embedded in Matrigel domes.

## **Materials and Methods**

### Preparation of microwells for organoid culture

Initially, microwell arrays (punched to size) were sterilized in a graded series of 2-propanol (VWR) (100–70–50–25–10%) and then washed twice with Dulbecco's Phosphate Buffered Saline (DPBS; Sigma-Aldrich). Afterwards, they were placed in 24-well plates and were secured at the bottom of each well using O-rings (ERIKS). O-rings are used to secure the polymer films at the bottom of the 24-well plates. These torus-shaped elastomers are slightly bigger than the diameter of a well of a 24-well plate so that their tight fit can be used to keep the films at the bottom of the wells in place.

### Organoid culture

Mouse intestinal organoids derived from the small intestine of C57BL/6 mice were purchased as cryopreserved fragments (STEMCELL Technologies) and cultured as previously described,<sup>13,30</sup> with minor modifications. Briefly, a mixture of 25  $\mu$ L Matrigel (Corning) and 25  $\mu$ L IntestiCult Organoid Growth Medium (50:50 mixture) containing organoids was placed dropwise in tissue culture-treated 24-well plates (Fisher Scientific), thus creating a 3D hydrogel dome. After polymerization at 37 °C and 5% CO<sub>2</sub> for 10 min, 650  $\mu$ L of IntestiCult was added. Medium changes were performed every two days, and organoids were passaged every 5–7 days (unless stated otherwise) using cold Gentle Cell Dissociation Reagent (GCDR; STEMCELL Technologies). After centrifugation at 290  $\times$  g for 5 min at 4 °C, the supernatant was removed, and the pelleted organoids were washed with cold Dulbecco's modified eagle medium with F-12 nutrients (DMEM/F-12) with 15 mM HEPES (STEMCELL Technologies), then centrifuged at 200  $\times$  g for 5 min at 4 °C. The supernatant was removed, and pelleted organoids were resuspended in a 50:50 mixture of Matrigel and IntestiCult. After incubation at 37 °C and 5% CO<sub>2</sub> for 10 min, Matrigel was polymerized and additional 650  $\mu$ L of IntestiCult was added. Only organoids with branching morphology (crypt-villus structures) were selected for analysis both for matrigel domes and microwells.

### Morphology assessment

The morphology of the organoids was assessed through images taken with a bright-field microscope (Nikon Eclipse TS100). The size of the organoids was measured using the image analysis software 'ImageJ' (National Institutes of Health, USA). More specifically, the projected contour of the organoid was manually retraced and the enclosed area was measured using the "Measure" option. The results are representative of five independent experiments performed with four organoids per

experimental group. Additionally, live imaging experiments were performed using a Nikon Inverted Research Microscope ECLIPSE Ti (see further details in the SI).

#### Scanning electron microscopy

Organoids were fixed with 4% paraformaldehyde in PBS for 30 min and dehydrated in a graded series of ethanol (at room temperature): 30% for 30 min (twice), 50% for 30 min, 70–80–90–96% for 10 min each and finally 100% for 10 min (thrice). Samples were dried overnight using hexamethyldisilazane (HMDS; Sigma-Aldrich) at room temperature and coated with a thin layer of gold (10 nm) in a sputter coater (Cressington 108auto). For imaging, SEM (FEI/Philips XL30) was used.

#### Viability assay

The viability of organoids was assessed by concurrently staining viable and dead cells with the fluorescent dyes calcein AM (Molecular Probes, Invitrogen) and ethidium homodimer-1 (EthD-1; Molecular Probes, Invitrogen), respectively, according to the supplier's instructions. Imaging was performed using Nikon Inverted Research Microscope ECLIPSE Ti. Quantification of viability was performed in total projection images. The percentage of area positively stained for EthD-1 was determined using ImageJ and was relative to the total organoid area. The results are representative of four independent experiments performed with four organoids per experimental group.

#### Immunostaining and confocal microscopy

Organoids were fixed with 4% paraformaldehyde (VWR) in phosphate-buffered saline (PBS; Sigma-Aldrich) followed by permeabilization with 0.2% Triton X-100 (VWR) and quenching with  $\text{NH}_4\text{Cl}$  (50 nM in PBS; Sigma-Aldrich), all at room temperature. After blocking with 5% bovine serum albumin (BSA; VWR) in PBS, primary antibodies were incubated overnight at 4 °C, and then secondary antibodies were added for 2 h at room temperature. Finally, samples were counterstained with DAPI (Sigma-Aldrich) and mounted using Lab Vision PermaFluor Aqueous Mounting Medium (Thermofisher). A full list of primary and secondary antibodies with respective dilutions is provided in SI Table 1. All stained samples were imaged using a confocal laser scanning microscopy (Leica TCS SP8) and processed with ImageJ.

#### Quantitative real-time PCR

Organoids grown in Matrigel domes or in microwells were dissociated using cold PBS and centrifugation at  $290 \times g$  for 5 min at 4 °C, after which the total RNA was

extracted using ISOLATE II RNA Mini Kit (Bioline). cDNA synthesis was performed using iScript cDNA Synthesis Kit (Bio-Rad). Quantification of gene expression was carried out using the iQ SYBR Green Supermix for quantitative real-time PCR (qPCR; Bio-Rad), on a CFX96 Real-Time PCR Detection System (Bio-Rad). Gene expression for each sample was normalized using glyceraldehyde-3-phosphate dehydrogenase (Gapdh) and hypoxanthine phosphoribosyltransferase (Hprt) housekeeping genes. Data analysis followed the  $2^{-\Delta\Delta C_t}$  method. The results are representative of four independent experiments. The primers are listed in SI Table 2.

#### Focused ion beam scanning electron microscopy

Organoids were fixed after 10 days in culture and prepared for 3D electron microscopy. Initially, samples were fixed with 2.5% glutaraldehyde (Merck) in 0.1 M cacodylic acid sodium salt trihydrate (cacodylate buffer; ACROS Organics) for 24 h at 4 °C. Subsequently, samples were washed with 0.1 M cacodylate buffer and postfixed with 1% osmium tetroxide (EMS) in the same buffer containing 1.5% potassium ferricyanide [ $K_3Fe(CN)_6$ ] (Merck) for 1 h in darkness at 4 °C. Then, organoids were dehydrated in a graded series of ethanol (70–90–100%) (Merck), with each step repeated twice for 30 min. Samples were infiltrated with Epon resin (LADD) for two days, embedded in the same resin and polymerized at 60 °C for 48 h. After fixation, the Epon blocks were trimmed down to the organoids using an UC6 ultramicrotome (Leica) and diamond trimming knife (Diatome). Blocks were glued onto SEM stubs using superglue, coated with a layer of carbon and embedded into silver paint to prevent charging. Samples were then transferred into the Scios DualBeam SEM (Thermofisher) and further processed for milling using the Slice & View software (version 3.0). The process started with a focused ion beam (FIB) that milled a nanometer thin layer from the sample, and subsequently each freshly produced surface was imaged with SEM.<sup>[56–58]</sup> These steps were consecutively repeated until the whole 3D object was ablated and imaged. Regular cross sections were milled at 30 kV and 1 nA beam current. Within each step, FIB removed 20 nm of the Epon blocks (containing organoids), and the fresh layers were imaged with SEM with an acceleration voltage of 2 keV. Dwell time was 300 ns per frame and volumetric range image integration (32 images) was performed. The pixel size was  $10 \times 10 \text{ nm}^2$  and the image dimensions were 6144 (width) and 4096 (height) in pixels. The individual FIB-SEM slices were aligned using the DipImage Matlab image processing toolkit (<http://www.diplib.org/>). Three-dimensional figures were rendered using Amira 6.5.0 (Thermofisher).

### Statistics

Statistical analysis was performed using GraphPad Prism 8. Unpaired Student's t-tests (two-tailed) with Welch's correction were used to determine statistical significance. Significant differences were defined as  $P < 0.05$ . P values of statistical significance are represented as \*\*\*\* $P < 0.0001$ , \*\*\* $P < 0.001$ , \*\* $P < 0.01$ , and \* $P < 0.05$ . The data were tested for normality with the D'Agostino & Pearson test. Error bars in figures indicate standard error of the mean (S.E.M).

## **Results and Discussion**

### Fabrication of microwell arrays

Microwell arrays were fabricated from 50  $\mu\text{m}$  thin polycarbonate films by microthermoforming.<sup>[31]</sup> Briefly, a brass mold was fabricated by ultra-precision micromilling comprising an array of 289 cylindrical dead-end holes, each with a diameter of 500  $\mu\text{m}$  and a depth of 800  $\mu\text{m}$ . The polymer film was clamped between the mold and a counter-plate. The latter contains openings for applying gas pressure and is connected to a pressure reservoir via high-pressure hoses and valves. The clamped mold and with it the polymer film were heated up to 153  $^{\circ}\text{C}$ , thereby softening the film. A differential gas pressure of 15 bar was then applied in order to three-dimensionally stretch the polymer film into the cavities of the mold. Afterwards, the film was cooled down, below its softening point (approximately 80  $^{\circ}\text{C}$ ), so that the gas pressure could be released and the polymer film retained its new shape. Finally, the gas pressure was released and the formed film was demolded (**Figure 1 A**; counter-plate not shown). The cavities formed using these conditions were 500  $\mu\text{m}$  in diameter and approximately 300  $\mu\text{m}$  in depth (Figure 1 B, C). Intestinal organoids present a characteristic crypt-villus architecture, which makes it hard to define their shape as circular, disc-like etc. Thus, the dimensions of the microwells were decided upon measurements of the area of organoids grown embedded in Matrigel. Morphometric characterization of the microwells was performed using a confocal laser scanning microscope (Keyence 3D Laser Scanning Microscope VK-X250K), corresponding analysis software (Keyence MultiFileAnalyzer), and a scanning electron microscope (SEM; FEI/Philips XL30). This process can be adapted in order to fabricate microwell arrays that fit into various cell culture plate formats, such as 96-well plates. Very recently, another microwell platform that accommodates intestinal organoid culture was designed using poly(ethylene glycol) (PEG)-based hydrogels. In that case, the arrays consisted of either 121 or 31 microcavities with a diameter of 400  $\mu\text{m}$  and the fabrication was performed directly onto the surface of cell culture plates.<sup>[32]</sup> Instead, our microwell arrays were microfabricated using very thin, thermoplastic polymer films that are

biocompatible and commercially available. The thin, transparent nature of these films facilitates high quality imaging.

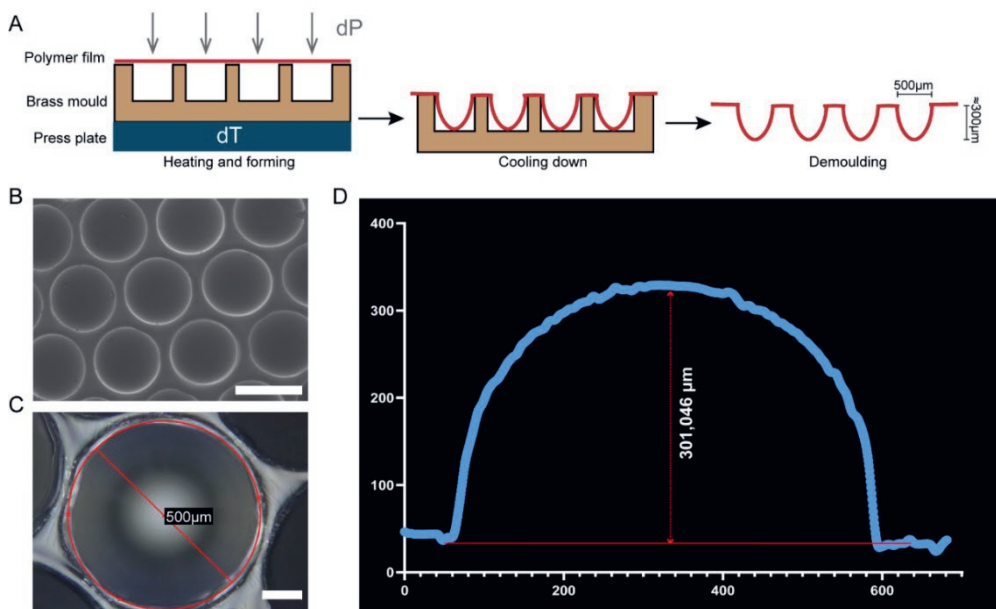


**Figure 1:** Fabrication and characterization of circular U-bottom microwells. (A) Schematic of the microthermoforming technique used to fabricate the microwell array (289 microwells arranged in a honeycomb-like fashion). Thermoforming was performed at 153 °C and 15 bar nitrogen pressure. (B) SEM image of a part of the array. Scale bar represents 500 μm. (C) & (D) Profile analysis of the formed microwells using confocal laser scanning microscope confirms the dimensions of 500 μm in diameter (C) and approximately 300 μm in depth (D). Scale bar represents 100 μm.

#### A method to culture intestinal organoids in microwells

In order to culture intestinal organoids in microwells (**Figure 2 A**), organoids were removed from Matrigel domes with cold Gentle Cell Dissociation Reagent (GCDR) and centrifuged as described in the methods section for passaging. Following the second centrifugation with DMEM/F-12 with 15 mM HEPES, the organoids' fragments were resuspended in IntestiCult containing 5% Matrigel, and 30 μL of this mixture was seeded onto the chip-type microwell arrays. Two hours post-seeding, an additional 600 μL of IntestiCult with 5% Matrigel was added. Medium was partially changed every 3-4 days. In order to avoid disruption of the organoids in microwells, the plate was slightly tilted and the medium was aspirated from the side walls. Organoids are not firmly attached to the surface of the microwells, thus they can be removed from microwells using GCDR and be passaged with the same procedure described above for the Matrigel domes. For our experiments, we used a

dilution of 1:2 (one Matrigel dome into two microwell arrays), although the seeding density is highly dependent on the initial density of organoids in Matrigel domes and can be adapted according to the experimental needs. However, additional work is required to further optimize the seeding process, e.g. by using more advanced low-volume cell dispensing techniques, in order to reliably have only one single organoid in each microwell. Because of the thin, transparent walls of the thermoformed microwells, standard immunostaining and imaging experiments can be performed on-chip.

As a proof of concept, we maintained organoids in microwell culture for 5 consecutive passages (from microwells to microwells) with no sign of deterioration. Specifically, we did not identify any difference in growth rate or morphology throughout serial passages. Organoids cultured for several passages in microwells can still be successfully transferred to Matrigel domes. This indicates that the organoids remain stable over multiple passages. Additionally, organoids were dissociated in single cells using Tryple, passed through a 40  $\mu\text{m}$  cell strainer and seeded in microwells (Figure S1A). In this case the medium was supplemented with Y-27632 (10  $\mu\text{M}$ ). Our results showed that after 6-8 days organoids present a mature architecture similar to organoids grown from fragments (Figure S1B).

Unlike previously suggested protocols that rely on the embedding of intestinal organoids in Matrigel domes,<sup>[13]</sup> or other types of hydrogels,<sup>[33–35]</sup> this microwell-based culture system allows for suspension-like culture of intestinal organoids. This overcomes the complex handling of fully embedded organoids.<sup>[33–35]</sup> For instance, in case of further downstream processing of organoids, gels need to be dissolved, a process that is labor-intensive and possibly leads to either disruption or loss of organoids. Further, without embedding, methods relying on controlled incubation with specific reagents (protein and metabolite production assays) would produce more accurate results, since gel absorbance and a changed diffusivity of reagents would not interfere with the assays.<sup>[36]</sup> This is an important feature of our platform, which could make it better suited for high-throughput screening purposes, where a higher diffusivity of the tested substances would lead to a more prompt response when compared to organoids embedded in higher viscous hydrogels. Additionally, organoids cultured within gels are usually localized at random positions in the matrix with various distances between them and it is known that organoids in close proximity could affect the growth of adjacent organoids, which overall can result in an increased variability of these gel-embedded systems.<sup>[32,37]</sup>



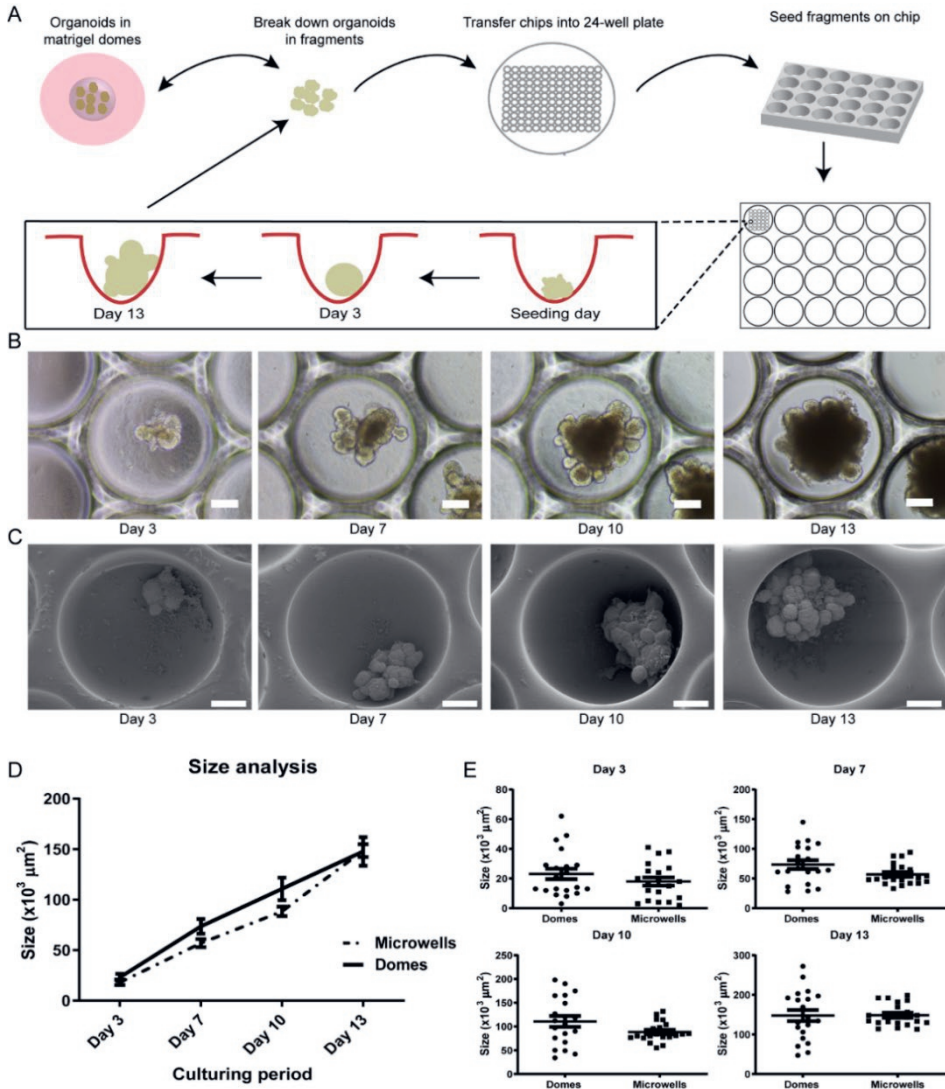


**Figure 2:** Microwell array-based organoid culture. (A) Schematic of the seeding procedure in microwells. Consistent with organoids grown in Matrigel domes, fragments of intestinal organoids grow as cyst-like spheres until day 3 and later they start budding, developing a crypt-villus architecture (day 13 shown). (B) Bright-field images showing the development of an organoid over a period of 13 days. Scale bars represent 100  $\mu\text{m}$ . (C) SEM images of microwells containing organoids after (left to right) 3, 7, 10, and 13 days in culture. Scale bars represent 100  $\mu\text{m}$ . (D) Graph represents the average sizes of organoids over 13 days of culture in microwells (non-filled triangles) and domes (filled circles). The same organoids were followed up over all the different time-points. Statistical analysis showed no significant difference between the two conditions at any of the time-points (mean  $\pm$  S.E.M,  $n=4$ ). (E) Scatter plot graphs display the variation in the size of organoids in each condition and at each time point. Each point represents an individual organoid; horizontal line and error bar indicate mean  $\pm$  S.E.M ( $n=4$ ).

In our method, one microwell typically harbors one organoid (52% one organoid per microwell, 5% two organoids and 2,5% three or more organoids per microwell; 40,5% of the microwells were empty; Figure S2) and all organoids are located in the same optical plane, so that the distance between the organoids is more defined and this contributes to increased homogeneity between the organoids. Similar approaches have been reported previously suggesting the culture of miniaturized kidney organoids in microwells (96 or 384-well plates) for high-throughput screenings<sup>[38]</sup> and suspension culture of kidney micro-organoids with higher yield.<sup>[39]</sup> Likewise, there are reports about the generation of colonoids in planar Matrigel scaffolds<sup>[40]</sup> and polystyrene “raft”- lined polydimethylsiloxane (PDMS) microwell platforms that support the co-culture of intestinal stem cells and Paneth cells for the generation and high-throughput analysis of enteroids.<sup>[41]</sup> However, in these approaches larger amounts of Matrigel were required. An effort to replace Matrigel and grow intestinal organoids in suspension was made by Takahashi et al.<sup>[42]</sup> Yet, organoids cultured in this system exhibited differences in the expression of cell markers, as well as a progressive decline in their growth rate.

#### Organoids grown in microwells have similar morphology and size as organoids in Matrigel domes

As a first step in the evaluation of our culture system, we used bright-field images (including also live cell imaging) and SEM images to evaluate their morphology and size (Figure 2 B, C; Supplementary Movie 1). Organoids grown in microwells presented a central cyst with crypt-like buds around it, consistent with the architecture of organoids embedded in Matrigel domes.<sup>[13,22]</sup> Using ImageJ, we measured the areas of the organoids grown inside the microwells and compared them with organoids grown with the “traditional” dome-based protocols at four different time points (day 3, 7, 10 and 13). Organoids grown in microwells were slightly smaller but not significantly different from those grown in Matrigel domes (Figure 2 D). The average areas of organoids in microwells were 18000  $\mu\text{m}^2$ , 57000  $\mu\text{m}^2$ , 89000  $\mu\text{m}^2$ , and 149000  $\mu\text{m}^2$ , at day 3, 7, 10, and 13 respectively; the average areas of organoids in Matrigel domes were 23000  $\mu\text{m}^2$ , 73000  $\mu\text{m}^2$ , 110000  $\mu\text{m}^2$  and 148000  $\mu\text{m}^2$  at the respective time points. Interestingly, we found that organoids grown in microwells showed less variation in size compared to organoids in the Matrigel domes. More specifically, analysis of variance showed that on day 3 the size variation in Matrigel domes was 40% higher than in microwells, with this rate elevating to 70% on day 7, 83% on day 10 and 80% on day 13 (Figure 2 E). These findings indicate that culturing organoids in microwells with 5% Matrigel in the culture medium (instead of 50:50 mixture of the Matrigel domes) results in the

formation of organoids with similar architecture and size as organoids grown in Matrigel domes but with less variation in projected area.

#### Organoids in microwells show lower cell death rates

To further evaluate our culture system, we performed live/dead staining of organoids grown in Matrigel domes and organoids grown in microwells with calcein AM and EthD-1, respectively, after 7, 10, and 13 days in culture. After 7 days in culture, an average of 14% of organoid area was stained positive for EthD-1, indicating dead cells, for organoids in microwells, whereas the rate reached 22% for organoids cultured in Matrigel domes (**Figure 3 A, D**). On day 10, 16% of the organoid area was found EthD-1<sup>+</sup> for organoids in microwells and 28% for organoids in Matrigel domes (**Figure 3 B, D**). Finally, on day 13 the difference was striking, with organoids in microwells having an average of 20% of total area of dead cells whereas the organoids in Matrigel domes had 40% (**Figure 3 C, D**). These results are consistent with previous reports, which indicate that organoids in Matrigel domes can stay in culture for up to 7 days before requiring passaging.<sup>[13,22]</sup> Our results suggest that organoids cultured in a microwell array can remain stable in culture for a longer period (up to 13 days). This prolongation in culture time reduces the labor required for passaging and makes the intestinal organoids amenable to longer-term assays, e.g. subchronic toxicity testing. One possible explanation for this extended stability is that with every medium exchange, culture debris is removed and the organoids in the microwells are in direct contact with fresh growth factors and other cytokines contained in the medium, whereas nutrients have to diffuse through the gel for organoids embedded in Matrigel domes and metabolic waste products are more likely to remain.<sup>[43]</sup> Alternatively, organoids grown in microwells may be exposed to higher and more equally distributed oxygen concentrations to facilitate growth and viability, as demonstrated previously for organoids in suspension cultures compared to ones grown embedded at different locations and different depths within dense gels. Okkelman et al.<sup>[37]</sup> demonstrated that organoids randomly distributed within Matrigel domes are not equally exposed to oxygen, imposing differences between organoids located close to the surface and deeper in the matrix.

#### Apico-basal polarity is better preserved throughout the whole culture period in microwells

Cell and tissue polarity are interrelated and play a pivotal role in normal tissue homeostasis.<sup>[3]</sup> Intestine is a highly organized tissue lined by a simple columnar epithelium of polarized cells. Apical and basolateral membranes differ in terms of protein and lipid compositions and serve different specialized functions. The apical

surface faces the lumen and is responsible for nutrient absorption, detection of microbial products and protection of the epithelium from noxious substances. The basolateral surface borders neighboring cells and the underlying basement membrane. Further, it mediates and governs the nutrient supply from the lumen to the bloodstream and the intercellular communication. Conservation of cell polarity in the gut is crucial for epithelial homeostasis, tumor suppression and innate immunity.<sup>42</sup> The strong apical-basal polarity in the intestine is marked by F-actin-rich brush border on the apical side and E-cadherin on the basolateral side.<sup>[3,4,16,44,45]</sup> Taking into account that the development and maintenance of polarity is necessary for proper intestinal function, we stained our organoids with E-cadherin and phalloidin at days 7, 10 and 13 in order to determine whether organization of the structure is preserved throughout the culture period. From organoids grown in microwells, we observed distinct expression of E-cadherin on the basolateral side and F-actin on the apical side during all the 13 days of culture (**Figure 4 A, B, C**; Supplementary Movie 2), indicating that intestinal structural organization was preserved. In contrast, organoids in Matrigel domes showed a well-organized epithelium on day 7 (Figure 4 A), but disrupted organization indicated by aberrant staining at later time points. More specifically, on day 10, low expression of F-actin was observed on the basal side of the organoids (Figure 4 B; Supplementary Movie 3), and on day 13, the expressions of E-cadherin and F-actin were distributed between the apical and basal side without distinct borders (Figure 4 C). In the microwells, however, the intestinal organoids remained stable for at least 13 days without any organizational disruptions. In combination with the results obtained from the viability assay and based on previous reports,<sup>[46,47]</sup> we hypothesize that the earlier loss of organization of intestinal organoids embedded in Matrigel domes is potentially caused by an impaired removal of metabolic waste and accumulation of senescent and dead cells in the gel. Shedding of high numbers of senescent and dead cells is expected for organoids that are faithfully recapitulating the physiology of an epithelium which, *in vivo*, has a very high turnover rate and completely self-renew within 2 to 6 days.<sup>[48]</sup>

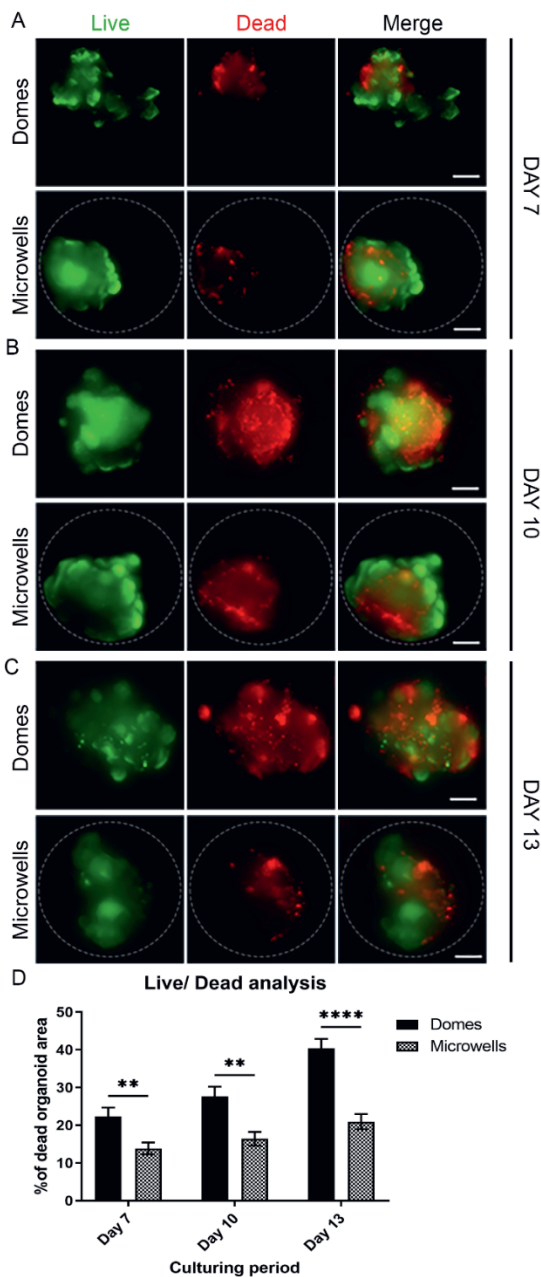


**Figure 3:** Viability assay. (A) Fluorescence microscopy images of organoids grown in Matrigel domes and in microwells. Viability assays were performed after (A) 7, (B) 10, and (C) 13 days in culture. At each time-point, the top row represents organoids grown in Matrigel domes and the bottom row organoids grown in microwells. Dashed circles represent the circumference of the microwells. Calcein (green, left column) marks the live organoid area and EthD-1 (red, middle column) the dead organoid area. Scale bar in merged image (right column) represents 100  $\mu\text{m}$ , and applies to the respective row. (D) Percentage of the total organoid area positively stained for cell death after 7, 10, and 13 days in culture, relative to the total organoid area. Unpaired Student's t-test with Welch's correction showed significantly lower cell death in organoids in microwells (white bars) comparing to the ones in Matrigel domes (black bars) at all time-points (mean  $\pm$  S.E.M, n=4).

### Maintenance of intestine-specific marker expression

Intestinal organoids are known to have a crypt-villus architecture and differentiate into the major intestine cell types, such as enterocytes, Paneth cells, goblet cells and enteroendocrine cells.<sup>[13,49-51]</sup> Paneth cells are located at the bottom of intestinal crypts, protecting the proliferative

cells by secreting bactericidal products and providing them with essential niche signal.<sup>45</sup> In order to ensure that our organoids maintained the intestinal phenotypic characteristics, we stained them for Ki67, a proliferation marker, lysozyme 1 for Paneth cells, chromogranin for enteroendocrine cells, and villin, which marks the apical face of enterocytes.<sup>[13,44,49,52]</sup> Confocal microscopy revealed the presence of

Ki67<sup>+</sup> proliferative cells in the crypts of organoids both in microwells and in Matrigel domes (**Figure 5 A**; Figure S3). In addition, Paneth cells (marked by lysozyme 1) were found adjacent to proliferative cells, as suggested by their protective role. Enteroendocrine cells, stained by chromogranin, were also found present in both systems (Figure 5 B; Figure S4). These results were consistent in organoids grown in microwells and Matrigel domes, at all time-points.

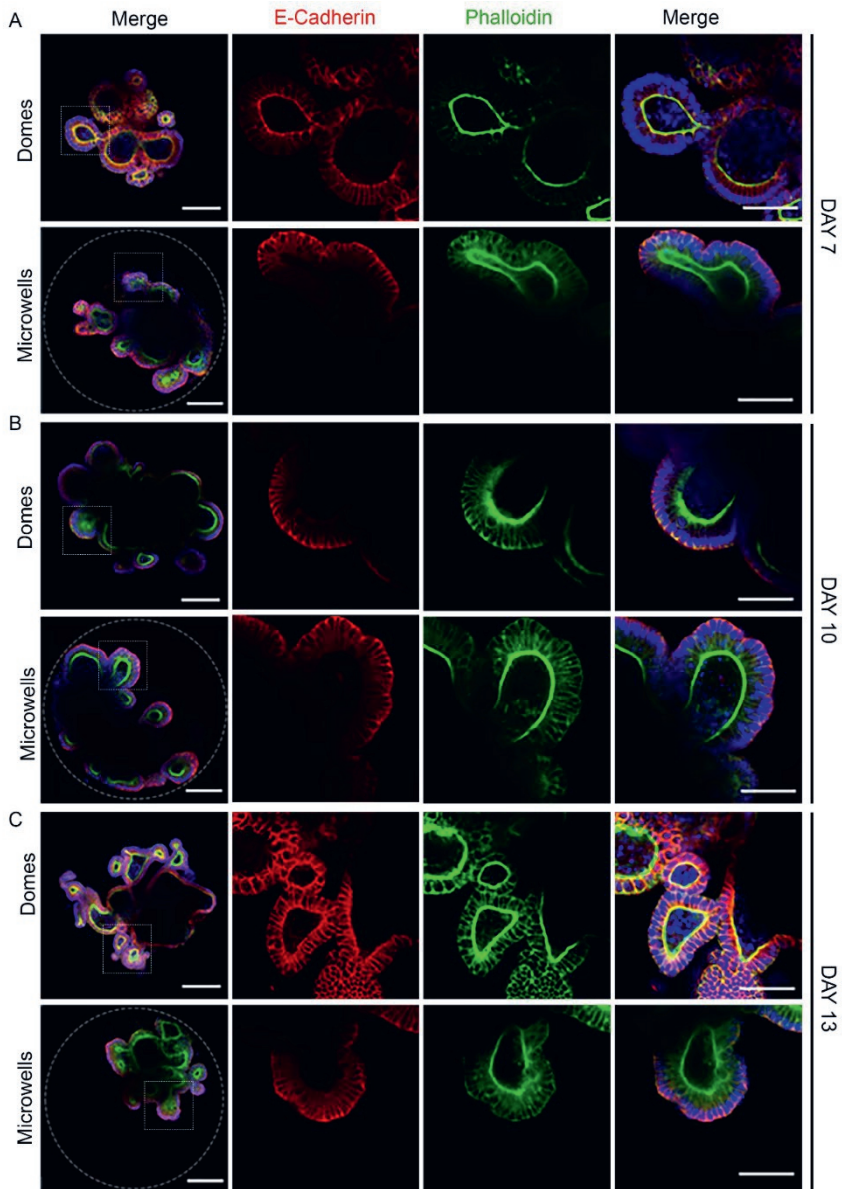




**Figure 4:** Apical-basolateral polar organization in organoids grown in microwells. Confocal microscopy of organoids after (A) 7, (B) 10, and (C) 13 days in culture. At each time-point, the top row represents organoids grown in Matrigel domes and the bottom row organoids grown in microwells. Dashed circles represent the circumference of the microwells. Dashed squares represent the area magnified in the respective columns to the right, in the same row. Basolateral side marked by E-Cadherin (red, middle left column) and apical side by phalloidin (green, middle right column). DAPI counterstain (blue) indicating the nucleus is shown in the merged images (left and right columns). All images represent a single z stack slice. Scale bars represent 100  $\mu\text{m}$ ; the scale bar in the right column applies also to the middle two columns.

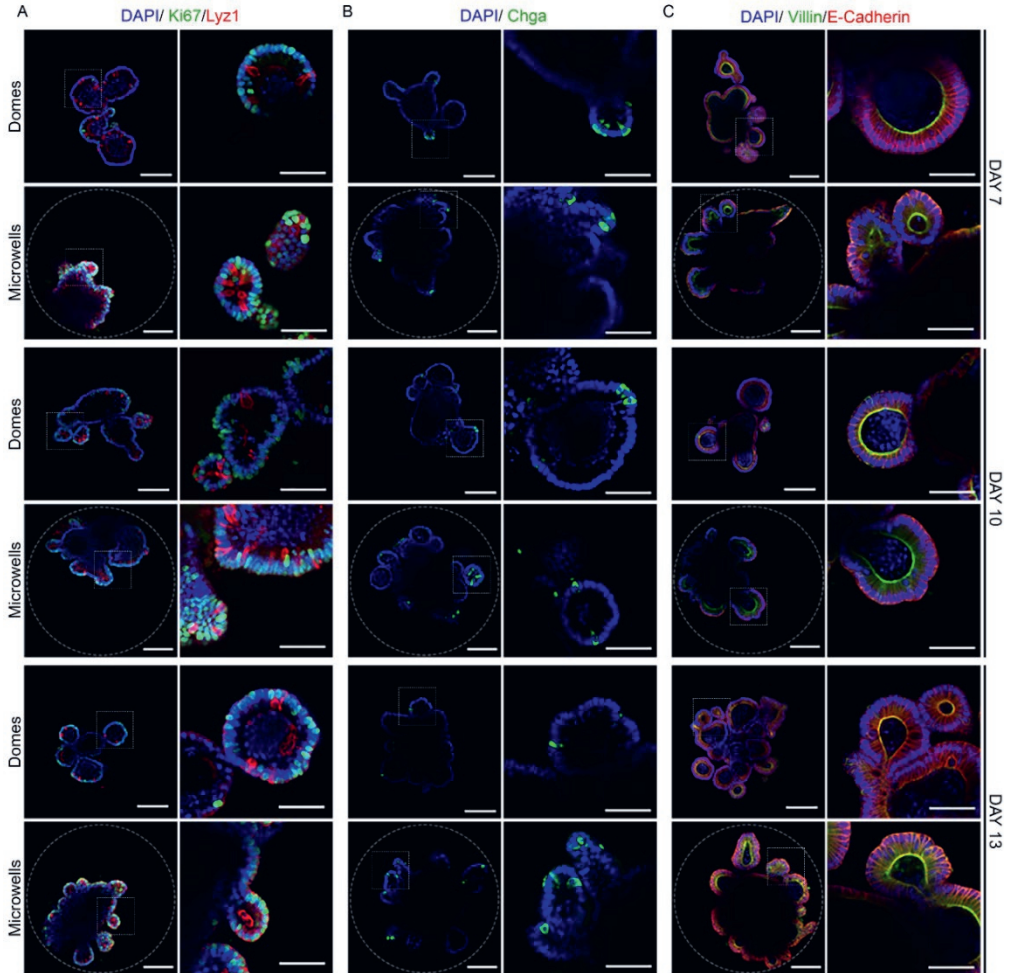


**Figure 5:** Organoids in microwells express intestine-specific markers for (A) proliferative and Paneth cells, (B) enteroendocrine cells and (C) enterocytes. Confocal microscopy of organoids on day 7 (top two rows), day 10 (middle two rows), and day 13 (bottom two rows). At each time-point, the top row represents organoids grown in Matrigel domes and the bottom row organoids grown in microwells. Dashed circles represent the circumference of the microwells. Dashed squares represent the area magnified in the corresponding image to the right. (A) Ki67 (green) demonstrates the presence of

proliferative cells and lysozyme (red) the Paneth cells. (B) Chromogranin (green) labels the enteroendocrine cells. (C) Villin (green) marks the apical side of enterocytes, and E-Cadherin (red) the basolateral side. In all panels, DAPI counterstain (blue) indicates cell nucleus. All images represent a single z stack slice. Scale bars represent 100  $\mu\text{m}$ .

To further examine the presence of the typical intestinal cell types in our system, qPCR was performed for organoids collected at all three time-points (day 7, 10 and 13). Organoids grown in microwells and Matrigel domes were examined for expression of the Wnt-associated stem cell marker *Lgr5* and for markers indicating intestinal differentiation (*Vill1* encoding villin, *Lyz* encoding lysozyme 1, *Chga* encoding chromogranin, as well as *Muc2* encoding mucin 2 secreted by goblet cells, and *Alpi* encoding alkaline phosphatase). The results showed similar expression levels of the genes studied, with no statistically significant differences, for the organoids embedded in Matrigel domes and the ones in microwells over the whole culture period (**Figure 6**). Altogether, these results indicate that, despite the differences in viability and polarity, organoids cultured in the microwells and in the Matrigel domes maintained similar gene expression levels after 13 days in culture.

#### Cellular morphology of the intestinal organoids by electron microscopy

We next sought to develop a protocol to evaluate the ultrastructural organization and maturity of the organoids grown in microwells. To this end, we optimized a 3D FIB-SEM protocol, which allows for the automatic generation of 3D images with superior resolution in all the axes (x, y and z). This technique is based on methods that have previously been used for ultrastructural imaging of 3D biological samples.<sup>[53]</sup> Organoids embedded in Matrigel domes have to be fixed on glass coverslips, which later requires the use of harsh chemicals to remove the glass for imaging. Instead, the organoids in the polymer microwells are embedded *in situ* and can be evaluated without processing with harsh chemicals, which considerably reduces the risk of damaging the organoids. Apart from simplifying the EM preparation, the absence of solidified Matrigel provided better results in terms of contrast and sharpness and the use of microwells eased the selection of the organoid that was sliced and imaged. The results of this analysis indicated the presence of mucus-secreting goblet cells and epithelial cells with apical microvilli, known as enterocytes (**Figure 7**; Supplementary Movie 4). The area imaged corresponds to the villi part of the organoid where mostly enterocytes and goblet cells are located.<sup>[54,55]</sup> Besides the confirmation of the presence of these cell types, FIB-SEM provided detailed information about the ultrastructural organization and visualized and confirmed the distinct apical-basolateral polarity of intestinal organoids that has previously shown using immunofluorescence microscopy.<sup>[4,16,44,45]</sup>



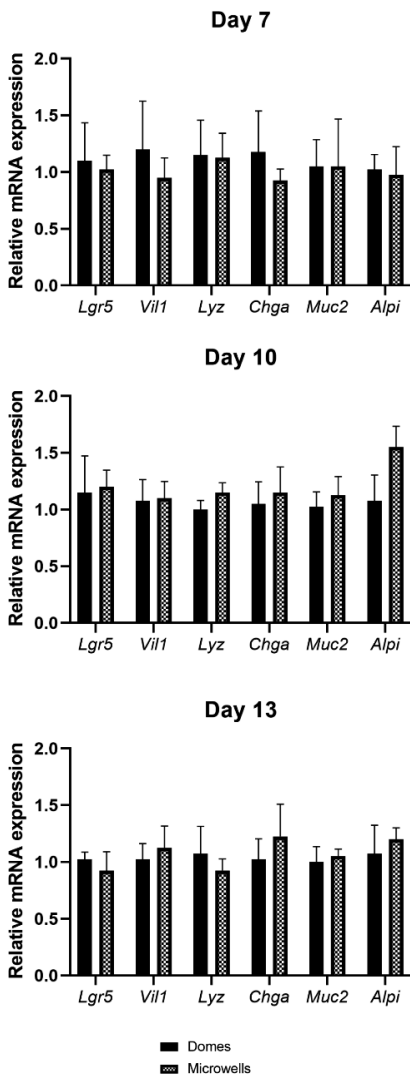


**Figure 6:** Organoids grown in Matrigel domes (black bars) and microwells (white bars) bars showed similar expression levels for proliferation (*Lgr5*) and differentiation markers (*Vill1*, *Lyz*, *Chga*, *Muc2*, *Alpi*) of the intestine at day 7 (top), day 10 (middle) and day 13 (bottom) of culture. Relative mRNA levels of the indicated genes were determined by qPCR and normalized to *Gapdh* and *Hprt* genes. Unpaired Student's t-test with Welch's correction showed no significant differences at all time-points (mean  $\pm$  S.E.M, n=4).

## Conclusion

In this study, we combined organoid technology with micro engineering and achieved an extended (up to 13 days, 86% longer than traditional protocols in Matrigel domes) and more controlled growth of mouse intestinal organoids in microwell arrays. Specifically, we circumvented the complications presented with gel embedding and achieved a more homogeneous culture of intestinal organoids. Indeed, our resulting organoids showed less variability in size compared to Matrigel dome cultures. The use of microwells also provides further advantages in regard to practical applications. Microwells facilitate sample preparation and assessment by imaging. For

example, they allow for easier selection of the organoid imaged simply because the position of the organoid is known and fixed throughout the entire experiment. This feature also helps to simplify organoid tracking throughout the experiment and promotes high-content image acquisition. Furthermore, microwell culturing of organoids facilitates additional experimental manipulations, such as microinjections<sup>[40,52,53]</sup> and co-culturing. Finally, this microwell-based organoid culture platform could be combined with other systems, such as microfluidics for screening applications, where the exchange of tested substances and soluble factors can be performed in a more controlled way, yet without necessarily creating

increased shear stress for the organoids, which are protected inside the microwells. These kinds of systems lay the foundation for even more advanced *in vitro* models in the future.

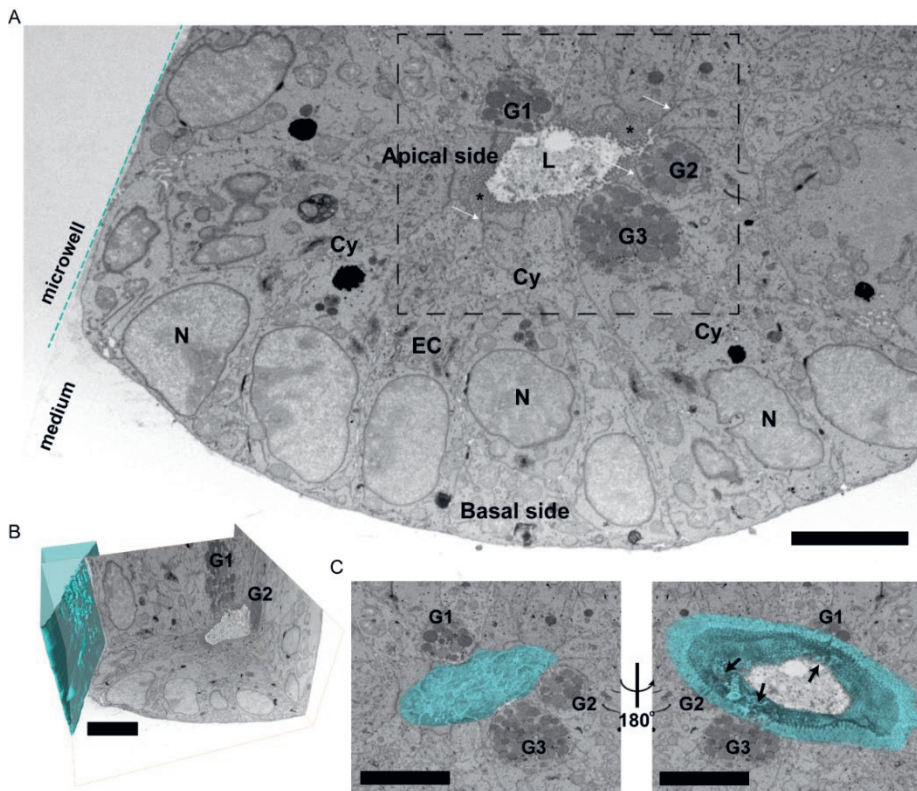


**Figure 7:** FIB-SEM of an organoid grown in a microwell after 10 days in culture showing enterocytes and goblet cells. (A) A slice from the FIB-SEM volume showing the interface between the microwell (indicated by the turquoise dashed line) and the organoid. In the dashed box, the luminal side of the organoid is apparent of which the surface is decorated with villi (asterisks). The G-numbers indicate three goblets cells that surface the lumen. N represents the cell nucleus, EC an enterocyte, Cy the cytosol and the thin white arrows the intercellular junctions. Scale bar represents 10  $\mu\text{m}$ . (B) 3D representation of the microwell and different orthoslices through the FIB-SEM volume. Scale bar represents 10  $\mu\text{m}$ . (C) Cropped detail of the dashed area in (A) with the surface of goblet cell membranes touching the organoid's lumen (blue) as seen from the cytosolic side (left). The same cross-section turned 180 degrees (right) shows the luminal side and the villi (arrows). Scale bars represent 5  $\mu\text{m}$ .

## References

- [1] H. Gehart, H. Clevers, *Nat. Rev. Gastroenterol. Hepatol.* **2019**, *16*, 19.
- [2] H. Clevers, *Cell* **2013**, *154*, 274.
- [3] K. Schneeberger, S. Roth, E. E. S. Nieuwenhuis, S. Middendorp, *Dis. Model.*

*Mech.* **2018**, *11*, dmm031088.

- [4] J. Y. Co, M. Margalef-Català, X. Li, A. T. Mah, C. J. Kuo, D. M. Monack, M. R. Amieva, *Cell Rep.* **2019**, *26*, 2509.
- [5] P. Buske, J. Przybilla, M. Loeffler, N. Sachs, T. Sato, H. Clevers, J. Galle, *FEBS J.* **2012**, *279*, 3475.
- [6] T. E. Wallach, J. R. Bayrer, *J. Pediatr. Gastroenterol. Nutr.* **2017**, *64*, 180.
- [7] A. Wodarz, I. Näthke, *Nat. Cell Biol.* **2007**, *9*, 1016.
- [8] A. C. Fasciano, J. Meccas, R. R. Isberg, *Microbiol. Spectr.* **2019**, *7*, DOI 10.1128/microbiolspec.BAI-0013-2019.
- [9] X. Zhao, M. Pack, *Methods Cell Biol.* **2017**, *138*, 241.
- [10] L. Yin, H. Yang, J. Li, Y. Li, X. Ding, G. Wu, Y. Yin, *Amino Acids* **2017**, *49*, 2099.
- [11] F. Hugenholtz, W. M. de Vos, *Cell. Mol. Life Sci.* **2018**, *75*, 149.
- [12] A. Bein, W. Shin, S. Jalili-Firoozinezhad, M. H. Park, A. Sontheimer-Phelps, A. Tovaglieri, A. Chalkiadaki, H. J. Kim, D. E. Ingber, *Cell. Mol. Gastroenterol. Hepatol.* **2018**, *5*, 659.
- [13] T. Sato, R. G. Vries, H. J. Snippert, M. Van De Wetering, N. Barker, D. E. Stange, J. H. Van Es, A. Abo, P. Kujala, P. J. Peters, H. Clevers, *Nature* **2009**, *459*, 262.
- [14] B. Zhang, A. Korolj, B. F. L. Lai, M. Radisic, *Nat. Rev. Mater.* **2018**, *3*, 257.
- [15] M. Huch, J. A. Knoblich, M. P. Lutolf, A. Martinez-Arias, *Development* **2017**, *144*, 938.
- [16] A. Fatehullah, S. H. Tan, N. Barker, *Nat. Cell Biol.* **2016**, *18*, 246.
- [17] H. Clevers, *Cell* **2016**, *165*, 1586.
- [18] R. Cruz-Acuña, A. J. García, *Exp. Cell Res.* **2019**, *377*, 109.
- [19] Y. Wang, D. B. Gunasekara, P. J. Attayek, M. I. Reed, M. Disalvo, D. L. Nguyen, J. S. Dutton, M. S. Lebhara, S. J. Bultman, C. E. Sims, S. T. Magness, N. L. Allbritton, *ACS Biomater. Sci. Eng.* **2017**, *3*, 2502.
- [20] A. Skardal, T. Shupe, A. Atala, *Drug Discov. Today* **2016**, *21*, 1399.
- [21] B. Ho, N. Pek, B.-S. Soh, *Int. J. Mol. Sci.* **2018**, *19*, 936.
- [22] M. M. Mahe, E. Aihara, M. A. Schumacher, Y. Zavros, M. H. Montrose, M. A. Helmuth, T. Sato, N. F. Shroyer, *Curr. Protoc. Mouse Biol.* **2013**, *3*, 217.
- [23] P. Samal, C. van Blitterswijk, R. Truckenmüller, S. Giselsbrecht, *Adv. Mater.* **2019**, *31*, 1805764.
- [24] J. Laurent, G. Blin, F. Chatelain, V. Vanneaux, A. Fuchs, J. Larghero, M. Théry, *Nat. Biomed. Eng.* **2017**, *1*, 939.
- [25] X. Yin, B. E. Mead, H. Safaei, R. Langer, J. M. Karp, O. Levy, *Cell Stem Cell* **2016**, *18*, 25.

- [26] J. A. Brassard, M. P. Lutolf, *Cell Stem Cell* **2019**, *24*, 860.
- [27] S. E. Park, A. Georgescu, D. Huh, *Science* (80-. ). **2019**, *364*, 960.
- [28] G. Rossi, A. Manfrin, M. P. Lutolf, *Nat. Rev. Genet.* **2018**, *19*, 671.
- [29] M. Viney, A. Bullock, M. Day, S. MacNeil, *Regen. Med.* **2009**, *4*, 397.
- [30] S. Giselbrecht, T. Gietzelt, E. Gottwald, C. Trautmann, R. Truckenmüller, K. F. Weibezahn, A. Welle, *Biomed. Microdevices* **2006**, *8*, 191.
- [31] R. Truckenmüller, S. Giselbrecht, N. Rivron, E. Gottwald, V. Saile, A. Van Den Berg, M. Wessling, C. Van Blitterswijk, *Adv. Mater.* **2011**, *23*, 1311.
- [32] N. Brandenburg, S. Hoehnel, F. Kuttler, K. Homicsko, C. Ceroni, T. Ringel, N. Gjorevski, G. Schwank, G. Coukos, G. Turcatti, M. P. Lutolf, *Nat. Biomed. Eng.* **2020**, *1*.
- [33] R. Cruz-Acuña, M. Quirós, A. E. Farkas, P. H. Dedhia, S. Huang, D. Siuda, V. García-Hernández, A. J. Miller, J. R. Spence, A. Nusrat, A. J. García, *Nat. Cell Biol.* **2017**, *19*, 1326.
- [34] N. Gjorevski, N. Sachs, A. Manfrin, S. Giger, M. E. Bragina, P. Ordóñez-Morán, H. Clevers, M. P. Lutolf, *Nature* **2016**, *539*, 560.
- [35] D. Jun, S. Y. Kim, J. C. Na, H. H. Lee, J. Kim, Y. E. Yoon, S. J. Hong, W. K. Han, *PLoS One* **2018**, *13*, e0206447.
- [36] F. Lee, C. Iliescu, F. Yu, H. Yu, *Constrained Spheroids/Organoids in Perfusion Culture*, Elsevier Inc., **2018**.
- [37] I. A. Okkelman, T. Foley, D. B. Papkovsky, R. I. Dmitriev, *Biomaterials* **2017**, *146*, 86.
- [38] S. M. Czerniecki, N. M. Cruz, J. L. Harder, R. Menon, J. Annis, E. A. Otto, R. E. Gulieva, L. V. Islas, Y. K. Kim, L. M. Tran, T. J. Martins, J. W. Pippin, H. Fu, M. Kretzler, S. J. Shankland, J. Himmelfarb, R. T. Moon, N. Paragas, B. S. Freedman, *Cell Stem Cell* **2018**, *22*, 929.
- [39] S. V. Kumar, P. X. Er, K. T. Lawlor, A. Motazedian, M. Scurr, I. Ghobrial, A. N. Combes, L. Zappia, A. Oshlack, E. G. Stanley, M. H. Little, *Dev.* **2019**, *146*, DOI 10.1242/dev.172361.
- [40] D. B. Gunasekara, M. DiSalvo, Y. Wang, D. L. Nguyen, M. I. Reed, J. Speer, C. E. Sims, S. T. Magness, N. L. Allbritton, *Anal. Chem.* **2018**, *90*, 1941.
- [41] A. D. Gracz, I. A. Williamson, K. C. Roche, M. J. Johnston, F. Wang, Y. Wang, P. J. Attayek, J. Balowski, X. F. Liu, R. J. Laurenza, L. T. Gaynor, C. E. Sims, J. A. Galanko, L. Li, N. L. Allbritton, S. T. Magness, *Nat. Cell Biol.* **2015**, *17*, 340.
- [42] Y. Takahashi, S. Sato, Y. Kurashima, T. Yamamoto, S. Kurokawa, Y. Yuki, N. Takemura, S. Uematsu, C. Y. Lai, M. Otsu, H. Matsuno, H. Osawa, T. Mizushima, J. Nishimura, M. Hayashi, T. Yamaguchi, H. Kiyono, *Stem Cell Reports* **2018**, *10*, 314.

- [43] C. W. Tan, Y. Hirokawa, A. W. Burgess, *Sci. Rep.* **2015**, *5*, 1.
- [44] S. Miura, A. Suzuki, *Cell Stem Cell* **2017**, *21*, 456.
- [45] T. Sato, H. Clevers, *Science* **2013**, *340*, 1190.
- [46] M. R. Schneider, M. Dahlhoff, D. Horst, B. Hirschi, K. Trülsch, J. Müller-Höcker, R. Vogelmann, M. Allgäuer, M. Gerhard, S. Steininger, E. Wolf, F. T. Kolligs, *PLoS One* **2010**, *5*, e14325.
- [47] A. Fatehullah, P. L. Appleton, I. S. Näthke, *Philos. Trans. R. Soc. B Biol. Sci.* **2013**, *368*, DOI 10.1098/rstb.2013.0014.
- [48] J. M. Williams, C. A. Duckworth, M. D. Burkitt, A. J. M. Watson, B. J. Campbell, D. M. Pritchard, *Vet. Pathol.* **2015**, *52*, 445.
- [49] T. Sato, J. H. van Es, H. J. Snippert, D. E. Stange, R. G. Vries, M. van den Born, N. Barker, N. F. Shroyer, M. van de Wetering, H. Clevers, *Nature* **2011**, *469*, 415.
- [50] P. Buske, J. Galle, N. Barker, G. Aust, H. Clevers, M. Loeffler, *PLoS Comput. Biol.* **2011**, *7*, e1001045.
- [51] J. R. Spence, C. N. Mayhew, S. A. Rankin, M. F. Kuhar, J. E. Vallance, K. Tolle, E. E. Hoskins, V. V. Kalinichenko, S. I. Wells, A. M. Zorn, N. F. Shroyer, J. M. Wells, *Nature* **2011**, *470*, 105.
- [52] E. Coudrier, M. Arpin, B. Dudouet, J. Finidori, A. Garcia, C. Huet, E. Pringault, S. Robine, C. Sahuquillo-Merino, D. Louvard, *Protoplasma* **1988**, *145*, 99.
- [53] K. Narayan, S. Subramaniam, *Nat. Methods* **2015**, *12*, 1021.
- [54] N. Sachs, Y. Tsukamoto, P. Kujala, P. J. Peters, H. Clevers, *Dev.* **2017**, *144*, 1107.
- [55] N. Barker, J. H. Van Es, J. Kuipers, P. Kujala, M. Van Den Born, M. Cozijnsen, A. Haegebarth, J. Korving, H. Begthel, P. J. Peters, H. Clevers, *Nature* **2007**, *449*, 1003.
- [56] C. S. Xu, K. J. Hayworth, Z. Lu, P. Grob, A. M. Hassan, J. G. García-Cerdán, K. K. Niyogi, E. Nogales, R. J. Weinberg, H. F. Hess, *Elife* **2017**, *6*, DOI 10.7554/eLife.25916.
- [57] C. Bosch, A. Martínez, N. Masachs, C. M. Teixeira, I. Feraud, F. Ulloa, E. Pérez-Martínez, C. Lois, J. X. Comella, J. DeFelipe, A. Merchán-Pérez, E. Soriano, *Front. Neuroanat.* **2015**, *9*, 60.
- [58] C. Villinger, H. Gregorius, C. Kranz, K. Höhn, C. Münzberg, G. Wichert, B. Mizaikoff, G. Wanner, P. Walther, *Histochem. Cell Biol.* **2012**, *138*, 549.

## Supporting Information

### Supplementary figures

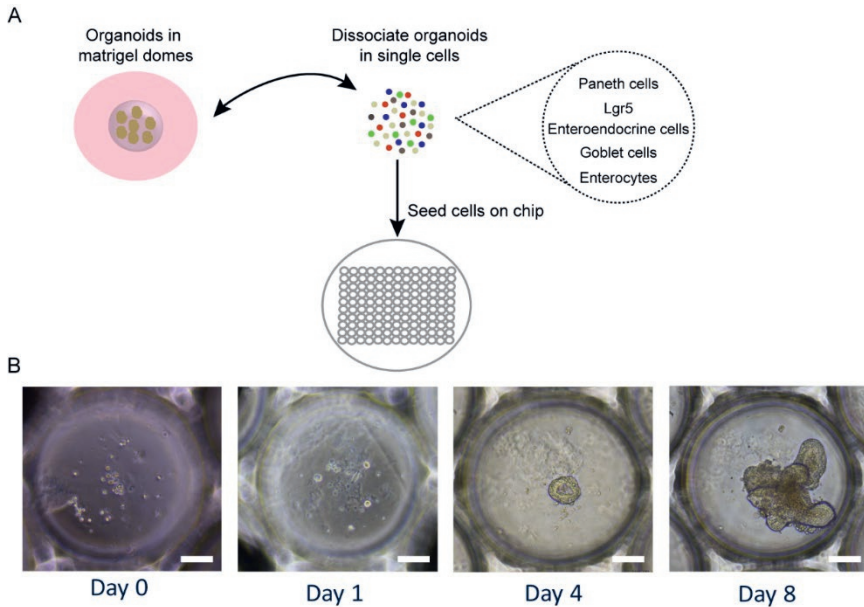


**Figure S1:** Single cell seeding in microwell arrays. (A) Schematic of the seeding procedure in microwells. (B) Bright-field images showing the development of an organoid from single cells over a period of 8 days. Scale bars represent 100  $\mu\text{m}$ .

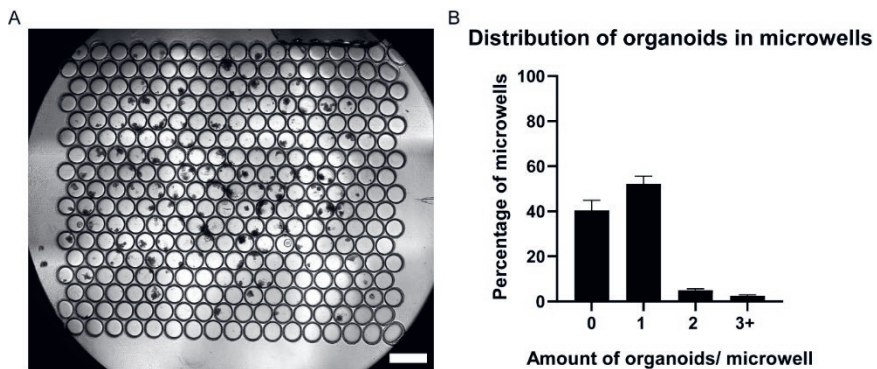


**Figure S2:** Distribution of organoids in microwell arrays. (A) Bright-field image showing organoids cultured in a microwell array for 4 days. Scale bar represent 1 mm. (B) Percentage of microwells containing zero, one, two and three or more organoids. The quantification was performed on day 4, following passaging of organoids with a dilution of 1:2 (one Matrigel dome into two microwell arrays) (mean  $\pm$  S.E.M, n=3).

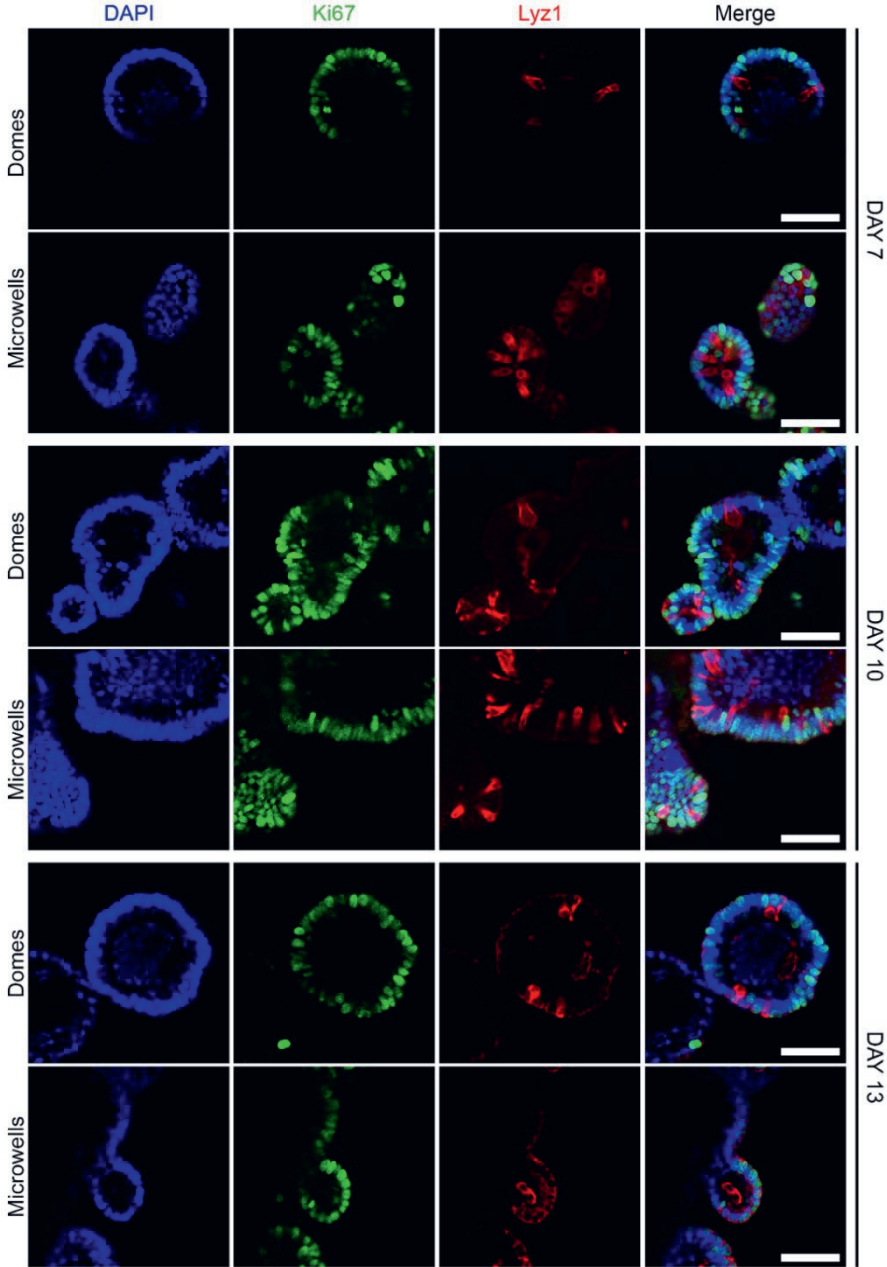


**Figure S3:** Organoids in microwells express intestine-specific markers for proliferative and Paneth cells. Confocal microscopy of organoids on day 7 (top two rows), day 10 (middle two rows), and day 13 (bottom two rows). At each time-point, the top row represents organoids grown in Matrigel domes and the bottom row organoids grown in microwells. Ki67 (green) demonstrates the presence of proliferative cells and lysozyme (red) the Paneth cells. In all panels, DAPI counterstain (blue) indicates cell nucleus. All images represent a single z stack slice. Scale bars represent 100  $\mu\text{m}$ .



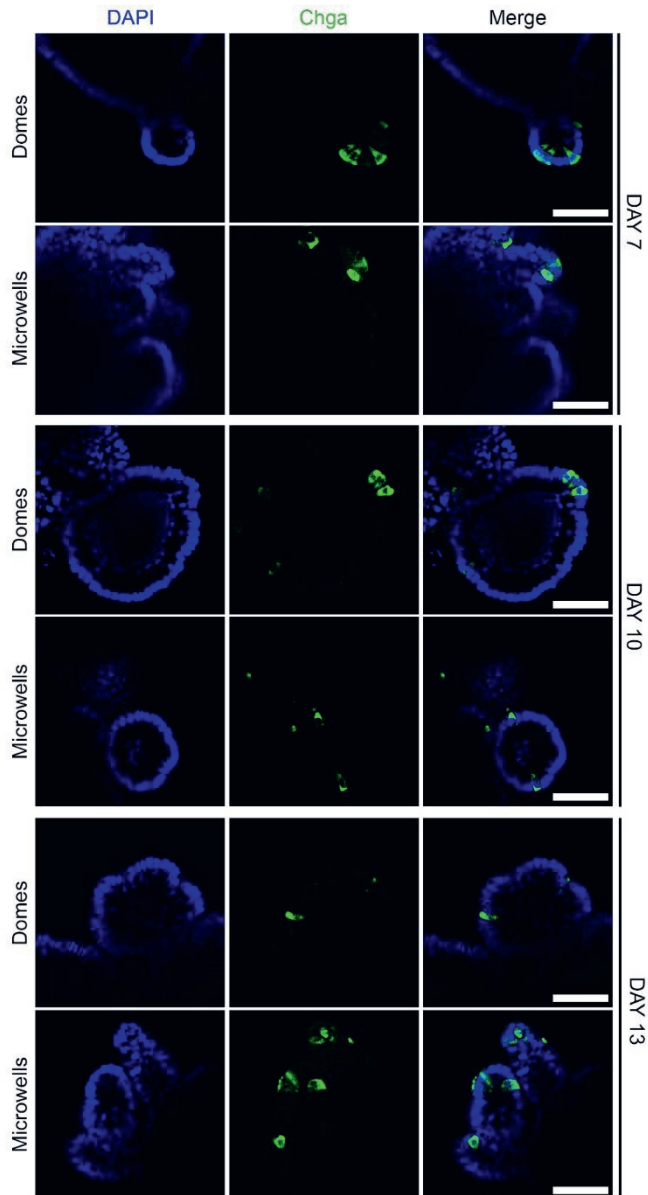


**Figure S4:** Organoids in microwells express intestine-specific markers for enteroendocrine cells. Confocal microscopy of organoids on day 7 (top two rows), day 10 (middle two rows), and day 13 (bottom two rows). At each time-point, the top row represents organoids grown in Matrigel domes and the bottom row organoids grown in microwells. Chromogranin (green) demonstrates the presence of enteroendocrine cells. In all panels, DAPI counterstain (blue) indicates cell nucleus. All images represent a single z stack slice. Scale bars represent 100  $\mu\text{m}$ .



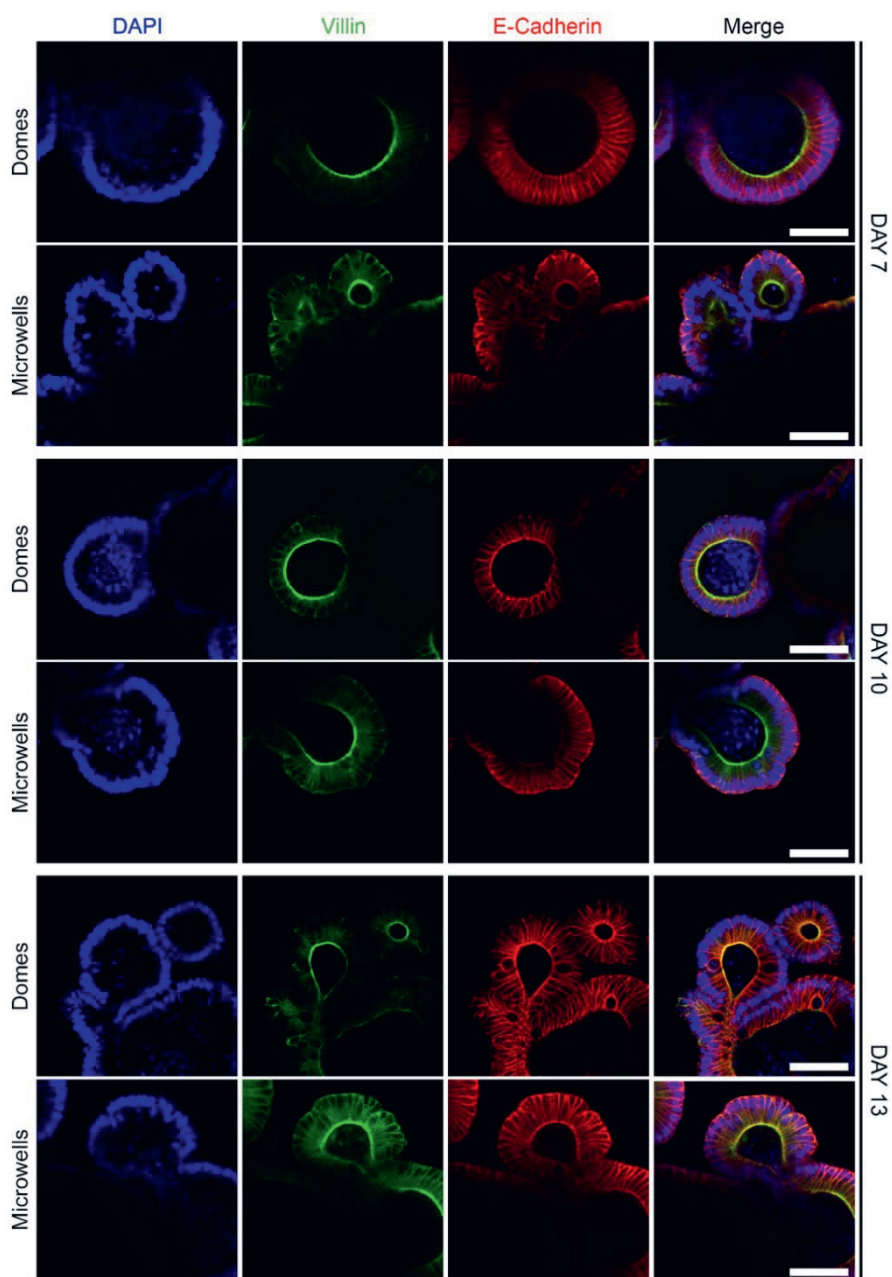


**Figure S5:** Organoids in microwells express intestine-specific markers for enterocytes. Confocal microscopy of organoids on day 7 (top two rows), day 10 (middle two rows), and day 13 (bottom two rows). At each time-point, the top row represents organoids grown in Matrigel domes and the bottom row organoids grown in microwells. Villin (green) marks the apical side of enterocytes, and E-Cadherin (red) the basolateral side. In all panels, DAPI counterstain (blue) indicates cell nucleus. All images represent a single z stack slice. Scale bars represent 100 μm.

Supplementary tables**Supplementary table 1.** List of antibodies

Antibodies	Supplier	Dilution	Catalog #	References
Ki67	MONOSAN Xtra	1:250	MONX10283	[1]
Chga	Santa Cruz	1:200	sc-393941	[2,3]
Villin	Santa Cruz	1:200	sc-58897	[3]
Lyz1	Agilent	1:1000	A009902-2	[2]
E-Cadherin	Life technologies	1:250	14-3249-82	N/A
Phalloidin	ThermoFisher	1:100	A12379	N/A
DAPI	Sigma-Aldrich	1.0 µg/mL	32670-5MG-F	[4]
Alexa Fluor 647	Invitrogen	1:500	A21247	N/A
Alexa Fluor 488	Invitrogen	1:500	A-11001	N/A
Alexa Fluor 647	Invitrogen	1:500	A-21245	N/A
Alexa Fluor 568	Invitrogen	1:500	A-11031	N/A

**Supplementary table 2.** List of primers used for qPCR

Gene	Forward primer	Reverse primer
<i>Lgr5</i>	ACATTCCCAAGGGAGCGTTC	ATGTGGTTGGCATCTAGGCG
<i>Vill</i>	TCAAAGGCTCTCTCAACATCAC	AGCAGTCACCATCGAAGAAGC
<i>Muc2</i>	ATGCCACCTCCTCAAAGAC	GTAGTTTCCGTTGGAACAGTGAA
<i>Lyz1</i>	GAGACCGAAGCACCGACTATG	CGGTTTTGACATTGTGTTTCGC
<i>Chga</i>	CCAAGGTGATGAAGTGCGTC	GGTGTTCGCAGGATAGAGAGGA
<i>Alpi</i>	AGGACATCGCCACTCAACTC	GGTTCAGACTGGTTACTGTCA
<i>Gapdh</i>	TGGCCTTCCGTGTTCTTAC	GAGTTGCTGTTGAAGTCGCA
<i>Hprt</i>	TCAGTCAACGGGGACATAAA	GGGGCTGTACTGCTTAACCAG

Supplementary movies

**Movie S1:** Time-lapse imaging of intestinal organoids growing in microwells. The starting point is day 2 post- seeding. Single plane images were taken every 60 minutes for 4 days.

**Movie S2:** Confocal stack of intestinal organoid grown inside a microwell for 10 days and stained for E-Cadherin (red) and Phalloidin (green).

**Movie S3:** Confocal stack of intestinal organoid grown embedded in Matrigel for 10 days and stained for E-Cadherin (red) and Phalloidin (green).

**Movie S4:** FIB-SEM stack of intestinal organoid cultured inside a microwell for 10 days.

**References**

- [1] N. Sachs, Y. Tsukamoto, P. Kujala, P.J. Peters, H. Clevers, *Development*. **2017**, 144
- [2] C.A. Thorne, I.W. Chen, L.E. Sanman, M.H. Cobb, L.F. Wu, S.J. Altschuler, *Developmental Cell*. **2018**, 44
- [3] M. Nam, S. Hahn, J. Jee, T. Hwang, H. Yoon, L.D. Hyeon, M. Kwon, J. Yoo, *Oncotarget*. **2017**, 9
- [4] T. Zietek, E. Rath, D. Haller, H. Daniel, *Scientific Reports* 2015, 5, DOI 10.1038/srep16831.








## CHAPTER IV

# **A MICROWELL-BASED INTESTINAL ORGANOID- MACROPHAGE CO-CULTURE SYSTEM TO STUDY INTESTINAL INFLAMMATION**

Panagiota Kakni, Roman Truckenmüller,  
Pamela Habibović, Martijn van  
Griensven and Stefan Giselbrecht

*Int. J. Mol. Sci.*  
23(23): 15364 (2022)



## **Abstract**

The mammalian intestinal epithelium contains more immune cells than any other tissue, and this is largely because of its constant exposure to pathogens. Macrophages are crucial for maintaining intestinal homeostasis, but they also play a central role in chronic pathologies of the digestive system. We have developed a versatile microwell-based intestinal organoid-macrophage co-culture system that enables us to recapitulate features of intestinal inflammation. This microwell-based platform facilitates the controlled positioning of cells in different configurations, continuous *in situ* monitoring of cell interactions and high-throughput downstream applications. Using this novel system, we compared the inflammatory response when intestinal organoids were co-cultured with macrophages versus when intestinal organoids were treated with the pro-inflammatory cytokine TNF- $\alpha$ . Furthermore, we demonstrated that the tissue-specific response differs according to the physical distance between the organoids and the macrophages and that the intestinal organoids show an immunomodulatory competence. Our novel microwell-based intestinal organoid model incorporating acellular and cellular components of the immune system can pave the way to unravel unknown mechanisms related to intestinal homeostasis and disorders.

## **Introduction**

The intestine comprises the largest compartment of the immune system, due to its continuous exposure to foreign antigens[1]. Immunological processes mainly take place in the mucosa that consists of the epithelium, the lamina propria and the muscularis mucosa. The crosstalk between immune cells and intestinal epithelial cells is important for gut homeostasis and alterations can result in inflammatory diseases, such as inflammatory bowel disease (IBD), which is a group of chronic inflammatory diseases of the digestive tract. This term is used to describe both ulcerative colitis and Crohn's disease, among others[2]. The pathogenesis of IBD involves a complex interplay among genetic, epigenetic, immunological and microbiological factors, and epithelial barrier dysfunction[2,3]. A lot of interest has been shifted towards the role of the immune system in the pathogenesis of IBD. In this disease, increased infiltration of inflammatory cells into the lamina propria and submucosa of the intestine is observed, accompanied by an increased expression of pro-inflammatory cytokines, such as interleukin-1 beta (IL-1 $\beta$ ) and tumor necrosis factor alpha (TNF- $\alpha$ ). These observations have led to the development of clinical immunomodulatory therapies, such as the treatment with infliximab. This is a

monoclonal antibody that binds with high affinity to TNF- $\alpha$  and neutralizes its biological activity, thus reducing inflammation[4,5]. However, patients often do not respond to such treatments. Thus, it is imperative to gain a better insight into the involvement of epithelial and other factors related to the pathogenesis of IBD[3]. Although mouse models have provided invaluable information over the years, they mostly focus on one aspect of IBD and they cannot fully recapitulate the complexity of human diseases[6,7]. Hence, establishing *in vitro* models that mimic both the epithelial and immune compartments is necessary to develop more effective therapies[8].

Intestinal organoids are self-organizing, three-dimensional (3D) mini-organs that can be derived from stem cells and recapitulate multiple features of the *in vivo* intestine[9,10]. Specifically, they have a multicellular composition, they are organized into crypt-villus structures and they are able to perform intestine-specific functions such as barrier formation and nutrient uptake[11]. Organoids recapitulate intestinal properties much closer than 2D monolayer systems (e.g., using Caco-2 cells) and allow for in-depth analysis of pathogen-host interactions and investigation of mechanisms related to development and disease. However, organoid systems usually lack immune system components, thus their applicability for investigating the mechanisms underlying certain diseases and disease modelling is limited[12].

In this study, we aimed to establish an intestinal organoid model to study the interactions of the epithelium with immune cells and to recapitulate aspects of intestinal inflammation. Hence, we developed a microwell-based co-culture system of mouse intestinal organoids and RAW 264.7 macrophages. This microwell-based co-culture system is highly versatile and facilitates the controlled positioning of different cell types in multiple configurations, the continuous monitoring of cell interactions during co-culture and high-throughput downstream applications. Additionally, there is no viscous and ill-defined hydrogel matrix (e.g. basement membrane extracts) that could interfere with or slow down the contact or interactions between the cells. Intestinal macrophages play a crucial role in intestinal immunity and homeostasis, but also in the development of intestinal inflammation[13,14]. When pathogens invade the intestinal epithelium, immune cells, mainly macrophages, get activated and they release a series of pro-inflammatory cytokines, such as TNF- $\alpha$ , IL1, and IL6[14]. Cytokines can affect the epithelium both positively and negatively. They can induce or restrict cell proliferation or cell death and also alter the barrier permeability[15]. For example, cytokines mediate mucosal healing



by controlling the epithelial cell activation, differentiation, survival, and migration[16]. However, aberrant and excessive secretion of those factors leads to chronic inflammation, a typical feature of IBD.

Using our microwell-based organoid culture model[17], we established a direct and an indirect co-culture system of mouse intestinal organoids with RAW 264.7 cells and compared the effects with TNF- $\alpha$  treatment, which is known to be the first cytokine secreted in the inflammation cascade[18]. We studied the effects of different numbers of macrophages on the intestinal organoids and compared it with organoids treated with different concentrations of TNF- $\alpha$ . We also showed that there are prominent differences when placing the macrophages in close proximity to the organoids, by comparing the direct (juxtacrine and paracrine signalling) with the indirect co-culture system (paracrine signalling). A quantification of a subpanel of cytokines, which are likely involved in the interactions between the intestinal epithelium and macrophages, was performed to identify other key players next to TNF- $\alpha$ . These experiments also revealed that organoids have an innate immunomodulatory function upon exposure to inflammatory cytokines.

## **Materials & Methods**

### Fabrication and preparation of microwells for organoid culture

Microwell arrays were fabricated using microthermoforming as previously described<sup>15,17</sup>. Briefly, 50  $\mu\text{m}$ -thin polycarbonate films were used to create arrays of 289 microwells. Morphometric characterization was performed using a confocal laser scanning microscope (Keyence 3D Laser Scanning Microscope VK-X250K) and the corresponding analysis software (Keyence MultiFileAnalyzer). Each microwell had a diameter of 500  $\mu\text{m}$  and a depth of  $\sim$ 300  $\mu\text{m}$ . For the indirect co-culture experiments, porous membranes with the same dimensions were used. The pore size was 0.8  $\mu\text{m}$  and the pore density was 1E06. Prior to cell culture, microwell arrays were punched to the size of a well of a 24-well plate and pre-wetted and sterilized in a graded series of 2-isopropanol (100%, 70%, 50%, 25%, 10%; VWR). Subsequently, they were washed twice in Dulbecco's phosphate buffered saline (PBS; Sigma-Aldrich) and placed at the bottom of non-tissue culture-treated 24-well plates, where there were kept in place by elastomeric O-rings (ERIKS).

### Intestinal organoid culture

Mouse intestinal organoids derived from the small intestine of C57BL/6 mice were purchased as cryopreserved fragments (STEMCELL Technologies). Organoids were

cultured embedded in Matrigel domes, as previously described<sup>7</sup> with minor modifications. Briefly, a 50:50 mixture of IntestiCult Organoid Growth Medium (STEMCELL Technologies) and Matrigel (Corning) containing organoids was placed dropwise in tissue culture-treated 24-well plates. After polymerization at 37 °C and 5% CO<sub>2</sub> for 10 min, Matrigel domes were covered with 650 µL of IntestiCult. Medium was refreshed every 2 days. Passaging of the organoids was performed every 5–7 days using Gentle Cell Dissociation Reagent (GCDR; STEMCELL Technologies).

To seed the organoid fragments in the microwells, following the organoid dissociation process, fragments were resuspended in IntestiCult medium supplemented with 2% Matrigel. Then, 50 µL of this mixture was added onto the microwell arrays, and fragments were let to settle for 2 h by gravity, before adding more medium.

#### Macrophage culture

The murine macrophage cell line RAW 264.7 was purchased from ECACC. Cells were cultured in Dulbecco's Modified Eagle Medium (DMEM; Gibco) supplemented with 10% fetal bovine serum (FBS; Sigma-Aldrich) and passaged every 3-4 days upon reaching confluence. The maximum passage number of the cells used in this study was 15.

#### Co-culture of intestinal organoids and macrophages

To perform direct co-culture, initially RAW 264.7 cells were seeded into the microwells. After centrifugation to accelerate the inoculation of the cells into the microwells, organoid fragments were added to the culture. The system was placed at 37 °C and 5% CO<sub>2</sub> for 2 h, so that the organoids settle into the microwells as well, and afterwards more organoid medium was added. Different concentrations of RAW 264.7 cells were tested, ranging from 12,500 cells/well to 100,000 cells/well.

To perform indirect co-culture, RAW 264.7 cells were initially seeded at the bottom of tissue culture-treated 24-well plate. Similar to the direct co-culture, different concentrations of RAW 264.7 cells were tested (12,500, 25,000, 50,000 and 100,000). Following that, a porous microwell array was placed in the same well, and organoid fragments were seeded into the microwells. To avoid contact of the microwell array with the macrophages, an O-ring was placed underneath the microwell array.

### Immunofluorescence and confocal microscopy

Initially, organoids and cells were fixed with 4% paraformaldehyde (VWR) in PBS. Next, permeabilization was performed with 0.5% Triton X-100 (Merck) in PBS for 30 min at room temperature (RT). For blocking, cells/organoids were incubated with 5% donkey serum (VWR) in permeabilization solution for 30 min at RT. Afterwards, primary antibodies against Lysozyme (Lyz1; Agilent), Ki67 (Abcam), CD11b (Abcam) and F4/80 (Abcam) diluted in blocking buffer were added and incubated overnight at 4 °C. The following day, the secondary antibodies and when applicable phalloidin (ThermoFisher), were incubated for 2 h at RT. Finally, samples were counterstained with 4',6-diamidino-2-phenylindole (DAPI; Sigma-Aldrich) and mounted using Dako Fluorescence Mounting Medium (Agilent). All stained samples were imaged using a TCS SP8 confocal laser scanning microscope (Leica) and processed with ImageJ.

### Enzyme-linked immunosorbent assay (ELISA)

The intestinal organoid medium was collected following the direct co-culture of organoids with RAW 264.7 cells (12,500, 25,000, 50,000, and 100,000 cells) or the addition of TNF- $\alpha$  (16, 32, 64, and 128 ng/mL) over three time-points (days 2, 4, and 5). The amount of TNF- $\alpha$  protein was measured with ELISA (R&D Systems) according to the manufacturer's instructions. Absorbance was measured at 450 nm using a CLARIOstar plate reader (BMG LABTECH).

### Luminex assay

The intestinal organoid medium was collected following the direct and indirect co-culture of organoids with RAW 264.7 cells or the addition of TNF- $\alpha$  and subsequent treatments (removal of TNF- $\alpha$  and/or removal of RAW 264.7 cells) over three time-points (days 2, 4, and 5). The amounts of cytokines were detected by the Bio-Plex Pro Mouse Cytokine 23-plex Assay, according to the manufacturer's guidelines. Fluorescence intensity was measured using a Luminex 100 Bio-Plex Liquid Array Multiplexing System (Bio-Rad).

### Scanning electron microscopy (SEM)

Microwell arrays were mounted on SEM stubs, sputter-coated with a thin layer of gold using a SC7620 Mini Sputter Coater (Quorum Technologies) and finally examined using a JSM-IT200 electron microscope (Jeol).

### Forskolin assay

Intestinal organoids cultured alone, treated with TNF- $\alpha$  and co-cultured with RAW 264.7 macrophages were treated with 5  $\mu$ M Forskolin and directly analyzed by live cell microscopy (Nikon Inverted Research Microscope ECLIPSE Ti).

### Statistical analysis

Statistical analysis was performed using Prism 9 software (GraphPad). Two-way ANOVA followed by Tukey's test were used to determine statistical significance. Significant differences were defined as  $P < 0.05$ . P values of statistical significance are represented as \*\*\*\*, \*\*\*, \*\* and \* for  $P < 0.0001$ ,  $P < 0.001$ ,  $P < 0.01$  and  $P < 0.05$ , respectively.

## **Results**

### Monocultures of intestinal organoids and RAW 264.7 macrophages in microwell arrays

Following microthermoforming, we performed characterization of the microwells. We verified that each microwell had a diameter of 500  $\mu$ m and a depth of approximately 300  $\mu$ m (Figure 1A). Our group has previously shown that these dimensions are appropriate for the culture of intestinal organoids[17]. Thus, we decided to use microwells with the same size to further advance this microwell-based organoid model by incorporating immune cells.

Prior to co-culture experiments, we assessed the efficiency of monocultures of organoids and macrophages. Our group has previously established a method to culture intestinal organoids in polymer film-based microwell arrays[17]. Here, we further improved this method by reducing the amount of Matrigel supplemented in the medium from 5% to 2%. This can be beneficial for the sequential seeding of different cells, where a medium with lower viscosity is superior to a medium with higher viscosity. After 5 days in culture, organoids demonstrated a crypt-villus architecture (Figure 1B), which is consistent with the architecture of organoids embedded in Matrigel[9] and the ones grown in microwells with 5% Matrigel[17]. Immunofluorescence stainings indicated that organoids maintained intestinal phenotypic characteristics as well (Figure 1C). Specifically, expression of phalloidin, which marks the F-actin located at the apical side of the epithelium, was identified at the inner surface of the organoids facing the organoid lumen[17]. Paneth cells, marked by lysozyme, were found adjacent to the proliferating cells (marked by

Ki67) as suggested by their protective role[19]. Collectively, these results indicate that intestinal organoids can be successfully cultured in microwell arrays with reduced amounts of Matrigel.

Following that, we cultured RAW 264.7 cells (50,000 cells/well) in microwells using IntestiCult medium. This was done to evaluate whether these macrophages survive in the organoid medium and maintain their phenotype. Bright-field images showed that RAW 264.7 macrophages attached to the inner surface of the microwells and maintained their normal cell morphology (Figure 1B). Immunofluorescence stainings demonstrated that these cells expressed the typical macrophage markers CD11b and F4/80, thus indicating that they maintain the macrophage phenotype (Figure 1D). Overall, these data confirm that RAW 264.7 cells can be efficiently cultured in microwell arrays, even in organoid medium.

#### Direct co-culture of intestinal organoids and RAW 264.7 macrophages in comparison with TNF- $\alpha$ treatment of intestinal organoid monocultures

The intestine *in vivo* is constantly exposed to foreign antigens, hence it accommodates the largest compartment of the immune system[20]. Macrophages play a crucial role in the maintenance of intestinal homeostasis and they provide a first line of innate immune defense. They are located under the epithelial monolayer, an ideal position to identify and eradicate any pathogen that crossed the epithelium[20]. When a pathogenic event occurs, apart from the tissue resident macrophages, additional macrophages infiltrate the intestinal mucosa and release cytokines[14]. However, when excessive secretion of cytokines persists, it leads to chronic inflammation, which is a characteristic of IBD. To create an *in vitro* model that mimics features of the intestinal inflammation, we developed here a 3D co-culture system in microwell arrays, in which mouse intestinal organoids are co-cultured in very close proximity and even in direct contact with the murine macrophage cell line RAW 264.7 (Figure 2A, Supplementary figure 1 and Supplementary video 1). In this co-culture system, there are both juxtacrine and paracrine cell signaling and it will be referred to as ‘direct co-culture’ (Supplementary table 1).

A microwell-based intestinal organoid-macrophage co-culture system to study intestinal inflammation

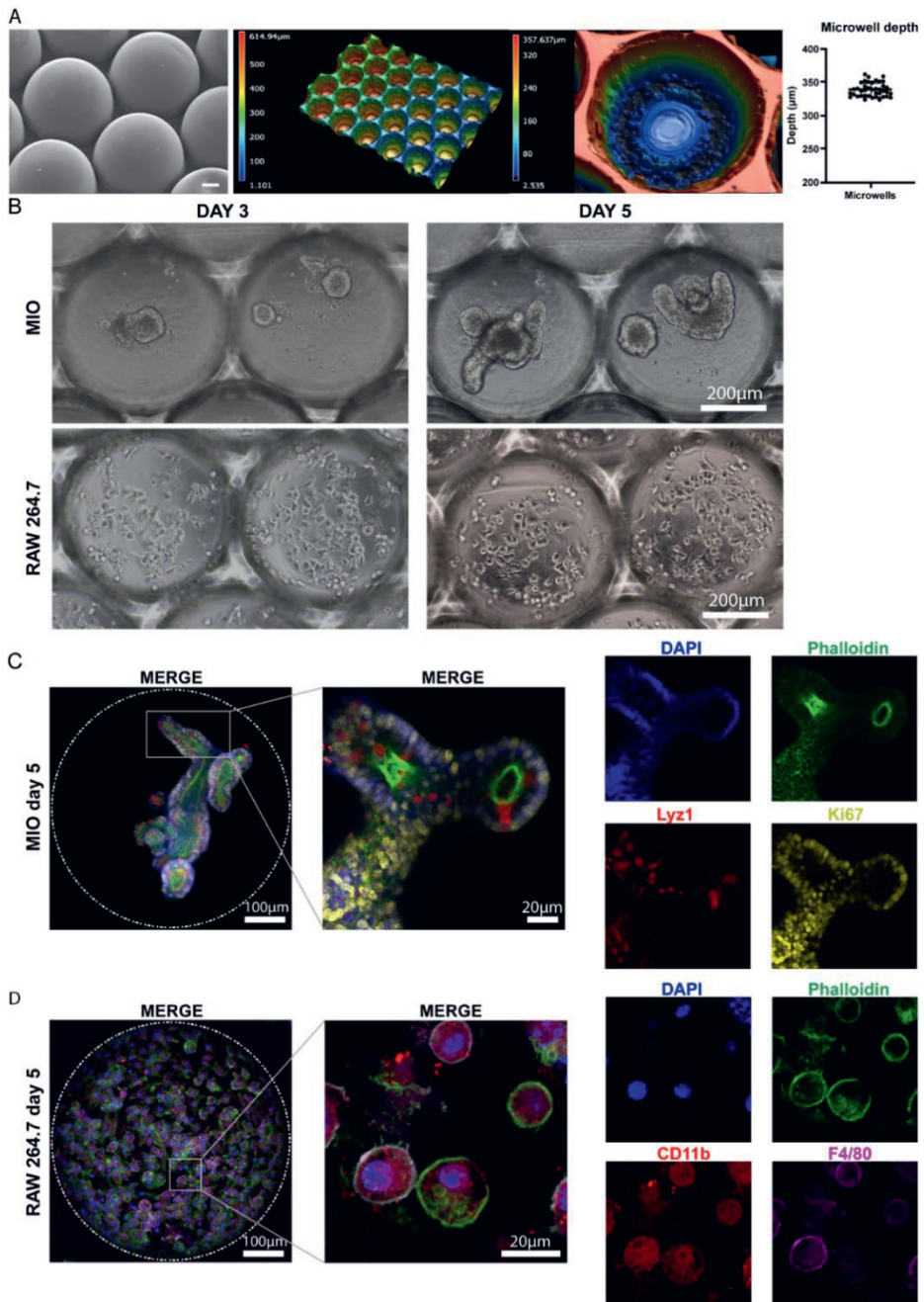


**Figure 1:** Monocultures of organoids (MIO) and RAW 264.7 cells in microwells. (A) Characterization of the thermoformed microwell arrays was performed using SEM and confocal laser scanning microscopy. The graph indicates the depth of the microwells. Data are presented as the mean  $\pm$  SEM. (n = 4). Scale bar represents 100  $\mu$ m. (B) Bright-field images demonstrating the growth of the organoids

(top) and macrophages (bottom) over a period of 5 days. (C) Immunofluorescence stainings of intestinal organoids grown in microwells for the F-actin marker phalloidin (green), the Paneth cell marker Lyz1 (red) and the proliferation marker Ki67 (yellow). Dashed circle represents the circumference of the microwells. The white square represents the area magnified in the respective column to the right. (D) Immunofluorescence stainings of RAW 264.7 cells grown in microwells for phalloidin (green) and the macrophage markers CD11b (red) and F4/80 (magenta). Dashed circle represents the circumference of the microwells. The white square represents the area magnified in the respective column to the right. Abbreviation: MIO, mouse intestinal organoid; DAPI, 4',6-diamidino-2-phenylindole.

Upon direct co-culture of organoids with different amounts of macrophages, we observed changes in organoids' morphology (Figure 2B). Specifically, organoids gradually lost their crypt-villus architecture and turned to spherical structures. Bright-field imaging with subsequent quantification showed that increasing numbers of RAW 264.7 cells had a faster and more prominent effect on the change of the organoid morphology from a crypt-villus to a more spherical shape (Figure 2C). One of the mechanisms mediating these morphological changes is the release of TNF- $\alpha$  from the macrophages[21–23]. TNF- $\alpha$  is a pro-inflammatory cytokine that affects the intestinal epithelial permeability by loosening the junctions between cells and hence it has been associated with diarrhea during inflammation[24–26]. To investigate further whether the change in organoid morphology is solely induced by TNF- $\alpha$ , we treated the organoids in a monoculture with TNF- $\alpha$  and evaluated their morphology over a period of 5 days (Figure 2D). Different concentrations of TNF- $\alpha$  were added to the organoid medium, ranging from 16 ng/mL to 128 ng/mL (Figure 2E). According to Hahn et al. 2017, treatment of organoids with less than 16 ng/mL TNF- $\alpha$  resulted in a less prominent effect on organoid morphology[21], thus we chose 16 ng/mL as a starting point. Similar to the increasing amounts of RAW 264.7 cells, higher concentrations of TNF- $\alpha$  had a more rapid and stronger effect on the organoids (Figure 2F). Specifically, with lower doses of TNF- $\alpha$ , some organoids retained their crypt-villus morphology and did not become spherical, whereas with higher doses, all of them became spherical after 5 days. However, when compared to the direct co-culture of organoids with macrophages, the effect of the added TNF- $\alpha$  on organoid morphology was less pronounced.

To test the functionality of the TNF- $\alpha$  treated organoids and the organoids co-cultured with RAW 264.7 cells, we performed a proof-of-concept Forskolin assay. This is a standard assay for the quantification of the Cystic Fibrosis Transmembrane Conductance Regulator (CFTR) function[27]. It has been reported that TNF- $\alpha$  affects the CFTR function by stimulating CFTR-mediated fluid secretion

[28]. We identified differences in the swelling of organoids among organoids cultured alone, organoids treated with TNF- $\alpha$  and organoids co-cultured with RAW 264.7 macrophages (Supplementary figure 2). Interestingly, in the last case organoids did not seem to swell upon treatment with Forskolin. Future studies are required to shed more light on the mechanisms underlying these differences. The use of microwells can facilitate the performance of such tests in a high-throughput manner.

#### TNF- $\alpha$ -induces changes in organoid morphology

To explore further the role of TNF- $\alpha$  on the morphological change of the organoids, we tested the removal of TNF- $\alpha$  from the culture and the addition of a TNF- $\alpha$  neutralizing antibody. We hypothesized that if the changes in the organoid morphology were solely dependent on TNF- $\alpha$ , neutralizing or completely removing TNF- $\alpha$  from the culture would allow organoids to rescue their crypt-villus morphology. Prior to testing this hypothesis, we aimed to determine the amount of TNF- $\alpha$  concentration in the organoid medium upon the co-culture of organoids with RAW 264.7 macrophages and the addition of TNF- $\alpha$  (Figure 3A). Similar concentrations of TNF- $\alpha$  were identified between RAW 264.7 cells cultured alone or in combination with organoids. Additionally, increasing numbers of RAW 264.7 cells increased the amounts of secreted TNF- $\alpha$  but not to a great extent. However, this was not the case for the added TNF- $\alpha$ , where higher amounts of added TNF- $\alpha$  resulted in substantially higher protein concentration. Noteworthy, the TNF- $\alpha$  concentration was significantly higher when TNF- $\alpha$  was added to the medium ( $\sim$ 0.9–15.96 ng/mL) comparing to when organoids were co-cultured with RAW 264.7 cells ( $\sim$ 0.45–0.8 ng/mL). Collectively, these results provided an indication about the amounts of TNF- $\alpha$  present in the culture medium.

Next, we tested the effects of a TNF- $\alpha$  neutralizing antibody and the removal of TNF- $\alpha$  from the medium by exchanging it with fresh medium (without TNF- $\alpha$ ) on the organoids morphology. According to a previous study, when TNF- $\alpha$  neutralizing antibody was added to the culture medium, the TNF- $\alpha$ -induced morphological changes could be reversed[21]. Thus, we aimed to evaluate whether this occurs only when TNF- $\alpha$  is added to our microwell-based organoid culture or also when organoids are co-cultured with macrophages. When organoids are in direct contact with RAW 264.7 cells, the addition of TNF- $\alpha$  neutralizing antibody (500 ng/mL) on day 3 had a minimal effect, with less than 10% of organoids reversing their morphology from spherical to budding (Figure 3B). This indicates that even



Chapter IV

though the amount of neutralizing antibody added was enough to neutralize the effects of TNF- $\alpha$  (according to our ELISA measurements), the spherical morphology was retained. In contrast, addition of neutralizing antibody or complete removal of TNF- $\alpha$  from the organoids (on day 3), which were initially treated with TNF- $\alpha$ , had a much more prominent effect on organoid morphology. We found that about 50% of the organoids that had initially become spherical returned to their crypt-villus architecture after treatment (Figure 3C). Collectively, these results indicate that, apart from TNF- $\alpha$ , other secreted factors and even the direct physical contact are involved in the morphological changes of the organoids, when they are in close proximity with RAW 264.7 cells.

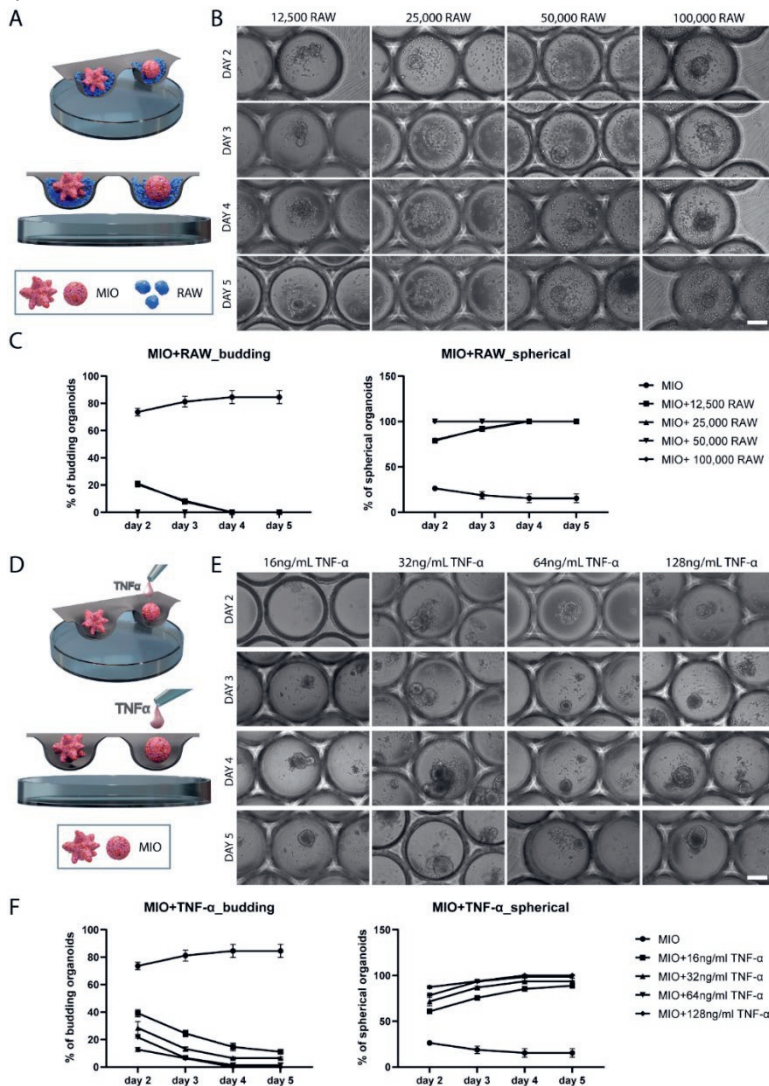


**Figure 2:** Morphological changes in organoids upon co-culture with macrophages or treatment with TNF- $\alpha$ . (A) Schematic illustration of the direct co-culture of intestinal organoids with RAW 264.7 cells in microwell arrays. (B) Representative bright-field images demonstrating the morphological changes in organoids upon co-culture with different amounts of macrophages (12,500, 25,000, 50,000, and 100,000 cells) over a period of 5 days. Scale bar represents 200  $\mu\text{m}$ . (C) Percentages of crypt-villus-structured and spherical organoids upon direct co-culture. Data are presented as the mean  $\pm$  SEM. (n = 3). (D) Schematic illustration of intestinal organoids treated with TNF- $\alpha$ . (E) Representative bright-field images demonstrating the morphological changes in organoids upon treatment with different concentrations of TNF- $\alpha$  (16, 32, 64, and 128 ng/mL) over a period of 5 days. Scale bar represents 200  $\mu\text{m}$ . (F) Percentages of budded and spherical organoids upon TNF- $\alpha$  treatment. Data presented as mean  $\pm$  S.E.M. (n = 3). Abbreviations: MIO, mouse intestinal organoids; RAW, RAW 264.7 cells; TNF- $\alpha$ , tumor necrosis factor alpha.

### Indirect co-culture of intestinal organoids and RAW 264.7 macrophages

To investigate the interactions between the macrophages and the organoids and test whether the immediate physical contact between them is playing a role in the morphological changes, we performed indirect co-culture of organoids with RAW 264.7 cells. Specifically, macrophages were seeded at the bottom of a 24-well plate and organoids were seeded inside the microwells (Figure 3D). Medium access was granted for both cell types both via the pores of the membrane and the sides of the insert. In this way, the crosstalk between the two cell types was mediated via the secretion of soluble factors by each cell line (paracrine signaling). This system will be referred to as ‘indirect co-culture’. After 5 days of indirect co-culture, the vast majority of organoids had a spherical morphology. Specifically, when 12,500 RAW 264.7 cells were added, 61% of the organoids became spherical, whereas when 100,000 RAW 264.7 cells were added 91% of the organoids became spherical. Hence, increasing numbers of RAW 264.7 cells resulted in increasing numbers of spherical organoids (Figure 3E).

Next, we assessed the morphology of the organoids after removing the RAW 264.7 cells from the culture or after adding TNF- $\alpha$  neutralizing antibody (500 ng/mL). Both treatments were found to have a similar effect on the organoid morphology. Almost all the organoids reversed their morphology and demonstrated budding architecture after 3 days (Figure 3E). Specifically, upon RAW 264.7 cells removal and TNF- $\alpha$  neutralizing antibody addition, 95% of the organoids co-cultured with 12,500 RAW 264.7 cells obtained crypt-villus morphology. When co-cultured with 100,000 RAW 264.7 cells, 82% of the organoids obtained crypt-villus morphology upon RAW 264.7 cells removal and 70% upon addition of TNF- $\alpha$  neutralizing antibody. Hence, TNF- $\alpha$  neutralizing antibody and RAW 264.7 cells removal have pronounced effects on organoid morphology when in indirect contact

Chapter IV

with macrophages, while, as discussed in the previous section, the effect of the TNF- $\alpha$  neutralizing antibody on organoids and macrophages in direct contact is less pronounced. Overall, these results indicate that there are prominent differences in the TNF- $\alpha$ -mediated morphological changes between organoids that are in direct or in indirect contact with macrophages.

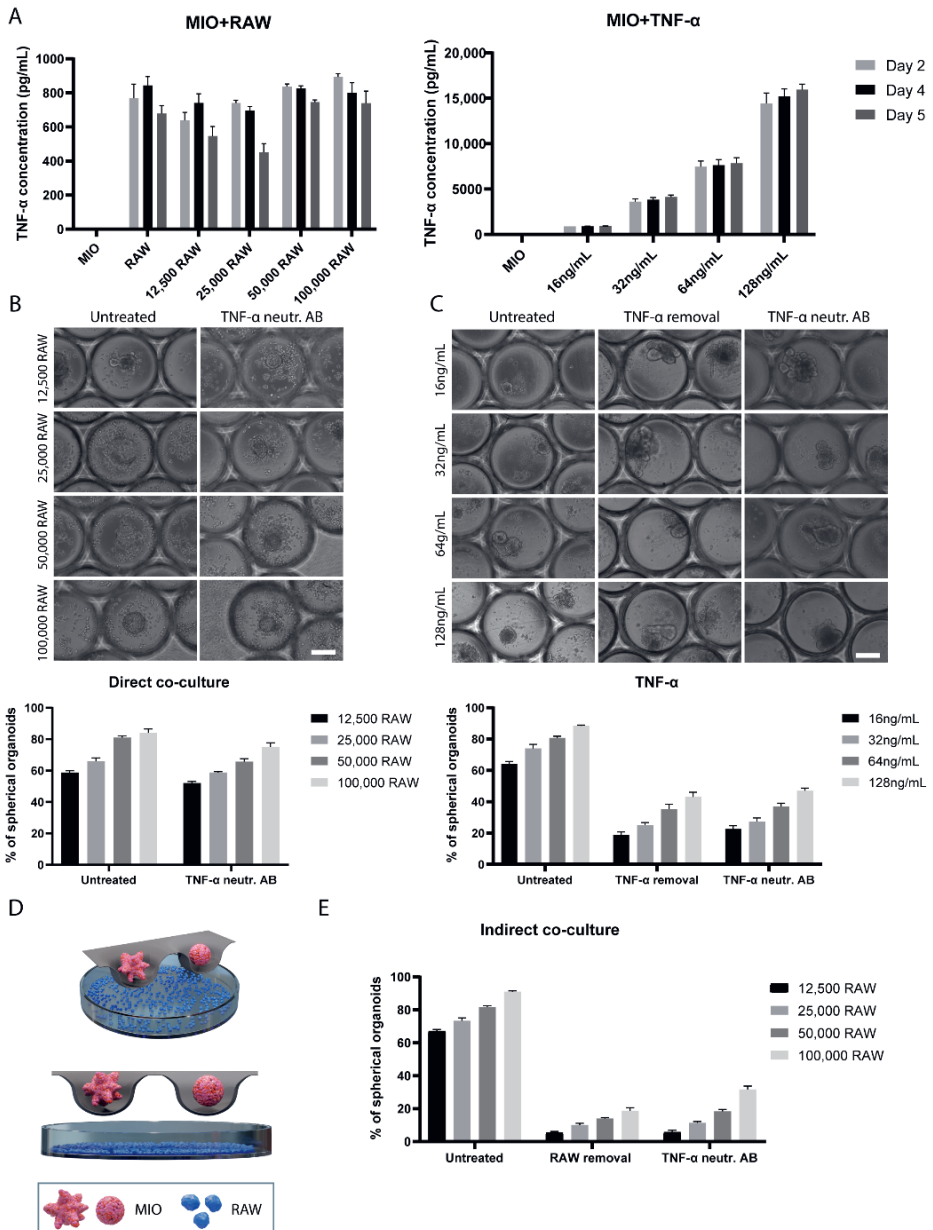


**Figure 3:** TNF- $\alpha$ -induced effects on organoid morphology. (A) Quantification of TNF- $\alpha$  concentration in the culture medium collected from organoids co-cultured with macrophages (left) and TNF- $\alpha$ -treated organoids (right) over a period of 5 days. Data are presented as the mean  $\pm$  SEM. (n = 3). (B) Bright-field images demonstrating the morphology of organoids co-cultured with macrophages upon treatment with TNF- $\alpha$  neutralizing antibody (500 ng/mL). Graph indicates the percentages of spherical organoids with and without treatment. Data are presented as the mean  $\pm$  SEM. (n = 3). Scale bar represents 200  $\mu$ m. (C) Bright-field images demonstrating the morphology of TNF- $\alpha$ -treated organoids upon additional treatment with TNF- $\alpha$  neutralizing antibody (500 ng/mL) and upon removal of TNF- $\alpha$  on day 3. Graph indicates the percentages of spherical organoids with and without additional treatments. Data are presented as the mean  $\pm$  SEM. (n = 3). Scale bar represents 200  $\mu$ m. (D) Schematic illustration of the indirect co-culture of intestinal organoids with RAW 264.7 cells in microwell arrays. (E) Graph indicates the percentages of spherical organoids upon indirect co-culture with macrophages, indirect co-culture with subsequent removal of macrophages and finally upon treatment with TNF- $\alpha$  neutralizing antibody on day 3 (500 ng/mL). Data are presented as the mean  $\pm$  SEM (n = 3). Abbreviations: MIO, mouse intestinal organoids; RAW, RAW 264.7 cells.

#### Luminex assay for TNF- $\alpha$ -treated intestinal organoids

To investigate the inflammatory responses of organoids upon exposure to the pro-inflammatory cytokine TNF- $\alpha$  and the mechanisms underlying the differences between the two co-culture systems and the TNF- $\alpha$  treatment further, we performed a luminex assay. Specifically, we collected the cell culture medium upon stimulation of organoids with 64 ng/mL TNF- $\alpha$  after 2, 4, and 5 days. We also tested cytokine expression in organoids that were treated with TNF- $\alpha$  for 3 days, after which TNF- $\alpha$  was removed from the culture medium. We identified expression of both pro- and anti-inflammatory cytokines that mediate immune responses. In particular, these included the interleukins IL1 $\alpha$ , IL1 $\beta$ , IL3, IL5, IL9, IL12p40, IL13, keratinocyte chemoattractant (KC), and TNF- $\alpha$  (Figure 4). Interestingly, the secretion of these cytokines continued in similar levels even after the removal of TNF- $\alpha$  from the culture. Except for KC and TNF- $\alpha$ , there was no statistically significant difference in the cytokine secretion after TNF- $\alpha$  removal. These results indicate that intestinal organoids show an innate immune response function that is activated upon exposure to TNF- $\alpha$ . Furthermore, the treatment of organoids with TNF- $\alpha$  can induce the secretion of some of the cytokines *in vitro*, in a similar way as has been described for IBD situations[29].

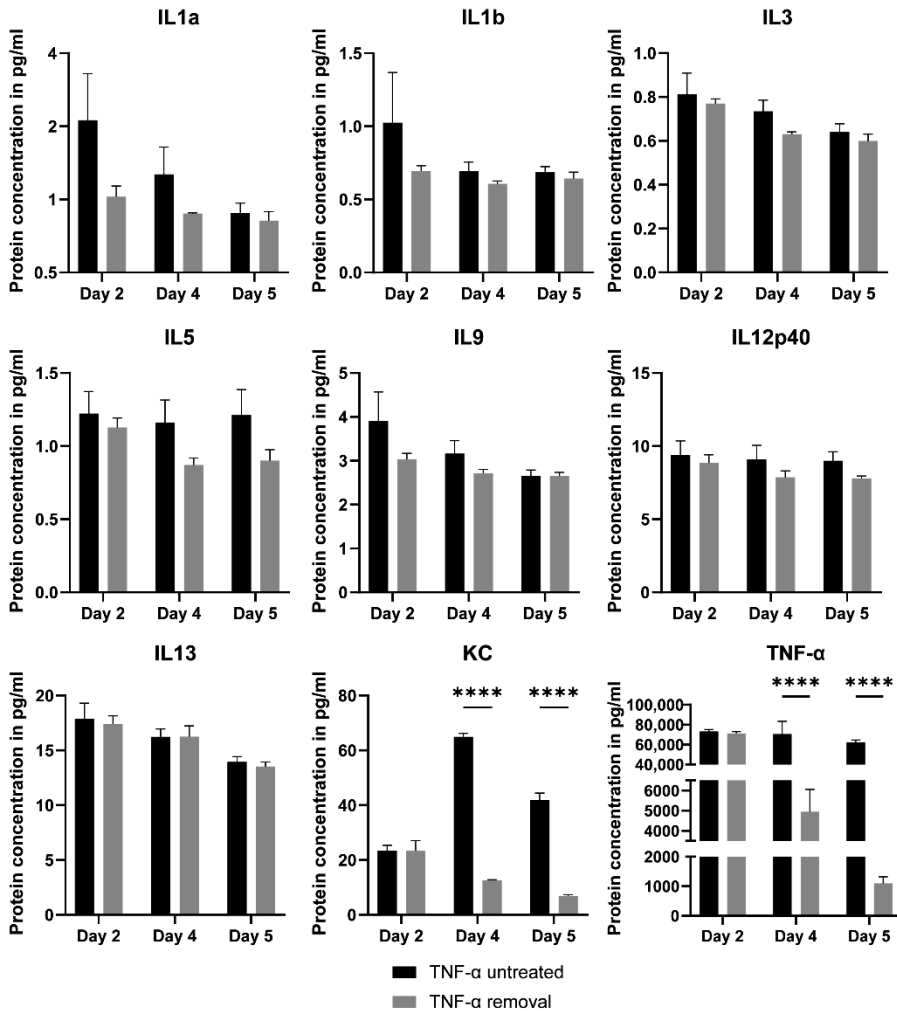


**Figure 4:** Luminex assay for TNF- $\alpha$ -treated intestinal organoids. Secretion of the cytokines IL1 $\alpha$ , IL1 $\beta$ , IL3, IL5, IL9, IL12p40, IL13, KC, and TNF- $\alpha$  was identified in organoid culture medium upon addition of 64 ng/mL TNF- $\alpha$  (TNF- $\alpha$  untreated). Except for the KC and TNF- $\alpha$ , removal of TNF- $\alpha$  from the medium did not seem to strongly affect the production of these proteins. Data are presented as the mean  $\pm$  SEM. (n = 4). \*\*\*\*, \*\*\*, \*\* and \* for P < 0.0001, P < 0.001, P < 0.01 and P < 0.05.

### Luminex assay for direct and indirect co-culture of intestinal organoids with macrophages

Next, we explored the cytokine release upon direct and indirect co-culture of intestinal organoids with 50,000 RAW 264.7 cells, after 2, 4, and 5 days. We also tested the secretion after removal of macrophages on day 3 from the culture (indirect culture only) and after monoculture of RAW 264.7 cells (50,000) in microwells. We

identified a list of pro- and anti-inflammatory cytokines secreted, including IL1 $\alpha$ , IL1 $\beta$ , IL2, IL3, IL4, IL5, IL6, IL9, IL10, IL12p40, IL12p70, IL13, KC, RANTES, Interferon (IFN)- $\gamma$ , and TNF- $\alpha$  (Figure 5).

Interestingly, the secretion of most of these cytokines (except KC and RANTES) was higher when RAW 264.7 were cultured alone. This suggests a sort of immunomodulatory function of the intestinal organoids, which seem to be able to modulate the immune response of the macrophages. In addition, the fact that these proteins are produced even after the removal of RAW 264.7 cells further supports our previous suggestion that organoids demonstrate an innate immune response function upon exposure to inflammatory cytokines (added or secreted by the macrophages). Furthermore, in most cases, the secretion of these proteins seemed to be downregulated over time, when macrophages were cultured alone or co-cultured indirectly with organoids. In contrast, when organoids are in direct contact with the RAW 264.7 cells, the secretion is more stable over the 5 days of culture. Noteworthy, the secreted levels of these proteins were higher when organoids were in direct contact with the macrophages comparing to indirect co-culture. For most cytokines, these differences were statistically significant at all time-points. Hence, the close proximity of intestinal organoids with the macrophages seemed to have a prominent effect on the crosstalk between the cells.

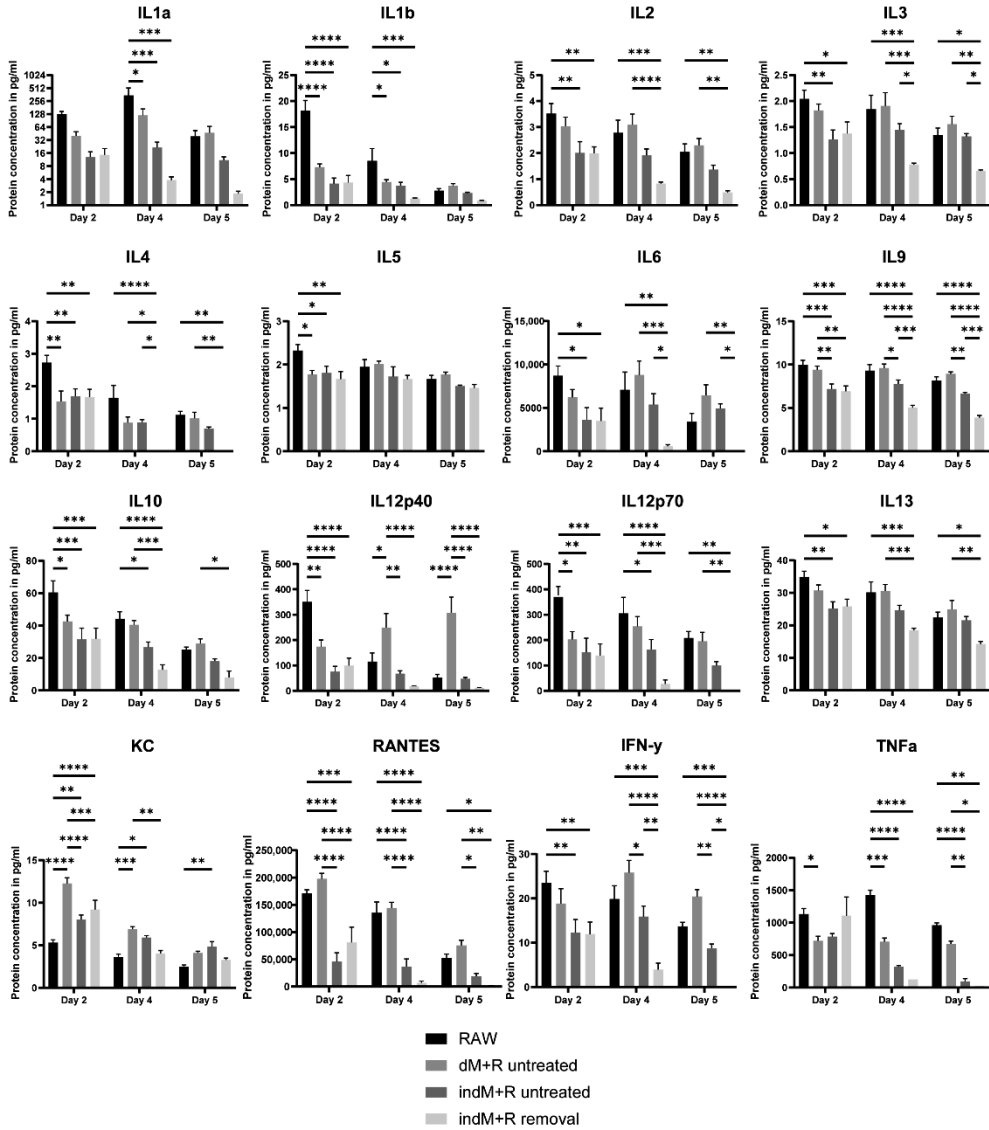


Figure 5: Luminescence assay for direct and indirect co-culture of intestinal organoids with macrophages. Pro- and anti-inflammatory cytokines were produced upon direct and indirect co-culture of organoids with RAW 264.7 cells over a period of 5 days. Removal of RAW 264.7 cells was performed after 3 days of co-culture. Data are presented as the mean  $\pm$  SEM. (n = 4). \*\*\*\*, \*\*\*, \*\* and \* for  $P < 0.0001$ ,  $P < 0.001$ ,  $P < 0.01$  and  $P < 0.05$ . Abbreviations: RAW, RAW 264.7 cells; dM+R, direct co-culture; indM+R, indirect co-culture.

## **Discussion**

In the past few years, significant progress has been made in the development of intestinal organoid models. Multiple features of the *in vivo* intestine, such as the crypt-villus organization and functions like barrier formation, drug absorption, and metabolism, can now be closely recapitulated by *in vitro* models. However, organoids still do not reflect the full complexity of the *in vivo* tissue, since important cues from surrounding tissues and cellular compartments are absent. Especially in the case of the intestine, the crosstalk between the epithelium and immune system is crucial to maintain homeostasis, since the intestine is constantly in contact with foreign materials. The development of more advanced 3D *in vitro* models incorporating immune components would be beneficial to unravel mechanisms involved in the defense system of the intestine but also for studying the pathogenesis of intestinal diseases, such as IBD. In this study, we incorporated immune cells in a microwell-based organoid model or added a pro-inflammatory cytokine and showed that organoids have an innate immunomodulatory function. This platform can be used to study intestinal inflammation in a more holistic way, since it allows modelling of both the intestinal epithelium and molecular/cellular components of the immune system and a controlled interaction between both compartments. Furthermore, this is a novel cell culture tool incorporating porous microwells for organoid culture in a compartmentalized, Transwell-like set-up. In this system, organoids can be co-cultured with different cell types, which can grow either on the inner or the outer surfaces of the microwells, or on the bottom of the culture plate. In this way, the interactions of multiple factors can be studied within the same system. In future studies, different types of stromal cells (macrophages, T cells, dendritic cells, vascular cells etc.) can be placed in several different configurations to decouple and explore the interactions between the compartments. Additionally, in our system organoids preserve their 3D architecture, whereas in traditional flat Transwell devices, organoids need to be dissociated to form cell monolayers[30–34]. This process requires a large amount of cells, hence a large number of organoids, which can be a pricey and time-consuming process. Thus, our microwell-based co-culture system can be particularly useful to study the interactions of the intestinal epithelium with immune and/or stromal cells.

Previously, efforts have been made to culture intestinal organoids in combination with immune cells. Specifically, mouse intestinal organoids have been co-cultured with RAW 264.7 macrophages before but in this case, organoids were embedded in Matrigel and macrophages were cultured on a Transwell insert, thus



the crosstalk between the cells was not entirely representative of the *in vivo* situation[21]. In another study, human monocyte-derived macrophages were co-cultured with human intestinal organoid-derived cell monolayers on opposite sides of a porous film[31]. Even though this model allows access to both apical and basolateral sides of the epithelium, the 3D architecture of the organoids is lost. Intraepithelial lymphocytes[35] and monocytes[36] were co-cultured with intestinal organoids inside Matrigel drops. However, these cell types are usually not embedded in Matrigel, which we hypothesize can affect their behavior as in physiological circumstances they are in suspension. Additionally, when embedded in Matrigel, organoids are not easy to track during culture. In contrast, when cultured in microwell arrays, organoids can be monitored easily throughout the whole culture period and can straightforwardly be harvested for further downstream analysis. Furthermore, in our system, the macrophages are added in suspension and then attached to the polymer films of the microwell arrays, thus behaving in a similar way to regular cell culture flasks. The close proximity of the organoids and the macrophages allowed for direct, physical interaction between the different cells in a more natural way. Apart from the small distance between the cells, the released cytokines did not have to diffuse over longer distances through Matrigel, which could also diminish and/or delay their effect. Overall, using a microwell system to perform co-culture allows for controlled positioning of the different cell types, which can benefit the modeling of certain *in vivo* conditions, and allows for a controlled decoupling of specific factors/interactions. For example, in IBD, there is infiltration of macrophages in the intestinal mucosa, which can only be achieved *in vitro* if cells are placed nearby and the cells can actively migrate.

The difference between the direct and indirect contact of organoids with macrophages was shown here both by the differences in the morphology of the organoids, but also in the series of released cytokines. The organoids' morphology was changed from crypt-villus to spherical upon co-culture with macrophages and one of the key mechanisms underlying this change is the release of the pro-inflammatory cytokine TNF- $\alpha$ . TNF- $\alpha$  has been associated with the loss of epithelial barrier integrity, via the phosphorylation of myosin light chain, the loss of zonula occludens-1 and the internalization of occludin within the cytoplasm[37–39]. Treatment with TNF- $\alpha$  neutralizing antibody failed to rescue the organoid architecture from spherical to budding when organoids were in direct contact with macrophages, whereas this was not the case when they were in indirect contact. In addition, the secretion of cytokines was higher and more stable over time when organoids were in direct contact with the macrophages, indicating that receptor

interactions may play a pivotal role. Thus, the direct co-culture system resembles more the conditions found in chronic intestinal inflammation, where we have excessive secretion of cytokines. The indirect system seems to better reflect conditions of a mild acute inflammation, where the secretion of cytokines stays lower and the immune response is less excessive. This notion is also supported by the fact that upon removal of RAW 264.7 cells following indirect co-culture with organoids, the effects of the secreted cytokines are minimized or even nullified.

In a comparison of immune responses between co-culture of organoids with macrophages and treatment with TNF- $\alpha$ , we identified that IL1 $\alpha$ , IL1 $\beta$ , IL3, IL5, IL9, IL12p40, IL13, KC, and TNF- $\alpha$  were secreted in both conditions, whereas IL2, IL4, IL6, IL10, IL12p70, RANTES, and IFN- $\gamma$  were solely secreted in the co-culture. A role of all these proteins have been associated previously with acute and/or chronic intestinal inflammatory responses[40]. For example, the pro-inflammatory cytokines IL1 $\alpha$ , IL1 $\beta$ , IL2, IL6, IL12, IFN- $\gamma$ , and TNF- $\alpha$  have been linked with initiation and progression of IBD, whereas the anti-inflammatory IL4, IL10, and IL13 have been associated with the pathogenesis of IBD by decreasing the production of pro-inflammatory cytokines[29,41,42]. Similarly, IL3 and IL5 have been regarded as pleiotropic regulators of inflammation and they are implicated in reducing intestinal inflammation[43,44]. IL9 has also been found to play a role in the pathogenesis of IBD and has been suggested as a disease severity marker and potential therapeutic candidate[45]. RANTES is a chemokine that is upregulated in IBD and the identification of differences in its expression patterns (granulomatous vs non-granulomatous) has been proposed as a possible method to distinguish between Crohn's disease and ulcerative colitis[46,47]. RANTES is also upregulated in gastrointestinal tumors[48]. Finally, KC is a chemokine that is induced by IL1 and TNF- $\alpha$ , and its expression is upregulated in IBD[49,50]. Collectively, these data indicate that a co-culture system of intestinal organoids with macrophages provides a more holistic approach to study inflammatory responses than an exogenous treatment of organoids with TNF- $\alpha$  only. However, this is still a simplified model compared to the *in vivo* situation, where more immune cell types are involved (e.g., T-cells, innate lymphoid cells) and more cytokines (e.g., IL8, IL17, IL21) are present during inflammatory responses. In the future, it would be interesting to use human cells and explore whether similar responses can be reproduced. It would also be intriguing to test different types or even combinations of immune cells and assess the directionality of the interactions among them. Using patient-derived organoids, treatments against more cytokines than just TNF- $\alpha$  could be explored, aiming for more efficient and even personalized therapies.

To conclude, we have developed a versatile microwell-based platform to perform co-culture of intestinal organoids with RAW 264.7 macrophages. Within this system, the positioning of the different cells can be controlled and the interactions of multiple factors can be studied simultaneously. Here, we placed RAW 264.7 cells either in direct contact with the intestinal organoids or in indirect contact, and in both systems, we identified characteristic secretion profiles of cytokines involved in inflammatory responses. These responses resembled aspects of the early and later phases (acute and more chronic) of inflammation. This indicates that our novel systems can be used to gain new insights into the mechanisms and interactions underlying intestinal inflammation. The microwell-based culture system facilitates a continuous monitoring of the macrophage-organoid interactions and the performance of high-throughput assays. For example, these models can be valuable alternatives for the development of more effective drug treatments against intestinal inflammatory diseases.

## **References**

1. Mowat, A.M.; Agace, W.W. Regional Specialization within the Intestinal Immune System. *Nat. Rev. Immunol.* **2014**, *14*, 667–685, doi:10.1038/nri3738.
2. Angus, H.C.K.; Butt, A.G.; Schultz, M.; Kemp, R.A. Intestinal Organoids as a Tool for Inflammatory Bowel Disease Research. *Front. Med.* **2019**, *6*, 334, doi:10.3389/FMED.2019.00334.
3. Wakisaka, Y.; Sugimoto, S.; Sato, T. Organoid Medicine for Inflammatory Bowel Disease. *Stem Cells* **2022**, *40*, 123–132, doi:10.1093/STMCLS/SXAB020.
4. Schneeweiss, S.; Korzenik, J.; Solomon, D.H.; Canning, C.; Lee, J.; Bressler, B. Infliximab and Other Immunomodulating Drugs in Patients with Inflammatory Bowel Disease and the Risk of Serious Bacterial Infections. *Aliment. Pharmacol. Ther.* **2009**, *30*, 253–264, doi:10.1111/J.1365-2036.2009.04037.X.
5. Ten Hove, T.; Van Montfrans, C.; Peppelenbosch, M.P.; Van Deventer, S.J.H. Infliximab Treatment Induces Apoptosis of Lamina Propria T Lymphocytes in Crohn's Disease. *Gut* **2002**, *50*, 206–211, doi:10.1136/GUT.50.2.206.
6. Joshi, A.; Soni, A.; Acharya, S. In Vitro Models and Ex Vivo Systems Used in Inflammatory Bowel Disease. *Vitr. Model. 2022 13* **2022**, *1*, 213–227, doi:10.1007/S44164-022-00017-W.
7. Mizoguchi, A. Animal Models of Inflammatory Bowel Disease. *Prog. Mol. Biol. Transl. Sci.* **2012**, *105*, 263–320, doi:10.1016/B978-0-12-394596-9.00009-3.

8. Kiesler, P.; Fuss, I.J.; Strober, W. Experimental Models of Inflammatory Bowel Diseases. *Cell. Mol. Gastroenterol. Hepatol.* **2015**, *1*, 154, doi:10.1016/J.JCMGH.2015.01.006.
9. Sato, T.; Vries, R.G.; Snippert, H.J.; Van De Wetering, M.; Barker, N.; Stange, D.E.; Van Es, J.H.; Abo, A.; Kujala, P.; Peters, P.J.; et al. Single Lgr5 Stem Cells Build Crypt-Villus Structures in Vitro without a Mesenchymal Niche. *Nature* **2009**, *459*, 262–265, doi:10.1038/nature07935.
10. Spence, J.R.; Mayhew, C.N.; Rankin, S.A.; Kuhar, M.F.; Vallance, J.E.; Tolle, K.; Hoskins, E.E.; Kalinichenko, V. V.; Wells, S.I.; Zorn, A.M.; et al. Directed Differentiation of Human Pluripotent Stem Cells into Intestinal Tissue in Vitro. *Nature* **2011**, *470*, 105–109, doi:10.1038/nature09691.
11. Kakni, P.; Truckenmüller, R.; Habibović, P.; Giselbrecht, S. Challenges to, and Prospects for, Reverse Engineering the Gastrointestinal Tract Using Organoids. *Trends Biotechnol.* **2022**, 932–944, doi:10.1016/J.TIBTECH.2022.01.006.
12. Günther, C.; Brevini, T.; Sampaziotis, F.; Neurath, M.F. What Gastroenterologists and Hepatologists Should Know about Organoids in 2019. *Dig. Liver Dis.* **2019**, *51*, 753–760.
13. Muller, P.A.; Matheis, F.; Mucida, D. Gut Macrophages: Key Players in Intestinal Immunity and Tissue Physiology. *Curr. Opin. Immunol.* **2020**, *62*, 54–61, doi:10.1016/J.COI.2019.11.011.
14. Han, X.; Ding, S.; Jiang, H.; Liu, G. Roles of Macrophages in the Development and Treatment of Gut Inflammation. *Front. Cell Dev. Biol.* **2021**, *9*, 385, doi:10.3389/FCCELL.2021.625423/BIBTEX.
15. Andrews, C.; McLean, M.H.; Durum, S.K. Cytokine Tuning of Intestinal Epithelial Function. *Front. Immunol.* **2018**, *9*, 1270, doi:10.3389/FIMMU.2018.01270/BIBTEX.
16. Neurath, M.F. Cytokines in Inflammatory Bowel Disease. *Nat. Rev. Immunol.* **2014**, *14*, 329–342, doi:10.1038/nri3661.
17. Kakni, P.; Hueber, R.; Knoop, K.; López-Iglesias, C.; Truckenmüller, R.; Habibovic, P.; Giselbrecht, S. Intestinal Organoid Culture in Polymer Film-Based Microwell Arrays. *Adv. Biosyst.* **2020**, 2000126, doi:10.1002/adbi.202000126.
18. Mashukova, A.; Wald, F.A.; Salas, P.J. Tumor Necrosis Factor Alpha and Inflammation Disrupt the Polarity Complex in Intestinal Epithelial Cells by a Posttranslational Mechanism. *Mol. Cell. Biol.* **2011**, *31*, 756–765, doi:10.1128/MCB.00811-10/ASSET/DA5268CF-0A04-4A27-BB60-53DF7943EB0B/ASSETS/GRAPHIC/ZMB9991089320005.JPEG.
19. Lueschow, S.R.; McElroy, S.J. The Paneth Cell: The Curator and Defender of the Immature Small Intestine. *Front. Immunol.* **2020**, *11*, 587, doi:10.3389/FIMMU.2020.00587/BIBTEX.
20. Bain, C.C.; Schridde, A. Origin, Differentiation, and Function of Intestinal Macrophages. *Front. Immunol.* **2018**, *9*, 2733,

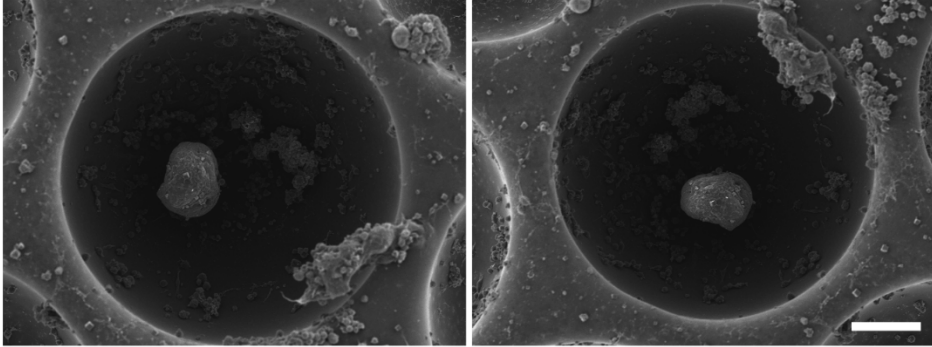
- doi:10.3389/FIMMU.2018.02733/BIBTEX.
21. Hahn, S.; Nam, M.O.; Noh, J.H.; Lee, D.H.; Han, H.W.; Kim, D.H.; Hahm, K.B.; Hong, S.P.; Yoo, J.H.; Yoo, J. Organoid-Based Epithelial to Mesenchymal Transition (OEMT) Model: From an Intestinal Fibrosis Perspective. *Sci. Rep.* **2017**, *7*, 1–11.
  22. Leppkes, M.; Roulis, M.; Neurath, M.F.; Kollias, G.; Becker, C. *Pleiotropic Functions of TNF- $\alpha$  in the Regulation of the Intestinal Epithelial Response to Inflammation*; **2014**, *26*, 509–515.
  23. Tanoue, T.; Nishitani, Y.; Kanazawa, K.; Hashimoto, T.; Mizuno, M. In Vitro Model to Estimate Gut Inflammation Using Co-Cultured Caco-2 and RAW264.7 Cells. *Biochem. Biophys. Res. Commun.* **2008**, *374*, 565–569, doi:10.1016/J.BBRC.2008.07.063.
  24. Ma, T.Y.; Boivin, M.A.; Ye, D.; Pedram, A.; Said, H.M. Mechanism of TNF- $\alpha$  Modulation of Caco-2 Intestinal Epithelial Tight Junction Barrier: Role of Myosin Light-Chain Kinase Protein Expression. *Am. J. Physiol. - Gastrointest. Liver Physiol.* **2005**, *288*, 422–430, doi:10.1152/ajpgi.00412.2004.
  25. Sun, L.; Rollins, D.; Qi, Y.; Fredericks, J.; Mansell, T.J.; Jergens, A.; Phillips, G.J.; Wannemuehler, M.; Wang, Q. TNF $\alpha$  Regulates Intestinal Organoids from Mice with Both Defined and Conventional Microbiota. *Int. J. Biol. Macromol.* **2020**, *164*, 548–556, doi:10.1016/J.IJBIOMAC.2020.07.176.
  26. Lee, C.; Hong, S.N.; Kim, E.R.; Chang, D.K.; Kim, Y.H. Epithelial Regeneration Ability of Crohn’s Disease Assessed Using Patient-Derived Intestinal Organoids. *Int. J. Mol. Sci.* **2021**, *22*, 6013, doi:10.3390/IJMS22116013/S1.
  27. Dekkers, J.F.; Wiegerinck, C.L.; De Jonge, H.R.; Bronsveld, I.; Janssens, H.M.; De Winter-De Groot, K.M.; Brandsma, A.M.; De Jong, N.W.M.; Bijvelds, M.J.C.; Scholte, B.J.; et al. A Functional CFTR Assay Using Primary Cystic Fibrosis Intestinal Organoids. *Nat. Med.* **2013**, *19*, 939–945, doi:10.1038/nm.3201.
  28. Baniak, N.; Luan, X.; Grunow, A.; Machen, T.E.; Ianowski, J.P. The Cytokines Interleukin-1 $\beta$  and Tumor Necrosis Factor- $\alpha$  Stimulate CFTR-Mediated Fluid Secretion by Swine Airway Submucosal Glands. *Am. J. Physiol. - Lung Cell. Mol. Physiol.* **2012**, *303*, 327–333, doi:10.1152/ajplung.00058.2012.
  29. Muzes, G.; Molnár, B.; Tulassay, Z.; Sipos, F. Changes of the Cytokine Profile in Inflammatory Bowel Diseases. *World J. Gastroenterol.* **2012**, *18*, 5848, doi:10.3748/WJG.V18.I41.5848.
  30. Hentschel, V.; Seufferlein, T.; Armacki, M. Intestinal Organoids in Coculture: Redefining the Boundaries of Gut Mucosa Ex Vivo Modeling. *Am. J. Physiol. - Gastrointest. Liver Physiol.* **2021**, *321*, G693–G704, doi:10.1152/AJPGI.00043.2021.
  31. Noel, G.; Baetz, N.W.; Staab, J.F.; Donowitz, M.; Kovbasnjuk, O.; Pasetti,

- M.F.; Zachos, N.C. A Primary Human Macrophage-Enteroid Co-Culture Model to Investigate Mucosal Gut Physiology and Host-Pathogen Interactions. *Sci. Reports* **2017**, *7*, 1–14, doi:10.1038/srep45270.
32. Kozuka, K.; He, Y.; Koo-McCoy, S.; Kumaraswamy, P.; Nie, B.; Shaw, K.; Chan, P.; Leadbetter, M.; He, L.; Lewis, J.G.; et al. Development and Characterization of a Human and Mouse Intestinal Epithelial Cell Monolayer Platform. *Stem Cell Reports* **2017**, *9*, 1976–1990, doi:10.1016/J.STEMCR.2017.10.013.
  33. Liu, Y.; Qi, Z.; Li, X.; Du, Y.; Chen, Y.G. Monolayer Culture of Intestinal Epithelium Sustains Lgr5+ Intestinal Stem Cells. *Cell Discov.* **2018**, *4*, 1–3, doi:10.1038/s41421-018-0036-z.
  34. VanDussen, K.L.; Marinshaw, J.M.; Shaikh, N.; Miyoshi, H.; Moon, C.; Tarr, P.I.; Ciorba, M.A.; Stappenbeck, T.S. Development of an Enhanced Human Gastrointestinal Epithelial Culture System to Facilitate Patient-Based Assays. *Gut* **2015**, *64*, 911–920, doi:10.1136/GUTJNL-2013-306651.
  35. Nozaki, K.; Mochizuki, W.; Matsumoto, Y.; Matsumoto, T.; Fukuda, M.; Mizutani, T.; Watanabe, M.; Nakamura, T. Co-Culture with Intestinal Epithelial Organoids Allows Efficient Expansion and Motility Analysis of Intraepithelial Lymphocytes. *J. Gastroenterol.* **2016**, *51*, 206–213.
  36. Jose, S.S.; De Zuani, M.; Tidu, F.; Hortová Kohoutková, M.; Pazzagli, L.; Forte, G.; Spaccapelo, R.; Zelante, T.; Frič, J. Comparison of Two Human Organoid Models of Lung and Intestinal Inflammation Reveals Toll-like Receptor Signalling Activation and Monocyte Recruitment. *Clin. Transl. Immunol.* **2020**, *9*, e1131, doi:10.1002/CTI2.1131.
  37. Marchiando, A.M.; Shen, L.; Vallen Graham, W.; Weber, C.R.; Schwarz, B.T.; Austin, J.R.; Raleigh, D.R.; Guan, Y.; Watson, A.J.M.; Montrose, M.H.; et al. Caveolin-1-Dependent Occludin Endocytosis Is Required for TNF-Induced Tight Junction Regulation in Vivo. *J. Cell Biol.* **2010**, *189*, 111–126, doi:10.1083/JCB.200902153/VIDEO-4.
  38. Cunningham, K.E.; Turner, J.R. Myosin Light Chain Kinase: Pulling the Strings of Epithelial Tight Junction Function. *Ann. N. Y. Acad. Sci.* **2012**, *1258*, 34–42, doi:10.1111/J.1749-6632.2012.06526.X.
  39. Feng, Y.; Teitelbaum, D.H. Tumour Necrosis Factor- $\alpha$ -Induced Loss of Intestinal Barrier Function Requires TNFR1 and TNFR2 Signalling in a Mouse Model of Total Parenteral Nutrition. *J. Physiol.* **2013**, *591*, 3709, doi:10.1113/JPHYSIOL.2013.253518.
  40. Feghali, C.A.; Wright, T.M. Cytokines in Acute and Chronic Inflammation. *Front. Biosci.* **1997**, *2*, doi:10.2741/A171.
  41. Chomarar, P.; Banchereau, J. Interleukin-4 and Interleukin-13: Their Similarities and Discrepancies. *Int Rev Immunol.* **2009**, *17*, 1–52, doi:10.3109/08830189809084486.
  42. West, G.A.; Matsuura, T.; Levine, A.D.; Klein, J.S.; Fiocchi, C. Interleukin 4 in Inflammatory Bowel Disease and Mucosal Immune Reactivity.

- Gastroenterology* **1996**, *110*, 1683–1695, doi:10.1053/GAST.1996.V110.PM8964392.
43. Dougan, M.; Dranoff, G.; Dougan, S.K. GM-CSF, IL-3, and IL-5 Family of Cytokines: Regulators of Inflammation. *Immunity* **2019**, *50*, 796–811, doi:10.1016/J.IMMUNI.2019.03.022.
  44. Borriello, F.; Galdiero, M.R.; Varricchi, G.; Loffredo, S.; Spadaro, G.; Marone, G. Innate Immune Modulation by GM-CSF and IL-3 in Health and Disease. *Int. J. Mol. Sci.* **2019**, *20*, doi:10.3390/IJMS20040834.
  45. Nalleweg, N.; Chiriac, M.T.; Podstawa, E.; Lehmann, C.; Rau, T.T.; Atreya, R.; Krauss, E.; Hundorfean, G.; Fichtner-Feigl, S.; Hartmann, A.; et al. IL-9 and Its Receptor Are Predominantly Involved in the Pathogenesis of UC. *Gut* **2014**, *64*, 743–755, doi:10.1136/GUTJNL-2013-305947/-/DC1.
  46. Ajuebor, M.N.; Swain, M.G. Role of Chemokines and Chemokine Receptors in the Gastrointestinal Tract. *Immunology* **2002**, *105*, 137, doi:10.1046/J.1365-2567.2002.01309.X.
  47. Ansari, N.; Abdulla, J.; Zayyani, N.; Brahmi, U.; Taha, S.; Satir, A.A. Comparison of RANTES Expression in Crohn's Disease and Ulcerative Colitis: An Aid in the Differential Diagnosis? *J. Clin. Pathol.* **2006**, *59*, 1066, doi:10.1136/JCP.2005.034983.
  48. Cao, Z.; Xu, X.; Luo, X.; Li, L.; Huang, B.; Li, X.; Tao, D.; Hu, J.; Gong, J. Role of RANTES and Its Receptor in Gastric Cancer Metastasis. *J. Huazhong Univ. Sci. Technol. Medical Sci.* **2011**, *31*, 342–347, doi:10.1007/S11596-011-0378-3.
  49. Puleston, J.; Cooper, M.; Murch, S.; Bid, K.; Makh, S.; Ashwood, P.; Bingham, A.H.; Green, H.; Moss, P.; Dhillon, A.; et al. A Distinct Subset of Chemokines Dominates the Mucosal Chemokine Response in Inflammatory Bowel Disease. *Aliment. Pharmacol. Ther.* **2005**, *21*, 109–120, doi:10.1111/J.1365-2036.2004.02262.X.
  50. Singh, U.P.; Singh, N.P.; Murphy, E.A.; Price, R.L.; Fayad, R.; Nagarkatti, M.; Nagarkatti, P.S. Chemokine and Cytokine Levels in Inflammatory Bowel Disease Patients. *Cytokine* **2016**, *77*, 44, doi:10.1016/J.CYTO.2015.10.008.
  51. Giselbrecht, S.; Gietzelt, T.; Gottwald, E.; Trautmann, C.; Truckenmüller, R.; Weibezahn, K.F.; Welle, A. 3D Tissue Culture Substrates Produced by Microthermoforming of Pre-Processed Polymer Films. *Biomed. Microdevices* **2006**, *8*, 191–199, doi:10.1007/s10544-006-8174-8.

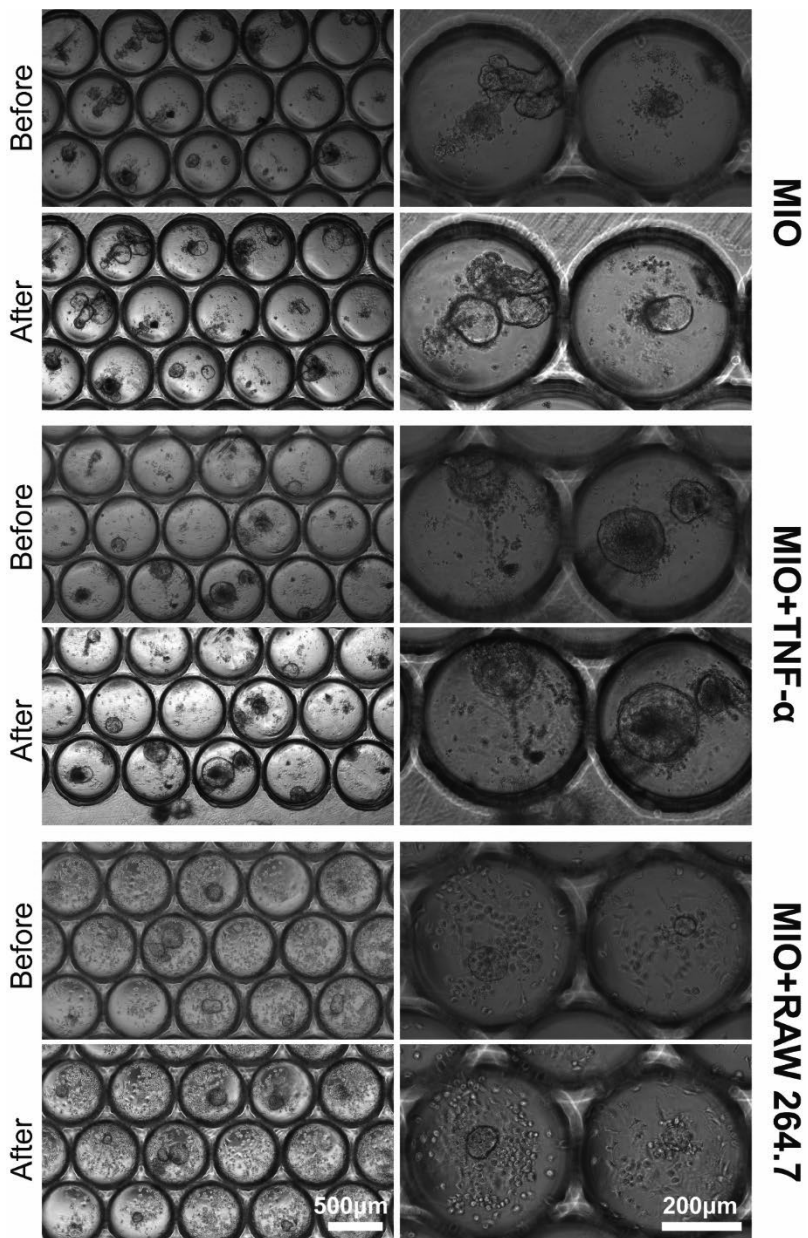
## **Supplementary Material**

### **Supplementary figures**



**Supplementary Figure 1.** SEM images demonstrating the direct co-culture of intestinal organoids with RAW 264.7 cells. Scale bar represents 100  $\mu\text{m}$ .





**Supplementary Figure 2.** Bright-field images demonstrating the swelling of organoids upon treatment with 5  $\mu$ M Forskolin for 3 hours.

## **Supplementary video**

**Supplementary video 1.** Time-lapse imaging of the direct co-culture of intestinal organoids with 50,000 RAW 264.7 cells. Single plane images were taken every 1 h for 3 days.





## CHAPTER V

# **REVERSING EPITHELIAL POLARITY IN PLURIPOTENT STEM CELL-DERIVED INTESTINAL ORGANIDS**

Panagiota Kakni, Carmen López-Iglesias,  
Roman Truckenmüller, Pamela Habibović  
and Stefan Giselbrecht

*Front. Bioeng. Biotechnol.*

10: 879024 (2022)



## **Abstract**

The inner surface of the intestine is a dynamic system, composed of a single layer of polarized epithelial cells. The development of intestinal organoids was a major breakthrough since they robustly recapitulate intestinal architecture, regional specification and cell composition *in vitro*. However, the cyst-like organization hinders direct access to the apical side of the epithelium, thus limiting their use in functional assays. For the first time, we show an intestinal organoid model from pluripotent stem cells with reversed polarity where the apical side faces the surrounding culture media and the basal side faces the lumen. These inside-out organoids preserve a distinct apico-basolateral orientation for a long period and differentiate into the major intestinal cell types. This novel model lays the foundation for developing new *in vitro* functional assays particularly targeting the apical surface of the epithelium and thus offers a new research tool to study nutrient/drug uptake, metabolism and host-microbiome/pathogen interactions.

## **Introduction**

The intestinal epithelium is a highly organized, self-renewing tissue mainly serving two roles. First, it forms a physical barrier to avoid the crossing of harmful substances in the intestinal lumen and second, it regulates the nutrient absorption and metabolism. Within this simple columnar epithelial layer, the establishment and maintenance of cell polarity with distinct apical and basolateral surfaces is considered crucial for the proper tissue development and function. Each of these compartments has a different structure, function and macromolecule composition (Klunder et al., 2017). The apical surface faces the lumen and is responsible for the absorption of nutrients while the basolateral surface faces the stroma and mediates nutrient transport. Apart from the apico-basolateral polar organization, the differentiation towards the major intestinal cell types (enterocytes, Paneth cells, goblet cells etc.) is of utmost importance for the proper functioning of the intestine. Various cell lines and animal models have been utilized to model the human intestinal epithelium but the full complexity of it has not yet been accurately recapitulated *in vitro*.

Advances in stem cell research made it possible to create *in vitro* 3D organ-like structures from either adult or pluripotent stem cells that better recapitulate the *in vivo* tissues than traditional 2D cell culture models. The generation of intestinal organoids was a major research breakthrough, yielding a new tool to study the intestinal epithelium (Sato et al., 2009; Sato and Clevers, 2013; Clevers, 2016). The

culture of intestinal organoids is a relatively simple process, requiring a tailored cell culture medium and hydrogels (e.g. basement membrane matrix secreted by Engelbreth-Holm-Swarm mouse sarcoma cells) serving as an extracellular matrix (ECM) substitute (Fatehullah et al., 2016). The resulting 3D multicellular constructs demonstrate an *in vivo*-like architecture with crypt-villus structures surrounding a central lumen and contain both proliferating and differentiated cell types. However, the enclosed position of the lumen hinders access to the apical surface of the epithelium, thus limiting studies related to nutrient uptake and host-microbiome/pathogen interactions. To overcome this, three different approaches have been taken so far. The first is the use of microinjection techniques where microbes or other infectious agents are injected directly to the lumen of organoids (Bartfeld et al., 2015; Hill et al., 2017; Williamson et al., 2018). This is a labor-intensive, time-consuming and often even disruptive process. The second is the formation of 2D cell monolayers by dissociating organoids (VanDussen et al., 2015; Kozuka et al., 2017; Wang et al., 2017; Altay et al., 2019). Although, in this way, access to both the apical and basolateral sides is granted, the 3D tissue-like structure of the organoids is lost thus making the system less physiologically relevant. Finally, the third method is the establishment of organoid models with reversed polarity (Co et al., 2019, 2021; Nash et al., 2021; Stroulios et al., 2021). In this case, the apical surface of the epithelium is facing the cell culture media thus allowing direct access to it. This method has been applied to human (Co et al., 2019, 2021; Stroulios et al., 2021), porcine (Li et al., 2020) and chicken (Nash et al., 2021) primary cell-derived intestinal organoids.

Here, we report the development of an intestinal organoid model with reversed polarity using pluripotent stem cells (PSCs). Following a stepwise directed differentiation protocol, we generated organoids consisting of a simple columnar epithelium patterned into crypt-like and villus-like structures. They contain the major intestinal differentiated cell types and are surrounded by a mesenchymal compartment. In our novel microwell-based culture protocol, the original embedding of organoids in a solid matrix was replaced by a suspension system, which allowed for a uniform, long-term reversal of the epithelial polarity. These novel pluripotent stem cell-derived apical-out organoids are a powerful new tool for studies relating but not limited to infectious diseases, gut microbiota, nutrient absorption and drug metabolism.

## **Materials and Methods**

### Maintenance of PSCs

The human embryonic stem cell line WA09 (H9) was obtained from WiCell and the induced pluripotent stem cell line iPSC72\_3 was obtained by the Pluripotent Stem Cell Facility at Cincinnati Children's Hospital Medical Center. ES and iPSC cell lines were maintained in feeder-free conditions on Matrigel (Corning®) using mTESR®1 (StemCell Technologies). Colonies were passaged every four to five days depending on colony density using Gentle Cell Dissociation reagent (StemCell Technologies).

### Fabrication and preparation of microwell arrays

Polymer film based microwell arrays were fabricated by microthermforming as described previously (Giselbrecht et al., 2006; Kakni et al., 2020). Every array accommodated 289 U-bottomed microwells and each microwell had a diameter of 500 µm and a depth of approximately 300 µm. Prior to cell culture, microwell arrays were sterilized in a graded series of 2-propanol (VWR) (100%–70%–50%–25%–10%) and then washed twice with Dulbecco's phosphate buffered saline (PBS; Sigma-Aldrich). Subsequently, they were placed at the bottom of non-treated 24-well plates, where they were kept in place by elastomeric O-rings (ERIKS).

### Differentiation of PSCs to definitive endoderm and hindgut in microwells

The protocol for directed differentiation of intestinal organoids was carried out as previously described (Spence et al., 2011) with small modifications. PSCs were dissociated into single cells using TrypLE™ Express Enzyme (Thermofisher) and seeded on microwell arrays at a density of 1000 cells/ microwell in mTesR1 supplemented with Y-27632 (10 µM; Tocris) to create embryoid bodies (EBs). The following three days, EBs were treated with Activin A (100 ng/ml; Cell guidance systems) in RPMI 1640 (Thermofisher) medium supplemented with increasing concentrations (0%, 0.2%, 2%) of Hyclone defined fetal bovine serum (dFBS; Fisher scientific). For hindgut specification, the DE spheroids were treated with a combination of FGF4 (500 ng/ml; R&D Systems) and CHIR99021 (3 µM; Stemgent) for four additional days. The medium was exchanged daily. In order to avoid the removal of the spheroids from the microwells, the plate was slightly tilted and the medium was aspirated from the sidewalls.

### Differentiation towards intestinal organoids

For the apical-in intestinal organoids, hindgut spheroids were collected, suspended in 50 µl Matrigel and plated as droplets into tissue culture treated 24-well plates. After letting the Matrigel solidify at 37°C and 5% CO<sub>2</sub> for 15 min, the Matrigel drops

containing the spheroids, were overlaid with Advanced DMEM/F-12 supplemented with B27, N2, Hepes, penicillin/streptomycin, L-glutamine (all Thermofisher), EGF (50 ng/ml; R&D systems), Noggin (100 ng/ml; R&D systems) and R-Spondin (500 ng/ml; R&D systems). The medium was refreshed every four days.

For the apical-out intestinal organoids, on day 8 the hindgut spheroids were placed in suspension culture in non-tissue culture-treated 6-well plates (plates with different sizes can be used as well). To avoid surface-cell adherence, the plates were coated with 1% Pluronic solution in PBS (Sigma-Aldrich) for 2 h at 37°C and then washed two times with PBS. The medium used, had the same composition as the apical-in organoids, but in this case Matrigel was added as a medium supplement at a concentration of 2%.

#### Immunofluorescence and confocal microscopy

EBs, DE spheroids, hindgut spheroids and intestinal organoids were fixed with 4% paraformaldehyde (VWR) in PBS for 30 min. Following that, permeabilization was performed with 0.5% Triton X-100 (Merck) in PBS for another 30 min at room temperature (RT). Blocking was performed with 5% donkey serum (VWR) in permeabilization solution for 30 min at RT as well. Afterwards, primary antibodies were incubated overnight at 4°C and the next day secondary antibodies were added for 2h at RT. Finally, samples were counterstained with 4',6-diamidino-2-phenylindole (DAPI) (Sigma-Aldrich) and mounted with Lab Vision PermaFluor Aqueous Mounting Medium (Thermofisher). A full list of antibodies is provided in the supplementary material. For the imaging of the immunostained samples, a confocal laser scanning microscopy (Leica TCS SP8) was utilized and the images were processed with ImageJ. Quantification was performed using the open access software QuPath.

#### RNA isolation and quantitative Real-Time PCR (qPCR)

Organoids were collected and the total RNA was extracted using the RNeasy Mini Kit (Qiagen) according to the manufacturer instructions. For the cDNA synthesis, the iScript cDNA Synthesis Kit (Bio-Rad) was utilized. Finally, qPCR was carried out using the iQ SYBR Green Supermix (Bio-Rad), on a CFX96 Real-Time PCR Detection System (Bio-Rad). Gene expression for each sample was normalized using the glyceraldehyde-3-phosphatedehydrogenase (*GAPDH*) or the hypoxanthine phosphoribosyltransferase (*HPRT*) housekeeping genes. *GAPDH* was used for DE and hindgut spheroids, whereas *HPRT* for intestinal organoids. The expression of *GAPDH* could be affected by the different oxygen levels(Caradec et al., 2010) we



expect between hydrogel embedded and suspension organoids, thus we chose to use *HPRT* for these samples. Data analysis followed the  $2^{-\Delta\Delta Ct}$  method. The results are representative of three independent experiments. The primer sequences are listed in the supplementary material.

#### Scanning Electron Microscopy (SEM)

Organoids were chemically fixed for 3 hours at room temperature with 1.5% glutaraldehyde in 0.067 M cacodylate buffered to pH 7.4 and 1% sucrose. Then they were washed with 0.1 M cacodylate buffer and postfixed with 1% osmium tetroxide in the same buffer containing 1.5% potassium ferricyanide for 1h in the dark at 4°C. After rinsing with MQ, organoids were dehydrated at RT in a graded ethanol series (70, 90, up to 100%). Then, organoids were dried using HMDS (Hexamethyldisilazane) (> 99.9%, Sigma Aldrich, Germany). After HMDS treatment, the samples were mounted on SEM stubs, coated with a thin layer of gold by a sputter coater SC7620 (Quorum Technologies, UK) and examined with the electron microscope (Jeol JSM-IT200, Japan).

#### Transmission Electron Microscopy (TEM)

Organoids were chemically fixed for 3 hours at room temperature with 1.5% glutaraldehyde in 0.067 M cacodylate buffered to pH 7.4 and 1% sucrose. Then they were washed with 0.1M cacodylate buffer and postfixed with 1% osmium tetroxide in the same buffer containing 1.5% potassium ferricyanide for 1h in the dark at 4°C. After rinsing with MQ, organoids were dehydrated at RT in a graded ethanol series (70, 90, up to 100%), infiltrated with Epon, embedded in the same resin and polymerized for 48h at 60°C. Ultrathin sections of 60 nm were cut using a diamond knife (Diatome) on a Leica UC7 ultramicrotome, and transferred onto 50 Mesh copper grids covered with a Formvar and carbon film. Sections were stained with 2% uranyl acetate in 50% ethanol and lead citrate. Then, sections were observed in a Tecnai T12 Electron Microscope equipped with an Eagle 4kx4k CCD camera (Thermofisher) or Veleta 2kx2k CCD camera (Olympus Soft Imaging, Germany).

#### Statistical analysis

All statistical analysis was performed using GraphPad Prism 9 software. Student's two-tailed t-test with Welch's correction (two groups) or one-way ANOVA followed by Tukey's test (> two groups) were used to determine statistical significance. Significant differences were defined as  $P < 0.05$ . P values of statistical significance are represented as \*\*\*\*P < 0.0001, \*\*\*P < 0.001, \*\*P < 0.01, and \*P < 0.05. Error bars in figures indicate standard error of the mean (S.E.M.).

## **Results**

### Embryoid body-based differentiation towards intestinal tissue

The generation of our PSC-derived intestinal organoids is based on the directed differentiation method developed by Spence and colleagues (Spence et al., 2011). Here, the human embryonic and induced pluripotent stem cells were dissociated into single cells and seeded onto microwell arrays in order to promote the formation of uniform embryoid bodies (EBs). Next, these EBs were differentiated stepwise towards intestinal organoids (definitive endoderm → hindgut → intestinal organoids) (Figure 1A). The microwell arrays were produced in-house with a custom-made design that fits the needs of our experiments. We identified that around 1000 cells per EB were adequate for the successful formation of intestinal tissue. These cell aggregates had a diameter of approximately 200  $\mu\text{m}$  (Figure 1B). Aggregates of smaller diameter failed to generate intestinal tissue later on. Additionally, to ensure that our cells remain pluripotent after the formation of EBs, we performed immunofluorescence stainings for the widely used pluripotency markers Oct3/4 and Nanog. The results showed co-localization of these markers, thus confirming their applicability for downstream differentiation. Initiation of the differentiation within a 2D culture system demands tightly regulated seeding densities and equal distribution of cells around the cell culture plates for the successful differentiation of PSCs towards intestinal organoids (McCracken et al., 2011). This process is very limiting and often fails. Our system overcomes this obstacle since the use of microwells offers a simple method to create uniform 3D EBs that can be used as the starting material for the differentiation towards intestinal tissue.

### Differentiation towards definitive endoderm and hindgut specification

The embryonic development of the intestine initiates during gastrulation when the primary germ layers, the endoderm, the mesoderm and the ectoderm, are formed. Specifically, the intestine derives from the definitive endoderm (DE), which following gastrulation transforms into the primitive gut tube that becomes regionally specified into the foregut, midgut and hindgut along the anterior-posterior axis. After this, the mid- and hindgut will give rise to the intestine (Zorn and Wells, 2009). To generate DE, we treated our EBs in the microwells with Activin-A, which is a nodal-related TGF- $\beta$  molecule (Figure 1D). After three days of treatment, immunofluorescence stainings showed that 90% of the cells in H9-derived DE spheroids (Figure 2A, B) and 92% of the cells in iPSC-derived DE spheroids (Figure S1A, B) were co-expressing the known DE markers SRY-Box Transcription Factor 17 (SOX17) and Forkhead Box A2 (FOXA2). Gene expression levels confirmed those results demonstrating a significant increase of *SOX17* and *FOXA2*

expression, compared to untreated cells, in DE spheroids derived from both cell sources (Figure 2C; Figure S1C). We also detected the expression of T-Box Transcription Factor T (*TBXT*), indicating the presence of mesoderm in our cultures, similar to what was previously reported by Spence et al.

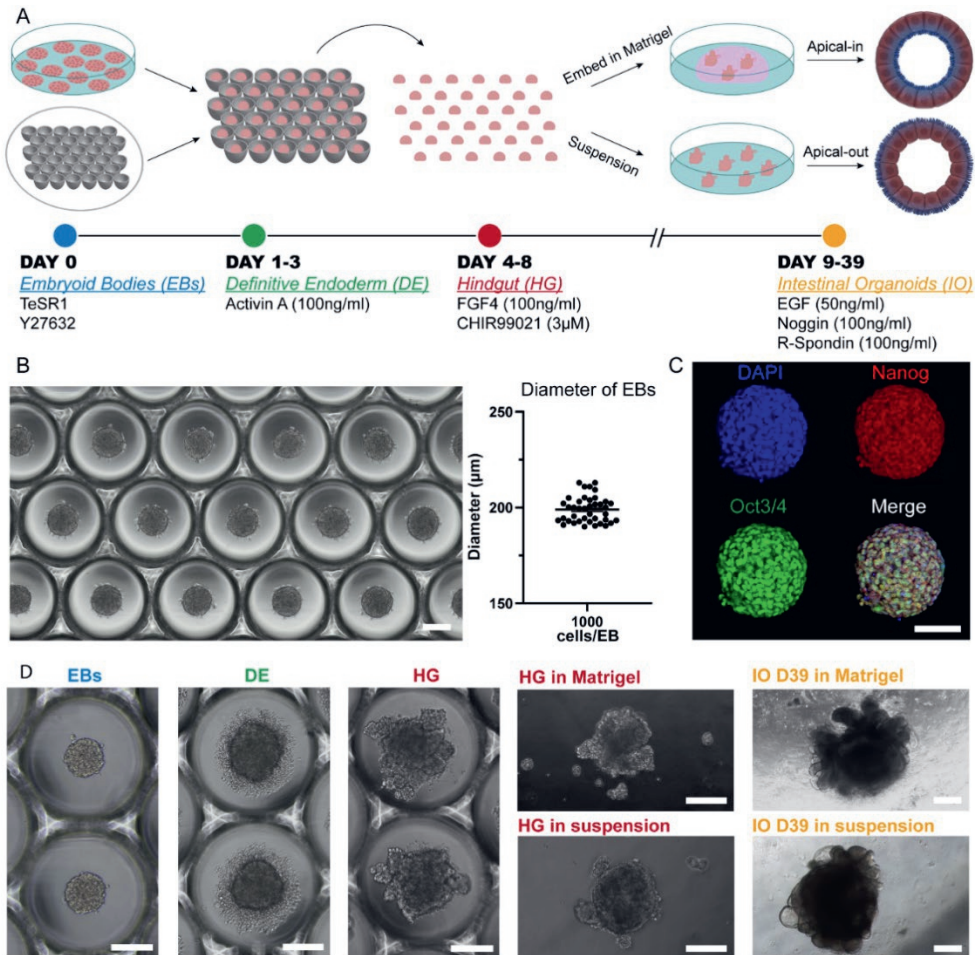


**Figure 1:** Overview of the *in vitro* culture system established for the directed differentiation of EBs towards intestinal organoids. (A) Schematic representation of the protocol. (B) Formation of EBs in thermoformed microwell arrays. The graph represents the diameter of EBs 24h after the cell seeding. Each point displays an individual EB; horizontal line and error bar indicate mean  $\pm$  S.E.M. ( $n = 3$ ). Scale bar: 200  $\mu$ m. (C) Fluorescence microscopy images of undifferentiated EBs stained for the pluripotency markers Oct3/4 (green) and Nanog (red) and counterstained with DAPI (blue). Scale bar: 100  $\mu$ m. (D) Bright-field images representative of each stage of the differentiation. Scale bars: 200  $\mu$ m.

To achieve hindgut specification, an appropriate combination of growth factors targeting the Fibroblast Growth Factor (FGF) and Wnt-related integration site (Wnt) pathways is required to repress the foregut and promote the hindgut development (Dessimoz et al., 2006; McCracken and Wells, 2017). For our experiments, we used a combination of FGF4 (500 ng/ml) and CHIR99021 (3  $\mu$ M). Four days of treatment were adequate to promote the hindgut endoderm specification in our DE spheroids (Figure 1D). The hindgut marker Caudal Type Homeobox 2 (*CDX2*) was expressed in 91% of the cells in H9-derived hindgut spheroids (Figure 2D, E) and in 90% of the cells in iPSC-derived ones (Figure S1D, E). The high levels of *CDX2* expression were confirmed by qPCR (Figure 2F; Figure S1F). The foregut marker Albumin (*ALB*) had very low expression without statistical significance, when compared to our undifferentiated controls, while Pancreatic and Duodenal Homeobox 1 (*PDX1*) was not detected. Mesenchyme was identified in our hindgut spheroids using qPCR, as indicated by the expression of Vimentin (*VIM*) (Figure 2F; Figure S1F). Overall, our results demonstrate that following a directed differentiation method, EBs can accurately recapitulate both the DE and the hindgut.

#### Reversal of epithelial polarity in organoids cultured in suspension

The intestinal epithelium is a highly organized tissue and the establishment of proper epithelial polarity is instrumental for balancing the communication between the lumen and surrounding body tissues. In the original protocol for PSC-derived intestinal organoids (Spence et al., 2011), hindgut spheroids are embedded in Matrigel thus leading to the formation of a simple columnar polarized epithelium where the apical surface is facing the enclosed lumen and the basal side the surrounding mesenchyme. In a similar manner, when we embedded our hindgut spheroids in Matrigel (Figure 1D), the resulting organoids demonstrated the same strong apical-basolateral polarity. Specifically, immunofluorescence stainings showed that Phalloidin, which marks the apical side of the organoids, is expressed at the inner side of the organoids facing the lumen, whereas E-cadherin, which marks the basolateral side, is expressed in the outer part facing the culture medium. The immunostainings were performed at days 7, 15, 30 and 50 after embedding the hindgut spheroids in Matrigel for both H9- and iPSC-derived organoids monitoring their structural organization during the whole culture period (Figure 3A; Figures S2 and S3). In addition, stainings for Villin, a marker of the apical side of the enterocytes, and Phalloidin (Figure 3B) verified our results.

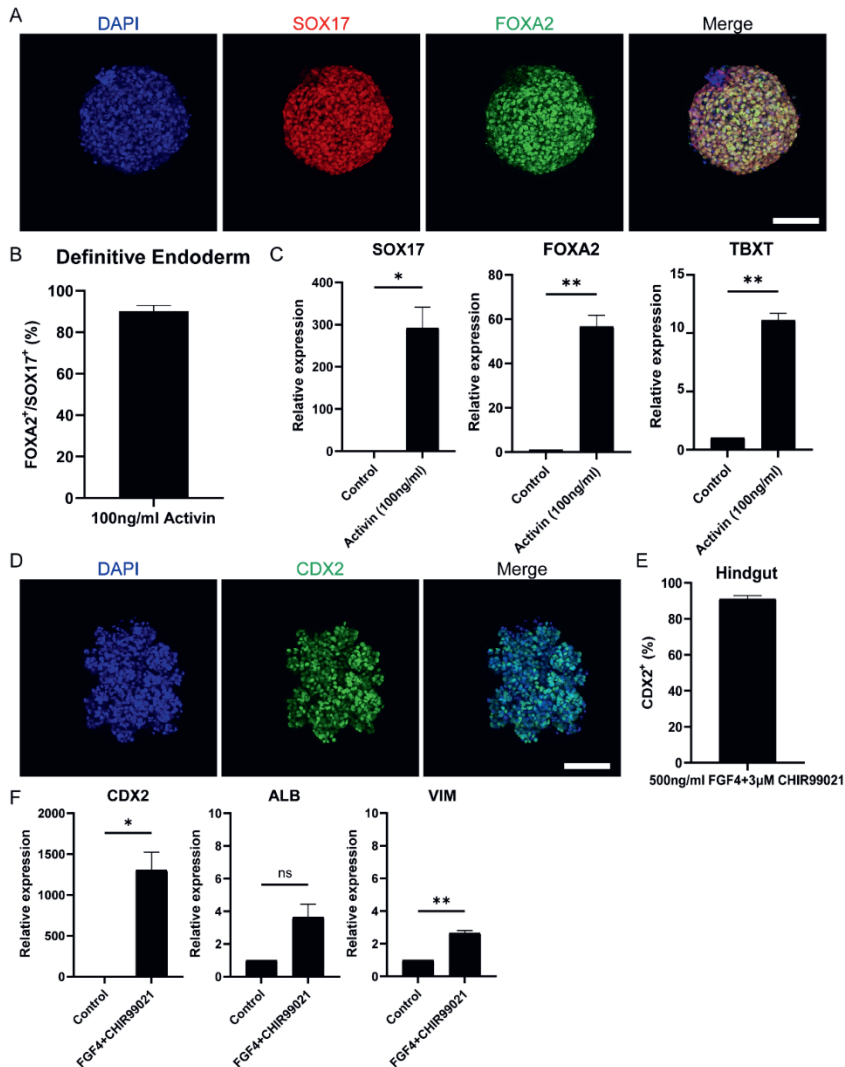


**Figure 2:** Differentiation towards definitive endoderm followed by hindgut specification. (A) H9-derived EBs were treated with 100 ng/ml Activin and the resulting spheroids were stained with the DE markers: SOX17 (red) and FOXA2 (green) and counterstained with DAPI (blue). Scale bar: 100  $\mu$ m. (B) Quantification of the fluorescent images showed that about 92% of the cells in Activin-treated EBs are co-expressing SOX17 and FOXA2. (C) qRT-PCR showed significantly increased expression of the DE genes *SOX17* and *FOXA2* and the mesoderm marker *TBXT* but in lower amounts. (D) DE spheroids were further treated with FGF4 and CHIR99021 to induce hindgut specification. After four days of treatment, the spheroids were stained for the hindgut marker CDX2. Scale bar: 100  $\mu$ m. (E) Quantification of the fluorescent images showed that about 90% of the cells were CDX2<sup>+</sup>. (F) qRT-PCR confirmed the robust expression of *CDX2*, whereas there was no significant expression of the foregut marker *ALB*. Low levels of the mesenchymal marker *VIM* were also detected. Error bars indicate mean  $\pm$  S.E.M. (n = 3).

To facilitate the studies of interactions between the epithelium and luminal contents, we aimed to reverse the polarity of our organoids while maintaining their 3D structure. To achieve that, we developed a suspension culture method that allows for hindgut spheroids to mature into intestinal tissue without being embedded in Matrigel (Figure 1A, D). Unlike the original protocol, Matrigel was added at a low concentration to the medium (2%). Already after seven days, the resulting organoids presented a reversed organization where the apical side was facing the culture medium and the basal side was facing the lumen. Notably, throughout the suspension method, the organoids were grown and matured solely in suspension, whereas in similar protocols the organoids are initially embedded in Matrigel and later on the Matrigel is removed in order to reverse the polarity (Co et al., 2019; Nash et al., 2021). We could show that organoids grown in suspension demonstrate a similar architecture to the Matrigel-embedded ones throughout the culture period, with crypt-villus structures surrounding a central lumen (Figure S4). Immunofluorescence stainings evidence the F-actin rich brush border (marked by Phalloidin) and the apical side of the enterocytes (marked by Villin) in the outer part of the organoids thus verifying the polarity reversal at all time-points in both H9- and iPSC-derived organoids (Figure 3A, B; Figures S2 and S3). Additionally, scanning electron microscopy (SEM) was utilized to verify the two different apico-basolateral organizations. Specifically, the Matrigel-embedded organoids seem to have a “smoother surface”, which is anticipated since the basal side of the organoids is visualized, whereas the suspension organoids exhibit a “rougher surface” in which we can clearly identify the presence of microvilli, further proving that a functional apical side of the organoids is facing outwards (Figure 3C). Finally, the presence of microvilli in reversed positions is illustrated by transmission electron microscopy (TEM; Figure 3D).

To examine the plasticity of these different polarity models, seven days before reaching full maturation (embedded/suspension day 23), organoids that were initially embedded in Matrigel were placed in suspension culture and organoids that were initially in suspension, were embedded in Matrigel for one week. Following this ECM manipulation, the samples were immunofluorescently labelled for E-Cadherin and Phalloidin and the amount of organoids that fully or partially reversed their polarity was quantified (Figure S5). Interestingly, none of the organoids (H9- or iPSC-derived) that were isolated from Matrigel and placed in suspension changed their polarity during these seven days. This indicates that the protocols (Co et al., 2019; Nash et al., 2021) previously described for reversing the polarity of established adult stem cell-derived organoids cannot be applied to reverse the polarity of PSC-derived organoids. We hypothesize that a possibly longer time is required to

manipulate the apico-basolateral organization of these organoids. In contrast to this, 90% of H9-derived and 85% of iPSC-derived organoids that were initially in suspension and then embedded in Matrigel reversed their polarity (apical side now facing the lumen). The remaining 10% and 15% of the organoids, respectively, demonstrated an intermediate polarity reversal, where the basal side was facing outwards in some regions of the organoids and in some other regions the apical side was facing outwards, suggesting that the apical-out intestinal organoids are more prone to polarity reversal when embedded in Matrigel.

#### Apical-out intestinal organoids display various intestinal cell types

Besides structural organization, the proper function of the intestine is highly dependent on the presence of different intestinal epithelial cell lineages. Indeed, one of the key advantages of organoids as an *in vitro* model is that they can recapitulate to a great extent the cellular diversity of the *in vivo* intestinal epithelium. Therefore, in a next step we verified that our apical-out organoids (derived from H9 or iPSCs) are able to fully mature and differentiate towards the major intestinal cell types. To visualize the intestinal cell differentiation, we used immunofluorescence against the proliferation marker Ki67 and Phalloidin (Figure 4A; Figure S6A), the intestinal differentiation marker CDX2, the goblet cell marker Mucin 2 (MUC2) (Figure 4B; Figure S6B) and the enteroendocrine marker Synaptophysin (Figure 4C; Figure S6C). These stainings were performed at 30 days post Matrigel embedment of hindgut organoids or their transfer to suspension culture. This time-point was selected according to Spence et al., 2011 and Janssen et al., 2020, who demonstrated that intestinal organoids embedded in Matrigel can reach sufficient maturation after approximately 28 days. Organoids from both culture conditions showed similar expression patterns of the mentioned markers. Further characterization of these organoids was performed using relative gene expression quantification. More specifically, the transcriptional expression of multiple intestinal cell lineages was quantified over three developmental stages: days 15, 30 and 50 (Figure 4D; Figure S6D). The expression of the intestinal differentiation marker *CDX2*, gradually increased between days 15 and 30, whereas at day 50 a significant decrease was observed. The proliferation markers sex determining region Y-box 9 (*SOX9*), Krueppel-like factor 5 (*KLF5*) and Achaete scute-like 2 (*ASCL2*) showed a similar trend with their peak expression at day 30, whereas leucine-rich repeat-containing G-protein-coupled receptor 5 (*LGR5*) expression peaked at day 15 and was reduced at later time-points. Lysozyme, which marks the presence of Paneth cells, was expressed at a low level on day 15 but was remarkably increased by day 30. The high expression levels were maintained over 50 days of culture. The expressions of Villin 1 (*VILI*) (brush border of the enterocytes) and Chromogranin A (*CHGA*)

(enteroendocrine cells) peaked at day 30 and decreased later on as well. Finally, in both apical-in and apical-out organoids we identified the presence of mesenchyme. The distal hindgut mesoderm marker Homeobox A13 (*HOXA13*) peaked at day 15 and gradually decreased over later time-points. In contrast, the expression of the mesenchymal markers Forkhead Box F1 (*FOXF1*) and *VIM* remained unchanged between days 15 and 30, whereas on day 50 it was notably reduced. The expression patterns of the basal-out and apical-out organoids were very similar and no statistical significance was identified at any time-point (both in H9- and iPSC-derived organoids). These results indicate that organoids on day 15 already express intestine-specific markers but are fairly immature, whereas by day 30 the *in vitro* maturation culminates. This is in accordance with findings from Spence et al., 2011 and Janssen et al., 2020. After 50 days in culture, we observed a general decrease in the expression of most markers, although still in detectable levels, showing that organoids' functionality in culture gradually deteriorates from day 30 day. Engraftment of organoids in mice would secure further maturation(Watson et al., 2014), overcoming the short-term culturing periods allowed by *in vitro* methods. However, it is unknown whether the apical-out organoids would be able to maintain their polarity.



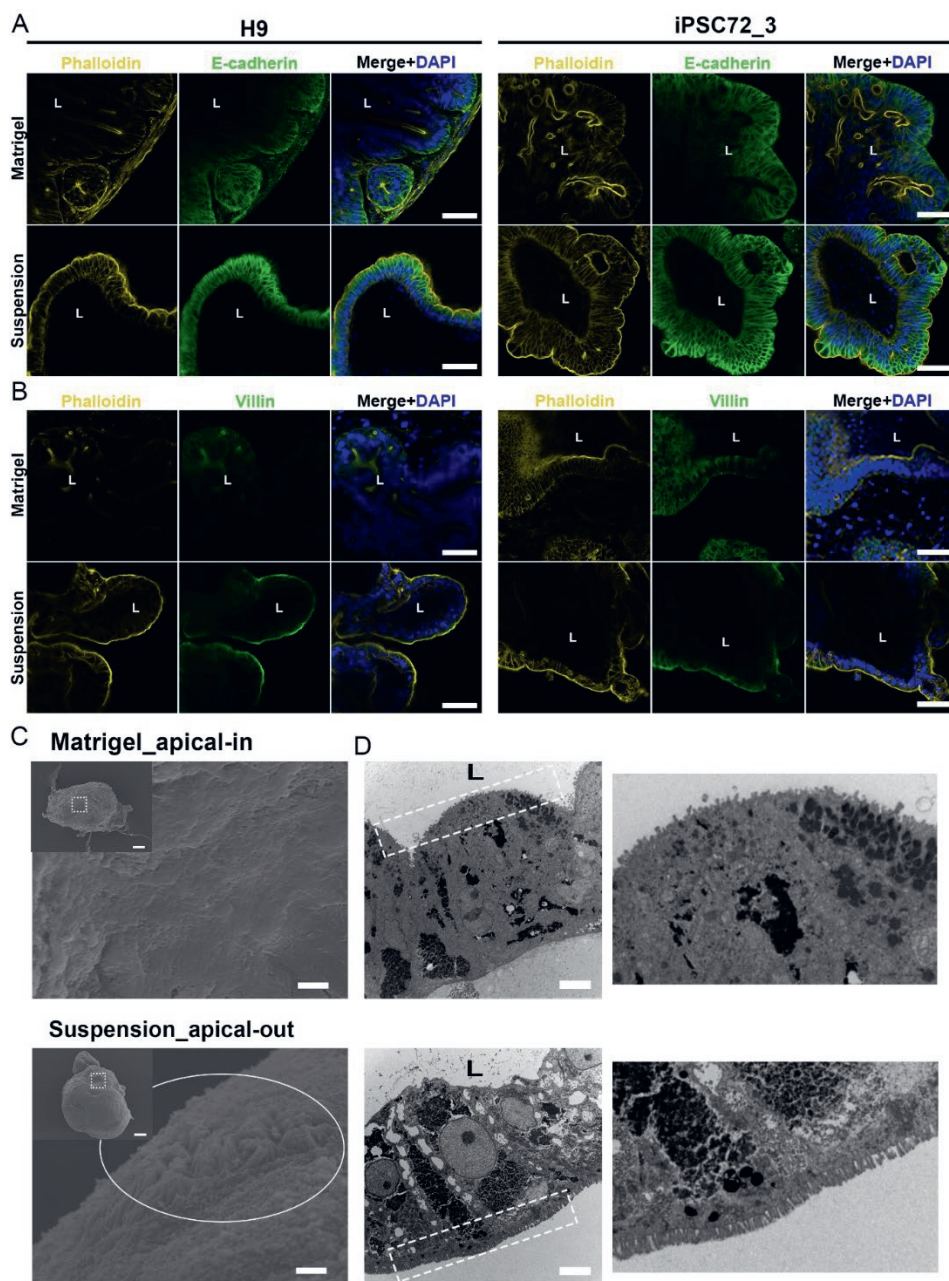


**Figure 3:** Apico-basolateral organization of human intestinal organoids after 30 days in culture. (A) Fluorescent staining of embedded (top) and suspension (bottom) intestinal organoids for the basolateral marker E-cadherin (green) and the apical marker Phalloidin (yellow) shows reversed polarity of the suspension organoids. The left panel demonstrates H9-derived organoids and the right one iPSC72\_3-derived organoids. Scale bar: 100  $\mu$ m. (B) These results were confirmed with Villin (green) and Phalloidin (yellow) stainings that were found to co-express in the apical side of the organoids. The left

panel demonstrates H9-derived organoids and thFe right one iPSC-derived organoids. Scale bar: 100  $\mu\text{m}$ . L: lumen. (C) SEM was performed in Matrigel embedded (top) and suspension (bottom) organoids showing the presence of microvilli (white circle) in the outer surface of the suspension organoids. Dashed squares represent the area magnified in the corresponding image. Scale bars: 100  $\mu\text{m}$  (inset) and 2  $\mu\text{m}$ . (D) TEM indicates that microvilli (white dotted squares) face the lumen in Matrigel embedded (top) organoids, whereas in suspension (bottom) organoids, microvilli face the outer surface. On the right, magnified images demonstrate the microvilli. Scale bars: 5  $\mu\text{m}$ .

## **Discussion**

In recent years, the advent of intestinal organoids has revolutionized the *in vitro* research of the intestinal epithelium. These organoids have been widely used in studies related to gut development, physiology and disease since they recapitulate the properties of the *in vivo* tissue with great fidelity. In the original method, the intestinal organoids demonstrate an organized structure, where the basal side is in contact with the ECM and facing outwards whereas the apical side is enclosed and facing the luminal compartment. Thus, access to the apical surface is restricted and microinjection techniques are required to deliver substances (Bartfeld et al., 2015; Hill et al., 2017; Williamson et al., 2018). Recent advances in the organoid field paved the way for easier access to the lumen by reversing epithelial polarity in adult stem cell-derived organoids (Co et al., 2019, 2021; Li et al., 2020; Giobbe et al., 2021; Nash et al., 2021), but whether the same method could be applied in PSC-derived organoids was uncertain. Here, we developed and validated a reversed polarity organoid model using PSCs. In these organoids the apical side is found on the outer surface of the organoids, and, thus, is directly accessible for testing compounds, particles or microbes. Apical-out organoids demonstrate similar functionality to the basal-out organoids as suggested by the retention of self-renewal capacity throughout the whole culture and the expression of all major intestinal cell types. One advantage of the apical-out organoids is that they are grown in a suspension system. In this way, the handling of organoids is uncomplicated since there is no viscous hydrogel surrounding them. This suggests that organoids can be easily selected and (re-) transferred e.g. into microwells for performing downstream experiments.

The intestinal epithelium acts as a highly selective barrier for the absorption, metabolism and release of nutrients and drugs. Currently, the investigation of these functions is mainly performed with cell monolayers (Transwell systems) and there are only few examples of organoid applications (Zietek et al., 2020; Youhanna and Lauschke, 2021). This is mainly due to the inaccessibility of the apical surface of the organoids. The formation of cell monolayers, either using cell lines (e.g. Caco-

2)(Sun et al., 2008) or dissociated organoids(VanDussen et al., 2015; Kozuka et al., 2017; Wang et al., 2017; Altay et al., 2019) provides access to both the apical and basal sides. However, in this case a large number of cells is required and usually several days of maturation. Also, the 3D organization is disrupted, thus making the system less physiologically relevant. Another limitation is that usually these monolayers are formed in Transwell systems, which restricts *in situ* monitoring, e.g. live cell imaging, during culture. In contrast to this, our apical-out intestinal organoids, both retain their 3D architecture and allow for easy tracking and monitoring throughout the culture period. Hence, apical-out organoids may represent a novel and improved model for nutrient uptake and drug absorption studies.

Although intestinal organoids constitute one of the most physiologically representative *in vitro* models, the integral gut microbiome is missing(Min et al., 2020). In order to incorporate this in organoid models, researchers utilize either microinjections or monolayer cultures. Reversing the polarity of organoids offers an easy access to the apical surface, in which the microbiota is residing *in vivo*. Hence, with this system, host-microbiome interactions can be studied simply by adding microorganisms in the culture medium of organoids. The same method can be applied for the study of host-pathogen interactions where unknown mechanisms of cell invasion can be explored, thus leading to novel, efficient therapies. First successful experiments with apical-out organoids and microorganisms have already been performed by Co et al., 2019; Li et al., 2020; Nash et al., 2021, but so far solely adult stem cell-derived organoids could be used for this. In case of PSC-derived organoids, microbial colonization and pathogen infections can be studied at different stages of development, which is particularly important since the early stages of gut microbiota development remains poorly understood(Senn et al., 2020).

In summary, apical-out intestinal organoids can be successfully generated in microwell arrays, from PSC-derived 3D EBs following a step-wise differentiation method. These organoids reflect the structural and functional characteristics of their *in vivo* counterparts. The long-term reversed polarity grants easy access to the apical compartment thus qualifying these organoids for a wide range of applications.

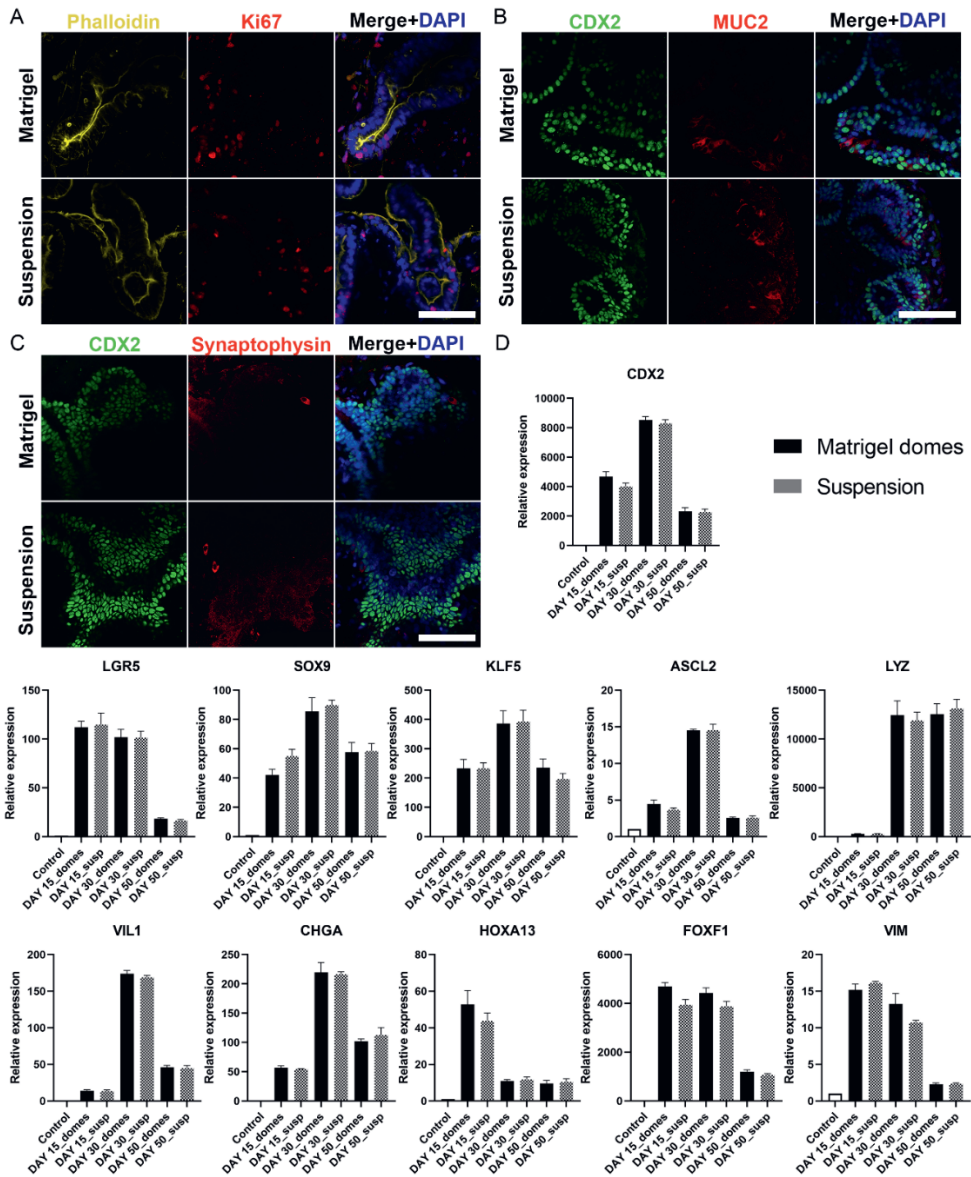


**Figure 4:** Characterization of H9-derived human intestinal organoids after 30 days in culture. (A-C) Immunofluorescence stainings of intestinal markers (Ki67: proliferative cells; CDX2: intestinal transcription factor; MUC2: goblet cells; Synaptophysin: enteroendocrine cells) show similar expression patterns in both embedded and suspension organoids. Scale bars: 100  $\mu$ m. (D) qRT-PCR analysis demonstrates the expression levels of proliferation genes (*LGR5*, *SOX9*, *KLF5*, *ASCL2*), intestinal differentiation genes (*CDX2*, *LYZ*, *VIL1*, *CHGA*, *HOXA13*) and mesenchymal genes (*FOXF1*, *VIM*) after 15, 30 and 50 days in culture. Untreated H9 cells were used as controls. Statistical analysis showed no significant difference between the organoids grown embedded in Matrigel and the organoids grown in suspension at any of the time-points. Error bars indicate mean  $\pm$  S.E.M. (n = 3).

## References

- Altay, G., Larrañaga, E., Tosi, S., Barriga, F. M., Batlle, E., Fernández-Majada, V., et al. (2019). Self-organized intestinal epithelial monolayers in crypt and villus-like domains show effective barrier function. *Sci. Reports* 2019 91 9, 1–14. doi:10.1038/s41598-019-46497-x.
- Bartfeld, S., Bayram, T., Van De Wetering, M., Huch, M., Begthel, H., Kujala, P., et al. (2015). In vitro expansion of human gastric epithelial stem cells and their responses to bacterial infection. *Gastroenterology* 148, 126-136.e6. doi:10.1053/j.gastro.2014.09.042.
- Caradec, J., Sirab, N., Keumeugni, C., Moutereau, S., Chimingqi, M., Matar, C., et al. (2010). ‘Desperate house genes’: the dramatic example of hypoxia. *Br. J. Cancer* 2010 1026 102, 1037–1043. doi:10.1038/sj.bjc.6605573.
- Clevers, H. (2016). Modeling Development and Disease with Organoids. *Cell* 165, 1586–1597. doi:10.1016/J.CELL.2016.05.082.
- Co, J. Y., Margalef-Català, M., Li, X., Mah, A. T., Kuo, C. J., Monack, D. M., et al. (2019). Controlling Epithelial Polarity: A Human Enteroid Model for Host-Pathogen Interactions. *Cell Rep.* 26, 2509-2520.e4. doi:10.1016/j.celrep.2019.01.108.
- Co, J. Y., Margalef-Català, M., Monack, D. M., and Amieva, M. R. (2021). Controlling the polarity of human gastrointestinal organoids to investigate epithelial biology and infectious diseases. *Nat. Protoc.* 2021 1611 16, 5171–5192. doi:10.1038/s41596-021-00607-0.
- Dessimoz, J., Opoka, R., Kordich, J. J., Grapin-Botton, A., and Wells, J. M. (2006). FGF signaling is necessary for establishing gut tube domains along the anterior–posterior axis in vivo. *Mech. Dev.* 123, 42–55. doi:10.1016/J.MOD.2005.10.001.
- Fatehullah, A., Tan, S. H., and Barker, N. (2016). Organoids as an in vitro model of human development and disease. *Nat. Cell Biol.* 18, 246–254. doi:10.1038/ncb3312.
- Giobbe, G. G., Bonfante, F., Jones, B. C., Gagliano, O., Luni, C., Zambaiti, E., et al. (2021). SARS-CoV-2 infection and replication in human gastric organoids. *Nat. Commun.* 2021 121 12, 1–14. doi:10.1038/s41467-021-26762-2.
- Giselbrecht, S., Gietzelt, T., Gottwald, E., Trautmann, C., Truckenmüller, R., Weibezahn, K. F., et al. (2006). 3D tissue culture substrates produced by microthermoforming of pre-processed polymer films. *Biomed. Microdevices* 8, 191–199. doi:10.1007/s10544-006-8174-8.
- Hill, D. R., Huang, S., Tsai, Y.-H., Spence, J. R., and Young, V. B. (2017). Real-time Measurement of Epithelial Barrier Permeability in Human Intestinal Organoids. *J. Vis. Exp.*, e56960. doi:10.3791/56960.
- Janssen, A. W. F., Duivenvoorde, L. P. M., Rijkers, D., Nijssen, R., Peijnenburg, A. A. C. M., Zande, M. van der, et al. (2020). Cytochrome P450 expression, induction

- and activity in human induced pluripotent stem cell-derived intestinal organoids and comparison with primary human intestinal epithelial cells and Caco-2 cells. *Arch. Toxicol.* 2020 953 95, 907–922. doi:10.1007/S00204-020-02953-6.
- Kakni, P., Hueber, R., Knoops, K., López-Iglesias, C., Truckenmüller, R., Habibovic, P., et al. (2020). Intestinal Organoid Culture in Polymer Film-Based Microwell Arrays. *Adv. Biosyst.*, 2000126. doi:10.1002/adbi.202000126.
- Klunder, L. J., Faber, K. N., Dijkstra, G., and van IJzendoorn, S. C. D. (2017). Mechanisms of Cell Polarity-Controlled Epithelial Homeostasis and Immunity in the Intestine. *Cold Spring Harb. Perspect. Biol.* 9, a027888. doi:10.1101/cshperspect.a027888.
- Kozuka, K., He, Y., Koo-McCoy, S., Kumaraswamy, P., Nie, B., Shaw, K., et al. (2017). Development and Characterization of a Human and Mouse Intestinal Epithelial Cell Monolayer Platform. *Stem Cell Reports* 9, 1976–1990. doi:10.1016/J.STEMCR.2017.10.013.
- Li, Y., Yang, N., Chen, J., Huang, X., Zhang, N., Yang, S., et al. (2020). Next-Generation Porcine Intestinal Organoids: an Apical-Out Organoid Model for Swine Enteric Virus Infection and Immune Response Investigations. *J. Virol.* 94. doi:10.1128/JVI.01006-20/ASSET/BCB7AACA-D4A6-4B5F-81F4-B11646C56C3C/ASSETS/GRAPHIC/JVI.01006-20-F0005.JPEG.
- McCracken, K. W., Howell, J. C., Wells, J. M., and Spence, J. R. (2011). Generating human intestinal tissue from pluripotent stem cells in vitro. *Nat. Protoc.* 6, 1920–1928. doi:10.1038/nprot.2011.410.
- Mccracken, K. W., and Wells, J. M. (2017). Seminars in Cell & Developmental Biology Mechanisms of embryonic stomach development. *Semin. Cell Dev. Biol.* 66, 36–42. doi:10.1016/j.semdb.2017.02.004.
- Min, S., Kim, S., and Cho, S. W. (2020). Gastrointestinal tract modeling using organoids engineered with cellular and microbiota niches. *Exp. Mol. Med.* 52, 227–237. doi:10.1038/s12276-020-0386-0.
- Nash, T. J., Morris, K. M., Mabbott, N. A., and Vervelde, L. (2021). Inside-out chicken enteroids with leukocyte component as a model to study host–pathogen interactions. *Commun. Biol.* 2021 41 4, 1–15. doi:10.1038/s42003-021-01901-z.
- Sato, T., and Clevers, H. (2013). Growing self-organizing mini-guts from a single intestinal stem cell: mechanism and applications. *Science* 340, 1190–4. doi:10.1126/science.1234852.
- Sato, T., Vries, R. G., Snippert, H. J., Van De Wetering, M., Barker, N., Stange, D. E., et al. (2009). Single Lgr5 stem cells build crypt-villus structures in vitro without a mesenchymal niche. *Nature* 459, 262–265. doi:10.1038/nature07935.
- Senn, V., Bassler, D., Choudhury, R., Scholkmann, F., Righini-Grunder, F., Vuille-

- dit-Bile, R. N., et al. (2020). Microbial Colonization From the Fetus to Early Childhood—A Comprehensive Review. *Front. Cell. Infect. Microbiol.* 10, 637. doi:10.3389/FCIMB.2020.573735/BIBTEX.
- Spence, J. R., Mayhew, C. N., Rankin, S. A., Kuhar, M. F., Vallance, J. E., Tolle, K., et al. (2011). Directed differentiation of human pluripotent stem cells into intestinal tissue in vitro. *Nature* 470, 105–109. doi:10.1038/nature09691.
- Stroulios, G., Stahl, M., Elstone, F., Chang, W., Louis, S., Eaves, A., et al. (2021). Culture Methods to Study Apical-Specific Interactions using Intestinal Organoid Models. *JoVE (Journal Vis. Exp.* 2021, e62330. doi:10.3791/62330.
- Sun, H., Chow, E. C. Y., Liu, S., Du, Y., and Pang, K. S. (2008). The Caco-2 cell monolayer: usefulness and limitations. <http://dx.doi.org/10.1517/17425255.4.4.395> 4, 395–411. doi:10.1517/17425255.4.4.395.
- VanDussen, K. L., Marinshaw, J. M., Shaikh, N., Miyoshi, H., Moon, C., Tarr, P. I., et al. (2015). Development of an enhanced human gastrointestinal epithelial culture system to facilitate patient-based assays. *Gut* 64, 911–920. doi:10.1136/GUTJNL-2013-306651.
- Wang, Y., DiSalvo, M., Gunasekara, D. B., Dutton, J., Proctor, A., Lebhar, M. S., et al. (2017). Self-renewing Monolayer of Primary Colonic or Rectal Epithelial Cells. *Cell. Mol. Gastroenterol. Hepatol.* 4, 165-182.e7. doi:10.1016/J.JCMGH.2017.02.011.
- Watson, C. L., Mahe, M. M., Múnera, J., Howell, J. C., Sundaram, N., Poling, H. M., et al. (2014). An in vivo model of human small intestine using pluripotent stem cells. *Nat. Med.* 20, 1310–1314. doi:10.1038/nm.3737.
- Williamson, I. A., Arnold, J. W., Samsa, L. A., Gaynor, L., DiSalvo, M., Cocchiario, J. L., et al. (2018). A High-Throughput Organoid Microinjection Platform to Study Gastrointestinal Microbiota and Luminal Physiology. *Cmgh* 6, 301–319. doi:10.1016/j.jcmgh.2018.05.004.
- Youhanna, S., and Lauschke, V. M. (2021). The Past, Present and Future of Intestinal In Vitro Cell Systems for Drug Absorption Studies. *J. Pharm. Sci.* 110, 50–65. doi:10.1016/J.XPHS.2020.07.001.
- Zietek, T., Giesbertz, P., Ewers, M., Reichart, F., Weinmüller, M., Urbauer, E., et al. (2020). Organoids to Study Intestinal Nutrient Transport, Drug Uptake and Metabolism – Update to the Human Model and Expansion of Applications. *Front. Bioeng. Biotechnol.* 0, 1065. doi:10.3389/FBIOE.2020.577656.
- Zorn, A. M., and Wells, J. M. (2009). Vertebrate Endoderm Development and Organ Formation. *Annu. Rev. Cell Dev. Biol.* 25, 221–251. doi:10.1146/annurev.cellbio.042308.113344.

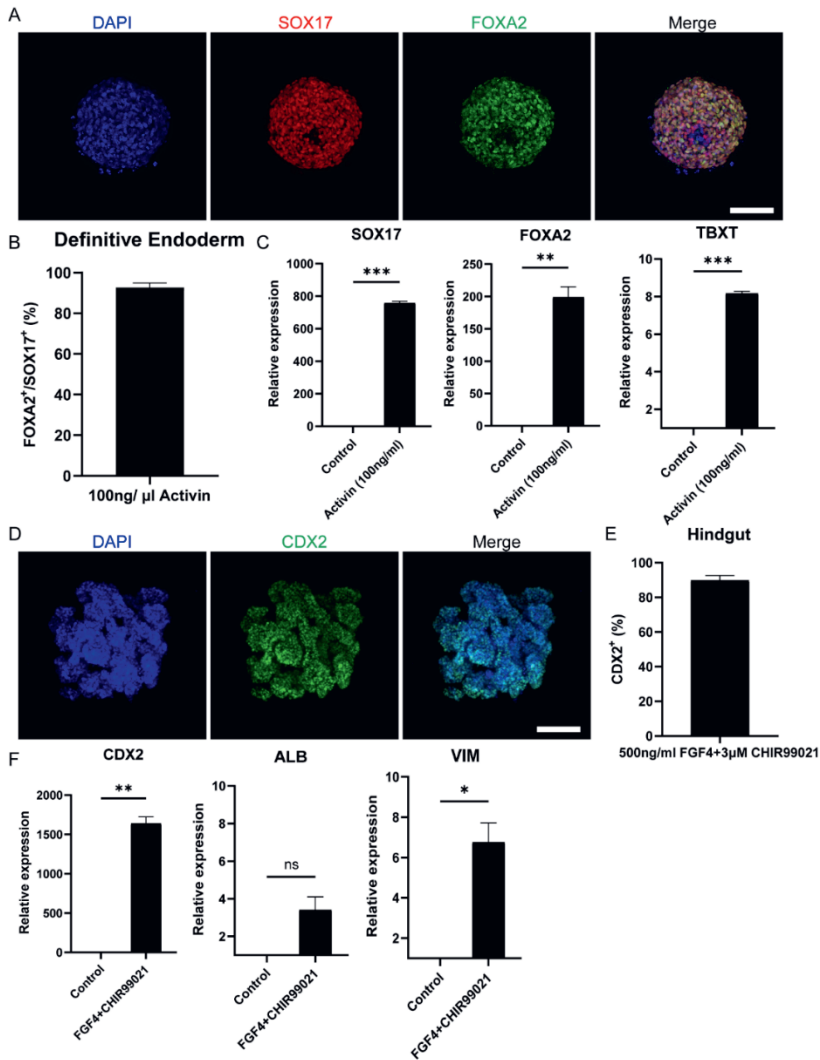
**Supporting Information**Supplementary Tables**Supplementary Table 1. List of antibodies**

Antibodies	Supplier	Host	Dilution
Oct-3/4	Santa Cruz	Mouse	1:500
Nanog	Abcam	Rabbit	1:500
E-Cadherin	Beckton Dickinson	Mouse	1:500
FOXA2	Novus Bio	Mouse	1:1000
SOX17	R&D	Goat	1:500
Ki67	Abcam	Rabbit	1:500
CDX2	Biogenex	Mouse	1:500
MUC2	Abcam	Rabbit	1:250
Synaptophysin 1	Synaptin systems	Guinea pig	1:200
Villin	Santa cruz	Mouse	1:250
Phalloidin 568	Invitrogen		1:500
Alexa Fluor 488	Invitrogen		1:500
Alexa Fluor 647	Invitrogen		1:500
Alexa Fluor 568	Invitrogen		1:500

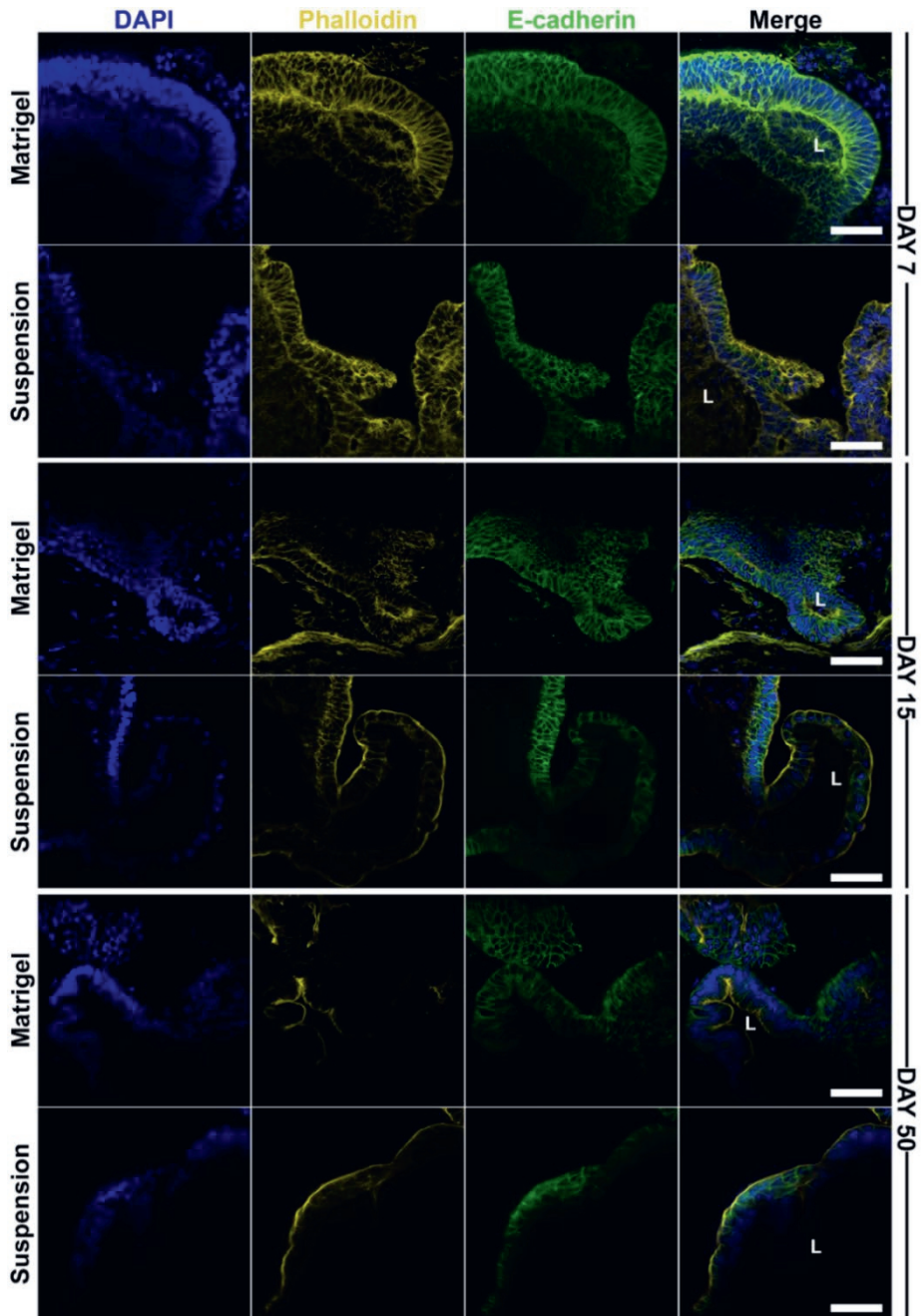
**Supplementary Table 2. Primer sequences**

Gene	5'-Forward- 3'	5'-Reverse- 3'
ALB	TGCAACTCTTCGTGAAACCTATG	ACATCAACCTCTGGTCTCACC
ASCL2	GCGTGAAGCTGGTGAACCTG	GGATGTACTCCACGGCTGAG
CDX2	GACGTGAGCATGTACCCTAGC	GCGTAGCCATTCCAGTCCT
CHGA	TAAAGGGGATACCGAGGTGATG	TCGGAGTGTCTCAAAACATTCC
FOXA2	CGACTGGAGCAGCTACTATGC	TACGTGTTTCATGCCGTTTCAT
FOXF1	GCGGCTTCCGAAGGAAATG	CAAGTGGCCGTTTCATCATGC
GAPDH	GGAGCGAGATCCCTCCAAAAT	GGCTGTTGTCATACTTCTCATGG
HOXA13	CTGCCCTATGGCTACTTCCGG	CCGGCGGTATCCATGTA
HPRT	GGACTCCAGATGTTTCCAACTC	TTGTTGTAGGATATGCCCTTGAC
KLF5	CCTGGTCCAGACAAGATGTGA	GAAGTGGTCTACGACTGAGGC
LGR5	CTCCCAGGTCTGGTGTGTTG	GAGGTCTAGGTAGGAGGTGAAG
LYZ	TCAATAGCCGCTACTGGTGTGA	ATCACGGACAACCCTCTTTGC
SOX17	GTGGACCGCACGGAATTTG	GGAGATTCACACCGGAGTCA
SOX9	AGCGAACGCACATCAAGAC	CTGTAGGCGATCTGTTGGGG
TBXT	TATGAGCCTCGAATCCACATAGT	CCTCGTTCTGATAAGCAGTCAC
VIL1	CTGAGCGCCCAAGTCAAAG	AGCAGTCACCATCGAAGAAGC
VIM	GACGCCATCAACACCGAGTT	CTTTGTCGTTGGTTAGCTGGT

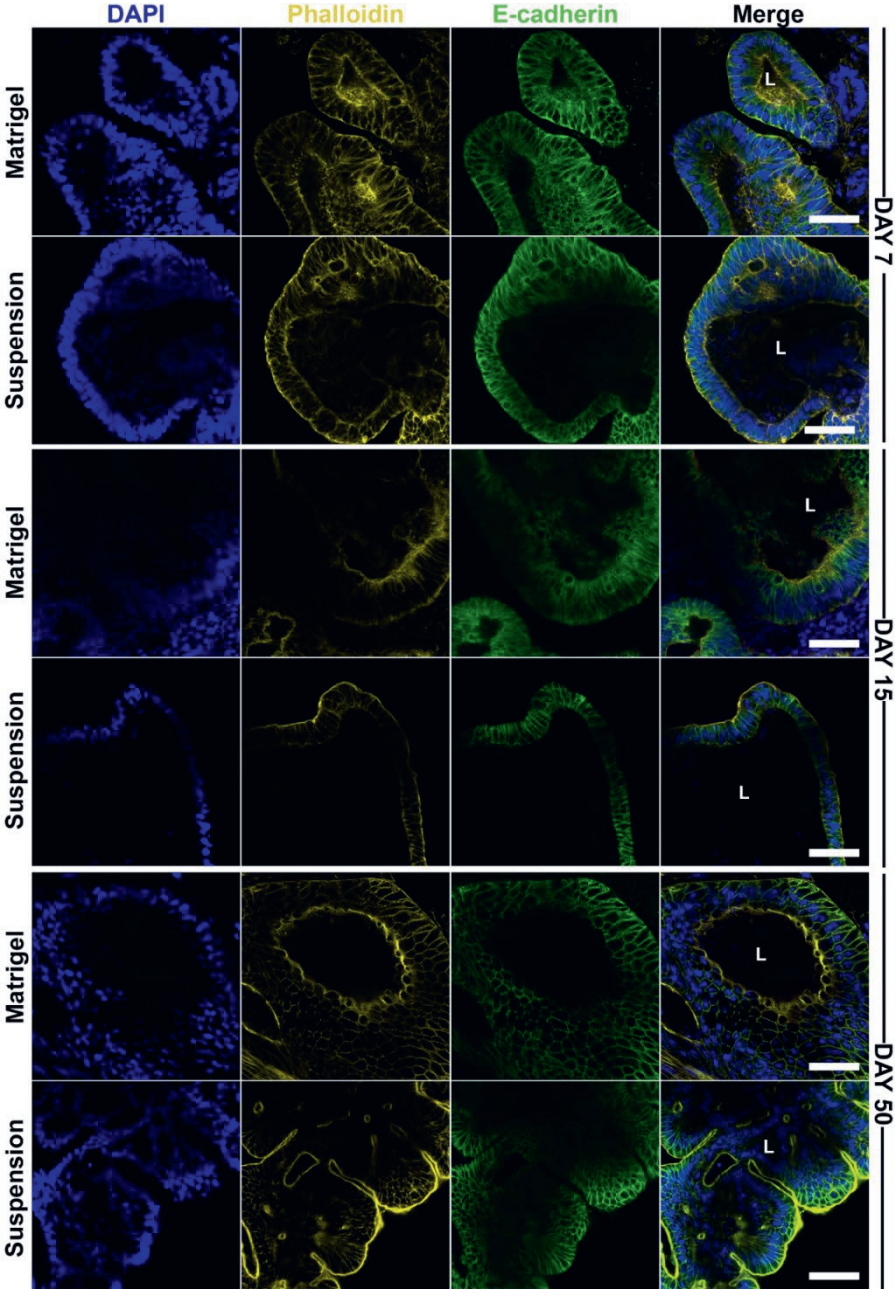




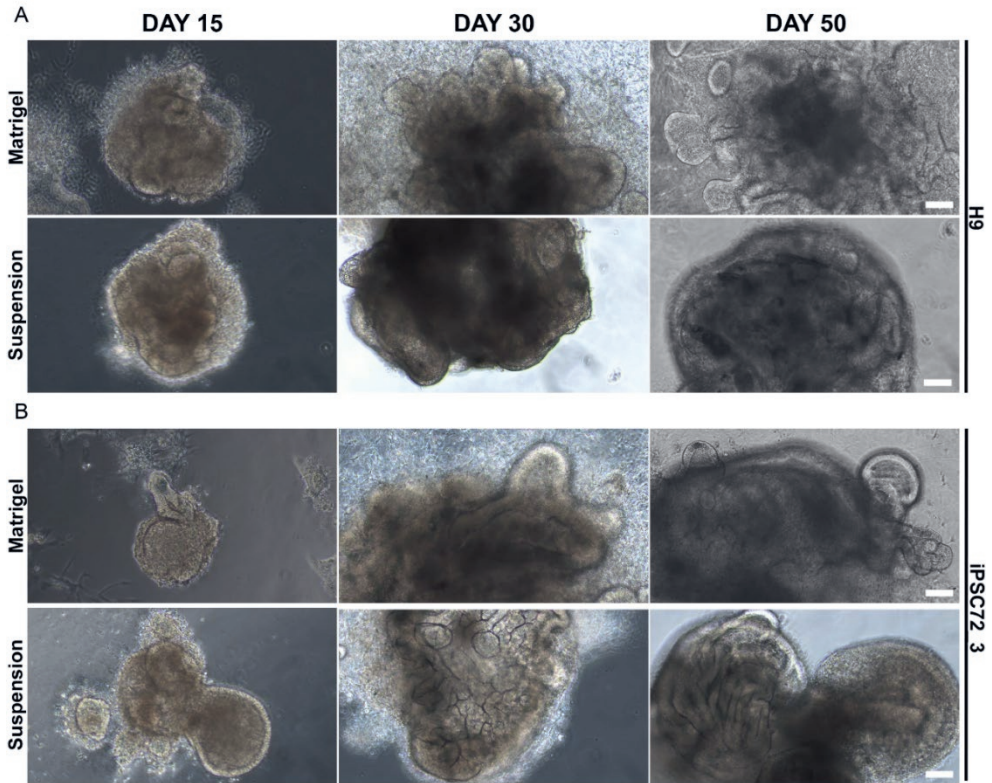
**Supplementary Figure 1:** Differentiation towards definitive endoderm followed by hindgut specification. (A) iPSC72\_3-derived EBs were treated with 100ng/ml Activin and the resulting spheroids were stained with the DE markers: SOX17 (red) and FOXA2 (green) and counterstained with DAPI (blue). Scale bar: 100µm. (B) Quantification of the fluorescent images showed that about 90% of the cells in Activin-treated EBs are co-expressing SOX17 and FOXA2. (C) qRT-PCR showed significantly increased expression of the DE genes SOX17 and FOXA2 and the mesoderm marker TBXT but in lower amounts. (D) DE spheroids were further treated with FGF4 and CHIR99021 to induce hindgut specification. After 4 days of treatment, the spheroids were stained for the hindgut marker CDX2. (E) Quantification of the fluorescent images showed that about 91% of the cells were CDX2<sup>+</sup>. (F) qRT-PCR confirmed the robust expression of CDX2, whereas there was no significant expression of the foregut marker ALB. Low levels of the mesenchymal marker VIM were also detected. Error bars indicate mean ± S.E.M. (n = 3).



**Supplementary Figure 2:** Apico-basolateral polar organization in different time-points. (A) H9-derived human intestinal organoids present reversed polarity (apical side out) already after 7 days in culture as shown by immunofluorescence staining with E-cadherin (green) and Phalloidin (yellow). Scale bar: 100 $\mu$ m. (B-C) Confocal imaging showed that these organoids maintain this organization after 15 (B) and even 50 days (C) in culture. Scale bar: 100 $\mu$ m.

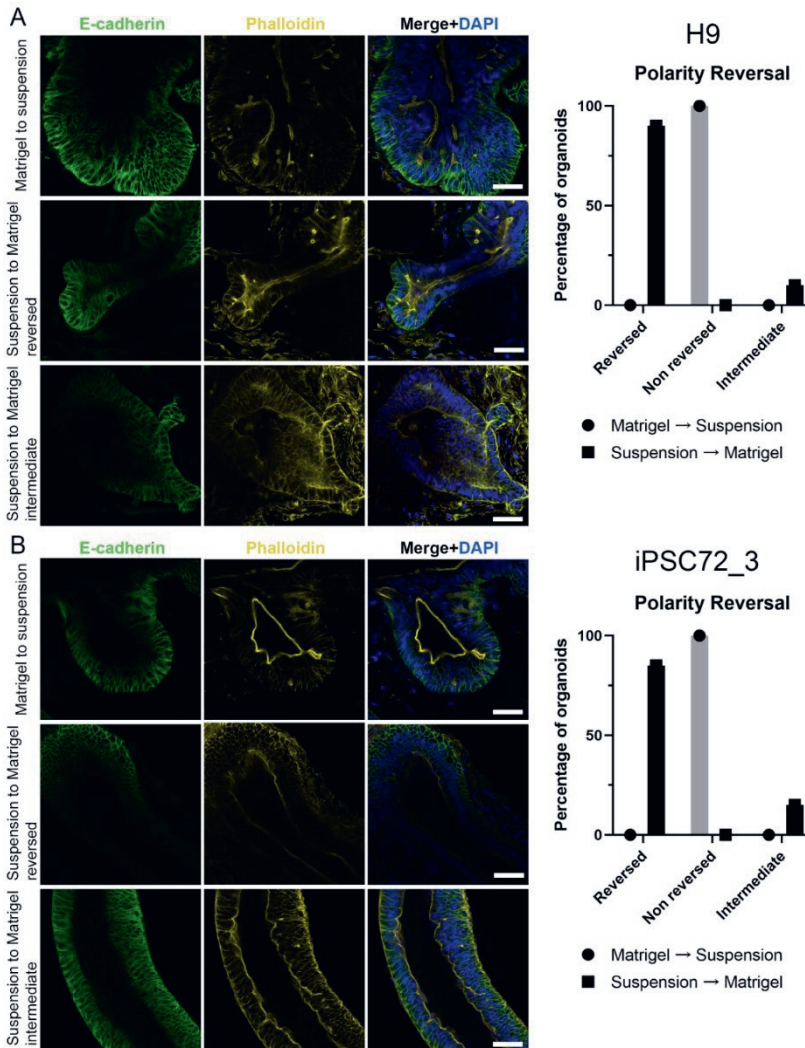


**Supplementary Figure 3:** Apico-basolateral polar organization in different time-points. (A) iPSC72\_3-derived human intestinal organoids present reversed polarity (apical side out) already after 7 days in culture as shown by immunofluorescence staining with E-cadherin (green) and Phalloidin (yellow). Scale bar:100µm. (B-C) Confocal imaging showed that these organoids maintain this organization after 15 (B) and even 50 days (C) in culture. Scale bar: 100µm.

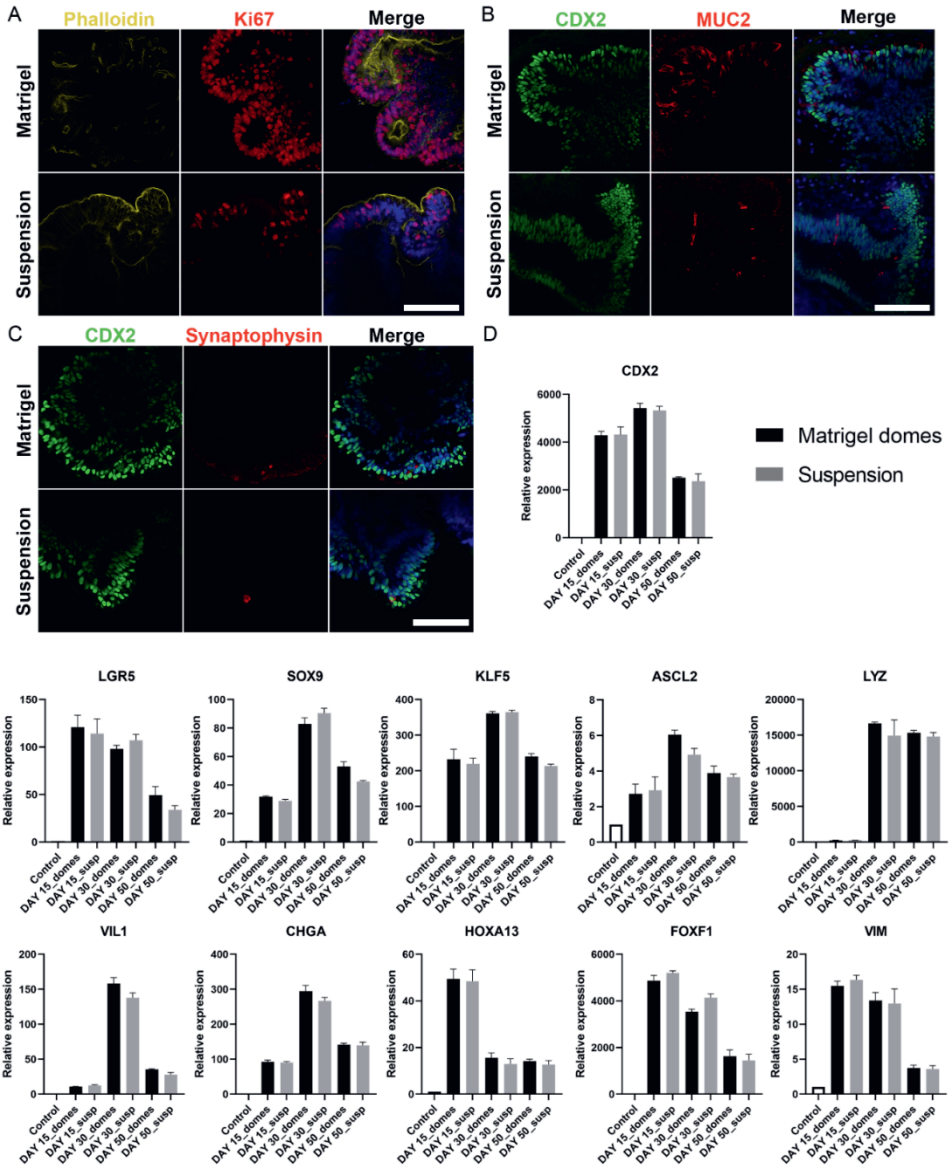


**Supplementary Figure 4:** Organoid morphology during culture. (A-B) Bright-field images demonstrating the growth and morphology of intestinal organoids after 15, 30 and 50 days in culture. The top panel indicates the H9-derived organoids (A) and the bottom one the iPSC72\_3-derived organoids (B). Scale bar: 200 $\mu$ m.





**Supplementary Figure 5:** Polarity reversal plasticity. (A) H9-derived organoids: Immunofluorescence stainings with E-cadherin (green) and Phalloidin (yellow) demonstrate that Matrigel embedded organoids that are placed in suspension culture for 7 days do not reverse polarity (top). When suspension organoids are embedded in Matrigel, the polarity is reversing in 90% of the organoids and the apical side is facing the organoid lumen (middle). The rest 10% is demonstrating an intermediate organization (bottom). Scale bars: 100 $\mu$ m. (n=4). (B) iPSC72\_3-derived organoids: Immunofluorescence stainings with E-cadherin (green) and Phalloidin (yellow) demonstrate that similar to H9-derived organoids Matrigel embedded organoids that are placed in suspension culture for 7 days do not reverse polarity (top). When suspension organoids are embedded in Matrigel, the polarity is reversing in 85% of the organoids and the apical side is facing the organoid lumen (middle). The rest 15% is demonstrating an intermediate organization (bottom). Scale bars: 100 $\mu$ m. (n=4).



**Supplementary Figure 6:** Characterization of iPSC72\_3-derived human intestinal organoids after 30 days in culture. (A-C) Immunofluorescence stainings of intestinal markers (Ki67: proliferative cells; CDX2: hindgut; MUC2: goblet cells; Synaptophysin: enteroendocrine cells) show similar expression patterns in both embedded and suspension organoids. Scale bars: 100 $\mu$ m. (D) qRT-PCR analysis demonstrates the expression levels of proliferation genes (*LGR5*, *SOX9*, *KLF5*, *ASCL2*), intestinal differentiation genes (*CDX2*, *LYZ*, *VIL1*, *CHGA*, *HOXA13*) and mesenchymal genes (*FOXF1*, *VIM*) after 15, 30 and 50 days in culture. Untreated iPSC72\_3 cells were used as controls. Statistical analysis showed no significant difference between the organoids grown embedded in Matrigel and the organoids grown in suspension at any of the time-points. Error bars indicate mean  $\pm$  S.E.M. (n = 3).





## CHAPTER VI

# **INTESTINAL ORGANOIDS WITH APICAL-OUT ORIENTATION AS A TOOL TO STUDY NUTRIENT UPTAKE, DRUG ABSORPTION AND METABOLISM**

Panagiota Kakni, Carmen López-Iglesias,  
Roman Truckenmüller, Pamela Habibović  
and Stefan Giselbrecht





## **Abstract**

Intestinal organoids recapitulate many features of the *in vivo* gastrointestinal tract and have revolutionized *in vitro* studies of intestinal function and disease. However, the restricted accessibility of the apical surface of the organoids facing the central lumen (apical-in) limits studies related to nutrient uptake and drug absorption and metabolism. Here, we demonstrate that pluripotent stem cell (PSC)-derived intestinal organoids with reversed epithelial polarity (apical-out) can successfully recapitulate tissue-specific functions. In particular, these apical-out organoids show strong epithelial barrier formation with all the major junctional complexes, nutrient transport and active lipid metabolism. Furthermore, the organoids express drug-metabolizing enzymes and relevant apical and basolateral transporters. The scalable and robust generation of functional, apical-out intestinal organoids lays the foundation for a completely new range of organoid-based high-throughput/high-content *in vitro* applications in the fields of nutrition, metabolism and drug discovery.

## **Introduction**

The intestinal epithelium is a highly organized, dynamic cell layer that creates a tight barrier between the luminal contents and the rest of the body. It is responsible for food digestion, nutrient transport and protection of the body from infections. Most of the orally administered drugs are also absorbed by the intestine and undergo first-pass metabolism. The establishment and maintenance of epithelial cell polarity, with distinct apical and basolateral surfaces, are pivotal for the proper conduction of these functions<sup>[1]</sup>. The apical side faces the intestinal lumen and mediates nutrient uptake and interactions with microorganisms. The basolateral side faces the basement membrane and surrounding tissues and is responsible for nutrient transport to the bloodstream and intercellular communication. Disruption of polarity has been associated with cancer<sup>[2]</sup>, microvillus inclusion disease, malnutrition, fetal diarrheal disorder and inflammatory bowel disease<sup>[1]</sup>. In the past years, animal models and cancer cell lines were considered the gold standard for modeling the functions of the intestine, but they do not accurately represent the human situation *in vivo*<sup>[3,4]</sup>.

Intestinal organoids are three-dimensional (3D) structures that recapitulate multiple features of the *in vivo* intestine: they contain all the major cell types (e.g. Lgr5<sup>+</sup> stem cells, Goblet cells, Paneth cells, enterocytes etc.) of the *in vivo* intestine<sup>[5,6]</sup>, organize into crypt-villus structures and possess tissue polarity, thus

mimicking the architecture and function of the intestinal epithelium. Intestinal organoids have been utilized in numerous studies related to nutrient transport, metabolism and drug development<sup>[4,7-11]</sup> and thus hold a great promise as a tool to study intestinal development, physiology and disorders<sup>[12,13]</sup>. Pluripotent stem cells (PSC) have shown a remarkable ability to differentiate towards all the cell types of the body and they can be used as a source for generating intestinal organoids. PSC-derived organoids have great potential for patient-specific disease modeling and high-throughput drug screenings. They have been found to express fundamental drug-metabolizing enzymes, and uptake and efflux transporters. However, the limited access to the apical surface of the organoid's epithelium hampers the assessment of intestinal permeability and drug or nutrient absorption. In addition, the presence of viscous gels surrounding the organoids, such as Matrigel, can further limit or slow down the diffusion of drugs or other compounds into the central lumen of the organoids. To overcome these, numerous studies have utilized organoids as cell sources to create 2D monolayers, e.g. on porous membranes of culture inserts. Even though this approach grants access to both the apical and basal surfaces, the intricate 3D structure of the organoids is largely lost. Recently, intestinal organoids with apical-out orientation were established using both adult<sup>[14-17]</sup> and pluripotent stem cells<sup>[18]</sup>. These innovative organoid models maintain the 3D architecture and function, and at the same time provide direct access to the apical side of the epithelium.

In this study, we utilized apical-out intestinal organoids, derived from human PSCs and we demonstrate their functionality with regard to nutrient uptake, drug transport and metabolism. Similar to a previously described method<sup>[18]</sup>, organoids were cultured in a suspension system following a stepwise differentiation method. After maturation, they expressed all the major cell types found in the *in vivo* intestine and they demonstrated strong epithelial barrier integrity, nutrient uptake, lipid metabolic functions and the presence of transporters, which are important drug and nutrient targets. Thus, these apical-out human intestinal organoids are a valuable *in vitro* model for future studies of nutrient transport, drug development and pharmacokinetics.

## **Experimental section**

### Maintenance of PSCs

The human embryonic stem cell (hESC) line WA09 (H9) was obtained from WiCell. The ES cell line was maintained in feeder-free conditions using mTESR1 (StemCell Technologies), and passaged onto Matrigel (Corning)-coated tissue culture dishes every 4 to 5 days.

### Fabrication and preparation of microwell arrays

Microthermoforming was used for the fabrication of microwells as described previously<sup>[51,52]</sup>. Briefly, 50 µm thick polymer films were used to form microwells, which were 500 µm wide and 300 µm deep. Each array contained 289 U-bottom microwells. For sterilization, microwells were treated stepwise with decreasing concentrations of 2-propanol (VWR) (100%–70%–50%–25%–10%) and then washed twice with Dulbecco's phosphate buffered saline (PBS; Sigma-Aldrich). When placed in 24-well plates, elastomeric O-rings (ERIKS) were mounted on top of the microwell arrays in order to keep them in place.

### Differentiation of PSCs towards intestinal organoids

The protocol for directed differentiation of intestinal organoids was carried out as previously described<sup>[18]</sup>. hESC colonies were dissociated into single cells using TrypLE™ Express Enzyme (Thermofisher) and seeded on microwell arrays at a density of 1000 cells/microwell in mTesR1 supplemented with Y-27632 (10 µM; Tocris) to create embryoid bodies (EBs). For definitive endoderm (DE) differentiation, EBs were treated with Activin A (100 ng/mL; Cell Guidance Systems) in RPMI 1640 (Thermofisher) medium supplemented with increasing concentrations (0%, 0.2%, 2%) of HyClone defined fetal bovine serum (dFBS; Thermofisher) for 3 days. The following 4 days, the DE spheroids were incubated with Fibroblast Growth Factor 4 (FGF4) (500 ng/ml; R&D Systems) and CHIR99021 (3 µM; Stemgent) to further differentiate towards hindgut. Medium exchange was performed daily. Thereby, to maintain the spheroids in the microwells, the plate was slightly tilted and the medium was aspirated from the sidewalls.

To promote intestinal differentiation, two different approaches were taken. Specifically, for organoids with the apical side in (facing the lumen), the hindgut spheroids were collected, embedded in 50 µl Matrigel and plated as droplets (Matrigel domes) into tissue culture-treated 24-well plates. Matrigel was allowed to polymerize at 37 °C and 5% CO<sub>2</sub> for 15 min and afterwards, the Matrigel drops

containing the spheroids were overlaid with Advanced Dulbecco's Modified Eagle Medium/Ham's F-12 (DMEM/F-12) supplemented with B27, N2, Hepes, penicillin/streptomycin, L-glutamine (all Thermofisher), Epidermal Growth Factor (EGF) (50 ng/mL; R&D systems), Noggin (100 ng/ml; R&D systems) and R-Spondin (500 ng/mL; R&D systems). The medium was refreshed every 4 days.

For organoids with the apical side out (facing the culture medium), the hindgut spheroids were collected on day 8 and placed in suspension culture in non-tissue culture-treated 6-well plates. To avoid surface-cell adherence, the plates were coated with 1% Pluronic F-108 (Sigma-Aldrich) solution in PBS for 2 h at 37 °C and then washed two times with PBS. The medium had the same composition as the apical-in organoids, but in this case, 2% Matrigel was added as a supplement. Apical-in and apical-out organoids reached full maturation after 30 days embedded in Matrigel or suspension culture respectively.

#### Epithelial barrier integrity

The permeability of fluorescence markers into the lumen of organoids was tested using 4 kDa fluorescein isothiocyanate (FITC)-labeled dextran (Sigma-Aldrich). Intact organoids were pelleted and resuspended in growth medium containing 2 mg/mL of FITC-dextran for 30 min at room temperature (RT). As a control, organoids were disrupted with 2 mM ethylenediamine tetraacetic acid (EDTA; VWR) in Hanks' balanced salt solution (no calcium and no magnesium; Thermofisher) on ice for 15 min and then resuspended in FITC-dextran solution. Finally, organoids were washed and mounted and immediately imaged using confocal laser scanning microscopy (Leica TCS SP8).

#### Fatty acid absorption assay

Apical-in organoids were treated with 5 mM EDTA in PBS for 1 h on a shaking platform at 4 °C to remove the Matrigel. All organoids (apical-in and apical-out) were washed with DMEM (Thermofisher) with no phenol red and incubated in a solution containing 5 µM fluorescent fatty acid analog C1-BODIPY-C12 (Thermofisher) and 5 µM fatty-acid-free bovine serum albumin (BSA; Sigma-Aldrich) for 30 min at 37 °C. Afterwards, organoids were fixed in 4% paraformaldehyde (VWR) in PBS for 30 min. Finally, samples were stained with phalloidin and counterstained with 4',6-diamidino-2-phenylindole (DAPI) (both Sigma-Aldrich), and imaged with confocal laser scanning microscopy (Leica TCS SP8).

### Drug treatments

Apical-in and apical-out intestinal organoids were treated with 20  $\mu$ M rifampicin (Sigma-Aldrich) and 100 nM 1,25-dihydroxyvitamin D3 (Sigma-Aldrich), which are known inducers of the cytochrome CYP3A4 and the apical transporter multidrug resistance mutation 1 (MDR1), for 48 h. In addition, organoids were treated with 100  $\mu$ M verapamil (Sigma-Aldrich) and 20  $\mu$ M ivacaftor (Selleck Chemicals), which are known inhibitors of CYP3A4 and MDR1, for 48 h. As controls, organoids were treated with 0.1% dimethyl sulfoxide (DMSO; VWR). Following treatment, organoids were harvested for RNA isolation.

### RNA isolation and quantitative real-time PCR (qPCR)

Organoids were collected and the total RNA was extracted using the RNeasy Mini Kit (Qiagen) as per manufacturer instructions. cDNA was synthesized using the iScript cDNA Synthesis Kit (Bio-Rad). qPCR was performed on a CFX96 real-time PCR detection system (Bio-Rad) using the iQ SYBR Green Supermix (Bio-Rad). Gene expression for each sample was normalized using the hypoxanthine phosphoribosyltransferase (HPRT) housekeeping gene. Data analysis was performed according to the  $2^{-\Delta\Delta C_t}$  method. The results represent the mean values of three independent experiments ( $n = 3$ ). The primer sequences are listed in the supplementary material.

### Transmission electron microscopy (TEM)

Initially, organoids underwent a chemical fixation for 3 h at RT with 1.5% glutaraldehyde (Merck) in 0.067 M cacodylate (Acros Organics) buffered to pH 7.4 and 1% sucrose (Merck). Later on, they were washed with 0.1 M cacodylate buffer and postfixed with 1% osmium tetroxide (Agar Scientific) in the same buffer containing 1.5% potassium ferricyanide (Merck) for 1 h in the dark at 4 °C. After rinsing with Mill-Q water, organoids were dehydrated at RT in a graded ethanol (Merck) series (70, 90, up to 100%), infiltrated with Epon, embedded in the same resin and polymerized for 48 h at 60 °C. Using a diamond knife (Diatome), ultrathin sections (60 nm) were cut on a Leica UC7 ultramicrotome and transferred onto 50 mesh copper grids covered with formvar and carbon film. Sections were then stained with 2% uranyl acetate in 50% ethanol and lead citrate. Finally, the sections were imaged in a Tecnai T12 electron microscope equipped with an Eagle 4k×4k CCD camera (Thermofisher) or Veleta 2k×2k CCD camera (Olympus Soft Imaging).

### Nile red staining

For lipid droplets visualization, the organoids were fixed in 4% paraformaldehyde in PBS for 30 min and then incubated with 500 nmol/L Nile red (Sigma-Aldrich) for 15 min at RT. Then, organoids were washed twice with PBS, counterstained with the nuclear dye DAPI and imaged with a confocal laser scanning microscope (Leica TCS SP8).

### Immunofluorescence and confocal microscopy

Intestinal organoids were fixed in 4% paraformaldehyde in PBS for 30 min and then washed with PBS. For permeabilization, organoids were treated with 0.5% Triton X-100 (Sigma-Aldrich) in PBS for 30 min at RT. For blocking, 5% donkey serum in the permeabilization solution was used. Incubation of primary antibodies (full list in Supplementary Materials) was performed overnight at 4 °C and the next day, secondary antibodies (Supplementary Materials) were added for 2 h at RT. Finally, the samples were counterstained with DAPI. For the imaging of the immunostained samples, confocal laser scanning microscopy (Leica TCS SP8) was utilized, and the images were processed with ImageJ. Quantification was performed using the open access software QuPath v0.3.2.

### Statistical analysis

Statistical analysis was performed using GraphPad Prism 9 software. Student's two-tailed t-test with Welch's correction and two-way ANOVA were used to determine statistical significance. Significant differences were defined as  $P < 0.05$ . P values of statistical significance are represented as \*\*\*\* $P < 0.0001$ , \*\*\* $P < 0.001$ , \*\* $P < 0.01$ , and \* $P < 0.05$ . Error bars in figures indicate standard error of the mean (S.E.M.).

## **Results**

### Apical-out intestinal organoids demonstrate epithelial barrier integrity

Culture of organoids in suspension with partial or complete removal of basement membrane(-like) matrix has led to the generation of organoids with reversed polarity, where the apical side is facing outwards to the surrounding culture medium<sup>[14,16–18]</sup>. To generate apical-out intestinal organoids from PSCs, we utilized a previously described stepwise differentiation method<sup>[18]</sup> (**Figure 1 A**). Briefly, H9 embryonic stem cells were seeded into microwell arrays (1000 cells/microwell) in order to create homogenous embryoid bodies, which were then differentiated towards definitive endoderm and hindgut without disrupting their 3D conformation.

Subsequently, hindgut spheroids were removed from the microwell arrays and transferred to a suspension culture system in order to further mature to intestinal organoids with reversed polarity (Supplementary Figure 1). This system has great potential to generate large numbers of organoids, since 289 homogenous hindgut spheroids, which will further mature into intestinal organoids, can be harvested from each microwell array. This number corresponds to almost 7000 organoids from a single 24-well plate. Thus, this system facilitates scaled-up production of apical-out organoids, which can be used in high-throughput applications, such as drug screenings.

One of the key functions of the intestinal epithelium is the formation and maintenance of a selective barrier, which allows the passage of essential nutrients but prevents the passage of harmful external factors, such as harmful microbes and toxins. This balance is also essential for the proper function of the intestinal epithelial cells. Special protein complexes are responsible to interconnect the individual cell membranes in order to maintain this barrier function and seal the intercellular space, while adhering the neighbor cells keeping them as an epithelial sheet. These include the desmosomes, adherent junctions and tight junctions<sup>[19,20]</sup>. These complexes have been previously identified in intestinal organoids<sup>[21]</sup>. Here, we aimed to explore whether such structures are present in intestinal organoids with reversed polarity. After establishing the inside-out intestinal organoids, we looked into their ultrastructural organization in order to identify the junctional complexes that are responsible for the cell adhesion and the barrier formation and maintenance (Figure 1 B). In a panoramic view of the middle and apical region of an enterocyte, we identified microvilli in the outer surface of the organoid, showing a well-developed glycocalyx and actin bundles deep in the terminal web area (Figure 1 B). Mitochondria, smooth and rough endoplasmic reticulum (ER) and Golgi complex appear very similar in morphology and localization to those present in the intestinal epithelium<sup>[22]</sup>. Additionally, junctional complexes including tight junctions, zonula adherens and desmosomes are present in the apical side of the cells. Basement membrane, mitochondria and collagen fibers were identified in the basal region. Taken together, the observations indicate that our apical-out intestinal organoids recapitulate fully functional enterocytes.

Intestinal organoids with apical-out orientation as a tool to study nutrient uptake, drug absorption and metabolism

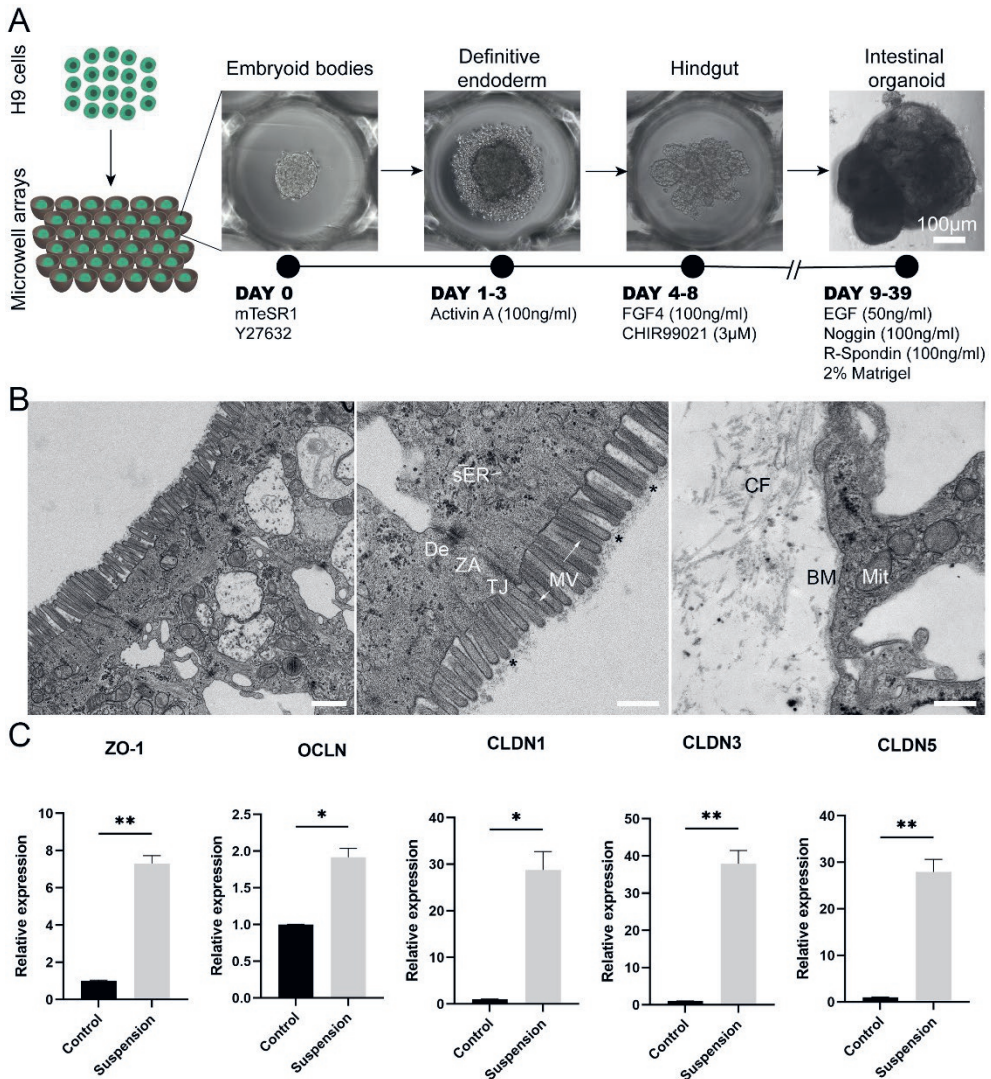


**Figure 1.** Apical-out intestinal organoids show tight barrier formation. (A) Overview of the protocol for the directed differentiation of H9 embryonic stem cells towards intestinal organoids with apical-out orientation. Scale bar: 100 µm. (B) On the left, a low magnification TEM image of the epithelial sheet of apical-out organoids demonstrating some enterocytes. In the middle image, TEM indicates the presence of apical microvilli (MV) on the outer surface of organoids. Functional ultrastructural features of the intestinal epithelium are indicated in the apical region of the enterocytes: microvilli (arrows) with core actin filaments and glycocalyx (stars), vesicles of smooth endoplasmic reticulum (sER) and intercellular junctions: tight junction (TJ), zonula adherens (ZA) and desmosome (De). In the basal region (right image), the indicated structures correspond to the basement membrane (BM), collagen fibers (CF) and the mitochondria (Mit). Scale bars: 1 µm (left) and 500 nm (middle and right). (C) qRT-PCR analysis shows significantly higher expression of the “leak pathway” regulators *ZO-1* and *OCLN*



and the “pore pathway” regulators *CLDNI*, *CLDN3*, *CLDN5* in the apical-out intestinal organoids compared to undifferentiated control stem cells. Error bars indicate mean  $\pm$  S.E.M. (n = 3).

To further assess the presence of junctional complexes, we performed gene expression analysis for zonula occludens 1 (*ZO-1*) and occludin (*OCLN*), which regulate the “leak pathway” that mediates the flux of large molecules (up to 6 nm) and claudin-1, 3 and 5 (*CLDNI*, *CLDN3*, *CLDN5*), which are responsible for the “pore pathway” that mediates the movement of small ions and solutes (up to 0.8 nm)<sup>[21,23]</sup>. In all cases, there was a significant increase in the expression levels compared to undifferentiated stem cells, thus further confirming that apical-out intestinal organoids harbor functional junctional complexes (Figure 1 C).

To determine the integrity of the organoid barrier, we performed a FITC-dextran diffusion assay, which has been used extensively to assess gut barrier integrity and permeability both in *in vivo*<sup>[24,25]</sup> and *in vitro*<sup>[26,27]</sup> systems. In our case, FITC-dextran of 4 kDa (FITC-D4) was added to the organoid culture medium for 30 min and its diffusion into the lumen of the organoids was observed using confocal microscopy (**Figure 2**). The apical-out intestinal organoids excluded entirely the FITC-D4, thus demonstrating strong epithelial barrier integrity. As a positive control, organoids were treated with 2 mM EDTA for 15 min, which is a chelating agent known to disrupt the tight junctions by depleting calcium in the medium and thus increasing permeation of compounds through the paracellular route<sup>[28,29]</sup>. In EDTA-treated organoids, the FITC-D4 diffused into the intercellular spaces and lumen of the organoids, thus showing a compromised epithelial barrier. These findings strongly support that apical-out intestinal organoids form an effective barrier that recapitulates multiple features of the *in vivo* intestinal epithelial barrier.

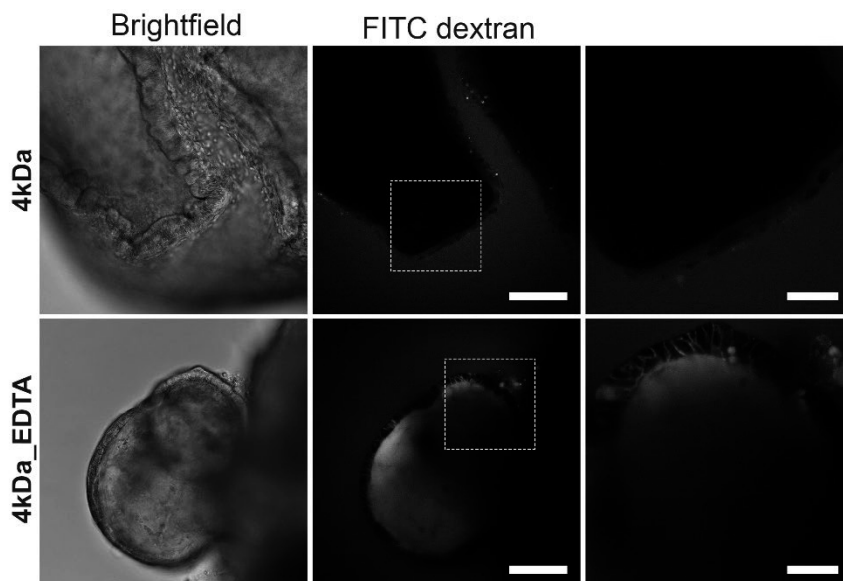


**Figure 2.** Apical-out intestinal organoids show epithelial barrier integrity by a FITC-dextran diffusion assay. Apical-out organoids exclude the 4 kDa FITC-dextran, showing tight epithelial barrier formation (top row). When organoids are treated with 2 mM EDTA (bottom row), the barrier is disrupted and FITC-dextran diffuses into the intracellular space and the organoid lumen. White boxes in the middle images delineate the areas shown in the zoomed images to the respective right. Scale bars: 100  $\mu\text{m}$  (left and middle) and 50  $\mu\text{m}$  (right).

### Nutrient transport and metabolism

The intestinal epithelium is a highly polarized cell layer that plays a pivotal role in nutrient absorption and metabolism. The uptake of fatty acids in the intestine is a multistep process that occurs through three different pathways<sup>[30]</sup>. For long- and medium-chain fatty acids, the fatty acid translocase (CD36) acts alone or in combination with the peripheral membrane protein plasma membrane-associated fatty acid-binding protein (FABP). Alternatively, these are transferred by the fatty acid transport protein 4. The short-chain fatty acids can transverse the epithelium by simple passive diffusion. Once inside the cells, fatty acids are transported to the endoplasmic reticulum where they are used for triglyceride synthesis. Triglycerides are packaged with lipoproteins, cholesterol and other lipids into chylomicrons. These particles are secreted from the enterocytes into the lymph across the basolateral membranes of the cells<sup>[31]</sup>. To assess the polarity-specific fatty acid absorption, we used the fluorescent fatty acid analog C1-BODIPY-C12 (**Figure 3**). We incubated both apical-in and apical-out organoids with 5  $\mu\text{M}$  BODIPY dye for 30 min and then we fixed and stained the organoids with phalloidin (indicating F-actin) and DAPI

(indicating cell nuclei). Confocal microscopy showed strong BODIPY signal in the apical-out organoids, demonstrating the successful absorption of the fatty acid analog from the surrounding medium. In comparison, in apical-in organoids, the BODIPY signal was significantly weaker and located in the outer surface of the organoids, indicating that fatty acids are not taken up from the medium and lipid droplets did not form. These data suggest that in apical-out organoids, the apical fatty acid transporters are directly accessible in the outer surface of the organoids.

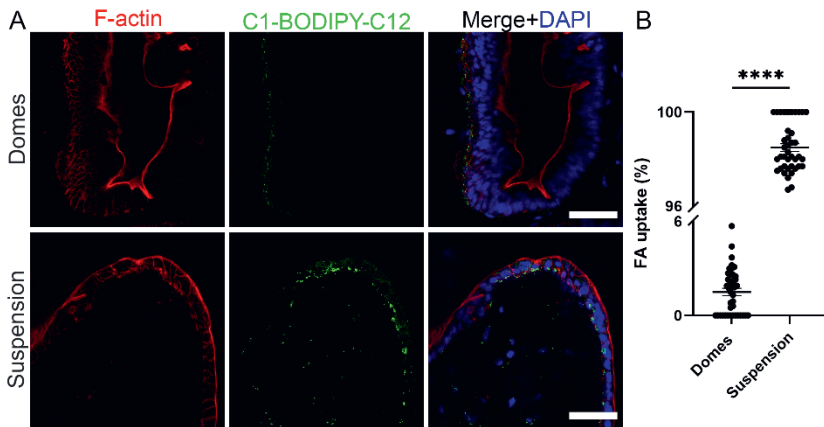


**Figure 3.** Apical-out intestinal organoids readily absorb fatty acids. (A) The fluorescent fatty acid (FA) analog C1-BODIPY-C12 (green) is only taken up when the apical surface of the organoids is facing outwards. Phalloidin (red) marks the apical side of the epithelium and DAPI (blue) the nuclei. Scale bars: 50  $\mu$ m, and apply to images in the respective row. (B) Quantification of the FA uptake in apical-in and apical-out intestinal organoids. The percentage of FA uptake corresponds to the amount of measured fluorescence in the intercellular space, over the total fluorescence. Error bars indicate mean  $\pm$  S.E.M. (n=4).

Next, we assessed whether the apical-out organoids can perform intestinal metabolic functions. First, we determined whether the apical-out organoids harbor chylomicrons and vesicles of smooth endoplasmic reticulum, which are involved in processing absorbed fatty acids and monoglycerides *in vivo*. TEM analysis indeed demonstrated the presence of these structures (Figure 4 A). Nile red staining indicated the formation of lipid droplets in the cytosol of the apical-out organoids (Figure 4 B). Cytosolic lipid droplets are organelles found in most tissues and they play a crucial role in energy storage, inter-organelle communication and cellular metabolic processes<sup>[32]</sup>. Then, we performed gene expression analysis for 14 different lipid metabolism markers (Figure 4 C). First, we investigated the expression of brush border enzymes and transporters, including Lactase (*LCT*), Sodium-hydrogen antiporter 3 regulator 1 (*SLC9A3R1*), Glutamyl aminopeptidase (*ENPEP*)

and Angiotensin-converting enzyme 2 (*ACE2*). Additionally, we assessed the expression of the lipoprotein metabolism-related gene *APOA4* and the expression of lipid digestion-related genes, such as the apolipoproteins A1 and 5 (*APOA1*, *APOA5*), the 3-hydroxy-3-methylglutarylCoA synthetase 2 (*HMGCS2*), the Phospholipid transfer protein (*PLTP*), the Cytosolic malic enzyme 1 (*ME1*) and the sterol 12- $\alpha$ -hydroxylase (*CYP8B1*). Finally, we evaluated the expression of lipase-related genes, including the Colipase (*CLPS*), lipase A (*LIPA*) and Lipoprotein lipase (*LPL*). Further information regarding the functions of these genes can be found in the supplementary table 3. The expression of all these genes was significantly increased in both apical-in and apical-out mature intestinal organoids when compared to undifferentiated stem cells. However, no significant difference was observed in gene expression levels between the two organoid models, indicating that our new apical-out intestinal organoids recapitulate intestinal metabolic functions similar to the already established apical-in intestinal organoids.

#### Apical-out organoids express drug-metabolizing enzymes and drug transporters

Apart from its key role in nutrient absorption, the intestine is involved in drug metabolism of orally administered drugs. Drug-metabolizing enzymes of the intestine contribute to first-pass drug metabolism and are responsible for the low oral bioavailability of numerous compounds<sup>[33]</sup>. So far, cell lines (e.g. Caco-2) have been utilized on either culture inserts or on-chip systems for drug absorption studies<sup>[3]</sup>. Organoids have not been widely used in such studies, mainly due to the limited accessibility of the lumen, which makes it more complicated to mimic a physiologically relevant drug transport<sup>[3]</sup>. However, apical-out intestinal organoids have the potential to overcome this technical difficulty and can become a valuable new tool for *in vitro* drug testing. Previous studies have shown that intestinal organoids express certain drug metabolizing enzymes and transporters<sup>[4,34,35]</sup>. Here, we aimed to explore whether the apical-out intestinal organoids express these enzymes and transporters at similar levels as apical-in organoids.

Initially, to visualize the position of apical and basal transporters, we performed immunofluorescence stainings against the basal glucose transporter 2 (GLUT2) and the apical bile acid receptor: Takeda G-protein-coupled receptor 5 (TGR5) (**Figure 5 A**). The expression of GLUT2 was identified in the outer surface of apical-in organoids and in the inner surface of apical-out organoids. Conversely, TGR5 was found in the inner part of apical-in and in the outer part of apical-out organoids. These data are consistent with previous studies with apical-in intestinal

organoids<sup>[8]</sup> and indicate that the transporters still show correct basal and apical localizations in apical-out organoids. Following that, we evaluated the gene expression levels of drug-metabolizing enzymes and transporters in apical-in and apical-out organoids using quantitative RT-PCR (Figure 5 B). Specifically, we assessed the expression of the cytochrome P450 family 2 subfamily C member 9 (*CYP2C9*), cytochrome P450 family 2 subfamily J member 2 (*CYP2J2*), *CYP3A4*, UDP glucuronosyltransferase family 1 member A1 (*UGT1A1*), UDP glucuronosyltransferase family 1 member A3 (*UGT1A3*), and carboxylesterase 2 (*CES2*). In both organoid models, these enzymes are expressed at similar levels without statistically significant differences. Next, we assessed the expression of several basolateral transporters. These include the multidrug resistance-associated protein 1, 3 and 5 (*MRP1*, *MRP3*, *MRP5*) and the organic solute transporter alpha and beta (*OSTA*, *OSTB*). Interestingly, in apical-in organoids (domes), the expression of these transporters was significantly higher compared to apical-out organoids (suspension). Then, we investigated the expression of the apical transporters: *MRP2*, *MRP4*, *MRP6*, multidrug resistance protein 1 (*MDR1*), breast cancer resistance protein (*BCRP*) and peptide transporter 1 (*PEPT1*). Unlike the basolateral transporters, the expression levels of the apical transporters were significantly higher in apical-out organoids.

After having confirmed that *CYP3A4* and *MDR1* are expressed in both apical-in and apical-out organoids, we aimed to assess their activity following drug treatments. *CYP3A4* is one of the most dominant and abundant drug-metabolizing enzymes<sup>[4]</sup> and *MDR1* (also known as P-glycoprotein or ABCB1) is actively involved in the transport of drugs and the modulation of the intracellular concentration of toxic compounds and drug components<sup>[36]</sup>. Induction of these enzymes is one of the major concerns for pharmacokinetic studies since they affect the oral bioavailability of drugs. We exposed apical-in and apical-out organoids to rifampicin and 1,25-dihydroxyvitamin D3, which are both known inducers of *CYP3A4* and *MDR1* (**Figure 6 A, B**). In both organoid models, there was a significant increase in the expression of *CYP3A4* and *MDR1* compared to DMSO-treated controls. In addition, we treated the organoids with the inhibitors verapamil and ivacaftor (weak inhibitor) (Figure 6 A, B). In this case, we found a significant decrease in the expression of both *CYP3A4* and *MDR1* compared to DMSO-treated controls. Collectively, these results indicate that the drug-metabolizing enzymes and transporters are not just present in the apical-out intestinal organoids, but they are also responsive to compound treatments.

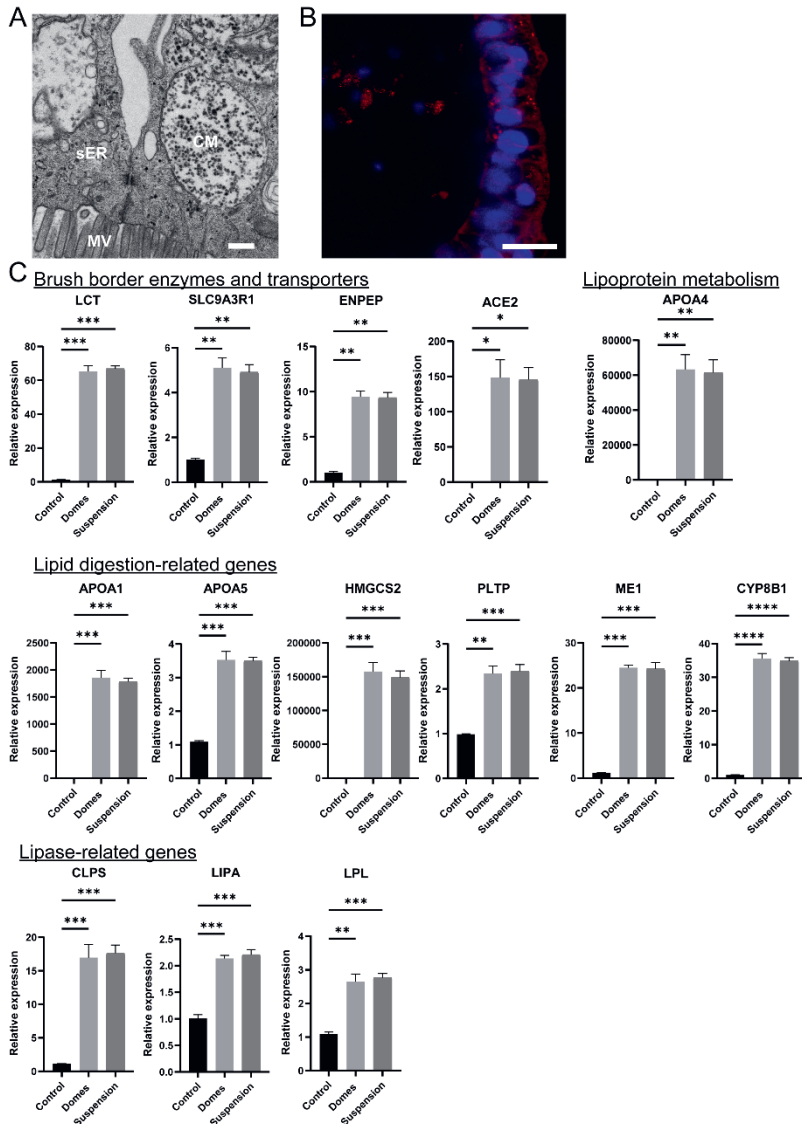


**Figure 4.** Apical-out intestinal organoids recapitulate *in vivo* metabolic activity. (A) TEM demonstrates the presence of chylomicrons (CM) and vesicles of smooth endoplasmic reticulum (sER) in apical-out organoids. MV: microvilli. Scale bar: 500 nm. (B) Nile red staining indicating the lipid droplets in the cytosol of apical-out intestinal organoids. Scale bar: 20  $\mu$ m. (C) qRT-PCR analysis demonstrates the expression levels of the brush borders enzymes and transporters (*LCT*, *SLC9A3R1*, *ENPEP*, *ACE2*); the lipoprotein metabolism-related gene (*APOA4*); the lipid digestion-related genes (*APOA1*, *APOA5*, *HMGCS2*, *PLTP*, *ME1*, *CYP8B1*) and the lipase-related genes (*CLPS*, *LIPA*, *LPL*) in both apical-in (domes) and apical-out (suspension) intestinal organoids. Untreated H9 embryonic stem cells were used as controls. Error bars indicate mean  $\pm$  S.E.M. (n=3).

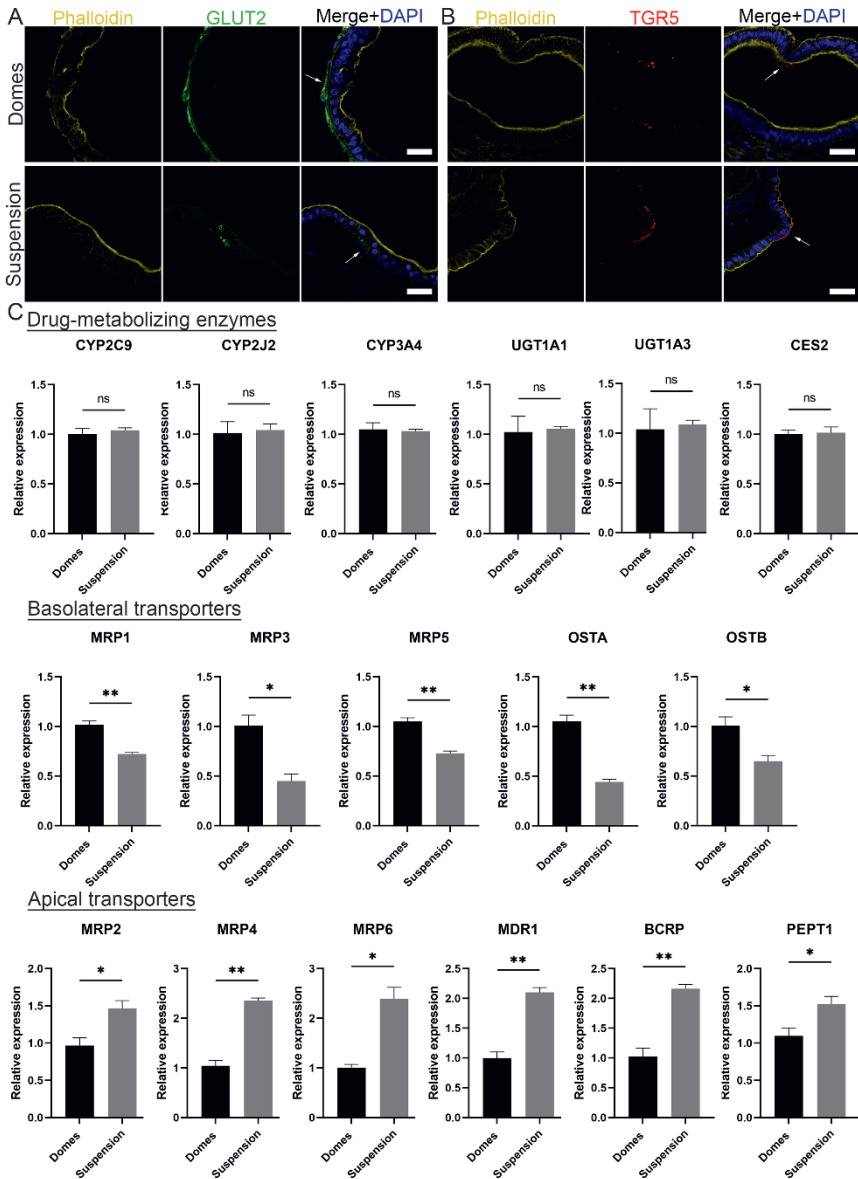


**Figure 5.** Apical-out intestinal organoids express drug-metabolizing enzymes and transporters. (A, B) Immunofluorescence stainings of the basal transporter GLUT2 (green) and the apical transporter TGR5 (red) in apical-in (top) and apical-out (bottom) organoids. Phalloidin (yellow) indicates F-actin and DAPI (blue) indicates cell nuclei. Scale bars: 50  $\mu$ m, and apply to the same group in each row. (C) Gene expression levels encoding drug-metabolizing enzymes (*CYP2C9*, *CYP2J2*, *CYP3A4*, *UGT1A1*, *UGT1A3* and *CES2*), basolateral transporters (*MRP1*, *MRP3*, *MRP5*, *OSTA* and *OSTB*) and apical transporters (*MRP2*, *MRP4*, *MRP6*, *MDR1*, *BCRP* and *PEPT1*) were measured by real time RT-PCR. Error bars indicate mean  $\pm$  S.E.M. (n=3).

## Discussion

In this study, we demonstrated for the first time that human PSC-derived intestinal organoids with apical-out orientation can successfully perform specialized intestinal functions, such as barrier formation, polarized nutrient uptake and drug absorption and metabolism. Exceptional advantages of this state-of-the-art model include the scalability of the system; approximately 7000 organoids can be derived from a single 24-well plate and the ability to generate organoids from various cell sources including both embryonic and induced PSCs (iPSCs)<sup>[18]</sup>. Considering that iPSCs can be generated from patients with various diseases, apical-out organoids derived from these cells could further contribute to the field of disease modeling and personalized

medicine, since various and combinatorial drug-treatments could be tested in simplified 3D assays in a high-throughput manner.

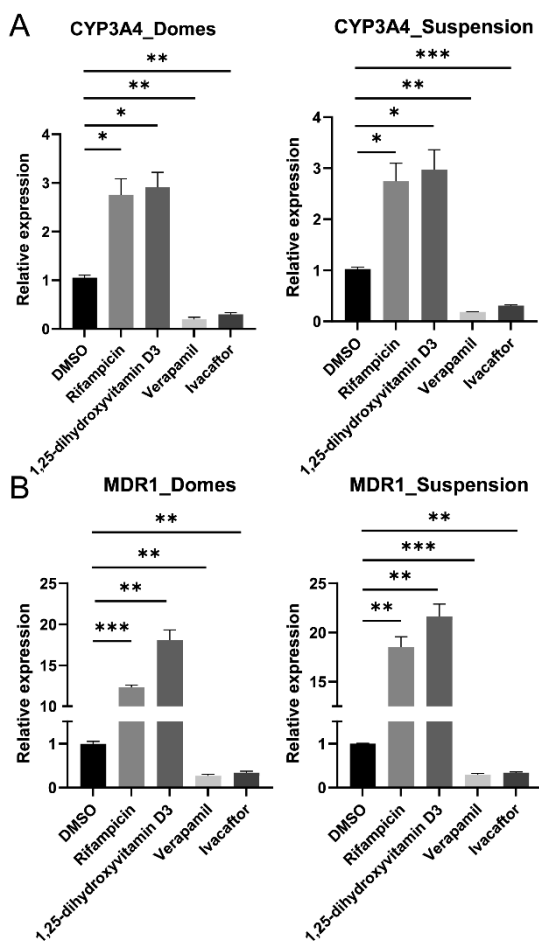


**Figure 6.** Induction and inhibition of *CYP3A4* and *MDR1*. (A, B) Assessment of *CYP3A4* (A) and *MDR1* (B) levels in apical-in and apical-out organoids, following drug treatment with the inducers rifampicin and 1,25-dihydroxyvitamin D3 and the inhibitors verapamil and ivacaftor for 48 h. In both organoid models, there are significant differences in the expression levels following treatments compared to DMSO-treated controls. Notably, the upregulation of *MDR1* expression following treatment with rifampicin and 1,25-dihydroxyvitamin D3 was more robust in the apical-out organoids than in the apical-in organoids. Error bars indicate mean  $\pm$  S.E.M. (n=3).



Looking into the gut epithelial barrier function in apical-out organoids, we identified all the junctional complexes that are responsible for the formation of a selective barrier. Specifically, we detected desmosomes, tight junctions and zonula adherens in the apical surface of the organoids, similar to the *in vivo* intestine<sup>[19]</sup>. The FITC-dextran diffusion assay demonstrated the tightness of our reversed-orientation epithelium. This is in accordance with previous publications on intestinal organoids with such an apical-out architecture<sup>[14,16]</sup>. Collectively, these results showed that apical-out organoids not only form a tightly sealed barrier but also have the “means” to allow selective transport of molecules. Increased intestinal permeability has been associated with numerous diseases including inflammatory bowel disease, irritable bowel syndrome, diabetes and Alzheimer’s disease<sup>[37]</sup>. This reversed polarity intestinal organoid model can be a valuable tool to evaluate intestinal permeability *in vitro*, thus assisting the detection of relevant diseases and later their treatment, since it can be used as (personalized) drug-screening platform. The exposure of the directly accessible apical surface to test probes (i.e. dextrans, polyethylene glycol of different molecular weights) can facilitate the process compared to the formation of 2D monolayers from organoid cells<sup>[38]</sup> or microinjections in the lumen of apical-in organoids<sup>[39,40]</sup>.

Almost all nutrients are absorbed and transported via the highly polarized intestinal epithelium *in vivo*. Fatty acids are absorbed from the lumen through the apical surface of the intestinal absorptive cells<sup>[30]</sup>. We demonstrated here that in organoids where the apical side is facing outwards, the fluorescent fatty acid analog BODIPY was absorbed through the apical surface whereas this was not observed in apical-in organoids (Figure 3). Similar results were previously shown for reversed polarity organoids derived from adult stem cells<sup>[14]</sup>. We took this finding a step further and demonstrated that these organoids recapitulate key metabolic functions. With a closer look into the ultrastructural organization of the apical-out organoids, we identified chylomicrons and vesicles of smooth endoplasmic reticulum, which indicate active processing of the dietary fats that are taken up by enterocytes. We also identified cytosolic lipid droplets that store the excess dietary triacylglycerols. Moreover, gene expression analysis showed also the presence of brush border enzymes and transporters, lipoprotein metabolism genes, lipid digestion-related genes and lipase-related genes, which map to the peroxisome proliferator-activated receptor (PPAR) signaling pathway, a key regulator of intestinal metabolism<sup>[41–43]</sup>. Taken together, these data confirm that apical-out intestinal organoids can successfully recapitulate nutrient uptake and metabolic functions, which are major

functions of the intestine. These intestinal functions profoundly affect the proper function of the whole body, since the availability and quality of nutrients are translated to substrates that are distributed to every organ in order to supply energy<sup>[44]</sup>. Nutrient transport and metabolism have not been widely studied in organoids since the architecture with an enclosed central lumen does not provide easy access to the apical surface, which is the nutrient absorption site. Therefore, our reversed polarity organoid model can further enhance the study of nutrient absorption, transport and metabolism because, by simply adding nutritional compounds to the culture medium, a physiologically relevant nutrient uptake via the apical surface and subsequent metabolism can be mimicked in a 3D organoid context.

The vast majority of drugs are administered orally, thus, it is important to predict their bioavailability. Absorption, distribution, metabolism and excretion are the processes that need to be studied in order to determine the bioavailability<sup>[45,46]</sup>. Here, we demonstrated that intestinal organoids with reversed polarity express drug metabolizing enzymes similar to established apical-in intestinal organoids<sup>[4,34]</sup>. However, we found a higher expression of apical transporters in apical-out organoids and higher expression of basolateral transporters in apical-in organoids (Figure 5 C). The expression of these transporters can be affected by endogenous and exogenous compounds, such as nutrients and hormones<sup>[47,48]</sup>. Therefore, we hypothesize that the differences in the expression levels of transporters between apical-in and apical-out organoids are mainly caused by the different concentrations of substances present in the enclosed organoid lumen or in the surrounding cell culture medium. Further studies would be required to shed light on the mechanisms underlying these gene expression differences, but this is beyond the scope of this paper. CYP3A4 is a dominant drug metabolizing enzyme and MDR1 plays an important role in intestinal absorption and excretion of drugs<sup>[4]</sup>. Treatment with rifampicin and 1,25-dihydroxyvitamin D3 induced the expression of CYP3A4 and MDR1 in both apical-in and apical-out organoids<sup>[4,9,34]</sup>. In contrast, treatment with verapamil<sup>[49]</sup> and ivacaftor<sup>[50]</sup> reduced their expression as suggested by their inhibitory role. To our knowledge, this is the first report showing that apical-out intestinal organoids contain functional drug metabolizing enzymes and transporters, which respond to drug treatments that were previously studied in apical-in organoids or 2D monolayer models. This organoid model is of great importance for future drug studies, since organoids are more physiologically relevant models than 2D cultures and the human

cell origin can overcome the species-specific differences that arise with animal-based testing, ultimately leading to faster and more successful drug development.

To conclude, we have used a scalable apical-out intestinal organoid model, derived from hPSCs, and demonstrated their ability to perform specialized intestinal functions. These organoids form a tight barrier, perform polarized nutrient absorption and lipid metabolism and express active drug metabolizing enzymes and transporters. The direct access to the apical surface of the organoids facilitate nutrient and drug absorption studies, since the tested substances can be simply added to the medium, bypassing the need for microinjections and gel diffusion. Therefore, this platform can be a timesaving and cost-efficient method for high-throughput and animal-free nutrition and drug discovery studies in the future.

## **References**

- [1] K. Schneeberger, S. Roth, E. E. S. Nieuwenhuis, S. Middendorp, *Dis. Model. Mech.* **2018**, *11*, dmm031088.
- [2] A. Fatehullah, P. L. Appleton, I. S. Näthke, *Philos. Trans. R. Soc. B Biol. Sci.* **2013**, *368*, DOI 10.1098/rstb.2013.0014.
- [3] S. Youhanna, V. M. Lauschke, *J. Pharm. Sci.* **2021**, *110*, 50.
- [4] R. Negoro, K. Takayama, K. Kawai, K. Harada, F. Sakurai, K. Hirata, H. Mizuguchi, *Stem Cell Reports* **2018**, *11*, 1539.
- [5] T. Sato, R. G. Vries, H. J. Snippert, M. Van De Wetering, N. Barker, D. E. Stange, J. H. Van Es, A. Abo, P. Kujala, P. J. Peters, H. Clevers, *Nature* **2009**, *459*, 262.
- [6] J. R. Spence, C. N. Mayhew, S. A. Rankin, M. F. Kuhar, J. E. Vallance, K. Tolle, E. E. Hoskins, V. V. Kalinichenko, S. I. Wells, A. M. Zorn, N. F. Shroyer, J. M. Wells, *Nature* **2011**, *470*, 105.
- [7] T. Zietek, P. Giesbertz, M. Ewers, F. Reichart, M. Weinmüller, E. Urbauer, D. Haller, I. E. Demir, G. O. Ceyhan, H. Kessler, E. Rath, *Front. Bioeng. Biotechnol.* **2020**, *0*, 1065.
- [8] T. Zietek, E. Rath, D. Haller, H. Daniel, *Sci. Rep.* **2015**, *5*, 1.
- [9] D. Onozato, M. Yamashita, A. Nakanishi, T. Akagawa, Y. Kida, I. Ogawa, T. Hashita, T. Iwao, T. Matsunaga, *Drug Metab. Dispos.* **2018**, *46*, 1572.
- [10] A. W. F. Janssen, L. P. M. Duivenvoorde, D. Rijkers, R. Nijssen, A. A. C. M. Peijnenburg, M. van der Zande, J. Lousse, *Arch. Toxicol. 2020 953* **2020**, *95*, 907.

- [11] M. Kasendra, R. Luc, J. Yin, D. V. Manatakis, G. Kulkarni, C. Lucchesi, J. Sliz, A. Apostolou, L. Sunuwar, J. Obrigewitch, K. J. Jang, G. A. Hamilton, M. Donowitz, K. Karalis, *Elife* **2020**, *9*, DOI 10.7554/ELIFE.50135.
- [12] C. Günther, T. Brevini, F. Sampaziotis, M. F. Neurath, *Dig. Liver Dis.* **2019**, *51*, 753.
- [13] P. Kakni, R. Truckenmüller, P. Habibović, S. Giselbrecht, *Trends Biotechnol.* **2022**, 932.
- [14] J. Y. Co, M. Margalef-Català, X. Li, A. T. Mah, C. J. Kuo, D. M. Monack, M. R. Amieva, *Cell Rep.* **2019**, *26*, 2509.
- [15] J. Y. Co, M. Margalef-Català, D. M. Monack, M. R. Amieva, *Nat. Protoc.* *2021 1611* **2021**, *16*, 5171.
- [16] T. J. Nash, K. M. Morris, N. A. Mabbott, L. Vervelde, *Commun. Biol.* *2021 41* **2021**, *4*, 1.
- [17] Y. Li, N. Yang, J. Chen, X. Huang, N. Zhang, S. Yang, G. Liu, G. Liu, *J. Virol.* **2020**, *94*.
- [18] P. Kakni, C. López-Iglesias, R. Truckenmüller, P. Habibović, S. Giselbrecht, *Front. Bioeng. Biotechnol.* **2022**, *0*, 669.
- [19] C. Chelakkot, J. Ghim, S. H. Ryu, *Exp. Mol. Med.* *2018 508* **2018**, *50*, 1.
- [20] K. R. Groschwitz, S. P. Hogan, *J. Allergy Clin. Immunol.* **2009**, *124*, 3.
- [21] S. C. Pearce, A. Al-Jawadi, K. Kishida, S. Yu, M. Hu, L. F. Fritzkly, K. L. Edelblum, N. Gao, R. P. Ferraris, *BMC Biol.* **2018**, *16*, 1.
- [22] I. S. Sesorova, N. R. Karelina, T. E. Kazakova, S. Parashuraman, M. A. Zdorikova, I. D. Dimov, E. V. Seliverstova, G. V. Beznoussenko, A. A. Mironov, *Histochem. Cell Biol.* **2020**, *153*, 413.
- [23] A. Monaco, B. Ovryn, J. Axis, K. Amsler, *Int. J. Mol. Sci.* *2021, Vol. 22, Page 7677* **2021**, *22*, 7677.
- [24] A. Woting, M. Blaut, *Nutr.* *2018, Vol. 10, Page 685* **2018**, *10*, 685.
- [25] M. F. A. Baxter, R. Merino-Guzman, J. D. Latorre, B. D. Mahaffey, Y. Yang, K. D. Teague, L. E. Graham, A. D. Wolfenden, X. Hernandez-Velasco, L. R. Bielke, B. M. Hargis, G. Tellez, *Front. Vet. Sci.* **2017**, *4*, 56.
- [26] J. Kowapradit, P. Opanasopit, T. Ngawhirunpat, A. Apirakaramwong, T. Rojanarata, U. Ruktanonchai, W. Sajomsang, *AAPS PharmSciTech* **2010**, *11*, 497.
- [27] P. Xu, E. Elamin, M. Elizalde, P. P. H. A. Bours, M. J. Pierik, A. A. M. Masclee, D. M. A. E. Jonkers, *Sci. Reports* *2019 91* **2019**, *9*, 1.
- [28] Y. B. Chung, K. Han, A. Nishiura, V. H. L. Lee, *Pharm. Res.* *1998 1512* **1998**, *15*, 1882.

- [29] Y. Zheng, Z. Zuo, A. H. Albert, *Int. J. Pharm.* **2006**, 309, 123.
- [30] T. Y. Wang, M. Liu, P. Portincasa, D. Q. H. Wang, *Eur. J. Clin. Invest.* **2013**, 43, 1203.
- [31] R. S. McLeod, Z. Yao, *Biochem. Lipids, Lipoproteins Membr. Sixth Ed.* **2016**, 459.
- [32] N. Auclair, L. Melbouci, D. St-Pierre, E. Levy, *Exp. Cell Res.* **2018**, 363, 1.
- [33] A. Fritz, D. Busch, J. Lapczuk, M. Ostrowski, M. Drozdziak, S. Oswald, *Basic Clin. Pharmacol. Toxicol.* **2019**, 124, 245.
- [34] S. Kondo, S. Mizuno, T. Hashita, T. Iwao, T. Matsunaga, *Biol. Open* **2020**, 9.
- [35] K. Sasaki, M. Inoue, M. Machida, T. Kawasaki, S. Tsuruta, H. Uchida, S. Sakamoto, M. Kasahara, A. Umezawa, H. Akutsu, *StemJournal* **2021**, 3, 1.
- [36] U. Hoffmann, H. K. Kroemer, <https://doi.org/10.1081/DMR-200033473> **2004**, 36, 669.
- [37] T. Vanuytsel, J. Tack, R. Farre, *Front. Nutr.* **2021**, 8, 585.
- [38] G. Altay, E. Larrañaga, S. Tosi, F. M. Barriga, E. Batlle, V. Fernández-Majada, E. Martínez, *Sci. Reports 2019 91* **2019**, 9, 1.
- [39] D. R. Hill, S. Huang, Y.-H. Tsai, J. R. Spence, V. B. Young, *J. Vis. Exp.* **2017**, e56960.
- [40] S. A. den Daas, U. Soffientini, S. Chokshi, G. Mehta, *STAR Protoc.* **2022**, 3, 101365.
- [41] H. M. de Vogel-van den Bosch, M. Bünger, P. J. de Groot, H. Bosch-Vermeulen, G. J. E. J. Hooiveld, M. Müller, *BMC Genomics* **2008**, 9, 1.
- [42] K. Duszka, M. Oresic, C. Le May, J. König, W. Wahli, *Int. J. Mol. Sci.* 2017, Vol. 18, Page 2559 **2017**, 18, 2559.
- [43] K. Duszka, A. Picard, S. Ellero-Simatos, J. Chen, M. Defernez, E. Paramalingam, A. Pigram, L. Vanoaica, C. Canlet, P. Parini, A. Narbad, H. Guillou, B. Thorens, W. Wahli, *Sci. Reports 2016 61* **2016**, 6, 1.
- [44] C. W. Ko, J. Qu, D. D. Black, P. Tso, *Nat. Rev. Gastroenterol. Hepatol.* 2020 173 **2020**, 17, 169.
- [45] A. Fedi, C. Vitale, G. Ponschin, S. Ayehunie, M. Fato, S. Scaglione, *J. Control. Release* **2021**, 335, 247.
- [46] J. Yu, R. L. Carrier, J. C. March, L. G. Griffith, *Drug Discov. Today* **2014**, 19, 1587.
- [47] M. Takano, R. Yumoto, T. Murakami, *Pharmacol. Ther.* **2006**, 109, 137.
- [48] M. R. Arana, G. N. Tocchetti, J. P. Rigalli, A. D. Mottino, S. S. M. Villanueva, *Pharmacol. Res.* **2016**, 109, 32.
- [49] J. Zhao, Z. Zeng, J. Sun, Y. Zhang, D. Li, X. Zhang, M. Liu, X. Wang, *Basic*

- Clin. Pharmacol. Toxicol.* **2017**, *120*, 250.
- [50] S. M. Robertson, X. Luo, N. Dubey, C. Li, A. B. Chavan, G. S. Gilmartin, M. Higgins, L. Mahnke, *J. Clin. Pharmacol.* **2015**, *55*, 56.
- [51] S. Giselbrecht, T. Gietzelt, E. Gottwald, C. Trautmann, R. Truckenmüller, K. F. Weibezahn, A. Welle, *Biomed. Microdevices* **2006**, *8*, 191.
- [52] P. Kakni, R. Hueber, K. Knoops, C. López-Iglesias, R. Truckenmüller, P. Habibovic, S. Giselbrecht, *Adv. Biosyst.* **2020**, 2000126.
- [53] E. H. H. M. Rings, E. H. van Beers, S. D. Krasinski, M. Verhave, R. K. Montgomery, R. J. Grand, J. Dekker, H. A. Büller, *Nutr. Res.* **1994**, *14*, 775.
- [54] S. Lin, S. Yeruva, P. He, A. K. Singh, H. Zhang, M. Chen, G. Lamprecht, H. R. de Jonge, M. Tse, M. Donowitz, B. M. Hogema, J. Chun, U. Seidler, C. C. Yun, *Gastroenterology* **2010**, *138*, 649.
- [55] J. M. Penninger, M. B. Grant, J. J. Y. Sung, *Gastroenterology* **2021**, *160*, 39.
- [56] R. S. Holmes, K. D. Spradling Reeves, L. A. Cox, *J. Data Mining Genomics Proteomics* **2017**, *8*, DOI 10.4172/2153-0602.1000211.
- [57] A. B. Kohan, F. Wang, C. M. Lo, M. Liu, P. Tso, *Am. J. Physiol. - Gastrointest. Liver Physiol.* **2015**, *308*, G472.
- [58] K. Shioji, T. Mannami, Y. Kokubo, Y. Goto, H. Nonogi, N. Iwai, *J. Hum. Genet. 2004 498* **2004**, *49*, 433.
- [59] M. Garelnabi, K. Lor, J. Jin, F. Chai, N. Santanam, *Clin. Biochem.* **2013**, *46*, 12.
- [60] M. B. Ruiz-Roso, J. Gil-Zamorano, M. C. López de las Hazas, J. Tomé-Carneiro, M. C. Crespo, M. J. Latasa, O. Briand, D. Sánchez-López, A. I. Ortiz, F. Visioli, J. A. Martínez, A. Dávalos, *Front. Genet.* **2020**, *11*, 707.
- [61] J. Huuskonen, V. M. Olkkonen, M. Jauhiainen, C. Ehnholm, *Atherosclerosis* **2001**, *155*, 269.
- [62] P. Jiang, W. Du, A. Mancuso, K. E. Wellen, X. Yang, *Nat. 2013 4937434* **2013**, *493*, 689.
- [63] I. Kim, S. H. Ahn, T. Inagaki, M. Choi, S. Ito, G. L. Guo, S. A. Kliewer, F. J. Gonzalez, *J. Lipid Res.* **2007**, *48*, 2664.
- [64] H. Van Tilbeurgh, S. Bezzine, C. Cambillau, R. Verger, F. Carrière, *Biochim. Biophys. Acta - Mol. Cell Biol. Lipids* **1999**, *1441*, 173.
- [65] H. Zhang, *Curr. Opin. Lipidol.* **2018**, *29*, 218.
- [66] K. L. Sylvers-Davie, B. S. J. Davies, *Encycl. Biol. Chem. Third Ed.* **2021**, *3*, 307.

**Supporting Information**Supplementary Tables**Supplementary Table 1.** List of antibodies

<b>Antibodies</b>	<b>Supplier</b>	<b>Host</b>	<b>Dilution</b>
E-Cadherin	Beckton Dickinson	Mouse	1:500
Villin	Santa cruz	Mouse	1:250
TGR5	Abcam	Rabbit	1:200
GLUT2	Santa cruz	Mouse	1:200
Phalloidin 568	Invitrogen		1:500
Alexa Fluor 488	Invitrogen		1:500
Alexa Fluor 647	Invitrogen		1:500
Alexa Fluor 568	Invitrogen		1:500

**Supplementary Table 2.** Primer sequences

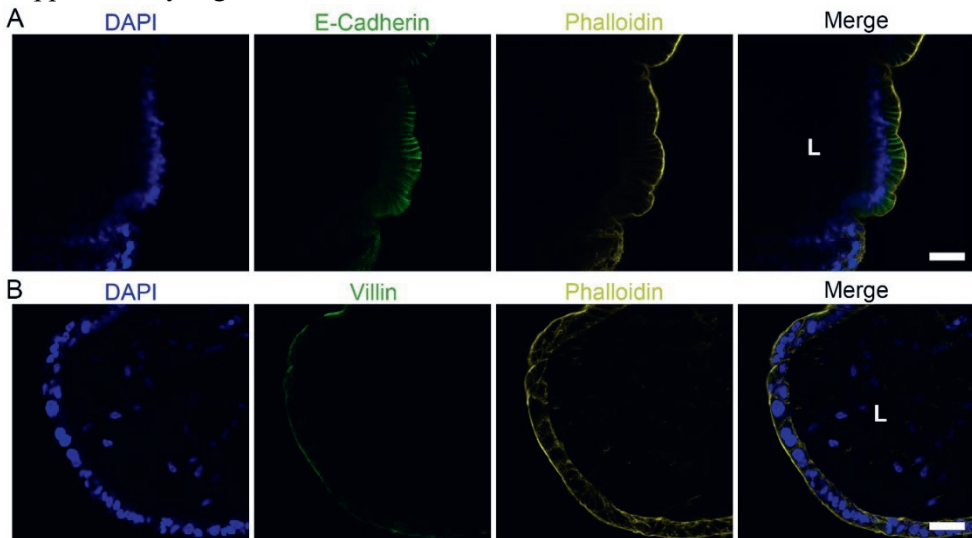
<b>Gene</b>	<b>5'–Forward– 3'</b>	<b>5'–Reverse– 3'</b>
<i>ACE2</i>	CAAGAGCAAACGGTTGAACAC	CCAGAGCCTCTCATTGTAGTCT
<i>APOA1</i>	CCCTGGGATCGAGTGAAGGA	CTGGGACACATAGTCTCTGCC
<i>APOA4</i>	CTCAAGGGACGCCTTACGC	GTCCTGAGCATAGGGAGCCA
<i>APOA5</i>	GCCAGCGACTTCAGGCTTT	AGCTTGCTCAGAACCCTGCC
<i>BCRP</i>	ACGAACGGATTAACAGGGTCA	CTCCAGACACACCACGGAT
<i>CES2</i>	CATGGCTTCCTGTATGATGGT	CTCCAAAGTGGGCGATATTCTG
<i>CLDN1</i>	CCCAGTCAATGCCAGGTACG	GGGCCTTGGTGTGGGTAAG
<i>CLDN3</i>	AACACCATTATCCGGGACTTCT	GCGGAGTAGACGACCTTGG
<i>CLDN5</i>	GCAGCCCCTGTGAAGATTGA	GTCTCTGGCAAAAAGCGGTG
<i>CLPS</i>	CTCTGCATGAATAGTGCCCAG	AGGGACACTTGTAGTAAATCCCA
<i>CYP2C9</i>	CAGAGACGACAAGCACAACCCT	ATGTGGCTCCTGTCTTGCATGC
<i>CYP2J2</i>	TGGCTTGCCCTTAATCAAAGAA	GGCCACTTGACATAATCAATCCA
<i>CYP3A4</i>	AAGTCGCCTCGAAGATACACA	AAGGAGAGAACTGCTCGTG
<i>CYP8B1</i>	ATTTGGATACCGTTCAGTGCAA	CAGAAGCGAAAAGAGGCTGTC
<i>ENPEP</i>	CTTGACCAGATCGTGTGACTC	GGCAGTCGAAAGTTTTCCAC
<i>HMGCS2</i>	CAGTCCAAGAGGACATCAACTC	CAGTGCCTACTTCCAGCCTG
<i>LCT</i>	ATCCAGACGAGAAAACAGTGC	GTCAGCAAAAGGCTTCGGTTC
<i>LIPA</i>	CCCACGTTTGCCTCATGTC	CCCAGTCAAAAGGCTTGAAACTT
<i>LPL</i>	TCATCCCGGAGTAGCAGAGT	GGCCACAAGTTTTGGCACC
<i>MDR1</i>	GGGATGGTCAGTGTTGATGGA	GCTATCGTGGTGGCAAAACAATA
<i>ME1</i>	GGGAGACCTTGGCTGTAATGG	TTCGGTCCCACATCCAGAAT
<i>MRP1</i>	TTACTCATTACAGCTCGTCTTGTC	CAGGGATTAGGGTCGTGGAT
<i>MRP2</i>	TCTCTCGATACTCTGTGGCAC	CTGGAATCCGTAGGAGATGAAGA
<i>MRP3</i>	CACCAACTCAGTCAAACGTGC	GCAAGACCATGAAAGCGACTC
<i>MRP4</i>	TGTGGCTTTGAACACAGCGTA	CCAGCACACTGAACGTGATAA
<i>MRP5</i>	GAACTCGACCGTTGGAATGC	TCATCCAGGATTCTGAGCTGAG

<i>MRP6</i>	AGATGGTGCTTGGATTGCGC	GCCACACAGTAGGATGAATGAG
<i>OCN</i>	CATTGCCATCTTTGCCTGTG	AGCCATAACCATAGCCATAGC
<i>OSTA</i>	ACCTCGTTTTATGCCGTGTG	AAGAAGGCGTATTGGAAAGGG
<i>OSTB</i>	ATGGTCCTCCTGGGAAGAAGCA	GCCTCATCCAAATGCAGGACTTC
<i>PEPT1</i>	GACAAGCAGTCACCTCAGTAAG	AGTCCCGAGAGCTATCAGGG
<i>PLTP</i>	AAGAGCGGATGGTGTATGTGG	ATGGGGAGTCAATCACTGCTG
<i>SLC9A3R1</i>	GGCTGGCAACGAAAATGAGC	TGTCGCTGTGCAGGTTGAAG
<i>UGT1A1</i>	CTGTCTCTGCCACTGTATTCT	TCTGTGAAAAGGCAATGAGCAT
<i>UGT1A3</i>	TTTCACCCTGACAACCTATGC	AGCTCCACACAAGACCTATGAT
<i>ZO-1</i>	CAACATACAGTGACGCTCACA	CACTATTGACGTTCCCCACTC

**Supplementary Table 3.** Functions of lipid metabolism markers

<b>Gene</b>	<b>Function</b>
<i>LCT</i>	instructs the production of lactase enzyme <sup>[1]</sup>
<i>SLC9A3R1</i>	encodes the Na <sup>+</sup> /H <sup>+</sup> exchanger regulatory factor 1 protein <sup>[2]</sup>
<i>ENPEP</i>	are involved in the control of sodium and water absorption, glucose uptake and absorption and digestion of peptides <sup>[3,4]</sup>
<i>ACE2</i>	
<i>APOA4</i>	is involved between others in chylomicron assembly, cholesterol transport and blood glucose homeostasis <sup>[5]</sup>
<i>APOA1</i>	is a major component of the high-density lipoprotein (HDL) <sup>[6]</sup>
<i>APOA5</i>	is a key regulator of triglyceride levels <sup>[7]</sup>
<i>HMGCS2</i>	encodes the rate-limiting enzyme in the production of ketone bodies <sup>[8]</sup>
<i>PLTP</i>	transfers phospholipid and cholesterol from apo B-containing lipoproteins to HDL <sup>[9]</sup>
<i>ME1</i>	generates nicotinamide adenine dinucleotide phosphate (NADPH) that is used in fatty acid and cholesterol biosynthesis <sup>[10]</sup>
<i>CYP8B1</i>	is required for the synthesis of cholic acid <sup>[11]</sup>
<i>CLPS</i>	is a cofactor of pancreatic lipase, which allows the lipase to anchor itself to the lipid-water interface <sup>[12]</sup>
<i>LIPA</i>	produces the lysosomal acid lipase <sup>[13]</sup>
<i>LPL</i>	hydrolyses circulating triglycerides and releases fatty acids that can be taken up by tissues <sup>[14]</sup>



Supplementary Figures

**Supplementary Figure 1: Apico-basolateral organization of human intestinal organoids.** (A) Immunofluorescence staining for the basolateral marker E-Cadherin (green) and the apical marker Phalloidin (yellow) indicated reversed polarity, where the apical side is facing outwards and the basal inwards. (B) The apical markers Villin (green) and Phalloidin (yellow) were co-expressed in the outer surface of the organoids. Scale bars: 50  $\mu\text{m}$ . L: lumen.

References

- [1] E. H. H. M. Rings, E. H. van Beers, S. D. Krasinski, M. Verhave, R. K. Montgomery, R. J. Grand, J. Dekker, H. A. Büller, *Nutr. Res.* **1994**, *14*, 775.
- [2] S. Lin, S. Yeruva, P. He, A. K. Singh, H. Zhang, M. Chen, G. Lamprecht, H. R. de Jonge, M. Tse, M. Donowitz, B. M. Hogema, J. Chun, U. Seidler, C. C. Yun, *Gastroenterology* **2010**, *138*, 649.
- [3] J. M. Penninger, M. B. Grant, J. J. Y. Sung, *Gastroenterology* **2021**, *160*, 39.
- [4] R. S. Holmes, K. D. Spradling Reeves, L. A. Cox, *J. Data Mining Genomics Proteomics* **2017**, *8*, DOI 10.4172/2153-0602.1000211.
- [5] A. B. Kohan, F. Wang, C. M. Lo, M. Liu, P. Tso, *Am. J. Physiol. - Gastrointest. Liver Physiol.* **2015**, *308*, G472.
- [6] K. Shioji, T. Mannami, Y. Kokubo, Y. Goto, H. Nonogi, N. Iwai, *J. Hum. Genet.* **2004**, *49*, 433.
- [7] M. Garelnabi, K. Lor, J. Jin, F. Chai, N. Santanam, *Clin. Biochem.* **2013**, *46*, 12.
- [8] M. B. Ruiz-Roso, J. Gil-Zamorano, M. C. López de las Hazas, J. Tomé-Carneiro, M. C. Crespo, M. J. Latasa, O. Briand, D. Sánchez-López, A. I. Ortiz, F. Visioli, J. A. Martínez, A. Dávalos, *Front. Genet.* **2020**, *11*, 707.

- [9] J. Huuskonen, V. M. Olkkonen, M. Jauhiainen, C. Ehnholm, *Atherosclerosis* **2001**, *155*, 269.
- [10] P. Jiang, W. Du, A. Mancuso, K. E. Wellen, X. Yang, *Nat. 2013 4937434* **2013**, *493*, 689.
- [11] I. Kim, S. H. Ahn, T. Inagaki, M. Choi, S. Ito, G. L. Guo, S. A. Kliewer, F. J. Gonzalez, *J. Lipid Res.* **2007**, *48*, 2664.
- [12] H. Van Tilbeurgh, S. Bezzine, C. Cambillau, R. Verger, F. Carrière, *Biochim. Biophys. Acta - Mol. Cell Biol. Lipids* **1999**, *1441*, 173.
- [13] H. Zhang, *Curr. Opin. Lipidol.* **2018**, *29*, 218.
- [14] K. L. Sylvers-Davie, B. S. J. Davies, *Encycl. Biol. Chem. Third Ed.* **2021**, *3*, 307.

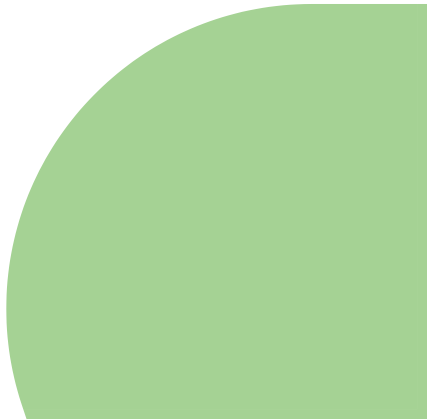




## CHAPTER VII

# **HYPOXIA-TOLERANT APICAL-OUT INTESTINAL ORGANOIDS TO MODEL HOST-MICROBIOME INTERACTIONS**

Panagiota Kakni, Barry Jutten, Daniel Teixeira  
Oliveira Carvalho, John Penders, Roman  
Truckenmüller, Pamela Habibović and  
Stefan Giselbrecht



## **Abstract**

Microbiome is an integral part of the gut and is essential for its proper function. Imbalances of the microbiota can be devastating and have been linked with several gastrointestinal conditions. Current gastrointestinal models do not fully reflect the *in vivo* situation. Thus, it is important to establish more advanced *in vitro* models to study host-microbiome/pathogen interactions. Here, we developed for the first time an apical-out human small intestinal organoid model in hypoxia, where the apical surface is directly accessible and exposed to a hypoxic environment. These organoids mimic the intestinal cell composition, structure and functions and provide easy access to the apical surface. Co-cultures with the anaerobic strains *Lactobacillus casei* and *Bifidobacterium longum* showed successful colonization and probiotic benefits on the organoids. These novel hypoxia-tolerant apical-out small intestinal organoids will pave the way for unraveling unknown mechanisms related to host-microbiome interactions and serve as a tool to develop microbiome-related probiotics and therapeutics.

## **Introduction**

The intestinal epithelium is a highly organized, dynamic cell layer with rapid self-renewing capacity<sup>1</sup>. Main functions of the intestine include the formation of a physical barrier between the luminal contents and the external environment, nutrient absorption and transport, and regulation of host-microbiome interactions<sup>2</sup>. Intestinal epithelial cells are polarized, featuring an apical and a basolateral membrane domain, which are characterized by different biochemical and functional properties. Maintenance of this organization is crucial for the proper function of the intestine. The apical surface is facing the intestinal lumen and is responsible for the uptake of nutrients and the formation of a defensive barrier against pathogens<sup>3</sup>. Trillions of bacteria, fungi and other microbes reside in the gut lumen and together create an interconnected community with symbiotic and/or pathogenic relationships. The gut microbiome has a key role in metabolism and training and homeostasis of the immune system regulation and thus a tremendous impact on overall health and disease of its host<sup>4,5</sup>. Disruption of the gut microbiome has been associated, amongst others, with inflammatory bowel disease, metabolic diseases, such as diabetes, obesity, and neurodevelopmental disorders<sup>4-6</sup>. Thus, there is a growing demand for advanced *in vitro* co-culture systems to reveal the mechanistic insights of the complex relationship and interactions between the microbiome and the intestinal epithelium, which often cannot be retrieved from more simple *in vitro* or *in vivo* models.

Intestinal organoids are three-dimensional (3D) *in vitro* models that have shown great potential in modeling intestinal physiology and disease. They recapitulate both the architecture and function of the *in vivo* tissue closer than traditional 2D culture systems. Specifically, they are structured into crypt and villus domains that surround a central lumen, they have self-renewal capacity, multicellular composition and they can perform numerous specialized intestinal functions<sup>1,7</sup>. Based on their proven capacity to closely resemble the intestinal epithelium, organoids have been used for the study of intestinal microbiota-host interactions<sup>8-10</sup>. Specifically, organoids have been co-cultured with commensal bacteria, such as *Lactobacillus*<sup>11-13</sup> and non-pathogenic *Escherichia coli* (*E. coli*) strains<sup>14</sup>, and pathogenic bacteria, such as *Cryptosporidium*<sup>15</sup>, *Salmonella enterica* serovar Typhimurium<sup>16,17</sup>, *E. coli* strains<sup>17-22</sup>, *Clostridioides difficile*<sup>23-25</sup>, and *Bacteroides thetaiotaomicron*<sup>26</sup>. In these systems, to bring the microorganisms in contact with the apical surface of the epithelial cells of the organoids, microinjections of the bacteria into the central lumen were necessary. Although with this method the microorganisms were placed in a hypoxic environment similar to the *in vivo* situation, microinjections are technically challenging, time-consuming and require skilled personnel.

As an alternative method to gain access to the apical surface that faces the lumen, researchers developed ways to reverse epithelial polarity. By culturing organoids in suspension, human adult<sup>27,28</sup>, human pluripotent stem cell<sup>29</sup>, and chicken<sup>30</sup> and porcine<sup>31</sup> adult stem cell-derived organoids reversed their polarity in a way that the apical surface is facing outwards to the culture medium. These organoids have been used to study infections by *Salmonella* Typhimurium, *Listeria monocytogenes*, influenza A virus strain PR8, *Eimeria tenella*, and transmissible gastroenteritis virus<sup>28,30,31</sup>. It has been shown that organoid models with reversed polarity facilitate such co-cultures since the microorganisms can simply be added to the culture medium. Although these apical-out models are highly valuable, with numerous advantages over microinjections, they do not resemble the low oxygen concentration environment that the apical surface of the intestine *in vivo* is exposed to. More specifically, *in vivo* there is an oxygen gradient from the intestinal lumen to the epithelium, ranging from 2% O<sub>2</sub> in the lumen to 8% in the crypt area<sup>32</sup>. Indeed, the apical surface of the apical-out organoids so far is exposed to approximately 18% O<sub>2</sub>, since it is in contact with the cell culture medium and the organoids are grown in a standard normoxia (21% O<sub>2</sub>) incubator<sup>33</sup>. The hypoxic intestinal lumen *in vivo* supports the growth and survival of anaerobic microorganisms, which constitute the predominant bacterial species in the gut<sup>32,34</sup>. Thus, co-culture of the current reversed

polarity organoids with anaerobic bacteria is not optimal, since the high oxygen levels are harmful to these microorganisms and in some cases even lethal<sup>35,36</sup>.

In this study, we aimed to establish an apical-out small intestinal organoid model in hypoxic conditions, in order to overcome the aforementioned issues and create an *in vitro* model that facilitates both the easy access to the apical surface and the survival of anaerobic bacteria. To this end, we adapted our previously described protocol to generate apical-out small intestinal organoids from pluripotent stem cells<sup>29</sup> to low oxygen conditions. Specifically, we cultured the organoids in a suspension system that was sustained in a hypoxic environment (5% O<sub>2</sub>). After assessing the differentiation capacity and functionality of these apical-out hypoxic organoids, we established co-culture systems with the probiotic strains *Lactobacillus casei* (*L. casei*) and *Bifidobacterium longum* (*B. longum*). These anaerobic bacteria reside in the intestine and have attracted a lot of interest from the food industry over the years because of their health-promoting probiotic benefits (e.g. epithelial barrier integrity and host immune response)<sup>37</sup>. Since multiple bacterial strains co-reside in the gut, we also performed a triple co-culture of organoids, *L. casei*, and *B. longum*. All co-culture experiments showed tighter barrier formation and increased mucin production in the organoids, compared to organoids without bacteria. This innovative, hypoxia tolerant apical-out small intestinal organoid model will be a valuable tool in future to decipher the complex gut-microbiome interactions, which have a great impact on health.

## **Materials and Methods**

### Maintenance of pluripotent stem cells

The human embryonic stem cell (ESC) line WA09 (H9) was purchased from WiCell. The cells were maintained in feeder-free conditions using mTESR<sup>®</sup>1 (StemCell Technologies). Every four to five days (depending on colony density), the ES cells were passaged onto Matrigel (Corning<sup>®</sup>)-coated tissue culture dishes.

### Fabrication and preparation of microwell arrays

Arrays of U-bottom microwells were fabricated using 50 µm thin polymer films by microthermoforming as previously described<sup>38,39</sup>. Each microwell had a diameter of 500 µm and depth of approximately 300 µm, and each array contained 289 microwells. Microwell arrays were sterilized in a graded series of 2-propanol (VWR) (100%–70%–50%–25%–10%) and then washed twice with Dulbecco's phosphate buffered saline (PBS; Sigma-Aldrich). The microwell arrays were mounted at the bottoms of 24-well plates using elastomeric O-rings (ERIKS).

Differentiation of pluripotent stem cells towards small intestinal organoids

Directed differentiation of ESCs towards intestinal organoids was performed as previously described<sup>29</sup>. Briefly, to create embryoid bodies (EBs), ESC colonies were dissociated into single cells with TrypLE™ Express Enzyme (Thermofisher), resuspended in mTesR1 supplemented with Y-27632 (10 µM; Tocris) and then seeded in the microwell arrays at a density of 1000 cells/microwell. A three-day incubation with Activin A (100 ng/mL; Cell guidance systems) in RPMI 1640 (Thermofisher) medium supplemented with increasing concentrations (0%, 0,2% and 2%) of Hyclone defined fetal bovine serum (dFBS; Fisher scientific) promoted the definitive endoderm (DE) differentiation. During the next four days, DE spheroids were treated with FGF4 (500 ng/mL; R&D Systems) and CHIR99021 (3 µM; Stemgent) to induce the hindgut formation. The medium was refreshed daily from the sidewalls of the well plates, to avoid disruption of the spheroids.

Differentiation of hindgut spheroids towards small intestinal organoids was performed in two ways in order to promote apical-in or apical-out epithelial polarity. For apical-in organoids, hindgut spheroids were collected and embedded in Matrigel. A 50 µl drop of Matrigel containing organoids (Matrigel dome) was placed in each well of a tissue cultured-treated 24-well plate, cross-linked at 37 °C for 20 min, and overlaid with Advanced DMEM/F-12 supplemented with B27, N2, HEPES, penicillin/streptomycin, L-glutamine (all Thermofisher), EGF (50 ng/mL; R&D systems), Noggin (100 ng/mL; R&D systems) and R-Spondin (500 ng/mL; R&D systems). For apical-out organoids, hindgut spheroids were collected and placed in suspension culture in non-tissue culture-treated 6-well plates. The plates were coated with 1% Pluronic solution in PBS (Sigma-Aldrich) for 2 h at 37 °C, to avoid cell-surface adherence. The same medium as for apical-in organoids was used, but in this case, it was supplemented with 2% Matrigel. The suspension cultures of apical-out organoids were performed either in a normoxic (21% O<sub>2</sub>) or in a hypoxic (5% O<sub>2</sub>) incubator (PHCbi) and they are referred to as suspension or suspension hypoxia, respectively.

Bacteria culture

*Lactobacillus casei* and *Bifidobacterium longum* (kindly provided by John Pender's lab at Maastricht University) were cultivated in de Man, Rogosa and Sharpe (MRS) broth (Thermofisher) at 37 °C in an anaerobic chamber. To evaluate bacterial growth in organoid media, *L. casei* and *B. longum* were anaerobically grown in MRS broth overnight at 37°C. The following day, the concentration of bacteria was established



by optical density measured at a wavelength of 600 nm ( $OD_{600}$ ). Bacteria were diluted to  $10^3$ /mL in organoid medium and incubated for 0, 6, 12, and 24 h at 5%  $O_2$ , 5%  $CO_2$  at 37 °C. Next, 0.1 and 1 mL of the culture were used to make pour plates using MRS agar (Sigma-Aldrich). Colonies were counted after 48 h of anaerobic incubation at 37 °C.

#### Co-culture of organoids with bacteria

Following differentiation, apical-out intestinal organoids were placed in 35 mm petri dishes (pre-coated with a 1% Pluronic solution). The concentration of bacteria was established by  $OD_{600}$ .  $10^7$  or  $10^8$  bacteria were added to the same 35 mm petri dish. The organoid-bacteria systems were co-cultured for 12 h at 37 °C in hypoxic conditions (5%  $O_2$ ). Following that, organoids were washed with PBS and collected for downstream experiments.

#### Epithelial barrier integrity

To test the epithelial barrier integrity, the permeability of the fluorescence marker 4 kDa Fluorescein isothiocyanate (FITC)-labeled dextran (Sigma-Aldrich) was evaluated. Intact organoids were collected and incubated in a solution containing 2 mg/mL 4 kDa FITC-dextran for 30 min at room temperature (RT). To disrupt the barrier integrity, organoids were treated with 2 mM ethylenediamine tetraacetic acid (EDTA; VWR) in Hanks' balanced salt solution (w/o calcium and magnesium; Thermofisher) on ice for 15 min. Afterwards, they were resuspended in the same FITC-dextran solution as intact organoids. Organoids were then mounted and immediately imaged using a confocal laser scanning microscope (Leica TCS SP8).

#### Fatty acid absorption assay

Initially, apical-in organoids were incubated with 5 mM EDTA in PBS for 1 h on a shaking platform at 4 °C, in order to remove the surrounding Matrigel. Both apical-in and apical-out organoids were then washed with DMEM without phenol red and treated with a solution containing 5  $\mu$ M fluorescent fatty acid analog C1-BODIPY-C12 (Thermofisher) and 5  $\mu$ M fatty-acid-free BSA (Sigma-Aldrich) for 30 min at 37 °C. Next, the organoids were fixed in 4% paraformaldehyde (VWR) in PBS for 30 min and stained for actin (phalloidin) and cell nuclei (4',6-diamidino-2-phenylindole; DAPI). Finally, organoids were imaged with a confocal laser scanning microscope (Leica TCS SP8). The intracellular fluorescent signal from C1-BODIPY-C12 was quantified in single confocal z-scans using QuPath 0.3.2.

### RNA isolation and quantitative Real-Time PCR (qPCR)

The total RNA was isolated from the organoids with the RNeasy Mini Kit (Qiagen) according to manufacturer's guidelines. The cDNA was synthesized from RNA using the iScript cDNA Synthesis Kit (Bio-Rad). All samples were analyzed on a CFX96 real-time PCR detection system (Bio-Rad) using the iQ SYBR Green Supermix (Bio-Rad). All gene expression levels were normalized using the hypoxanthine phosphoribosyltransferase (HPRT) housekeeping gene. Data analysis followed the  $2^{-\Delta\Delta C_t}$  method. The results are representative of three independent experiments. The primer sequences are listed in the supplementary material.

### Scanning Electron Microscopy (SEM)

Organoids were chemically fixed with 1.5% glutaraldehyde (Merck) in 0.067 M cacodylate (Acros Organics) buffered to pH 7.4 and 1% sucrose (Merck) for 3 h at RT. Subsequently, they were washed with 0.1 M cacodylate buffer and postfixed with a mixture of 1% osmium tetroxide (Agar Scientific) and 1.5% potassium ferricyanide (Merck) in the same buffer, for 1 h in the dark at 4 °C. After washing with Milli-Q water, the organoids were dehydrated in a graded series of ethanol (Merck) (70, 90, up to 100%) at RT and dried with hexamethyldisilazane (HMDS) (>99.9%, Sigma-Aldrich). Finally, the samples were mounted onto SEM stubs, coated with a thin layer of gold by a sputter coater SC7620 (Quorum Technologies) and examined with an electron microscope (Jeol JSM-IT200).

### Transmission Electron Microscopy (TEM)

Organoids were chemically fixed with 1.5% glutaraldehyde in 0.067 M cacodylate buffered to pH 7.4 and 1% sucrose for 3 h at RT. Following that, they were washed with 0.1 M cacodylate buffer and postfixed with a mixture of 1% osmium tetroxide and 1.5% potassium ferricyanide in the same buffer, for 1 h in the dark at 4 °C. After washing with Milli-Q water, the organoids were dehydrated in a graded series of ethanol (70, 90, up to 100%) at RT. Next, organoids were infiltrated with Epon, embedded in the same resin and polymerized for 48 h at 60 °C. Using a diamond knife (DiATOME), ultrathin sections of 60 nm were cut on a Leica UC7 ultramicrotome. The sections were transferred to 50 Mesh copper grids and covered with a formvar and carbon film. They were then imaged on a Tecnai T12 Electron Microscope equipped with an Eagle 4k×4k CCD camera (Thermofisher) and a Veleta 2k×2k CCD camera (Olympus Soft Imaging).

### Immunofluorescence and confocal microscopy

Organoids were fixed with 4% paraformaldehyde in PBS for 30 min and washed three times with PBS. Permeabilization was performed with 0.5% Triton X-100 (Merck) in PBS for 30 min and blocking with 5% donkey serum (VWR) in permeabilization solution for 1 h, all at RT. Primary antibodies were incubated overnight at 4 °C and the following day secondary antibodies were added and incubated for 2 h at RT. Nuclei were counterstained with DAPI and actin with phalloidin. A full list of antibodies is provided in the supplementary material. All samples were imaged with a confocal laser scanning microscope (Leica TCS SP8) and the images were processed with ImageJ.

### Oxygen measurements

Self-adhesive sensor dots (PreSens Precision Sensing GmbH) were autoclaved (121 °C, 15 min) and batch calibrated using a two-point calibration in oxygen-free water and air-saturated water, according to the manufacturer's guidelines. The oxygen-free standard was made by dissolving Na<sub>2</sub>SO<sub>3</sub> (1 g) and Co(NO<sub>3</sub>)<sub>2</sub> standard solution (50 µL) ( $\rho(\text{Co}) = 1000 \text{ mg/L}$ ; in nitric acid 0.5 mol/L) in water (100 mL). Air-saturated water was obtained by blowing air into a stirred water-filled beaker for 20 min under agitation. We observed no significant changes in the signal acquisition of non- vs autoclaved sensor dots, suggesting that sterilization did not affect the sensing capability. Next, sensor dots were glued onto 24-well plate wells pre-coated with 1% Pluronic solution in PBS (Sigma-Aldrich) for 2 h at 37 °C, and seeded with organoids embedded in a drop of Matrigel or suspended in cell culture medium. Plates were incubated at 37 °C for 7 days at normoxic (21% O<sub>2</sub>) and hypoxic (5% O<sub>2</sub>) conditions. Cell culture medium was refreshed after 4 days of culture. The concentration of dissolved oxygen was measured every 5 min from the bottom side of the 24-well plate by using a fluorescence transmitter (Oxy-SMA, PreSens Precision Sensing GmbH) connected to polymeric optic fibers and processed by using the PreSens Measurement Studio 2 software.

### Statistical analysis

Statistical analyses were performed in GraphPad Prism 9 software. Student's two-tailed t-test with Welch's correction and one- or two-way ANOVA were used to determine statistical significance. Significant differences were defined as  $P < 0.05$ . P values of statistical significance are represented as \*\*\*\*P < 0.0001, \*\*\*P < 0.001, \*\*P < 0.01, and \*P < 0.05. Error bars in figures indicate standard error of the mean (S.E.M.).

## **Results**

### Differentiation of apical-out organoids in hypoxia

Recently, human intestinal organoid models with reversed polarity have been described in order to facilitate the access to the apical surface of the organoids<sup>28,29</sup>. Based on our existing reversed polarity intestinal organoid model<sup>29</sup>, here, we developed apical-out intestinal organoids in hypoxic conditions (5% O<sub>2</sub>), aiming to create a more physiologically relevant *in vitro* model for host-microbiome and host-pathogen interaction studies. Briefly, human embryonic stem cells (H9 cells) were aggregated to create homogeneous EBs using polymer film-based microwell arrays (Figure 1 A). In the next days, EBs were differentiated stepwise, first towards definitive endoderm and then towards hindgut. Ultimately, hindgut spheroids were removed from the microwells and placed in a suspension culture system to differentiate them further towards intestinal organoids. This system provides a scalable platform to produce up to 7000 intestinal organoids with reversed polarity, from a single 24-well plate. Scaled-up production of apical-out organoids can be particularly useful for high-throughput downstream applications, such as drug screenings.

For the proper function of the intestine, maintenance of structural organization and presence of diverse epithelial cell lineages are pivotal. Previous reports have shown that pluripotent stem cell-derived organoids recapitulate closely the cellular composition of the *in vivo* intestine<sup>29,40</sup>. To assess the differentiation capacity and maturation level of apical-out organoids in hypoxic conditions, we performed gene expression analysis for both proliferation and differentiation of intestinal cell lineages after 30 days in culture and compared them with apical-in organoids grown embedded in Matrigel domes and with apical-out organoids grown in normoxic conditions (21% O<sub>2</sub>) (Figure 1 B). Specifically, we evaluated the expression of the leucine-rich repeat-containing G-protein-coupled receptor 5 (*LGR5*), the sex determining region Y-box 9 (*SOX9*), the Krueppel-like factor 5 (*KLF5*) and the Achaete scute-like 2 (*ASCL2*), all indicators of proliferation. For differentiation, the expression of the intestinal differentiation marker Caudal Type Homeobox 2 (*CDX2*), the enterocyte brush border marker Villin 1 (*VILL1*), the Paneth cell marker Lysozyme (*LYZ*), and the enteroendocrine cell marker Chromogranin A (*CHGA*) were examined. Presence of mesenchyme was identified by the expression of the distal hindgut mesoderm marker Homeobox A13 (*HOXA13*) and the mesenchymal markers Forkhead Box F1 (*FOXF1*) and Vimentin (*VIM*). The expression levels of all these markers were similar in all three systems (Matrigel

domes, suspension, and suspension hypoxia) and no statistically significant differences were identified. We also performed immunofluorescence stainings to visualize the expression of the proliferation marker Ki67 and phalloidin, the intestinal differentiation marker CDX2, the goblet cell marker Mucin 2 (MUC2) and the enteroendocrine marker Synaptophysin (Supplementary Figure 1). Collectively, these results indicate that apical-out intestinal organoids can be differentiated efficiently in a hypoxic environment.

Next, we examined the structural organization of these organoids. Confocal microscopy demonstrated the expression of the basolateral surface marker E-cadherin in the inner part of the apical-out organoids. In contrast, the expression of phalloidin, which visualizes F-actin, and Villin, which visualizes the apical brush border of the enterocytes, were identified in the outer part of the organoids (Figure 1 C). Transmission electron microscopy (TEM) verified the reversal of epithelial polarity. Microvilli were found on the exterior surface of the organoids, facing the surrounding culture medium (Supplementary Figure 2). Overall, these data confirm that organoids cultured in suspension in hypoxic conditions, have a reversed epithelial polarity, similar to organoids grown in normoxic conditions.

#### HIF-1 $\alpha$ -induced effects on the organoids

Intestine is exposed to a unique oxygen gradient from the highly vascularized subepithelial mucosa towards the hypoxic lumen<sup>41</sup>. The hypoxia-inducible factors (HIFs) are the main regulators of oxygen homeostasis, mediating both oxygen delivery and adaptation to oxygen deprivation<sup>42</sup>. HIFs are heterodimers consisting of an oxygen sensitive  $\alpha$ -subunit and a constitutively expressed  $\beta$ -subunit. Under normoxic conditions, the HIF- $\alpha$  subunits are hydroxylated but under hypoxic conditions, this function is inhibited, thus leading to stabilization of HIF- $\alpha$  subunits that heterodimerize with the HIF- $\beta$  subunits<sup>33</sup>. The HIF-1 $\alpha$  isoform contributes to the proper function of the intestinal barrier and the maintenance of mucosal homeostasis<sup>43</sup>. In this study, we aimed to evaluate the response of apical-out organoids upon exposure to hypoxia, by investigating the expression of HIF-1 $\alpha$  and its downstream targets.

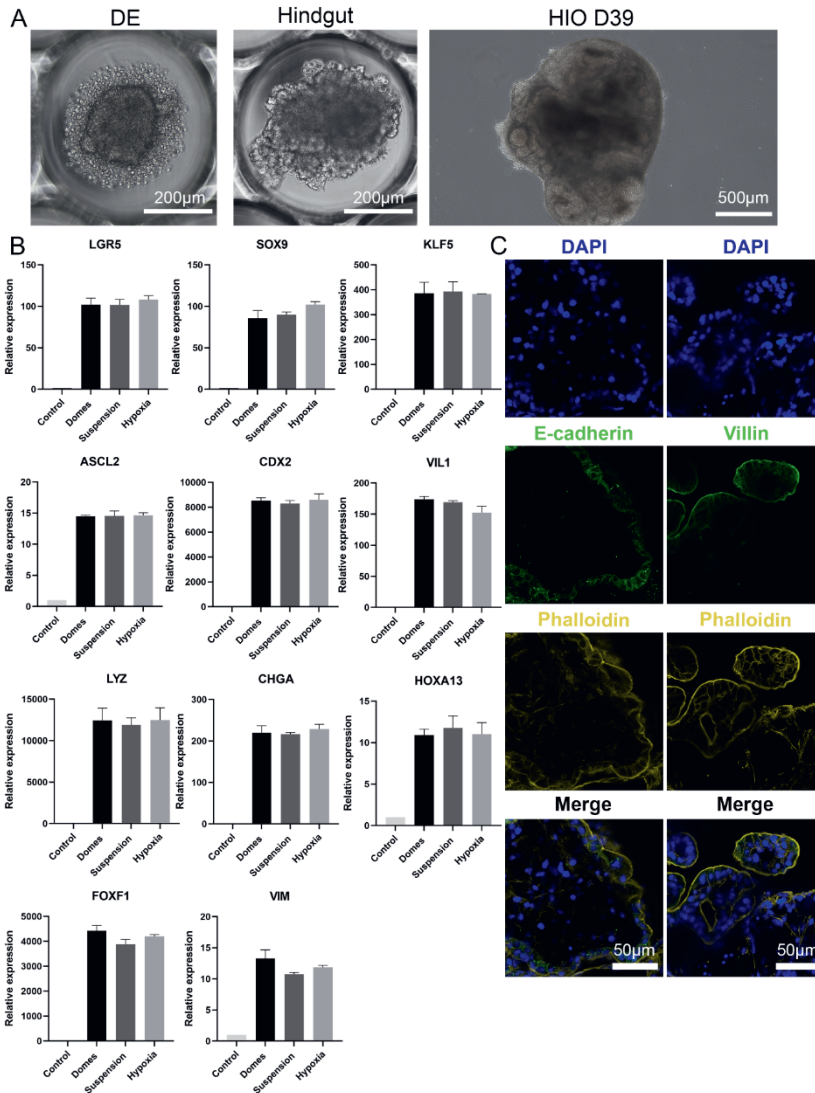


**Figure 1:** Apical-out small intestinal organoid differentiation in hypoxic conditions. (A) Bright-field images indicating each step of the directed differentiation of ESCs towards intestinal organoids (Definitive endoderm → Hindgut → Human Intestinal Organoids). (B) qRT-PCR analysis demonstrated the expression levels of proliferation genes (*LGR5*, *SOX9*, *KLF5*, and *ASCL2*), intestinal differentiation genes (*CDX2*, *VIL1*, *LYZ*, *CHGA*, and *HOXA13*) and mesenchymal genes (*FOXF1* and *VIM*) in Matrigel-embedded (domes), suspension normoxia and suspension hypoxia organoids. Untreated H9 cells were used as controls. Statistical analysis showed no significant difference between the three organoid models at any of the time-points. Error bars indicate mean ± S.E.M. (n = 3). (C) Confocal microscopy demonstrated the expression of the basolateral marker E-cadherin (green, left column) in the inner part of the organoids, whereas the apical markers phalloidin (yellow, both columns) and Villin (green, right column) in the outer part of the organoids, thus indicating a successful reversal of epithelial polarity.

Initially, we assessed the oxygen levels in each different culture system (Matrigel-embedded, suspension and suspension hypoxia) (Figure 2 A). To do that, we measured the concentration of dissolved oxygen using an oxygen optic sensor over a period of 7 days. On the one hand, organoids cultured in suspension in a hypoxic incubator (5% O<sub>2</sub>) had similar oxygen levels as organoids embedded in Matrigel and cultured in a normoxic incubator (~3-5% O<sub>2</sub>). On the other hand, the oxygen levels in organoids cultured in suspension in a normoxic incubator were much higher (15-18% O<sub>2</sub>). These results are consistent with previous studies showing that inside a Matrigel dome, the oxygen levels range between 2.8–9.7%<sup>44</sup> and in suspension cultures, the oxygen concentration in cell culture medium is ~18% for a standard normoxic incubator and ~2% for a 2% O<sub>2</sub> incubator<sup>32</sup>.

After the estimation of oxygen levels in the different organoid culture systems, we aimed to evaluate the protein expression of HIF-1 $\alpha$  (Figure 2 B). Immunofluorescence staining indicated increased HIF-1 $\alpha$  expression in organoids grown embedded in Matrigel and in hypoxia suspension. HIF-1 $\alpha$  expression was detected in both the nucleus and the cytoplasm of the intestinal organoids' cells. However, no expression was identified in suspension organoids cultured in a normoxic incubator, since the high levels of oxygen do not allow for HIF-1 $\alpha$  stabilization. Following the confirmation of HIF-1 $\alpha$  expression, we evaluated the expression of certain HIF-1 $\alpha$  target genes (Figure 2 C). A number of mucosal barrier formation-related genes are critically regulated by HIF-1 $\alpha$ , including the Mucins 2 and 3A (*MUC2* and *MUC3A*) and the intestinal trefoil factor 3 (*TFF3*)<sup>45</sup>. We indeed found significant upregulation of these genes in both Matrigel-embedded and suspension hypoxia organoids. Higher expression levels of keratin 20 (*KRT20*), a marker of mature enterocytes and goblet cells, were detected in hypoxia, which is in accordance with previously reported data<sup>46</sup>. Finally, the glucose transporter solute carrier family 2 member 1 (*SLC2A1*, also known as *GLUT1*) is also responsive to hypoxia<sup>47</sup>. This was confirmed in our organoids grown in low oxygen conditions (Matrigel-embedded and suspension hypoxia). Collectively, these results show that the apical surface of suspension hypoxia organoids is exposed and responds to the hypoxic environment, similar to the *in vivo* situation. Upon exposure to the hypoxic environment, HIF-1 $\alpha$  was activated and the expression of its downstream targets was upregulated, too.

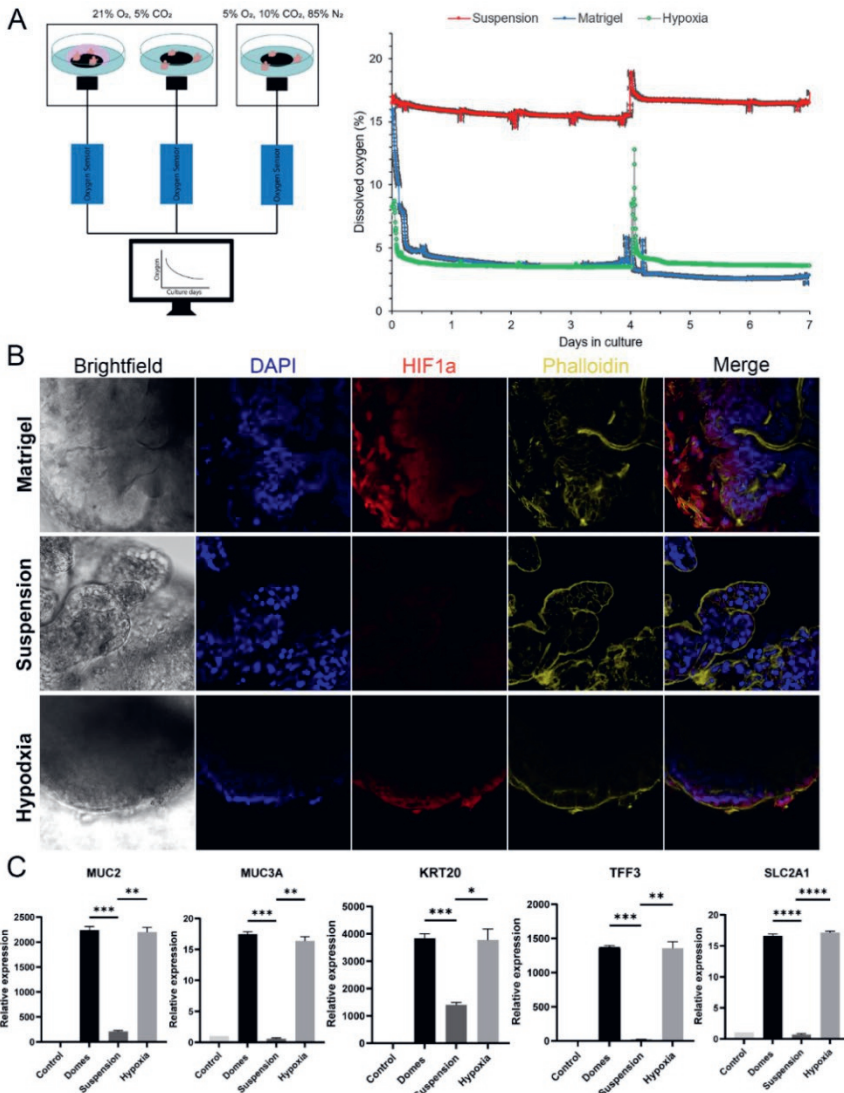


**Figure 2:** HIF-1 $\alpha$ -induced effects on apical-out small intestinal organoids. **(A)** Sensor measurements of oxygen levels in organoids cultured in Matrigel domes, suspension normoxia, and suspension hypoxia over a period of 7 days. For organoids grown in suspension normoxia, the dissolved oxygen concentration was about 15-18%, whereas in Matrigel-embedded and suspension hypoxia cultures, the dissolved oxygen concentration was about 3-5%. The peak at day 4 corresponds to medium refreshment. Error bars indicate mean  $\pm$  S.E.M. (n = 3). **(B)** Immunofluorescence stainings indicated the expression of HIF-1 $\alpha$  in low oxygen conditions (Matrigel-embedded and hypoxia suspension). No expression was identified in organoids grown in suspension normoxia. **(C)** Comparison of gene expression levels of HIF-1 $\alpha$  targets, including *MUC2*, *MUC3A*, *KRT20*, *TFF3*, and *SLC2A1* between the three culture conditions. All these genes were significantly upregulated in low oxygen conditions. Error bars indicate mean  $\pm$  S.E.M. (n = 3).



Barrier integrity in hypoxic apical-out organoids

One of the fundamental functions of the intestinal epithelium is to act as a physical and biochemical barrier between the luminal contents and the underlying tissue. Disruption of the intestinal barrier has been associated with various diseases, such as inflammatory bowel disease and irritable bowel syndrome. To evaluate the epithelial barrier function in our hypoxic apical-out organoids, we performed a fluoresceinyl isothiocyanate (FITC)-dextran diffusion assay. This is a common way to evaluate barrier function both *in vivo*<sup>48,49</sup> and *in vitro*<sup>50,51</sup>. Apical-out organoids were incubated in a 4 kDa FITC-dextran (FITC-D4) solution for 30 min. Subsequently, we observed its diffusion into the organoid lumen using a confocal microscope (Figure 3). This experiment showed that the apical-out organoids cultured in hypoxic conditions excluded the FITC-D4, thus indicating intact epithelial barrier integrity. As a positive control, we treated organoids with EDTA, a chelating agent known to disrupt tight junctions and compromise barrier integrity<sup>52</sup>. Treatment of apical-out organoids with 2 mM EDTA for 15 min led to disruption of barrier integrity, as suggested by the diffusion of FITC-D4 in the intercellular spaces of the organoids. Collectively, these results support that apical-out small intestinal organoids grown in hypoxic conditions demonstrate intact epithelial barrier function.

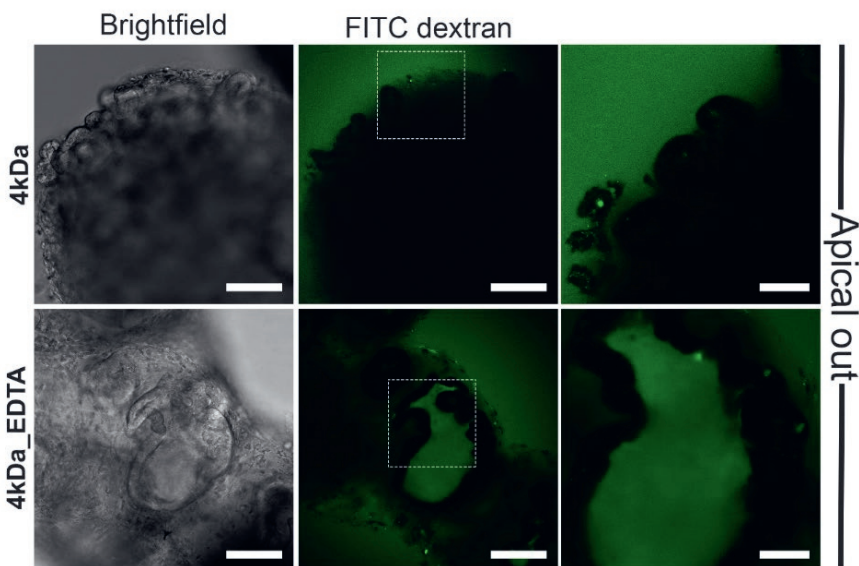


**Figure 3:** Epithelial barrier integrity in hypoxia apical-out organoids. Confocal microscopy demonstrated that no diffusion of the 4 kDa FITC-dextran solution in untreated organoids (top row) occurred, thus indicating strong barrier integrity. In contrast, treatment of organoids with 2 mM EDTA (bottom row) disrupted the junctions and the dextran diffused into the intercellular space. Scale bars: 100  $\mu\text{m}$  (left and middle) and 50  $\mu\text{m}$  (right).

Polarized nutrient absorption

The formation of a strong epithelial barrier is key to another major function of the intestinal epithelium, the controlled nutrient absorption. This function is mediated by certain transport proteins that are located in the apical and/or basal membrane domains<sup>53</sup>. Fatty acids enter into the apical membranes of the enterocytes through the following transport proteins: cluster of differentiation 36 (CD36, also known as fatty acid translocase), plasma membrane-associated fatty acid-binding protein (FABPpm) and/or fatty acid transport proteins 1-6 (FATP1-6)<sup>54</sup>. Once inside the enterocytes, fatty acids are transported towards the endoplasmic reticulum where they contribute to the synthesis of phospholipids, triacylglycerols, and cholesterol esters. These lipids are assembled into chylomicrons or stored in the cytosol as lipid droplets<sup>55</sup>. To assess the fatty acid uptake in apical-out organoids grown in hypoxic conditions, we used the fluorescent fatty acid analog C1-BODIPY-C12 and compared its uptake to the uptake in apical-in organoids. Both apical-in and apical-out organoids were incubated with a solution containing the BODIPY dye for 30 min. Afterwards, organoids were fixed and stained with phalloidin (indicating F-actin) and DAPI (indicating nuclei) (Figure 4). Visualization with a confocal microscope and subsequent quantification demonstrated strong fluorescent signal only in apical-out organoids, thus showing that these organoids can successfully absorb the fatty acid analog from the surrounding medium (>96% uptake). In apical-in organoids, the fluorescent signal was weak, thus indicating that there was no uptake of fatty acids in these organoids. Overall, these results support the presence of active fatty acid transport proteins directly accessible in the outer apical surface of apical-out organoids grown in hypoxia.

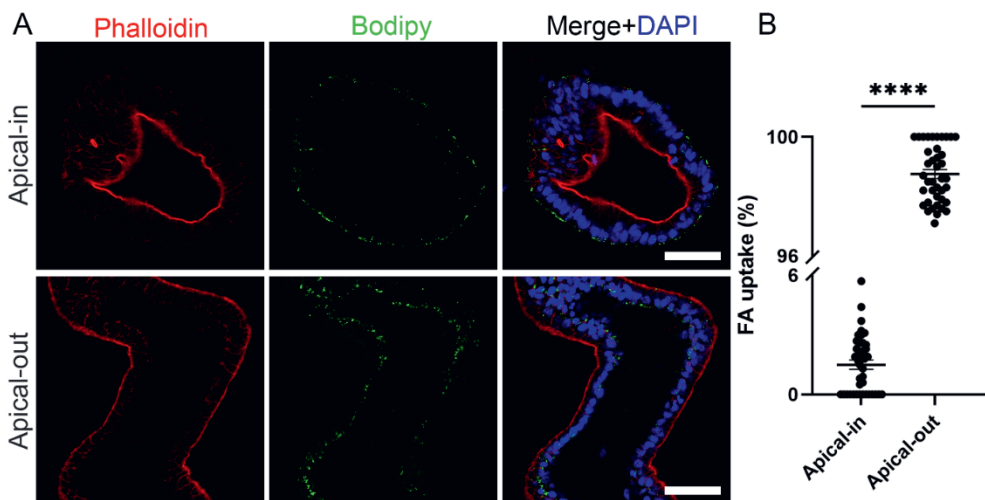


**Figure 4:** Polarized nutrient uptake. (A) Representative images of apical-in and apical-out organoids incubated with the fluorescent fatty acid (FA) analog C1-BODIPY-C12 (green). Only apical-out organoids took up the BODIPY. DAPI (blue) marked the nuclei and phalloidin (red) the apical side of the epithelium. Scale bars: 50  $\mu\text{m}$ . (B) Quantification of the FA uptake in apical-in and apical-out organoids. Error bars indicate mean  $\pm$  S.E.M. (n=4).

#### Co-culture of organoids with *Lactobacillus casei*

Lactobacilli are among the dominant bacteria in the gut and can be found in several dietary sources (i.e. kefir, yoghurt, sourdough bread etc.). They provide numerous benefits to the host, such as the enhancement of gut barrier integrity, the strengthening of tight junctions, and the regulation of mucin expression and immune responses<sup>56</sup>. *L. casei* is a facultative anaerobic strain that is proven very promising for the prevention of intestinal inflammation and the protection of the mucosal barrier<sup>57</sup>. Here, we aimed to evaluate the effects of *L. casei* cells and metabolites on small intestinal organoids with apical-out orientation in hypoxic conditions. To this end, we either co-cultured organoids with  $10^7$  or  $10^8$  bacteria cells or we added 10  $\mu\text{g}/\text{mL}$  bacteria lysates to the organoid medium for 12 h. Higher amounts of bacteria ( $> 10^8$ ) have proven to be toxic and led to severe cell death in the organoids.

Prior to the co-culture experiments, we cultured the bacteria in organoid medium in hypoxia, to evaluate their growth over time (Figure 5 A). Even though bacteria did not seem to replicate during the 24 h incubation period, more than 80% of the bacteria survived. Since *L. casei* is an anaerobic strain, we assume that a possible reason for the small amount of bacterial cells' death are the oxygen levels differences that arise during the handling (e.g. measuring concentration, transfer in the organoid medium). Alternatively, another reason could be the reduced fitness of bacteria in the organic medium of the organoids. Then, we aimed to identify whether the *L. casei* cells colonize the apical epithelial surface of the small intestinal organoids. Hence, we performed SEM imaging and observed that *L. casei* cells attached on the apical surface of the organoids (Figure 5 B), which is in accordance with previous *in vivo* and *in vitro* studies<sup>58</sup>.

To evaluate the effects of *L. casei* on the barrier integrity of apical-out organoids, we performed gene expression analysis for the junction markers zonula occludens 1 (*ZO-1*), claudin-1, 3 and 5 (*CLDN1*, *CLDN3*, *CLDN5*), and occludin (*OCN*) (Figure 5 C). *ZO-1* and *OCN* mediate the transport of large molecules up to 6 nm via the Leak Pathway, whereas *CLDN1*, *CLDN3*, and *CLDN5* regulate the transport of smaller ions and solutes (up to 0.8 nm) via the Pore Pathway<sup>59,60</sup>. All these markers were found upregulated when *L. casei* cells or lysates were added to

the culture. This response was “dose-dependent”, meaning that increasing amounts of bacteria led to increasing gene expression of junction markers. Probiotic bacteria strains have also been found to affect mucin expression, thus regulating the properties of the mucus layer and indirectly the intestinal immune system<sup>57</sup>. To examine whether this is occurring in apical-out intestinal organoids, we conducted quantitative real-time PCR for major secreted and membrane-bound mucins and mucin-related genes. Our analysis included *MUC2*, *MUC3A*, *MUC13*, *MUC17*, and *TFF3*. Similar to the junction markers, we found the expression of these genes significantly upregulated and positively correlated with the increasing numbers of microorganisms added. In summary, these results indicate that the presence of *L. casei* cells or lysates enhances the barrier formation and mucus production in apical-out organoids, when compared to untreated organoids. Noteworthy, it is important to highlight that viable bacterial cells have a much stronger effect on the organoids when compared to the lysates. To achieve sufficient quantities of protein content in lysates (10µg/mL), approximately  $3.4 \times 10^8$  bacteria were required. This is more than three times higher than the amount of bacteria co-cultured with the organoids and yet the effects were less robust. Thus, this indicates the importance of direct organoid-bacteria contact. Overall, apical-out small intestinal organoids grown in hypoxia can be used to explore further the mechanisms underlying the probiotic effects of *L. casei* on the intestinal epithelium.

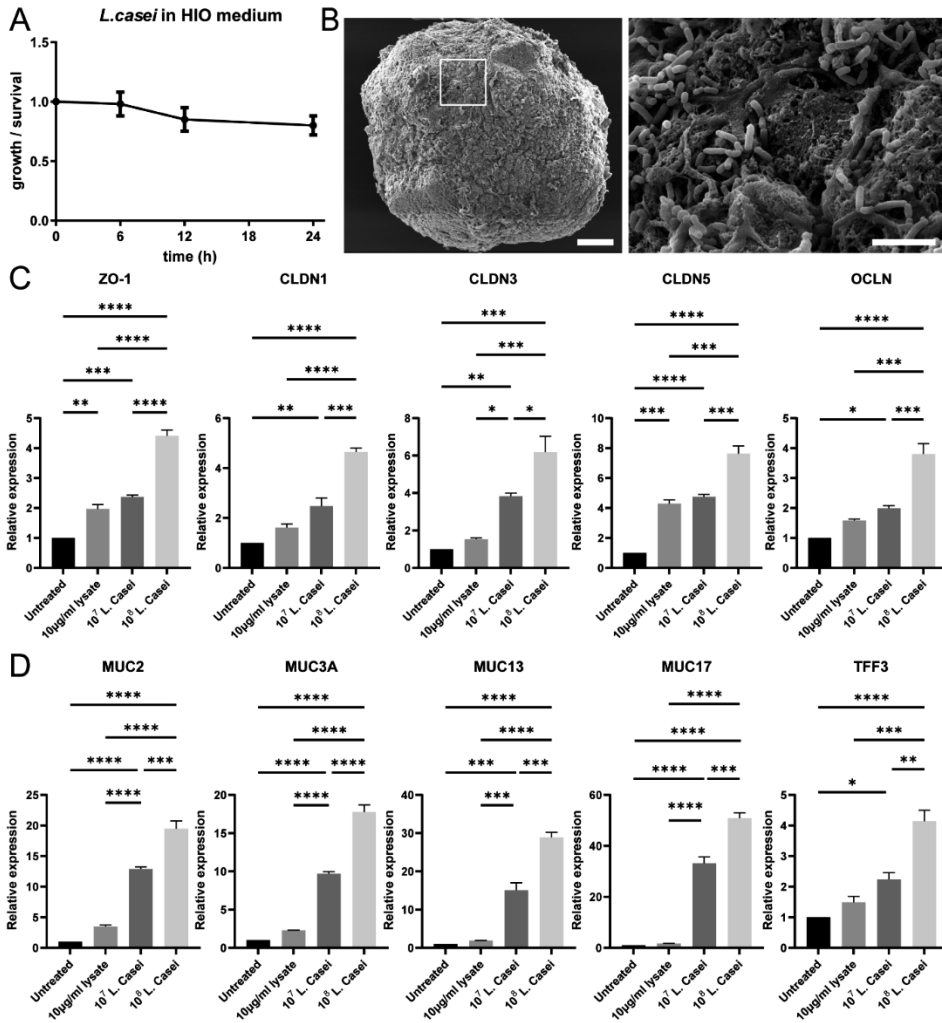


**Figure 5:** Co-culture of organoids with *L. casei*. **(A)** Anaerobic culture of *L. casei* cells in human intestinal organoid (HIO) medium. Error bars indicate mean ± S.D. (n = 4). **(B)** SEM microscopy showed colonization of *L. casei* bacteria on the apical surface of the organoids. White box represents the area magnified in the corresponding image on the right. Scale bars: 100 µm and 5 µm. **(C-D)** qRT-PCR analysis demonstrated the expression levels of the junction markers: *ZO-1*, *OCLN*, *CLDN1*, *CLDN3* and *CLDN5* (C) and the mucins markers: *MUC2*, *MUC3A*, *MUC13*, *MUC17*, and *TFF3* (D) in organoids co-cultured with *L. casei*-derived lysates and two concentrations of *L. casei* cells (10<sup>7</sup> and 10<sup>8</sup>). Error bars indicate mean ± S.E.M. (n = 3).

Co-culture of organoids with *Bifidobacterium longum*

Together with lactobacilli, bifidobacteria are among the first colonizers of the neonatal gut and rank among the ten most dominant bacteria. Bifidobacteria are probiotics and they can be found in many food types, including yogurt, kefir,

seaweed, and whole grains. They are known to prevent the invasion of pathogens by modulating the pro-inflammatory responses<sup>37</sup>, promote intestinal barrier integrity<sup>61</sup>, and improve the mucosal barrier function<sup>62</sup>. *B. longum* is a nonpathogenic, microaerotolerant anaerobic strain that is considered to be one of the earliest colonizers of the infants' gastrointestinal tract. In this study, we investigated the effects of *B. longum* cells and metabolites on apical-out small intestinal organoids in anaerobic conditions. Similar to *L. casei*, we either performed co-culture of organoids with  $10^7$  or  $10^8$  bacteria cells or we added 10  $\mu\text{g}/\text{mL}$  bacteria lysates to the organoid medium for 12 h. Higher numbers of *B. longum* bacteria were cytotoxic for the organoids.

Preceding the co-culture of bacteria with the organoids, we also evaluated the growth of *B. longum* in organoid medium in hypoxia (Figure 6 A). We observed that up to 12 h later, the bacteria moderately replicated in organoid medium, whereas after 24 h they stopped proliferating, but they maintained high viability levels (99%). According to previous studies, *B. longum* adherence to the gastrointestinal tract is important to colonize the gut and exert their probiotic effects<sup>63,64</sup>. To explore whether *B. longum* attached to the surface of apical-out organoids we performed SEM analysis (Figure 6 B). The results indicated that *B. longum* adhered to the apical surface of the organoids, thus showing successful colonization.

We also aimed to evaluate the probiotic effects of *B. longum* on the apical-out intestinal organoids. Similar to *L. casei*, we initially assessed the effect on barrier integrity. We conducted quantitative analysis of gene expression for the junction markers *ZO-1*, *CLDN1*, *CLDN3*, *CLDN5*, and *OCN* (Figure 6 C). In comparison to the untreated organoids, they were all significantly upregulated when bacterial cells or lysates were added to the culture. Also in the case of *B. longum*, there was a positive correlation between the number of bacteria and the gene expression levels of the junction markers. Next, to evaluate whether the presence of *B. longum* has an impact on the mucous modulation, we analyzed the gene expression of *MUC2*, *MUC3A*, *MUC13*, *MUC17*, and *TFF3* (Figure 6 D). A dose-dependent trend towards increased expression of these markers was observed upon addition of bacterial cells or lysates. Together these results indicate that the *B. longum* bacteria can successfully colonize the apical-out organoids and establish probiotic effects *in vitro*. Also in the case of *B. longum*, the direct contact of organoids with bacterial cells, led to more robust effects. Collectively, small intestinal organoids with reversed polarity, grown in hypoxia are a suitable *in vitro* model to unravel unknown

mechanisms underlying the probiotic effects of *B. longum* on the intestinal epithelium.

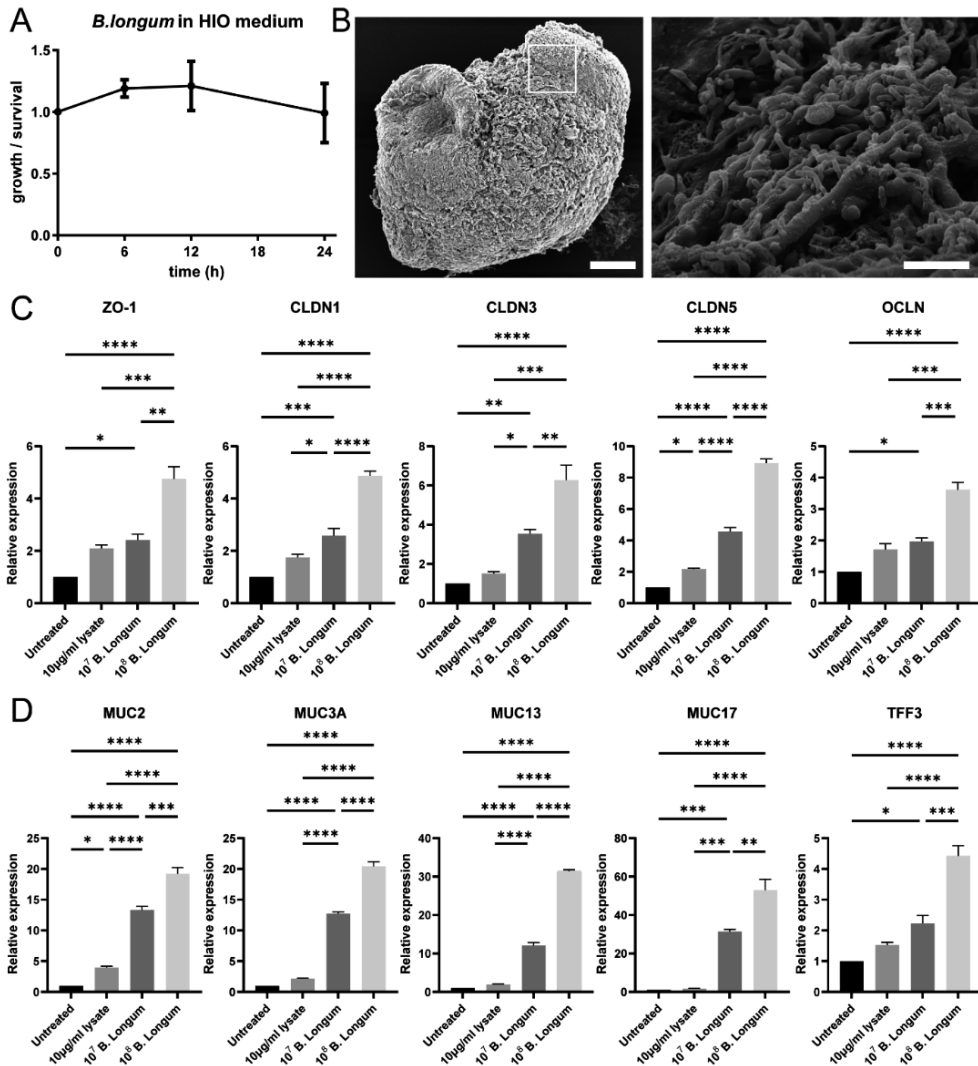


**Figure 6:** Co-culture of organoids with *B. longum*. (A) Anaerobic culture of *B. longum* cells in intestinal organoid medium. Error bars indicate mean  $\pm$  S.D. (n = 4). (B) SEM microscopy indicated colonization of *B. longum* bacteria on the apical surface of the organoids. White box represents the area magnified in the corresponding image on the right. Scale bars: 100  $\mu$ m and 5  $\mu$ m (C-D) qRT-PCR analysis demonstrated the expression levels of the junction markers *ZO-1*, *OCLN*, *CLDN1*, *CLDN3*, and *CLDN5* (C) and the mucins markers *MUC2*, *MUC3A*, *MUC13*, *MUC17*, and *TFF3* (D) in organoids co-cultured with *B. longum*-derived lysates and two concentrations of *B. longum* cells (10<sup>7</sup> and 10<sup>8</sup>). Error bars indicate mean  $\pm$  S.E.M. (n = 3).

**Triple co-culture of organoids, *L. casei* and *B. longum***

Intestinal microbiota is a complex, dynamic population of microorganisms that consists of thousands of different species. Alterations in the microbiota has been associated with chronic immune disorders, such as inflammatory bowel disease, obesity, and diabetes. Lactobacilli and bifidobacteria are among the dominant species and the most widely used probiotic bacteria in food supplements<sup>37</sup>. Probiotic supplements usually consist of a combination of bacteria, and they are beneficial for the host immune health. In this study, apart from studying the effects of single bacteria strains, we aimed to evaluate whether we can recapitulate the probiotic effects of a combination of *L. casei* and *B. longum* on apical-out small intestinal organoids. This is a step further towards mimicking closer the *in vivo* situation, where thousands of different bacteria co-reside in the gastrointestinal tract.

Apical-out small intestinal organoids were either co-cultured with  $10^7$  or  $10^8$  bacteria cells or incubated with 10  $\mu\text{g}/\text{mL}$  bacteria lysates for 12 h in anaerobic conditions. The ratio between the amounts of bacteria cells or lysates added, was 50:50 (*L. casei* : *B. longum*). Also in the case of multiple bacteria strains, we observed bacterial cell adherence on the apical surface of the organoids, using electron microscopy (Figure 7 A). Similar to the effects of single bacteria strains, we identified significantly elevated gene expression of the junction-related markers *ZO-1*, *CLDN1*, *CLDN3*, *CLDN5*, and *OCLN* (Figure 7 B) and the mucin-related markers *MUC2*, *MUC3A*, *MUC13*, *MUC17*, and *TFF3* (Figure 7 C). These results indicate that the two bacteria strains can successfully interact with and colonize the apical surface of human small intestinal organoids and improve barrier formation and mucin regulation.

**Discussion**

In the past few years, the role of the gut microbiome in health and disease has attracted a lot of interest. However, this remains a rather unexplored field with about 71% of the species lacking a culture representative<sup>65</sup>. Hence, there is an urgent need for physiologically relevant and robust *in vitro* models to shed light on the complex gut-microbiome interactions. In this study, we developed for the first time, an apical-out small intestinal organoid model in hypoxia. These organoids contain all the major intestinal cell types and mimic structural and functional properties of the *in vivo* intestine. The directly accessible apical membrane in the outer surface of the organoids facilitates, amongst others, nutrient, drug or other compound screenings in high-throughput, since thousands of organoids with reversed polarity can be



derived from a single 24-well plate. Here, we focused on the study of host-microbiome interactions. A unique advantage of this reversed polarity small intestinal organoid model is that the apical surface is exposed to a hypoxic environment, thus recapitulating closer the *in vivo* situation. These culture conditions enable the studies of the interactions with anaerobic microorganisms, which constitute the vast majority of the gut microbiota species.

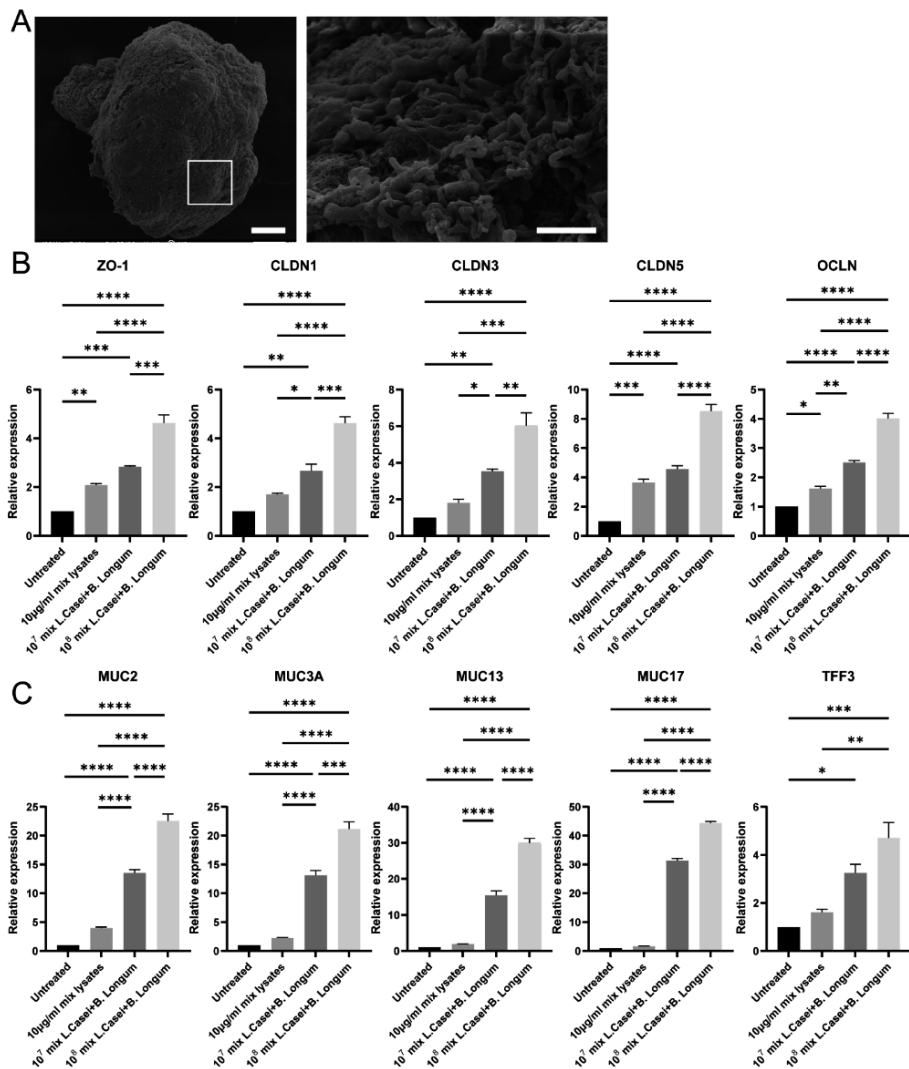


**Figure 7:** Triple co-culture of organoids with *L. casei* and *B. longum*. (A) SEM microscopy indicated colonization of *L. casei* and *B. longum* bacteria on the apical surface of the organoids. The white box in the left image represents the area magnified in the corresponding image on the right. Scale bars: 100  $\mu$ m and 5  $\mu$ m. (B-C) qRT-PCR analysis demonstrated the expression levels of the junction markers

*ZO-1*, *OCN*, *CLDN1*, *CLDN3*, and *CLDN5* (B) and the mucins markers *MUC2*, *MUC3A*, *MUC13*, *MUC17*, and *TFF3* (C) in organoids co-cultured with a 50:50 mix of *L.casei*- and *B.longum*-derived lysates (final concentration 10 µg/ml) and a 50:50 mix of *L.casei* and *B. longum* cells (final concentrations: 10<sup>7</sup> and 10<sup>8</sup>). Error bars indicate mean ± S.E.M. (n = 3).

Lately, intestinal organoids with apical-out orientation have been described using human<sup>28</sup>, chicken<sup>30</sup>, and porcine<sup>31</sup> adult stem cells. However, in none of these models, the apical surface was exposed to a hypoxic environment. Thus, co-cultures with anaerobes is not optimal, since obligate anaerobes will not be able to survive and facultative anaerobes show differences in their growth in the presence of higher or “normal” (normoxic) oxygen concentrations<sup>66</sup>. For the study of anaerobic strains, usually microinjections are performed into the hypoxic lumen of apical-in organoids<sup>13,67</sup>. Alternatively but no longer in a 3D organoid context, bacteria have been co-cultured with 2D monolayers of intestinal epithelial cells in cell culture devices (inserts or microfluidic systems), which were designed to control oxygen concentrations and gradients<sup>68,69</sup>. However, microinjections are tedious, and monolayers do not recapitulate the 3D architecture of the *in vivo* tissues. Our group has previously established an apical-out small intestinal organoid model using pluripotent stem cells in normoxia<sup>29</sup>. Here, we followed the same stepwise differentiation protocol but in hypoxic conditions. The organoids can be differentiated with the same high efficiency as in normoxia and show a reversed epithelial polar organization. Adding on to the presence of the major small intestinal cell types and proper structural organization, we demonstrated that our hypoxia-tolerant, apical-out intestinal organoids recapitulate functional characteristics of the intestine. Specifically, in the *in vivo* intestine, the adaptation to hypoxia is mainly regulated by hypoxia-inducible factors (HIFs). After verifying the presence of reduced oxygen concentration in our culture system, we identified increased protein expression of the HIF-1 $\alpha$  isoform in the hypoxia organoids. Gene expression analysis showed that HIF-1 $\alpha$  targets are significantly upregulated as well. Therefore, apical-out small intestinal organoids actively respond and adapt to low oxygen conditions, via similar mechanisms as *in vivo*<sup>33</sup>. This is particularly important since deficiencies of HIF-1 $\alpha$  have been associated with pathological conditions, including inflammatory bowel disease and colorectal cancer<sup>33,70</sup>. Similar to other apical-out organoid models, we demonstrated that these hypoxia-tolerant organoids form a tight epithelial barrier, which is one of the main functions of the intestine<sup>71</sup>. Additionally, successful apical-specific nutrient uptake was verified by the absorbance of a fluorescent fatty acid analogue. In summary, these results indicate that we have established an effective and robust protocol to reverse epithelial polarity in hypoxia. This method can be successfully adapted to various culture conditions and

constitutes a valuable *in vitro* tool for the study of nutrient uptake, drug absorption, and host-microbiome interactions. The versatility of this system is particularly useful for the study of the complex microbiome, where different microorganisms require different culture conditions.

The human gut microbiota is composed of about  $10^{14}$  microorganisms (mostly anaerobic) and is crucial for the nutrition and health status of the organism<sup>37,72</sup>. Probiotics are living microorganisms, which are known to provide health benefits for the host. These benefits include the improvement of gut barrier formation, maintenance of mucosal homeostasis, and immunomodulation<sup>37</sup>. In this study, we co-cultured for the first time apical-out organoids with the anaerobic strains *L. casei* and *B. longum*. We identified that these probiotic bacteria can successfully colonize the apical surface of the organoids and have beneficial effects on them. We also highlighted the importance of direct contact of organoids with the bacterial cells. Collectively, these results show that this novel hypoxia-tolerant organoid model can be a valuable tool to explore the mechanisms underlying the probiotic effects of these microorganisms in greater depth. This would be of great interest for the production of more efficient probiotic supplements, the demand of which has immensely increased in the past decades<sup>73</sup>. Furthermore, since the probiotic benefits have mainly been investigated in pathogenic situations<sup>73</sup>, this model can be useful to determine their importance for healthy individuals as well. Additionally, these organoids can be used to study the effects of other known bacterial strains or even aid the discovery of unknown ones through the co-culture with microbiota, derived straight from human stool specimens. For such studies, it would be interesting in the future to grow these apical-out organoids in even lower oxygen levels, since there are microorganisms that require  $<0.1\%$  oxygen to survive. Further research and identification of bacterial strains will benefit the investigation of their synergistic effect on the host as well.

Gut microbiota consists of approximately 300 to 500 bacterial species, which comprise a complex ecosystem<sup>74</sup>. Hence, apart from the study of single microorganisms, it is crucial to study how multiple species interact when they are cultured together and what their combined effects on the host are. Here, we performed a triple co-culture system with the hypoxia apical-out organoids and the probiotic strains *L. casei* and *B. longum*, and identified efficient adherence on the apical surface and active probiotic effects on the organoids. The interactions of different *Lactobacillus* and *Bifidobacterium* strains - the predominant species of gastrointestinal microbiota - have been studied before but using a colorectal

adenocarcinoma cell line (Caco-2)<sup>37</sup>, which is less physiologically relevant than organoids. Various probiotic supplements include combinations of different bacterial strains, thus a high-throughput 3D *in vitro* model that facilitates the study of effects of multiple bacterial strains on a host can be a particularly useful tool for identifying new beneficial combinations of bacteria and testing new food supplements. Furthermore, in this study, we used a 50:50 ratio of the two bacteria strains, but it would be interesting in a larger combinatorial screen to systematically test different ratios of various bacteria strains. Finally, future steps could include the exposure of these apical-out organoids co-cultured with probiotics to different pathogenic bacteria to further assess the functionality of the mucosal barrier integrity.

To conclude, we have developed a novel, scalable hypoxia-tolerant, apical-out small intestinal organoid model. These organoids contain the major intestinal cell lineages and recapitulate structural and functional characteristics of the *in vivo* tissue. Specifically, they have distinct apical and basolateral surfaces, they form a strong barrier and perform polarized nutrient uptake. The directly accessible apical surface facilitates also the investigation of host-microbiome interactions, since microorganisms can simply be added to the culture medium. The hypoxic environment allows for the first time, the study of anaerobes using organoids with reversed polarity. Overall, this system has great potential to simplify and advance not only research related to host-microbiome and host-pathogen interactions, but also pharmaceutical and nutritional studies.

## **References**

1. Merker SR, Weitz J, Stange DE. Gastrointestinal organoids: How they gut it out. *Developmental Biology* 2016; 420: 239–250.
2. Peterson LW, Artis D. Intestinal epithelial cells: regulators of barrier function and immune homeostasis. *Nat Rev Immunol* 2014; 14: 141–153.
3. Schneeberger K, Roth S, Nieuwenhuis EES, et al. Intestinal epithelial cell polarity defects in disease: lessons from microvillus inclusion disease. *Dis Model Mech* 2018; 11: dmm031088.
4. Cani PD. Human gut microbiome: hopes, threats and promises. *Gut* 2018; 67: 1716–1725.
5. Jandhyala SM, Talukdar R, Subramanyam C, et al. Role of the normal gut microbiota. *World J Gastroenterol* 2015; 21: 8787.
6. Kho ZY, Lal SK. The human gut microbiome - A potential controller of

- wellness and disease. *Front Microbiol* 2018; 9: 1835.
7. Singh A, Poling HM, Spence JR, et al. Gastrointestinal organoids: a next-generation tool for modeling human development. *Am J Physiol Liver Physiol* 2020; 319: G375–G381.
  8. Kakni P, Truckenmüller R, Habibović P, et al. Challenges to, and prospects for, reverse engineering the gastrointestinal tract using organoids. *Trends Biotechnol* 2022; 932–944.
  9. Bozzetti V, Senger S. Organoid technologies for the study of intestinal microbiota–host interactions. *Trends Mol Med* 2022; 28: 290–303.
  10. Min S, Kim S, Cho SW. Gastrointestinal tract modeling using organoids engineered with cellular and microbiota niches. *Experimental and Molecular Medicine* 2020; 52: 227–237.
  11. Hou Q, Ye L, Liu H, et al. Lactobacillus accelerates ISCs regeneration to protect the integrity of intestinal mucosa through activation of STAT3 signaling pathway induced by LPLs secretion of IL-22. *Cell Death Differ* 2018; 25: 1657–1670.
  12. Shaffiey SA, Jia H, Keane T, et al. Intestinal stem cell growth and differentiation on a tubular scaffold with evaluation in small and large animals. *Regen Med* 2016; 11 (1): 45-61.
  13. Son YS, Ki SJ, Thanavel R, et al. Maturation of human intestinal organoids in vitro facilitates colonization by commensal lactobacilli by reinforcing the mucus layer. *FASEB J* 2020; 34: 9899–9910.
  14. Hill DR, Huang S, Nagy MS, et al. Bacterial colonization stimulates a complex physiological response in the immature human intestinal epithelium. *Elife* 2017; 6: e29132.
  15. Heo I, Dutta D, Schaefer DA, et al. Modelling Cryptosporidium infection in human small intestinal and lung organoids. *Nat Microbiol* 2018; 3: 814–823.
  16. Forbester JL, Goulding D, Vallier L, et al. Interaction of Salmonella enterica Serovar Typhimurium with Intestinal Organoids Derived from Human Induced Pluripotent Stem Cells. *Infect Immun* 2015; 83: 2926–2934.
  17. Wilson SS, Tocchi A, Holly MK, et al. A small intestinal organoid model of non-invasive enteric pathogen–epithelial cell interactions. *Mucosal Immunol* 2014; 8: 352–361.
  18. Zhang YG, Wu S, Xia Y, et al. Salmonella-infected crypt-derived intestinal organoid culture system for host–bacterial interactions. *Physiol Rep* 2014; 2: e12147.
  19. Karve SS, Pradhan S, Ward D V., et al. Intestinal organoids model human responses to infection by commensal and Shiga toxin producing Escherichia

- coli. *PLoS One* 2017; 12: e0178966.
20. In J, Foulke-Abel J, Zachos NC, et al. Enterohemorrhagic *Escherichia coli* Reduces Mucus and Intermicrovillar Bridges in Human Stem Cell-Derived Colonoids. *Cell Mol Gastroenterol Hepatol* 2016; 2: 48-62.e3.
  21. VanDussen KL, Marinshaw JM, Shaikh N, et al. Development of an enhanced human gastrointestinal epithelial culture system to facilitate patient-based assays. *Gut* 2015; 64: 911–920.
  22. Pleguezuelos-Manzano C, Puschhof J, Rosendahl Huber A, et al. Mutational signature in colorectal cancer caused by genotoxic pks<sup>+</sup> *E. coli*. *Nature* 2020; 580: 269–273.
  23. Leslie JL, Huang S, Opp JS, et al. Persistence and toxin production by *Clostridium difficile* within human intestinal organoids result in disruption of epithelial paracellular barrier function. *Infect Immun* 2015; 83: 138–145.
  24. Engevik MA, Yacyshyn MB, Engevik KA, et al. Human *Clostridium difficile* infection: Altered mucus production and composition. *Am J Physiol - Gastrointest Liver Physiol* 2014; 308: G510–G524.
  25. Engevik MA, Engevik KA, Yacyshyn MB, et al. Human *Clostridium difficile* infection: Inhibition of NHE3 and microbiota profile. *Am J Physiol - Gastrointest Liver Physiol* 2014; 308: G497–G509.
  26. Engevik MA, Aihara E, Montrose MH, et al. Loss of NHE3 alters gut microbiota composition and influences *Bacteroides thetaiotaomicron* growth. *Am J Physiol - Gastrointest Liver Physiol* 2013; 305: 697–711.
  27. Co JY, Margalef-Català M, Monack DM, et al. Controlling the polarity of human gastrointestinal organoids to investigate epithelial biology and infectious diseases. *Nat Protoc* 2021; 16: 5171–5192.
  28. Co JY, Margalef-Català M, Li X, et al. Controlling Epithelial Polarity: A Human Enteroid Model for Host-Pathogen Interactions. *Cell Rep* 2019; 26: 2509-2520.e4.
  29. Kakni P, López-Iglesias C, Truckenmüller R, et al. Reversing Epithelial Polarity in Pluripotent Stem Cell-Derived Intestinal Organoids. *Front Bioeng Biotechnol* 2022; 0: 669.
  30. Nash TJ, Morris KM, Mabbott NA, et al. Inside-out chicken enteroids with leukocyte component as a model to study host–pathogen interactions. *Commun Biol* 2021; 4: 1–15.
  31. Li Y, Yang N, Chen J, et al. Next-Generation Porcine Intestinal Organoids: an Apical-Out Organoid Model for Swine Enteric Virus Infection and Immune Response Investigations. *J Virol* 2020; 94: e01006-20.
  32. Newby D, Marks L, Lyall F. Dissolved oxygen concentration in culture

- medium: assumptions and pitfalls. *Placenta* 2005; 26: 353–357.
33. Singhal R, Shah YM. Oxygen battle in the gut: Hypoxia and hypoxia-inducible factors in metabolic and inflammatory responses in the intestine. *Journal of Biological Chemistry* 2020; 295: 10493–10505.
  34. Konjar Š, Pavšič M, Veldhoen M. Regulation of Oxygen Homeostasis at the Intestinal Epithelial Barrier Site. *Int J Mol Sci* 2021; 22: 9170.
  35. Rolfe RD, Hentges DJ, Campbell BJ, et al. Factors Related to the Oxygen Tolerance of Anaerobic Bacteria. *Appl Environ Microbiol* 1978; 36: 306.
  36. Hentges DJ. Anaerobes: General Characteristics. *Med Microbiol*. 4<sup>th</sup> ed Galveston, 1996.
  37. Candela M, Perna F, Carnevali P, et al. Interaction of probiotic *Lactobacillus* and *Bifidobacterium* strains with human intestinal epithelial cells: Adhesion properties, competition against enteropathogens and modulation of IL-8 production. *Int J Food Microbiol* 2008; 125: 286–292.
  38. Giselbrecht S, Gietzelt T, Gottwald E, et al. 3D tissue culture substrates produced by microthermoforming of pre-processed polymer films. *Biomed Microdevices* 2006; 8: 191–199.
  39. Kakni P, Hueber R, Knoops K, et al. Intestinal Organoid Culture in Polymer Film-Based Microwell Arrays. *Adv Biosyst* 2020; 2000126.
  40. Spence JR, Mayhew CN, Rankin SA, et al. Directed differentiation of human pluripotent stem cells into intestinal tissue in vitro. *Nature* 2011; 470: 105–109.
  41. Van Welden S, Selfridge AC, Hindryckx P. Intestinal hypoxia and hypoxia-induced signalling as therapeutic targets for IBD. *Nat Rev Gastroenterol Hepatol* 2017; 14: 596–611.
  42. Zheng L, Kelly CJ, Colgan SP. Physiologic hypoxia and oxygen homeostasis in the healthy intestine. A review in the theme: Cellular responses to hypoxia. *Am J Physiol - Cell Physiol* 2015; 309: C350–C360.
  43. Sun L, Li T, Tang H, et al. Intestinal epithelial cells-derived hypoxia-inducible factor-1 $\alpha$  is essential for the homeostasis of intestinal intraepithelial lymphocytes. *Front Immunol* 2019; 10: 806.
  44. Okkelman IA, Foley T, Papkovsky DB, et al. Live cell imaging of mouse intestinal organoids reveals heterogeneity in their oxygenation. *Biomaterials* 2017; 146: 86–96.
  45. Kumar T, Pandey R, Chauhan NS. Hypoxia Inducible Factor-1 $\alpha$ : The Curator of Gut Homeostasis. *Front Cell Infect Microbiol* 2020; 10: 227.
  46. Hu X, Wu R, Shehadeh LA, et al. Severe hypoxia exerts parallel and cell-specific regulation of gene expression and alternative splicing in human

- mesenchymal stem cells. *BMC Genomics* 2014; 15: 303.
47. Karhausen J, Furuta GT, Tomaszewski JE, et al. Epithelial hypoxia-inducible factor-1 is protective in murine experimental colitis. *J Clin Invest* 2004; 114: 1098–1106.
  48. Woting A, Blaut M. Small Intestinal Permeability and Gut-Transit Time Determined with Low and High Molecular Weight Fluorescein Isothiocyanate-Dextran in C3H Mice. *Nutr* 2018; 10: 685.
  49. Baxter MFA, Merino-Guzman R, Latorre JD, et al. Optimizing fluorescein isothiocyanate dextran measurement as a biomarker in a 24-h feed restriction model to induce gut permeability in broiler chickens. *Front Vet Sci* 2017; 4: 56.
  50. Kowapradit J, Opanasopit P, Ngawhirunpat T, et al. In vitro Permeability Enhancement in Intestinal Epithelial Cells (Caco-2) Monolayer of Water Soluble Quaternary Ammonium Chitosan Derivatives. *AAPS PharmSciTech* 2010; 11: 497.
  51. Xu P, Elamin E, Elizalde M, et al. Modulation of Intestinal Epithelial Permeability by Plasma from Patients with Crohn's Disease in a Three-dimensional Cell Culture Model. *Sci Reports* 2019; 9: 1–11.
  52. Zheng Y, Zuo Z, Albert AH. Lack of effect of  $\beta$ -cyclodextrin and its water-soluble derivatives on in vitro drug transport across rat intestinal epithelium. *Int J Pharm* 2006; 309: 123–128.
  53. Kiela PR, Ghishan FK. Physiology of Intestinal Absorption and Secretion. *Best Pract Res Clin Gastroenterol* 2016; 30: 145–159.
  54. Wang TY, Liu M, Portincasa P, et al. New insights into the molecular mechanism of intestinal fatty acid absorption. *Eur J Clin Invest* 2013; 43: 1203–1223.
  55. Hussain MM. Intestinal Lipid Absorption and Lipoprotein Formation. *Curr Opin Lipidol* 2014; 25: 200.
  56. Camilleri M. Human Intestinal Barrier: Effects of Stressors, Diet, Prebiotics, and Probiotics. *Clin Transl Gastroenterol* 2021; 25: e00308 12.
  57. La Fata G, Weber P, Mohajeri MH. Probiotics and the Gut Immune System: Indirect Regulation. *Probiotics Antimicrob Proteins* 2018; 10: 11.
  58. Vélez MP, De Keersmaecker SCJ, Vanderleyden J. Adherence factors of *Lactobacillus* in the human gastrointestinal tract. *FEMS Microbiol Lett* 2007; 276: 140–148.
  59. Pearce SC, Al-Jawadi A, Kishida K, et al. Marked differences in tight junction composition and macromolecular permeability among different intestinal cell types. *BMC Biol* 2018; 16: 1–16.



60. Monaco A, Ovryn B, Axis J, et al. The Epithelial Cell Leak Pathway. *Int J Mol Sci* 2021; 22: 7677.
61. Hsieh CY, Osaka T, Moriyama E, et al. Strengthening of the intestinal epithelial tight junction by *Bifidobacterium bifidum*. *Physiol Rep* 2015; 3: e12327.
62. Yao S, Zhao Z, Wang W, et al. *Bifidobacterium Longum*: Protection against Inflammatory Bowel Disease. *J Immunol Res*; 2021; 2021: 8030297.
63. Xiong Y, Zhai Z, Lei Y, et al. A Novel Major Pilin Subunit Protein FimM Is Involved in Adhesion of *Bifidobacterium longum* BBMN68 to Intestinal Epithelial Cells. *Front Microbiol* 2020; 11: 2929.
64. Westermann C, Gleinser M, Corr SC, et al. A Critical Evaluation of Bifidobacterial Adhesion to the Host Tissue. *Front Microbiol* 2016; 7: 1220.
65. Almeida A, Nayfach S, Boland M, et al. A unified catalog of 204,938 reference genomes from the human gut microbiome. *Nat Biotechnol* 2020; 39: 105–114.
66. André AC, Debande L, Marteyn BS. The selective advantage of facultative anaerobes relies on their unique ability to cope with changing oxygen levels during infection. *Cell Microbiol* 2021; 23: e13338.
67. Williamson IA, Arnold JW, Samsa LA, et al. A High-Throughput Organoid Microinjection Platform to Study Gastrointestinal Microbiota and Luminal Physiology. *Cmgh* 2018; 6: 301–319.
68. Jalili-Firoozinezhad S, Gazzaniga FS, Calamari EL, et al. A complex human gut microbiome cultured in an anaerobic intestine-on-a-chip. *Nat Biomed Eng* 2019; 3: 520–531.
69. Kim R, Attayek PJ, Wang Y, et al. An in vitro intestinal platform with a self-sustaining oxygen gradient to study the human gut/microbiome interface. *Biofabrication* 2019; 12: 015006.
70. Rohwer N, Jumpertz S, Erdem M, et al. Non-canonical HIF-1 stabilization contributes to intestinal tumorigenesis. *Oncogene* 2019; 38: 5670–5685.
71. Chelakkot C, Ghim J, Ryu SH. Mechanisms regulating intestinal barrier integrity and its pathological implications. *Exp Mol Med* 2018; 50: 1–9.
72. Nicholson JK, Holmes E, Kinross J, et al. Host-gut microbiota metabolic interactions. *Science* 2012; 336: 1262–1267.
73. Khalesi S, Bellissimo N, Vandelanotte C, et al. A review of probiotic supplementation in healthy adults: helpful or hype? *Eur J Clin Nutr* 2018; 73: 24–37.
74. Quigley EMM, Eamonn D, Quigley MM. Gut Bacteria in Health and Disease. *Gastroenterol Hepatol* 2013; 9: 560.

## Supplementary Material

### Supplementary Tables

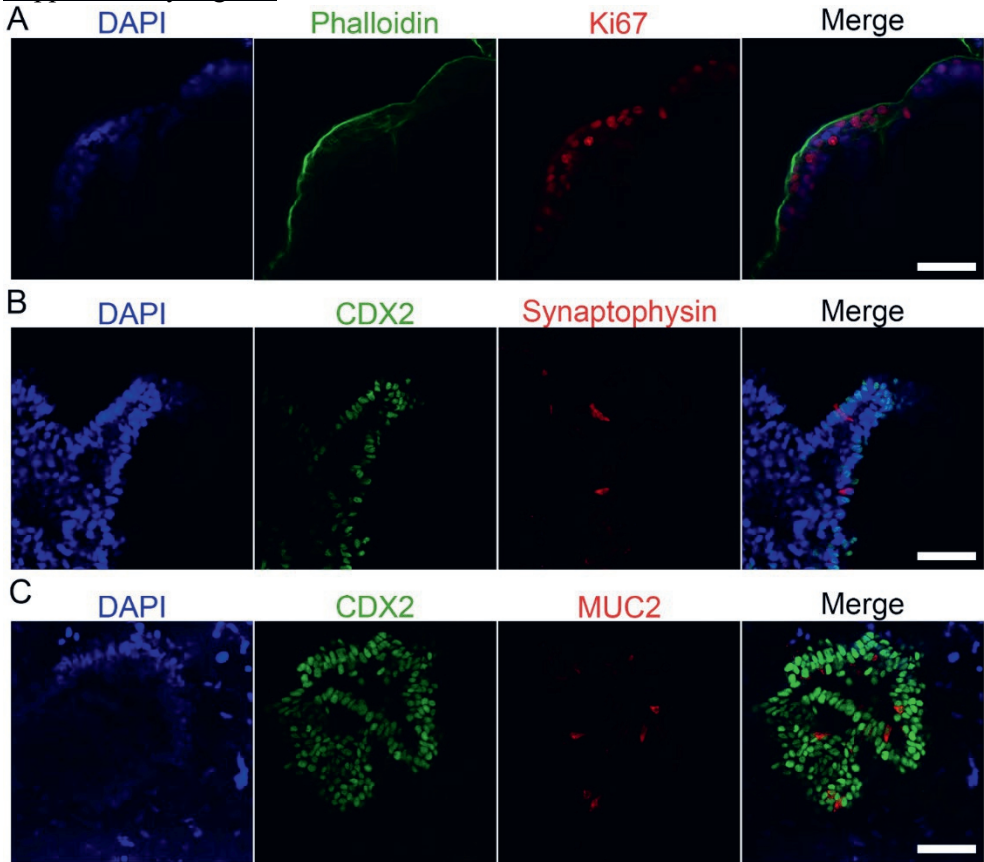
**Supplementary Table 1.** List of antibodies

Antibodies	Supplier	Host	Dilution
E-Cadherin	Beckton Dickinson	Mouse	1:500
Ki67	Abcam	Rabbit	1:500
CDX2	Biogenex	Mouse	1:500
MUC2	Abcam	Rabbit	1:250
Synaptophysin 1	Synaptin systems	Guinea pig	1:200
Villin	Santa cruz	Mouse	1:250
HIF1a	Novus Biologicals	Rabbit	1:500
Phalloidin 568	Invitrogen		1:500
Alexa Fluor 488	Invitrogen		1:500
Alexa Fluor 647	Invitrogen		1:500
Alexa Fluor 568	Invitrogen		1:500

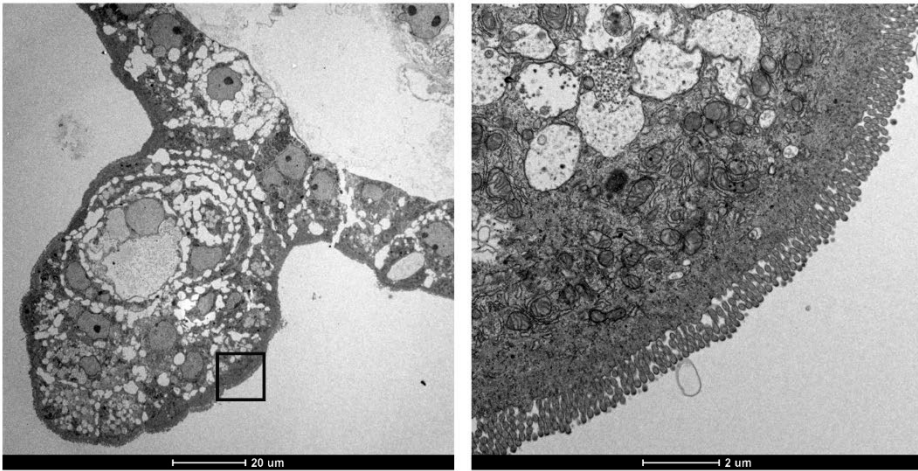
**Supplementary Table 2.** Primer sequences

Gene	5'–Forward– 3'	5'–Reverse– 3'
ASCL2	GCGTGAAGCTGGTGAACCTG	GGATGTACTCCACGGCTGAG
CDX2	GACGTGAGCATGTACCCTAGC	GCGTAGCCATTCCAGTCTT
CHGA	TAAAGGGGATACCGAGGTGATG	TCGGAGTGTCTCAAAACATTCC
CLDN1	CCCAGTCAATGCCAGGTACG	GGGCCTTGGTGTGGGTAAG
CLDN3	AACACCATTATCCGGGACTTCT	GCGGAGTAGACGACCTTGG
CLDN5	GCAGCCCCTGTGAAGATTGA	GTCTCTGGCAAAAAGCGGTG
FOXF1	GCGGCTTCCGAAGGAAATG	CAAGTGGCCGTTTCATCATGC
HOXA13	CTGCCCTATGGCTACTTCGG	CCGGCGGTATCCATGTACT
HPRT	GGACTCCAGATGTTTCCAAACTC	TTGTTGTAGGATATGCCCTTGAC
KLF5	CCTGGTCCAGACAAGATGTGA	GAAGTGGTCTACGACTGAGGC
KRT20	GAACCTAAATGACCGTCTAGCG	GGTTTCGTACCACTGCTTGATT
LGR5	CTCCCAGGTCTGGTGTGTTG	GAGGCTAGGTAGGAGGTGAAG
LYZ	TCAATAGCCGCTACTGGTGTA	ATCACGGACAACCCTCTTTGC
MUC2	GGAGATACCAATGACTGCGA	GAATCGTTGTGGTCAACCCTTG
MUC3A	GACAACGCCATCGACTGTCA	CGTGTCCGGTGGAGTAGCAG
MUC13	CGGATGACTGCCTCAATGGT	AAAGACGCTCCCTTCTGTCTC
MUC17	GGGCCAGCATAGCTTCGA	GCTACAGGAATTGTGGGAGTTCA
OCN	CATTGCCATCTTTGCCTGTG	AGCCATAACCATAGCCATAGC
SLC2A1	GGTTGTGCCATACTCATGACC	CAGATAGGACATCCAGGGTAGC
SOX9	AGCGAACGCACATCAAGAC	CTGTAGCGCATCTGTTGGGG
TFF3	GCTGCTGCTTTGACTCCAG	TGGAGGTGCCTCAGAAGGT
VIL1	CTGAGCGCCAAAGTCAAAG	AGCAGTCAACCATCGAAGAAGC
VIM	GACGCCATCAACACCGAGTT	CTTTGTCGTTGGTTAGCTGGT
ZO-1	CAACATACAGTGACGCTTCACA	CACTATTGACGTTTCCCCACTC

Supplementary Figures



**Supplementary Figure 1:** Characterization of H9-derived, apical-out human intestinal organoids in hypoxia. (A-C) Immunofluorescence stainings of the intestinal markers (Ki67: proliferative cells; CDX2: intestinal transcription factor; MUC2: goblet cells; Synaptophysin: enteroendocrine cells) show that reversed polarity hypoxic organoids differentiate successfully towards intestinal cell lineages. Scale bars: 50  $\mu$ m.



**Supplementary Figure 2:** TEM characterization of epithelial polarity. The microvilli are facing outwards in hypoxic apical-out intestinal organoids. Black box indicates the magnified area in the corresponding image to the right. Scale bars: 20 µm (left) and 2 µm (right).





## CHAPTER VIII

# **GENERAL DISCUSSION**



The objective of this thesis was the development of advanced small intestinal organoid models that overcome limitations and expand the range of applications of current organoid models. Over the years, numerous systems have been described that recapitulate multiple structural and functional characteristics of the small intestine. These include *in vivo* models, 2D cell culture systems, 3D organoid models and bioengineered 2D and 3D systems<sup>1</sup>. Each one of these systems has various advantages, but also certain limitations. In the past few years, organoids have gained an elevated interest, but there are still certain issues that restrict their widespread applicability. For example, there is extended use of animal-derived extracellular matrix analogs, which increases the variation in organoid cultures and limits the applicability of organoids in translational applications. Additionally, there is lack of the required complexity (e.g., lack of immune and vascular systems) to act as true tissue replicas<sup>2</sup>. To address some of the issues, in the context of this thesis we developed different bioengineered intestinal organoid systems using microengineered tools. Initially we established a microwell-based intestinal organoid model, which facilitates both high-throughput downstream applications (e.g. drug screenings) and co-cultures of organoids with other cell types (chapter III). Capitalizing on the acquired knowledge and established model, we used this platform to co-culture intestinal organoids with macrophages, thus creating a more complex and physiologically relevant organoid model (chapter IV). In chapter V, we developed a different intestinal organoid model, where organoids had a reversed polar organization (apical surface facing outwards), in order to facilitate the *in vitro* study of processes that are conducted through the apical side of the intestinal epithelium, such as nutrient uptake and host-microbiome interactions. In chapter VI, we further investigated functional applications of this apical-out system, including nutrient uptake, metabolism and barrier formation. Finally, in chapter VII we modified this system, by adapting it for hypoxic culture conditions, thus creating a more physiologically relevant environment for studying interactions between the host (intestine) and the anaerobic microorganisms that reside there.

In this chapter, we discuss current *in vivo* and *in vitro* models of the intestine, which rely solely on biological or on the combination of biological and engineering tools. We highlight the strengths and opportunities offered, as well as the drawbacks and challenges raised by the use of each system. Finally, we contextualize our findings and envision the future of 3D intestinal models.

## **Current intestinal models**

The intestinal epithelium is the fastest renewing epithelium in the human body, with a complete renewal every 4-5 days<sup>3</sup>. This highly dynamic tissue, hosts multiple cell types that ensure its proper function. Its structural and functional complexities make the proper *in vitro* tissue modeling challenging. At the same time, the animal models have extensive similarities in anatomy, physiology and genetics, but also major differences in the structure and microbiome of their gastrointestinal tract (as will be discussed below)<sup>4,5</sup>. Even though there are multiple deviations from the human tissue, both *in vitro* systems and *in vivo* animal models have provided valuable information about the physiological and pathophysiological conditions of the intestine.

### *Animal models*

As mentioned before, animal models show various similarities with the human intestine and they provide a high level of biological complexity. This allows researchers to study organ responses in complex environments, thus in a more holistic manner than in isolated parts. Especially rodent models have been widely used in biological research, since they are relatively small, easy to maintain in large numbers, they can be genetically modified and they have about 85% of their genetic sequences in common with humans<sup>5</sup>. One important difference is the size of the intestinal tract, which is almost 20 times shorter than in humans. This affects also the microbiome composition, hence numerous factors have to be considered during experimental design and interpretation. To overcome this, larger animal models can be used, such as canids and monkeys. Each of them have their own advantages but they do not fully recapitulate the features of the human intestine<sup>6</sup>. Another important deviation between humans and animal models is the interaction between host and pathogens. For example, *Listeria monocytogenes* does not infect rodent species, but listeriosis is a serious infectious disease in humans<sup>7</sup>. Furthermore, a study using rats indicated that rat models can successfully predict oral drug absorption, but not drug metabolism or oral bioavailability in humans<sup>8</sup>. As a consequence, despite the prosperous pre-clinical animal testing, over 90% of clinical trials for novel drugs fail<sup>9</sup>. Apart from these differences with the human organism, animal models require extended time for growth and experimentation, sufficient space and specialized facilities, which translate to financial and time-related burdens. On top of these, there are also ethical concerns about the use of animals in experiments and current guidelines recommend the “3R” principles: “Replace, Reduce and Refine”<sup>10</sup>. For all



these reasons, *in vitro* models are constantly developed and improved in order to extend their applicability in fundamental studies and preclinical research.

### *In vitro* systems

Various standardized *in vitro* models of the small intestine have been described over the years for preliminary studies of permeability, absorption, toxicity and effects of foods and drugs. Cancer-derived cell lines are usually the front-runners for such *in vitro* studies, since they are highly proliferative, easy to culture, and cheap to use. Currently there is a large number of such cell lines available, including Caco-2 and HT-29<sup>1,6,11</sup>. Caco-2 are human epithelial cells derived from the colon tissue of a male with colorectal adenocarcinoma. Caco-2 cells are predominating the *in vitro* studies of differentiation, permeability and absorption since they spontaneously differentiate into a polarized epithelium with typical finger-like villi, upon reaching confluence<sup>12</sup>. The HT-29 cell line is a human colorectal adenocarcinoma cell line with epithelial morphology that is derived from a female with colorectal adenocarcinoma. HT-29 is considered to be a pluripotent intestinal cell line and upon treatment with specific growth factors can differentiate towards either enterocytes or mucin producing goblet-like cells<sup>11</sup>. However, these come with certain limitations as well. For example, there is high variation in terms of proliferation, differentiation state and metabolic properties, possibly due to the cancer origin of the cells<sup>1</sup>. Additionally, in their majority, they usually recapitulate only the enterocytes and not all the cell lineages that are found in the *in vivo* intestine. For instance, there are no stem cells in these systems, which are crucial to maintain the integrity and the regeneration capacity of the intestinal epithelium<sup>13</sup>. Another drawback of these cell lines is that they carry multiple gene mutations (e.g. Caco-2 are aneuploid and harbor a mutated p53 gene)<sup>1</sup>. Apart from these, conventionally used 2D cultures do not reflect the 3D architecture of the intestine, which is fundamental for its functionality.

In 2009, the development of 3D intestinal organoids was a major breakthrough for the gastrointestinal research. Organoids can be derived from multiple sources, including human and mouse tissue-resident stem cells, induced pluripotent stem cells and embryonic stem cells<sup>14</sup>. These self-organizing structures recapitulate the 3D architecture of the intestine, since they are organized into crypt-villus units and the epithelium retains distinct apical and basolateral surfaces. This unique architecture of the intestine facilitates its primary functions (e.g., digestion, nutrient absorption and secretion)<sup>15</sup>, thus to better mimic intestinal functions *in vitro*, it is important to also mimic the intestinal structure. The crypt hosts actively cycling intestinal stem cells and differentiated secretory paneth cells. The crypt stem cells

continuously undergo self-renewal and generate transit-amplifying cells that move up towards the villus and produce all the differentiated intestinal cell types, including (but not limited to) paneth cells, goblet cells and enterocytes<sup>16,17</sup>. Several tissue functions, such as barrier formation, nutrient uptake and metabolism can be successfully modeled *in vitro* using intestinal organoids<sup>2</sup>. Growing such representative 3D tissue surrogates in a dish has opened up the possibility to study development, model diseases and test personalized medicine approaches *in vitro*. The ability of stem cells to self-renew and differentiate has even raised hopes for future transplantation therapies, hence bypassing the need for organ donations<sup>14</sup>. However, it is important not to create false expectations for the near future, since organoid models still have limitations that need to be overcome. Organoids often lack reproducibility and show high levels of variation, which limits their applicability in drug testing, developmental studies and disease modeling. For example, there are differences in organoid formation efficiency, morphology and function, which impose a high level of variation within organoid cultures. The inherent formation of an enclosed lumen in intestinal organoids, limits the access to the apical surface of the epithelium. Therefore, studies related to nutrient/ drug uptake and host-microbiome interactions are also restricted. The need for several materials (e.g., growth factors, extracellular matrix (ECM) substitutes) and extended culture periods drastically increases the cost of organoid studies, thus posing another issue for extending the applicability of organoids.

Employing bioengineering tools can greatly benefit both 2D and 3D cell culture systems, by offering the possibility to increase the number of controllable parameters during culture. Such approaches can help to achieve more robust, reproducible and representative *in vitro* models. In the following section, we will discuss advantages and disadvantages of such methods.

### *Bioengineered systems*

In an attempt to overcome certain limitations of *in vivo* and cellular *in vitro* models, various microfabrication and tissue engineering techniques have been described. These systems aim to develop better-controlled and standardized *in vitro* models that recapitulate key structural and functional properties of the *in vivo* intestine.

### On-chip

Over the years, numerous small intestine-on-chip models have been described aiming to increase the complexity of *in vitro* cell models and emulate better the intestinal physiology<sup>18,19</sup>. On-chip platforms have profoundly evolved, from simple

2D structures to comprehensive systems with various functionalities<sup>19</sup>. The first devices only contained two channels (upper and lower) separated by a semipermeable membrane on which the cells (Caco-2) were forming a polarized monolayer epithelium<sup>18,20</sup>. Later on, further advances in the microfabrication techniques promoted the generation of more complex devices that stimulated several features of the intestinal environment, such as peristalsis, fluid flow and formation of villi structures. In addition, integration of sensors or other analytical probes provided the opportunity for real-time monitoring during the culture. Furthermore, the combination of tight control over the culture conditions (e.g. oxygen levels) and fluid flow facilitated the investigation of host-microbiome interactions and especially the study of anaerobic microorganisms<sup>21</sup>. The possibility to implement multiple cell types in one device (e.g. intestinal cells with vascular and/or immune cells) in a controlled environment, further increases the complexity of the system, and thus mimics closer the *in vivo* situation. The modular nature of such devices facilitates the connection of multiple chips, each one representing a different tissue, to create body-on-chip systems. These offer a holistic approach to study inter-organ communication and multi-tissue responses<sup>22,23</sup>. Overall, all the afore-mentioned systems have greatly benefited not only the study of intestinal development, physiology and disease, but also studies related to absorption, distribution, metabolism and excretion (ADME) of nutrients and drugs. Despite all the advantages and wide applicability of the on-chip systems, some challenges still remain. A major pitfall is the lack of reproducibility and robustness between different laboratories, pushing forward the need for implementation of standardization strategies. Intestine-on-chip systems display more functional characteristics than simple *in vitro* models, by incorporating medium flow and peristalsis-like movements, which provide biomimetic shear stress to the cells and affect the epithelial cells' differentiation and the resident microorganisms<sup>21</sup>. However, they still do not fully recapitulate the complexity of the *in vivo* intestine. For example, they still lack 3D organization and multicellular composition that are essential for the proper intestinal function. Furthermore, intestine-on-chip models usually incorporate Caco-2 cells, which as mentioned before, are not an ideal tissue representative, since they lack multiple structural and functional aspects of the intestine. For instance, Caco-2 cells differentiate towards enterocytes, but not towards the other intestinal cell types (e.g., paneth cells and goblet cells) that are important for the proper function of the intestine. Also Caco-2-based models lack the intestinal stem cell niche, which is fundamental for the regeneration and homeostasis<sup>13</sup>. The use of cells derived from dissociated intestinal organoids is becoming more and more prevalent, but in this case, the 3D architecture of the organoids is usually lost. Several devices have been

described that accommodate whole organoids as well, but this field is still in its infancy<sup>24</sup>. Further progress in both biofabrication techniques and organoid technology are required to overcome the current challenges and create reproducible and highly physiologically relevant bioengineered *in vitro* systems.

### 3D scaffolds

As mentioned before, the highly organized 3D architecture of the intestine is crucial for its proper function. Microfabrication techniques and synthetic materials were implemented to create scaffolds that mimic the crypt-villus structure of the intestine, based on guided cell organization. Among those techniques are photolithography, soft-lithography, PEG hydrogels and 3D printing<sup>1</sup>. Several studies focused on the reproduction of the crypt structures using crypt-like microwells<sup>1</sup>. These mainly indicated that such topography favors a stem cell-like phenotype. Other studies reported the successful villi formation after long-term culture of Caco-2 cells<sup>19</sup>. These vary from “simple” collagen scaffolds replicating the geometry of intestinal microvilli, to more complex “all-in-one” systems that apart from the proper geometry include fluid flow, mechanical stretching and co-cultures with other cell types. The villi microstructures are crucial for the intestine *in vivo*, in order to form and act as a physiological barrier, but most importantly, to increase and facilitate the absorption of ingested molecules. Thus, proper representation of these structures *in vitro* is fundamental for nutrition, metabolism and drug development studies. However, one limitation of such scaffolds is that they usually represent either the crypts or the villi and not both; hence, they do not fully recapitulate the *in vivo* structure. Only recently, this was overcome using micropatterned scaffolds and bioprinting approaches<sup>25-27</sup>. Combined with the use of dissociated intestinal organoid cells instead of Caco-2 cells and the intraluminal perfusion, these models are highly physiologically relevant and show great progress compared to previously described models. Specifically, the perfusable tubular mini-guts that were developed within predefined spatial boundaries, demonstrated the emergence of rare cell types (such as M cells) and the potential to regenerate consequent epithelial damage and to model long-term parasite infection<sup>26</sup>. Co-cultures with immune and vascular cells were also tested to closer mimic the organ-level complexity. All these place this model in a unique position among current organoid models, since it provides a high level of complexity and closely recapitulates the architecture and function of the *in vivo* intestine. However, the culture of cells in complex scaffolds requires sophisticated handling and is difficult to set up and control, hence the reproducibility between different laboratories is a major concern.

## **Advancing *in vitro* intestinal models: our approaches**

It is beyond any doubt that organoids are currently the most promising 3D *in vitro* cell model. Insights into the development and homeostasis of the gastrointestinal tract laid the foundation for the generation and culture of intestinal organoids. However, despite the tremendous progress in the field over the past decade, organoids still face numerous challenges. A combination of such tissue analogues with bleeding edge technological tools will greatly enhance *in vitro* models to the benefit of basic and preclinical research.

In chapter III, we developed a method to culture intestinal organoids in microwell arrays<sup>28</sup>. Initially, we fabricated the microwell platform, using microthermoforming. Important advantages of our system comparing to a similar hydrogel platform<sup>29</sup>, are the high transparency of our microwells and the ability to remove and transfer the whole platform (microwells with organoids) from the well plate, for downstream applications. More specifically, the microwell arrays are only 50  $\mu\text{m}$  thick, and allow for high quality *in situ* imaging and monitoring of organoids throughout the whole culture period and downstream experiments. In addition, the size of our platform can be adapted according to the experimental needs (i.e. different sizes of microwells that can fit into different well plate formats). When cultured in microwells, organoids maintained their crypt-villus organization, multicellular composition and distinct apico-basolateral polarity, thus indicating both proper structure and function. In contrast to intestinal organoids embedded in Matrigel, these organoids were viable for up to thirteen days, they demonstrated increased homogeneity and the amount of Matrigel was significantly reduced, since only 5% of it was added to the medium as a supplement. This system paves the way towards more controlled organoid culture systems that can be beneficial for a wide range of applications. An example is the use in drug/nutrient screenings, where the direct contact of the organoids with the tested substances circumvents the need for diffusion through viscous gels, thus leading to more direct responses that mimic closer the *in vivo* situation. Additionally, when in microwells, organoids are kept in a fixed position throughout the whole culture period, hence facilitating organoid tracking in high-throughput applications. Finally, this culture system can support the controlled co-culture of organoids with other cell types. Nonetheless, apart from all the benefits of this system, there are also certain limitations. For instance, this study (chapter III) was performed using mouse cells, thus it would be interesting in the future to substitute those with human cells and even patient-derived cells. Furthermore, the seeding of organoids could be improved by using automated pick and place systems. In that way, the placement of a single organoid per microwell can

be ensured. Reversing epithelial polarity of the organoids cultured in microwells could further facilitate studies related to drug/nutrient screenings, since the apical surface of the organoids would be in direct contact with the tested substances. This would more closely mimic the *in vivo* situation where nutrients and drugs are absorbed through the apical side of the villus<sup>30</sup>.

Based on our microwell-based intestinal organoid model, in chapter IV we developed a co-culture system incorporating intestinal organoids and macrophages. We tested two different configurations, in which organoids were in direct (juxtacrine and paracrine signalling) or in indirect (paracrine only) contact with the macrophages. When in direct contact, the system represented a chronic inflammatory state, where there is infiltration of macrophages in the lamina propria of the intestine and excessive cytokine release. The indirect system represented the acute inflammatory response. This was the first time that the importance of the distance between the cells is highlighted. Controlled positioning of the different cell types in a co-culture system can benefit the modeling of certain *in vivo* conditions. For example, the infiltration of macrophages in the intestinal mucosa during intestinal bowel disease (IBD) can only be recapitulated *in vitro*, if the cells are placed in close proximity and can actively migrate. Further studies focusing on the tracking of macrophage movement, when in co-culture with organoids, are necessary to shed more light on the infiltration process. Additionally, we identified an intrinsic immunomodulatory response of the intestinal organoids that were able to regulate the secretion of cytokines by the macrophages. When organoids were co-cultured with macrophages, more different cytokines were released than when organoids were stimulated with the pro-inflammatory cytokine TNF- $\alpha$ . The cytokines found in our system have been previously associated with IBD<sup>31,32</sup>. Hence, a co-culture system can more closely recapitulate intestinal inflammatory states than external addition of cytokines. However, it is noteworthy to mention that not all the cytokines associated with IBD were present in our system. For instance, we did not detect IL8 and IL11. This can be partially because we only used macrophages, whereas there are more cell types involved in immune responses, such as T cells and lymphoid cells<sup>32</sup>. Thus, this system is still a simplified model of intestinal inflammation. Future studies incorporating more than one immune cell components in organoid systems could further improve the *in vitro* modeling of intestinal inflammation. The use of microwell-based models can allow for *in situ* monitoring of the interaction between the organoids and the macrophages (or other cell types) and they can facilitate high-throughput applications such as drug screenings. This can be particularly important to test different therapeutic agents against IBD, even in a personalized medicine

approach, where specific treatments can be tested on patient-derived organoids. Collectively, this system can benefit research related to the complex mechanisms underlying the intestinal inflammation that still remain elusive. Better understanding of these processes can lead to more effective treatments, since current therapeutics are not always efficient.

In chapter V, we developed a novel human pluripotent stem cell (PSC)-derived intestinal organoid model where organoids showed a reversed epithelial polar organization<sup>33</sup>. By employing a microwell platform at the initial stages of differentiation, we created homogeneous embryoid bodies that were ultimately differentiated towards small intestinal organoids. This method differs from the original protocol by Spence et al.<sup>17</sup>, since the whole differentiation process is performed in 3D. In contrast, Spence et al., initiated the differentiation by placing the PSCs in 2D culture and only after hindgut formation 3D spheroids are formed. Our method provides an easy and robust way to start the differentiation process, bypassing the issues of tightly regulated seeding densities and equally distributed cells around the cell culture plates that 2D methods require. At the same time, this suspension system has the potential to generate large numbers of apical-out organoids. Specifically, up to 7000 organoids can be harvested from a single 24-well plate. The scalability of our model opens up possibilities for high-throughput applications. This was the first report of apical-out intestinal organoids derived from human PSCs, since previous approaches were only focusing on human ASCs<sup>34</sup>, chicken ASCs<sup>35</sup> or porcine ASCs<sup>36</sup>. A difference of our system with the previous models is that our apical-out organoids were solely cultured in suspension, whereas the previous models were initially embedded in Matrigel and later on placed in suspension. Previous studies using Madin-Darby canine kidney (MDCK) cells-derived epithelial cysts have suggested that  $\beta 1$  integrins play a crucial role in the regulation of epithelial cell polarity<sup>37</sup>. Integrin receptors mediate the interaction between the ECM and the epithelium<sup>38</sup> and as a consequence, changes in ECM proteins affect the  $\beta 1$  integrin signalling, leading to changes in the orientation of epithelial polarity. This mechanism was identified in human ASC-derived enteroids with reversed polarity<sup>34</sup>, hence we suspect that the same mechanism mediates the polarity reversal of our PSC-derived organoids. Further experiments using  $\beta 1$  integrin function-blocking antibody could provide more information about this mechanism. To validate our novel organoid model, we evaluated the differentiation efficiency in every step of the differentiation process (definitive endoderm  $\rightarrow$  hindgut  $\rightarrow$  intestinal organoids). Furthermore, we used various imaging methods to demonstrate the reversal in the epithelial polar organization. We showed that these

organoids, even though they have an inside-out polar organization, still organize into crypt-villus structures and express the major intestinal cell types, thus reflecting structural and functional characteristics of the *in vivo* intestine. It is particularly important to ensure the functionality of the organoids, before proceeding to study intestinal functions. Reversal of epithelial polarity grants easy access to the apical surface of the organoids, which otherwise is facing the enclosed lumen, thus qualifying these organoids for a wide range of applications, including nutrient uptake, drug metabolism and host-microbiome/pathogen interactions studies. Although, this system is beneficial for such studies, it would be interesting in the future to include fluid flow using a bioreactor or a micro-/macro-fluidic device, since it is known that the flow of luminal contents affects these functions in the *in vivo* intestine<sup>39</sup>.

In chapter VI, we focused on the functionality of this newly developed intestinal organoid model. Initially, we looked into whether these organoids form a selective barrier, which is one of the fundamental roles of the intestine<sup>40</sup>. Indeed, we identified all the junctional complexes that are responsible for this function and using a diffusion assay, we further validated the integrity of our reversed-orientation epithelium. Next, we investigated whether these apical-out organoids can perform nutrient absorption and metabolic functions. *In vivo*, almost all the nutrients have been absorbed and transported by the intestinal epithelium. Fatty acids have been absorbed from the lumen via the apical surface of enterocytes<sup>41</sup>. Thus, we first assessed the fatty acid absorption in both apical-in and apical-out organoids and we found that only when the apical surface was facing outwards, such molecules could be absorbed. With a closer look into the ultrastructural organization of these organoids, we identified chylomicrons and vesicles of smooth endoplasmic reticulum, which point towards active metabolism of dietary fats. Further investigation into the gene expression of lipid metabolism markers, showed that apical-out intestinal organoids can successfully perform metabolic functions. Finally, considering that intestine is involved in drug metabolism of orally administered drugs, we demonstrated that these organoids express certain drug metabolizing enzymes and apical and basolateral transporters, which were also found to be functional, after assessing their activity following drug treatment. Overall, all these data confirm the suitability of this organoid model for studies related to nutrient and drug uptake and metabolism. So far, such studies were mainly performed using cell monolayers (mainly Caco-2)<sup>42</sup> and rarely with organoids with apical-in polar organization<sup>43</sup>. However, even though with monolayers access to both apical and basal side is granted, these systems require large numbers of cells and they do not



have a 3D organization, thus making the system less physiologically relevant. In the case of apical-in organoids, microinjections are required to access the apical surface, which is a tedious and time-consuming process that requires skilled personnel. The direct access to the apical surface, combined with the scalability of our system, place these apical-out organoids in a unique position as a tool for high-throughput and animal-free nutrition and drug discovery studies in the future. Nonetheless, it is worth mentioning that PSC-derived organoids resemble the early fetal-stage tissues<sup>44</sup>, thus we assume that there will be differences in the expression levels of transporters and drug metabolizing enzymes, when compared to the adult intestine. To assess these differences, it would be interesting in the future to compare these expression levels among PSC-derived apical-out organoids, human fetal intestinal tissue and human adult intestinal tissue.

In chapter VII, we developed a second apical-out intestinal organoid model, but this time in hypoxia. Considering that the intestinal lumen is hypoxic and the microbiota mostly consists of anaerobes<sup>45</sup>, we hypothesized that the most optimal way to study host-microbiome interactions *in vitro* using apical-out organoids would be to adapt our system to hypoxic conditions. The gut microbiome has a key role in metabolism and immune system regulation, thus a tremendous impact on the overall health and disease of the host<sup>46</sup>. So far in reversed polarity intestinal organoid models, the apical surface is exposed to high levels of oxygen (~18%)<sup>33-36,47</sup>, which is not optimal for the study of anaerobes. Instead, our model facilitates the study of anaerobic microorganisms, since the apical surface is directly accessible, the culture conditions are tightly controlled and the microorganisms can simply be added to the culture medium. Previous methods to study anaerobic species include microinjections in the lumen of the organoids<sup>48</sup>, or co-culture with 2D epithelial monolayers inside microfluidic devices that control the oxygen concentration<sup>49</sup>. To characterize our system, we initially evaluated the differentiation efficiency in low oxygen conditions and verified the reversal of epithelial polarity. Following that, we assessed the functionality of these organoids, by testing the epithelial barrier integrity, the nutrient uptake and the response to hypoxia. All of these functions were performed successfully by our hypoxia-tolerant apical-out organoids, similar to the *in vivo* intestine. After the validation of our model, we performed co-culture experiments with the anaerobic probiotic strains *Lactobacillus casei* (*L. casei*) and *Bifidobacterium longum* (*B. longum*). Furthermore, since multiple bacteria species co-reside in the intestine, we performed a triple co-culture with organoids, *L. casei* and *B. longum*. We identified successful colonization of both strains on the apical surface of the organoids and probiotic benefits, such as enhanced barrier integrity

and mucus production. These results confirmed our initial hypothesis that culturing apical-out organoids in low oxygen conditions can facilitate the co-culture with anaerobes, overcoming the need for tedious microinjections in the organoid lumen. Future experiments with human stool specimens could be useful to identify unknown bacterial strains. Additionally, it would be interesting to study the host-pathogen interactions using apical-out organoids co-cultured with both probiotics and pathogens (e.g., *Salmonella* and invasive *Escherichia coli*). Fabrication of micro- or macro-fluidic devices that can accommodate these apical-out organoids and enable continuous fluid flow would further benefit the studies of the gut microbiome, since bacteria can overgrow and contaminate the cell cultures<sup>50</sup>. Collectively, this system has great potential to facilitate and advance research related to host-microbiome/pathogen interactions, but also pharmaceutical and nutritional studies.

### **What comes next?**

Among the current *in vitro* gut models, organoids seem to have the greatest potential for studying intestinal development, physiology and disease. The future of intestinal organoid models lies in the combination of advanced biology and engineering approaches. With such technologies, current limitations can be overcome and make organoids a suitable model for a wider range of applications in basic and clinical research. For example, substituting Matrigel with synthetic matrices may drastically reduce the variation in organoid systems and overcome the issues that arise with its animal origin (e.g., organoids are unsuitable for clinical applications)<sup>51,52</sup>. Furthermore, synthetic dynamic matrices can guide morphogenetic processes to remodel organoids into desired shapes, thus allowing for better control over the organoid architecture<sup>26</sup>. Template-guided morphogenesis can increase the homogeneity in organoid cultures, since organoids will pattern in a pre-defined shape and facilitate the studies of specific regions (e.g., crypt or villus)<sup>53</sup>. Fabrication of micro- or macro-fluidic devices that accommodate organoids can further increase the complexity of organoid models by implementing fluid flow and mechanical stimulation. Such systems would benefit studies related to nutrient/drug uptake and bacterial growth, since these are affected by the motility of the intestine. Besides this, generation of organoids inside devices that can tightly control the culture conditions (e.g., medium composition) can promote the growth of multilineage organoid models. Additionally, body-on-chip platforms containing organoids instead of 2D cells can increase the biological complexity and provide a holistic *in vitro* approach to study body functions. Such approaches could provide valuable tools for drug discovery, since effects in secondary tissues can be studied along the

target site. This is particularly important since secondary effects can induce toxicity leading to failure in later clinical use. Finally, all these can only be achieved, if the methods developed are accessible, robust and reproducible, meaning that certain standards on organoid development, device fabrication and downstream analysis/testing should be agreed upon.

## **References**

1. Creff, J., Malaquin, L. & Besson, A. In vitro models of intestinal epithelium: Toward bioengineered systems. *J. Tissue Eng.* **12**, 2041731420985202 (2021).
2. Kakni, P., Truckenmüller, R., Habibović, P. & Giselbrecht, S. Challenges to, and prospects for, reverse engineering the gastrointestinal tract using organoids. *Trends Biotechnol.* 932–944 (2022). doi:10.1016/J.TIBTECH.2022.01.006
3. Gehart, H. & Clevers, H. Tales from the crypt: new insights into intestinal stem cells. *Nature Reviews Gastroenterology and Hepatology* **16**, 19–34 (2019).
4. Nguyen, T. L. A., Vieira-Silva, S., Liston, A. & Raes, J. How informative is the mouse for human gut microbiota research? *Dis. Model. Mech.* **8**, 1–16 (2015).
5. Hugenholtz, F. & de Vos, W. M. Mouse models for human intestinal microbiota research: a critical evaluation. *Cell. Mol. Life Sci.* **75**, 149–160 (2018).
6. Jung, S. M. & Kim, S. In vitro Models of the Small Intestine for Studying Intestinal Diseases. *Front. Microbiol.* **12**, 4102 (2022).
7. Drolia, R. & Bhunia, A. K. Crossing the Intestinal Barrier via Listeria Adhesion Protein and Internalin A. *Trends Microbiol.* **27**, 408–425 (2019).
8. Cao, X. *et al.* Why is it challenging to predict intestinal drug absorption and oral bioavailability in human using rat model. *Pharm. Res.* **23**, 1675–1686 (2006).
9. Mak, I. W. Y., Evaniew, N. & Ghert, M. Lost in translation: animal models and clinical trials in cancer treatment. *Am. J. Transl. Res.* **6**, 114 (2014).
10. Guidelines for the treatment of animals in behavioural research and teaching. *Anim. Behav.* **59**, 253–257 (2000).
11. Simon-Assmann, P., Turck, N., Sidhoum-Jenny, M., Gradwohl, G. & Kedinger, M. In vitro models of intestinal epithelial cell differentiation. *Cell Biol Toxicol* **23**, 241–256 (2007).
12. Fois, C. A. M. *et al.* Models of the Gut for Analyzing the Impact of Food and Drugs. *Adv. Healthc. Mater.* **8**, 1900968 (2019).
13. Barker, N. Adult intestinal stem cells: critical drivers of epithelial homeostasis and regeneration. *Nat. Rev. Mol. Cell Biol.* 2013 151 **15**, 19–33 (2013).

14. Huch, M., Knoblich, J. A., Lutolf, M. P. & Martinez-Arias, A. The hope and the hype of organoid research. *Development* **144**, 938–941 (2017).
15. Kwon, O., Han, T. S. & Son, M. Y. Intestinal Morphogenesis in Development, Regeneration, and Disease: The Potential Utility of Intestinal Organoids for Studying Compartmentalization of the Crypt-Villus Structure. *Front. Cell Dev. Biol.* **8**, 1192 (2020).
16. Sato, T. *et al.* Single Lgr5 stem cells build crypt-villus structures in vitro without a mesenchymal niche. *Nature* **459**, 262–265 (2009).
17. Spence, J. R. *et al.* Directed differentiation of human pluripotent stem cells into intestinal tissue in vitro. *Nature* **470**, 105–109 (2011).
18. Bein, A. *et al.* Microfluidic Organ-on-a-Chip Models of Human Intestine. *Cell. Mol. Gastroenterol. Hepatol.* **5**, 659–668 (2018).
19. Xiang, Y. *et al.* Gut-on-chip: Recreating human intestine in vitro. *J. Tissue Eng.* **11**, 2041731420965318 (2020).
20. Kimura, H., Yamamoto, T., Sakai, H., Sakai, Y. & Fujii, T. An integrated microfluidic system for long-term perfusion culture and on-line monitoring of intestinal tissue models. *Lab Chip* **8**, 741–746 (2008).
21. Ashammakhi, N. *et al.* Gut-on-a-chip: Current progress and future opportunities. *Biomaterials* **255**, 120196 (2020).
22. Ingber, D. E. Human organs-on-chips for disease modelling, drug development and personalized medicine. *Nat. Rev. Genet.* **2022** 238 **23**, 467–491 (2022).
23. Sung, J. H. *et al.* Recent Advances in Body-on-a-Chip Systems. *Anal. Chem.* **91**, 330–351 (2019).
24. Park, S. E., Georgescu, A. & Huh, D. Organoids-on-a-chip. *Science (80-. )*. **364**, 960–965 (2019).
25. Wang, Y. *et al.* A microengineered collagen scaffold for generating a polarized crypt-villus architecture of human small intestinal epithelium. *Biomaterials* **128**, 44–55 (2017).
26. Nikolaev, M. *et al.* Homeostatic mini-intestines through scaffold-guided organoid morphogenesis. *Nature* doi:10.1038/s41586-020-2724-8
27. Brassard, J. A., Nikolaev, M., Hübscher, T., Hofer, M. & Lutolf, M. P. Recapitulating macro-scale tissue self-organization through organoid bioprinting. *Nat. Mater.* 1–8 (2020). doi:10.1038/s41563-020-00803-5
28. Kakni, P. *et al.* Intestinal Organoid Culture in Polymer Film-Based Microwell Arrays. *Adv. Biosyst.* 2000126 (2020). doi:10.1002/adbi.202000126
29. Brandenburg, N. *et al.* High-throughput automated organoid culture via stem-cell aggregation in microcavity arrays. *Nat. Biomed. Eng.* 1–12 (2020). doi:10.1038/s41551-020-0565-2
30. Kiela, P. R. & Ghishan, F. K. Physiology of Intestinal Absorption and Secretion. *Best Pract. Res. Clin. Gastroenterol.* **30**, 145–159 (2016).
31. Muzes, G., Molnár, B., Tulassay, Z. & Sipos, F. Changes of the cytokine profile in inflammatory bowel diseases. *World J. Gastroenterol.* **18**, 5848

- (2012).
32. Neurath, M. F. Cytokines in inflammatory bowel disease. *Nat. Rev. Immunol.* **2014** *145* **14**, 329–342 (2014).
  33. Kakni, P., López-Iglesias, C., Truckenmüller, R., Habibović, P. & Giselbrecht, S. Reversing Epithelial Polarity in Pluripotent Stem Cell-Derived Intestinal Organoids. *Front. Bioeng. Biotechnol.* **0**, 669 (2022).
  34. Co, J. Y. *et al.* Controlling Epithelial Polarity: A Human Enteroid Model for Host-Pathogen Interactions. *Cell Rep.* **26**, 2509-2520.e4 (2019).
  35. Nash, T. J., Morris, K. M., Mabbott, N. A. & Vervelde, L. Inside-out chicken enteroids with leukocyte component as a model to study host–pathogen interactions. *Commun. Biol.* **2021** *41* **4**, 1–15 (2021).
  36. Li, Y. *et al.* Next-Generation Porcine Intestinal Organoids: an Apical-Out Organoid Model for Swine Enteric Virus Infection and Immune Response Investigations. *J. Virol.* **94**, (2020).
  37. Ojakian, G. K. & Schwimmer, R. Regulation of epithelial cell surface polarity reversal by  $\beta$  1 integrins. *J. Cell Sci.* **107**, 561–576 (1994).
  38. Lee, J. L. & Streuli, C. H. Integrins and epithelial cell polarity. *J. Cell Sci.* **127**, 3217–3225 (2014).
  39. Codutti, A., Cremer, J. & Alim, K. Changing Flows Balance Nutrient Absorption and Bacterial Growth along the Gut. *Phys. Rev. Lett.* **129**, 138101 (2022).
  40. Groschwitz, K. R. & Hogan, S. P. Intestinal barrier function: Molecular regulation and disease pathogenesis. *J. Allergy Clin. Immunol.* **124**, 3–20 (2009).
  41. Wang, T. Y., Liu, M., Portincasa, P. & Wang, D. Q. H. New insights into the molecular mechanism of intestinal fatty acid absorption. *Eur. J. Clin. Invest.* **43**, 1203–1223 (2013).
  42. Youhanna, S. & Lauschke, V. M. The Past, Present and Future of Intestinal In Vitro Cell Systems for Drug Absorption Studies. *J. Pharm. Sci.* **110**, 50–65 (2021).
  43. Zietek, T. *et al.* Organoids to Study Intestinal Nutrient Transport, Drug Uptake and Metabolism – Update to the Human Model and Expansion of Applications. *Front. Bioeng. Biotechnol.* **0**, 1065 (2020).
  44. Liang, J., Li, X., Dong, Y. & Zhao, B. Modeling Human Organ Development and Diseases With Fetal Tissue–Derived Organoids. *Cell Transplant.* **31**, (2022).
  45. Singhal, R. & Shah, Y. M. Oxygen battle in the gut: Hypoxia and hypoxia-inducible factors in metabolic and inflammatory responses in the intestine. *Journal of Biological Chemistry* **295**, 10493–10505 (2020).
  46. Cani, P. D. Human gut microbiome: hopes, threats and promises. *Gut* **67**, 1716–1725 (2018).
  47. Newby, D., Marks, L. & Lyall, F. Dissolved oxygen concentration in culture medium: assumptions and pitfalls. *Placenta* **26**, 353–357 (2005).
  48. Williamson, I. A. *et al.* A High-Throughput Organoid Microinjection

- Platform to Study Gastrointestinal Microbiota and Luminal Physiology. *Cmgh* **6**, 301–319 (2018).
49. Jalili-Firoozinezhad, S. *et al.* A complex human gut microbiome cultured in an anaerobic intestine-on-a-chip. *Nat. Biomed. Eng.* **3**, 520–531 (2019).
  50. Bein, A. *et al.* Microfluidic Organ-on-a-Chip Models of Human Intestine. *Cell. Mol. Gastroenterol. Hepatol.* **5**, 659 (2018).
  51. Gjorevski, N. *et al.* Designer matrices for intestinal stem cell and organoid culture. *Nature* **539**, 560–564 (2016).
  52. Cruz-Acuña, R. *et al.* Synthetic hydrogels for human intestinal organoid generation and colonic wound repair. *Nat. Cell Biol.* **19**, 1326–1335 (2017).
  53. Hofer, M. & Lutolf, M. P. Engineering organoids. *Nat. Rev. Mater.* **2021** 65 **6**, 402–420 (2021).





CHAPTER IX

**IMPACT PARAGRAPH**





In this chapter, we discuss the potential impact of the research described in the context of this thesis. Specifically, we deliberate over how these intestinal organoid models fit within the societal needs and what the possible scientific and commercial applications are.

The digestive system is one of the most complex organ systems. It contains diverse cell types that are responsible for a wide range of functions that are crucial for life. Apart from digestion, absorption, secretion and excretion, the gastrointestinal (GI) tract acts as a barrier to harmful compounds and microorganisms, thus contributing significantly to the defense mechanisms of the body. Trillions of bacteria and other microorganisms reside within the GI tract that collectively make up the microbiota. GI tract cells communicate also with the central nervous system and the endocrine system, thus its function is regulated and affected by multiple factors. The complexity of the system along with the variation exhibited among different individuals entangle not only basic research related to the understanding of mechanisms underlying the normal and diseased state of the GI tract, but also translational research related to the treatment of these disorders. Thus, currently disorders of the digestive system (e.g., irritable bowel syndrome, Crohn's disease, GI cancers) are a major cause of morbidity in the elderly population. Every year, up to 370 million people are diagnosed with a digestive disorder globally<sup>1,2</sup>. This raises the need for the development of more advanced and representative *in vitro* models. 3D organoid systems can be tremendously beneficial for studying such complex tissues *in vitro* and are expected to revolutionize the conventional paradigm in pharmaceutical industry and drug discovery in the future. Currently there are 70 organoid research model companies globally, which focus on drug discovery using organoid models<sup>3</sup>. Till November 2020, there were globally 21 ongoing organoid clinical trials, a number which is expected to increase in the next few years, owing to the progress in the scientific field and improvements in infrastructures<sup>4,5</sup>. The sales of organoids had an increase of 5% in the period between 2016 and 2020 and investments in organoid products are constantly rising<sup>4</sup>. Solely the National Institute of Health in the U.S. awarded research grants, which exceeded \$251 million between 2015 and 2019<sup>4</sup>. The global organoid market size was evaluated at \$516.6 million in 2021 and is expected to reach \$1.2 billion by 2031<sup>5</sup>. Among organoid models, intestinal organoids are expected to exhibit the highest sales in the market<sup>4</sup>. All these data indicate the importance and great potential of organoid models.

In the past decade, numerous 3D organoid models recapitulating different tissues have been developed. These mini-organs mimic structural and functional

characteristics of the *in vivo* tissues with great fidelity and they have been widely used to study physiology and disease. However, their use in drug development and clinical applications is still restricted because of certain limitations such as the use of animal-derived extracellular matrices substitutes, the low throughput and the lack of surrounding tissue microenvironment. With the research performed here, we managed to overcome some of these issues and broaden the applicability of organoid technology in basic and translational research.

Currently, drug discovery is a long and expensive process, which often turns out fruitless upon reaching the clinical trial phase. Specifically, it can take between 12 and 15 years from the discovery of a drug until its approval and requires an investment of \$1 billion<sup>6</sup>. Furthermore, out of a million molecules screened, only a single one will reach the clinical trials<sup>6</sup>. This urges the need for improvements in the predictive power of the preclinical phase. Personalized drug testing with organoids could be particularly useful to bridge the gap between preclinical drug development and clinical trials. In the Netherlands, cystic fibrosis patients that would respond well to a certain treatment were identified after a drug screening in patient-derived organoids with different mutations<sup>7</sup>. This was a first step towards extending the application of organoids for personalized medicine purposes. The use of organoids can also reduce drug/compound testing in animals, which is currently an ongoing ethical debate topic. All these may also result in financial benefit, since experiments with organoids are cheaper than *in vivo* studies; therefore, the budget spent on unsuccessful clinical studies may be minimized since drug candidates will be better “filtered” during the preclinical phase. The microwell-based intestinal organoid model developed in chapter III allows for a better-controlled organoid culture with limited use of Matrigel and it facilitates downstream applications, such as drug-screenings, in high-throughput. Such systems could be adopted by pharmaceutical companies in the future to improve, reduce the cost of and accelerate preclinical drug testing.

To improve the drug discovery process, it is particularly important to understand the mechanisms underlying the physiology and disease. Although organoids represent multiple tissue features, they lack the surrounding microenvironment. Tissue communication plays a crucial role among others in homeostasis, in the development of certain diseases and in the responses to drugs/treatments. For instance, the immune system includes multiple components (innate and adaptive) in all tissues and is crucial for the host defense against harmful agents. With that in mind, in chapter IV we incorporated macrophages in our

microwell-based intestinal organoid culture system in two different ways. In the first configuration, organoids are in very close proximity and even direct contact with macrophages, mimicking chronic inflammation states. In the second configuration, the communication between organoids and macrophages is performed only by paracrine signaling and this situation mimics closer acute inflammation. These two systems could immensely benefit research related to the complex mechanisms underlying the immune responses in the intestine. For example, inflammatory bowel disease (IBD) has become a global disease with accelerating incidences and its pathogenesis is not fully understood yet. Consequently, there is no cure for this disease and current treatments only aim to reduce symptoms and prevent complications. Currently, the annual costs of care for IBD patients are approximately \$23,000, which could reach up to \$37,759 if a single visit to the emergency department is required<sup>8</sup>. Considering that up to 70,000 new IBD cases per year are diagnosed only in the U.S, there is a tremendous burden on healthcare. Using these intestinal organoid-macrophage models, studies focusing on the mechanisms underlying such diseases could be facilitated. Subsequently, therapeutic agents could be tested in a high-throughput manner in order to develop more efficient treatments.

For the proper validation of drug and other nutrition compounds, the characterization of absorption, distribution, metabolism, and excretion (ADME) properties is pivotal. In the intestine, orally administered nutrients and drugs are taken up via the apical surface. Currently, around 60% of the drug products that are commercially available are administered via the oral route<sup>9</sup>. However, in intestinal organoid models the apical side is facing the enclosed lumen, thus access to it is challenging. To facilitate ADME studies, we developed intestinal organoids with reversed epithelial polarity, where the apical surface is facing outwards to the culture medium (chapters V and VI). This scalable organoid model could facilitate nutrient and pharmaceutical studies, since it mimics more closely the *in vivo* situation where there is direct contact between the apical surface and the substances. Apart from that, organoids with apical-out orientation could be used to study the gut barrier function. This is important for the assessment of permeability, which again is connected to nutrient and drug uptake. Barrier dysfunction has been associated with several diseases such as food allergies, microbial infections, irritable bowel syndrome and diabetes, thus the use of such advanced intestinal organoid models could pave the way for unravelling unknown mechanisms underlying the relationship between barrier dysfunction and disease and later on, for testing new therapeutic agents.

The apical surface of the intestine is also exposed to the complex gut microbiota, which mainly consists of anaerobic microorganisms. To recapitulate closer this *in vivo* situation, we developed apical-out organoids in a hypoxic environment and performed co-culture with two of the most dominant probiotic bacteria species of the intestine; Lactobacillus and Bifidobacterium (chapter VII). Probiotics are known for their health-promoting benefits (e.g. epithelial barrier integrity and host immune response) and in the past decade, there is growing demand for probiotic supplements. Specifically, the amount of consumers taking probiotics increased by 66% in the U.S., 188% in Italy and 108% in China between November 2019 and May 2020. The global probiotics market was \$58.17 billion in 2021 and is expected to expand tremendously in the upcoming years<sup>10</sup>. Thus, such advanced 3D *in vitro* models could benefit food industry (global market amount to \$8.66 trillion<sup>11</sup>), since they can be used as bacteria testing platforms to develop new, efficient probiotic supplements.

Overall, the research described in this thesis advanced our understanding in organoid models and provided powerful platforms to study intestinal physiology and disease, and conduct high-throughput nutrient and drug screenings. These models could be mainly used by researchers for fundamental research or for nutrient/ drug screening applications. Overall, these are critical steps towards novel treatment options for digestive disorders, which affect almost 40% of the adult population worldwide with varying severity.

## **References**

1. GI Alliance. Digestive disease continues to rise among Americans digestive disease continues to rise among Americans. *GI Alliance: Nation's Premier Gastroenterology Practice* (2021). at <https://gialliance.com/gastroenterology-blog/digestive-disease-continues-to-rise-among-americans>.
2. New report reveals Major Health and economic impact of digestive diseases across Europe. *UEG* (2022). at <https://ueg.eu/a/306>.
3. Top Organoid Research Models Startups. *Tracxn.com* (2022). at <https://tracxn.com/d/trending-themes/Startups-in-Organoid-Research-Models>.
4. Organoids Market. *Futuremarketinsights.com* (2021). at <https://www.futuremarketinsights.com/reports/organoids-market>.
5. Vikita, T. & Onkar, S. Organoids Market | Spheroids Market Statistics | Forecast - 2031. *Allied Market Research* (2022). at <https://www.alliedmarketresearch.com/organoids-and-spheroids-market-A17036>.

6. Deore, A., Dhumane, J., Wagh, R. & Sonawane, R. The Stages of Drug Discovery and Development Process. *Asian Journal of Pharmaceutical Research and Development* **7**, 62-67 (2019).
7. Kingwell, K. 3D cell technologies head to the R&D assembly line. *Nature Reviews Drug Discovery* **16**, 6-7 (2016).
8. Park, K. et al. The Cost of Inflammatory Bowel Disease: An Initiative From the Crohn's & Colitis Foundation. *Inflammatory Bowel Diseases* **26**, 1-10 (2019).
9. Alqahtani, M. S., Kazi, M., Alsenaidy, M. A. & Ahmad, M. Z. Advances in oral drug delivery. *Frontiers in Pharmacology* **12**, (2021).
10. Probiotics Market Size | Industry Report, 2021-2030. *Grandviewresearch.com* at <https://www.grandviewresearch.com/industry-analysis/probiotics-market>.
11. Food - Worldwide | Statista Market Forecast. *Statista* (2022). at <https://www.statista.com/outlook/cmo/food/worldwide>.







EPILOGUE

**SUMMARY**

**SAMENVATTING**

**ACKNOWLEDGEMENTS**

**LIST OF PUBLICATIONS**

**CURRICULUM VITAE**





## Summary

The advent of organoid systems has revolutionized biomedical research by offering powerful three-dimensional *in vitro* models, which closely recapitulate the architecture, cellular heterogeneity and function of specific organs. Even though such systems might be of great potential for translational applications, such as drug discovery and regenerative medicine, organoids are not without limitations. This thesis focused on identifying ways to overcome current limitations of organoids and expand their range of applications. To achieve that, we used both adult (ASC) and pluripotent (PSC) stem cell-derived intestinal organoids, since they are one of the most well-established organoid models and we developed different methods to culture them. In chapter I, we provide a general introduction to intestinal organoid models development and present a thesis overview. In chapter II, we review the current challenges of intestinal organoid models and discuss the available approaches to overcome them. Additionally, we envision the next-generation of gastrointestinal tract organoids as integrated models that recapitulate structural and functional characteristics of multiple regions of the digestive tube in a single *in vitro* model. In chapter III, we develop a microwell-based intestinal organoid model, where organoids cultured with limited amounts of basement membrane extract, demonstrate reduced variability and survive for prolonged time periods, compared to organoids embedded in hydrogels. This system facilitated the *in situ* monitoring of organoids during culture as well as the downstream processes, enabling the possibility of high-throughput screenings. In chapter IV, we increase the system complexity to more accurately model its *in vivo* counterpart, by integrating immune cells, which surround the intestinal epithelium. Using a combination of organoids and macrophages in tightly controlled spatial conformation, we were able to model both acute and chronic intestinal inflammation states. In chapter V, we develop a novel PSC-derived intestinal organoid model with reversed epithelial polar organization, where the apical surface of the organoid is directly accessible, facing the culture medium. This system facilitated nutrient and drug uptake and metabolism studies, as well as studies related to host-microbiome and host-pathogen interactions. In chapter VI, we present the functional aspects of the system by performing a polarity-specific nutrient uptake assay and testing barrier formation and integrity, metabolic functions, as well as the presence of functional apical and basal transporters and drug metabolizing enzymes. In chapter VII, we follow up with the applications of reversed polarity organoids and adapt the protocol described in chapter V to hypoxic conditions. More specifically, we establish hypoxia-tolerant apical-out intestinal organoids in order to study host-microbiome interactions. Most

of microorganisms in the intestine are anaerobic, suggesting that they survive and grow only in environments with low or no oxygen and therefore, the hypoxia-tolerant apical-out intestinal organoid system allows for the first time the study of the complex gut-microbiome interactions in low oxygen conditions using apical-out organoids. In chapter VIII, we provide a historical and critical perspective of preclinical intestinal *in vitro* and *in vivo* models, we contextualize our findings in this context and provide our vision on the future of intestinal organoids. Finally, in chapter IX, we explore the scientific and social impact of the organoid systems developed in the context of this thesis.

To conclude, this thesis provides valuable insights into the development of more advanced and representative *in vitro* organoid models. The new methods established here to culture intestinal organoids, can be a steppingstone to overcome current limitations and expand the range of applications of organoid models.

## Samenvatting

De komst van organoïde systemen heeft de wetenschap voorzien van krachtige drie-dimensionale *in vitro* modellen, welke de architectuur, de cellulaire heterogeniteit en functie van een specifiek weefsel samenvat. Hoewel deze systemen veel kunnen betekenen voor translationele toepassingen, zoals medicijnontwikkeling en regeneratieve geneeskunde, zijn organoïden niet zonder beperkingen. Dit proefschrift richt zich op het zoeken naar methoden om deze beperkingen weg te nemen en hun toepassingen uit te breiden. Om dit te bereiken zijn organoïden gebruikt die gederiveerd zijn van zowel volwassenen als van pluripotente stamcellen, omdat deze tot de meest gebruikte organoïden modellen horen. Tevens hebben we verschillende methoden ontwikkeld om ze te kweken. In hoofdstuk I geven we een algemene introductie over de ontwikkeling van organoïden en een overzicht van deze thesis. In hoofdstuk II bespreken we de huidige uitdagingen van de darm organoïden en de beschikbare benaderingen om deze uitdagingen te overwinnen. Tevens schetsen we een beeld van de volgende generatie organoïden van het maag-darm kanaal, waarin de structurele en functionele kenmerken van meerdere regio's van de spijsverteringsbuis geïntegreerd zijn in één enkel *in vitro* model. In hoofdstuk III ontwikkelen we een 'microwell' gebaseerd darm organoïden. In dit model vertonen organoïden minder variabiliteit en overleven ze voor langere tijd wanneer ze gekweekt worden met beperkte hoeveelheden basaalmembraan extract. Met dit systeem kunnen zowel organoïden *in situ*, tijdens de kweek, als in de daaropvolgende stappen gevolgd worden, waardoor screenings met een hoge doorvoer mogelijk worden. In hoofdstuk IV vergroten we de complexiteit van het model om zo te komen tot een model dat meer lijkt op de *in vivo* situatie. Dit werd gedaan door de toevoeging van immuun cellen welke het darmepitheel omringen. Door gebruik te maken van een combinatie van organoïden en macrofagen in een sterk gecontroleerde ruimtelijke conformatie, was het mogelijk om zowel acute als chronische darmontsteking na te bootsten. In hoofdstuk V ontwikkelen we een nieuw pluripotent stamcel afgeleid darm organoïde model met omgekeerd epitheliale polarisatie, waarbij het apicaal oppervlak van de organoïden direct toegankelijk is voor het kweekmedium. Dit model maakt het mogelijk om studies te verrichten gefocust op de opname van voedingsstoffen en medicijnen, en gastheer-microbioom en gastheer-pathogeen interacties. In hoofdstuk VI presenteren we de functionele aspecten van het model aan de hand van een polariteit-specifiek voedingsstoffen opname experiment. We tonen zowel barrière formatie als integriteit aan, welke betrokken zijn bij de metabole functie. Tevens worden de aanwezigheid van functionele apicale en basale transporters en enzymen die geneesmiddelen omzetten

aangetoond. In hoofdstuk VII hebben we meer toepassingen voor de omgekeerde polariteit organoïden onderzocht en het protocol zoals beschreven in hoofdstuk V aangepast voor zuurstofarme kweek omgeving (hypoxie). Meer specifiek, we hebben hypoxie tolerante organoïden met de apicale oppervlak aan de buitenkant ontwikkeld om de gastheer-microbioom interacties te bestuderen. De meeste micro-organismen in de darmen zijn anaeroob, zij kunnen alleen overleven en groeien in een omgeving met weinig of geen zuurstof. Het is voor het eerst dat de complexe darm-microbioom interactie in hypoxie bestudeerd kan worden door gebruik te maken van het hypoxie tolerante organoïde model met de apicale oppervlak aan de buitenkant. In hoofdstuk VIII bieden we een historisch en kritisch perspectief van preklinische *in vitro* en *in vivo* darmmodellen, we contextualiseren onze bevindingen in dit opzicht en stellen ons de toekomst voor van darm organoïden. Tot slot, in hoofdstuk IX, onderzoeken we de wetenschappelijke en maatschappelijke impact van de organoïde modellen die in de context van dit proefschrift zijn ontwikkeld. Concluderend voegt dit proefschrift fundamentele kennis toe aan de ontwikkeling van meer geavanceerde en representatieve *in vitro* organoïde modellen. De nieuwe methoden die hier zijn ontwikkeld om darm organoïden te kweken, kunnen een springplank zijn om de huidige beperkingen te overwinnen en het scala aan toepassingen van organoïde modellen uit te breiden.

## Acknowledgements

Finally, this part marks the end of a unique roller-coaster ride. Pursuing a PhD was quite a journey and reaching the end of it now, I would like to take some time to thank all the people that supported me on the way and made this journey more fun and enjoyable.

Initially, I would like to thank my supervisors Stefan, Pamela and Roman that gave me the opportunity to start this journey and supported me all the way through it. Stefan, I am forever grateful for your guidance and mentorship and I could never ask for a better supervisor. You always gave me the confidence to carry out my research projects with freedom. You lead by example and you are a true inspiration for all of us. Pamela and Roman, I know that organoids are not your cup of tea, but I am very thankful for bringing in your perspectives and always trying to help in any way possible.

A special thanks goes to my family. I have no words to describe my gratitude to my parents for providing me the best values and education to become who I am today. Thank you for your unconditional love, support and guidance in every step of my life. I wish every child on earth could have parents like you! To my sister Niki, for always being by my side and never stops believing in me. Remember, no matter where I live, I will always be one call away.

Next, I would like to thank everyone that contributed to the projects described in this thesis. Especially Barry with whom we spent a lot of (fun) hours in the lab and played a part in multiple projects. Another special thanks goes to Carmen López Iglesias, who was always willing and enthusiastic to work with new projects together.

Moving to Maastricht, I was lucky to meet many people with different cultural and educational backgrounds. MERLN is a unique, diverse working place and it was a pleasure pursuing a PhD there. But, I think we can all agree that life without fun is unbearable! So I would like to thank all the people that made this journey more enjoyable. To Francesca, Tristan, Ane, Maria, Joanna, Gabriella, Pere, Daniel, Tony, Lou, Julia, Paula, Gabriele, Nello, Shivesh, Claudia, Mirco, Clarissa, Adrian, Kike, Carlos, Pierpaolo, Helen and Monize, I will never forget our incredible parties and dinners.

Special shout out to Francesca, with whom we met during our interviews back in December 2017 and here we are in December 2022 getting through the last steps of this journey together. Thank you for listening to all my complains and be there

through thick and thin. Tristan, my roomie, thank you for sticking by my side all these years. A lot of good times (full of alcohol and laughs) were spent with you and I am grateful for those. Ane, my favorite e-spanish, thank you for all the e-spanish you e-taught me, all the great trips we took (and the next that are yet to come) and all the fun hours we spent at the gym. Maria, my Greek twin, even though we only met during the last year, the bonding was instant and I am very grateful for our friendship.

Another big thanks goes to my friends from Greece, Nina, Zefi, Andreas and Christina. Even if we are far away, the time we spend together is always fun and I am very thankful for your support all these years. Nina, thank you for picking me up when I was down and for always being there to celebrate my wins. Zefi, thank you for cheering me up and for making all these years fun and full of great memories.

Lastly, I would like to thank the members of the assessment committee Prof. Dr. Lorenzo Moroni, Prof. Dr. Daisy Jonkers, Prof. Dr. Daniel Keszthelyi, Dr. Adrian Ranga and Dr. Hans Bouwmeester for taking the time to critically evaluate and provide feedback on this thesis.

## List of Publications

1. **Kakni, P.**, Hueber, R., Knoops, K., López-Iglesias, C., Truckenmüller, R., Habibovic, P., & Giselbrecht, S. Intestinal Organoid Culture in Polymer Film-Based Microwell Arrays. *Advanced Biosystems*, 4 (10), 2000126 (2020). <https://doi.org/10.1002/adbi.202000126>
2. **Kakni, P.**, Truckenmüller, R., Habibovic, P., & Giselbrecht, S. Challenges to, and prospects for, reverse engineering the gastrointestinal tract using organoids. *Trends in Biotechnology*, 40 (8), 932-944 (2022). <https://doi.org/10.1016/j.tibtech.2022.01.006>
3. **Kakni, P.**, López-Iglesias, C., Truckenmüller, R., Habibović, P. & Giselbrecht, S. Reversing Epithelial Polarity in Pluripotent Stem Cell-Derived Intestinal Organoids. *Frontiers in Bioengineering and Biotechnology*, 10, 879024 (2022). <https://doi.org/10.3389/fbioe.2022.879024>
4. **Kakni, P.**, Truckenmüller, R., Habibović, P., van Griensven, M., & Giselbrecht, S. A microwell-based intestinal organoid-macrophage co-culture system to study intestinal inflammation. *Int. J. Mol. Sci.* 23 (23) 15364 (2022). <https://doi.org/10.3390/ijms232315364>
5. **Kakni, P.**, López-Iglesias, C., Truckenmüller, R., Habibović, P. & Giselbrecht, S. Intestinal organoids with apical-out orientation as a tool to study nutrient uptake, drug absorption and metabolism. (under review)
6. **Kakni, P.**, Jutten, B., Teixeira Oliveira Carvalho, D., Penders, J., Truckenmüller, R., Habibović, P. & Giselbrecht, S. Hypoxia-tolerant apical-out intestinal organoids to model host-microbiome interactions (under review)

# Curriculum Vitae

Panagiota Kakni was born on 30<sup>th</sup> of April 1994 in Thessaloniki, Greece. She received her Bachelor's degree in Molecular Biology and Genetics at Democritus University of Thrace. Afterwards, she moved to Edinburgh in order to continue her studies and obtain her Master's degree in Integrative Neuroscience. For her master thesis, she performed an internship at the Centre for Integrative Physiology of the University of Edinburgh, focusing on the evaluation of brain organoids as an *in vitro* model of brain development and disease. In February 2019, she moved to Maastricht to start her PhD research at the MERLN Institute for Technology-Inspired Regenerative Medicine, under the supervision of



Stefan Giselbrecht, Pamela Habibović and Roman Truckenmüller. Her PhD project was focused on the development of more advanced and physiologically relevant 3D *in vitro* models of the intestine. These newly developed models can be a steppingstone to overcome current limitations and expand the range of applications of organoid models.



